POLYTECHNIQUE

École Polytechnique
Laboratoire d'Hydrodynamique

Thèse présentée pour obtenir le grade de

DOCTEUR DE L'ÉCOLE POLYTECHNIQUE

Spécialité : Physique Théorique

par

Anaël LEMAÎTRE

Systèmes chaotiques couplés : comportements collectifs et universalité

---

soutenue le 27 juillet 1998
devant le jury composé de :

M. Jean Bricmont	
M. Hugues Chaté	
M. Pierre Collet	Président du jury
M. Peter Grassberger	
M. Vincent Hakim	Rapporteur
M. Raymond Kapral	Rapporteur
M. Paul Manneville	Directeur de thèse
M. Arkady Pikovsky	

POLYTECHNIQUE

École Polytechnique
Laboratoire d'Hydrodynamique

Thèse présentée pour obtenir le grade de

DOCTEUR DE L'ÉCOLE POLYTECHNIQUE

Spécialité : Physique Théorique

par

Anaël LEMAÎTRE

Systèmes chaotiques couplés : comportements collectifs et universalité

---

soutenue le 27 juillet 1998
devant le jury composé de :

M. Jean Bricmont	
M. Hugues Chaté	
M. Pierre Collet	Président du jury
M. Peter Grassberger	
M. Vincent Hakim	Rapporteur
M. Raymond Kapral	Rapporteur
M. Paul Manneville	Directeur de thèse
M. Arkady Pikovsky	

L'essentiel du travail présenté dans ce mémoire a été effectué au Laboratoire d'Hydrodynamique de l'École Polytechnique (LadHyX), ainsi qu'au Service de Physique de l'État Condensé du CEA (SPEC).

Il est difficile de résumer en quelques lignes ce que furent les années pré-fa du LadHyX, mais il est certain qu'elles me laisseront le souvenir de moments intenses par l'intérêt de mon étude, la richesse du sujet, et aussi le sentiment d'avoir vécu une période privilégiée, grâce à l'ambiance heureuse qui y régnait ; ce sont en tout cas pour moi des instants inoubliables.

Je dois en premier lieu remercier Paul Manneville, qui a accepté d'être le directeur de cette thèse, me permettant ainsi d'aborder un sujet aussi passionnant et sur lequel j'ai eu beaucoup de plaisir à travailler ; j'ai toujours apprécié pouvoir discuter avec lui et tenter de comprendre sa vision intuitive de la thermodynamique.

Hugues Chaté a accompagné cette thèse tout au long de son déroulement, il en a suivi toutes les péripéties ; interlocuteur à la fois attentif et critique, il a toujours été un soutien. Que dire de plus ?... si ce n'est que je me rejouis de la perpective de poursuivre et d'étendre cette collaboration dans de nombreux projets.

Toute thèse ayant une fin, je remercie les membres du jury de l'intérêt qu'ils ont manifesté pour ce travail et de leur... présence le jour de la soutenance, de leur disponibilité malgré une organisation quelque peu «chaotique».

L'ambiance chaleureuse et néanmoins sérieuse du LadHyX-Circus a beaucoup compté au cours de ces années de thèse, parfois semées d'embûches ; la magie de cette assemblée a toujours été un réconfort, et je tiens à en saluer les différents personnages. Quelle fut donc l'alchimie concoctée par Don P. Huerre avec l'aide de son fidèle J.-M. Chomaz ? Pourquoi ont-ils attaqué le phare de Beg-Rohu ? Quel rôle mystérieux ont donc joué Tatie Thérèse, et Tonio l'homme de mains ? Les ethnologues y répondront peut-être un jour : derrière ces questions se cache une recette de succès. Il faudrait encore se demander comment l'espresso vibré horizontalement fut mis au point par Al-Olivier-

bin-Sabl et Carolus le curiace ou encore comment le respectable père d'une famille de cinq filles finit par jouer avec sa pomme de douche et son tuyau d'arrosage... Sans peut-être les nommer tous, je citerai Yvan dans son rôle de barde, Stéphanie la Marseillaise qui heureusement ne l'a pas chantée, Le Grand Duc Majuscule aux Interminables Pinaillages en Maints Langages et Scriptages, le Beau Thomas, Dame Sabine, Paulo le clown stratifié, l'Ours des Carpates dans son numéro de funambule, ainsi que la troupe des roumains et enfin Jack, le monteur de gabu, dompteur de gibis, sans lesquels les calculs eussent été plus longs.

Ce travail ayant necessité de longues heures de calcul sur les machines du LadHyX et sur celles du SPEC, je salue la patience de tous devant des processeurs (hum !),... parfois un petit peu surchargés.

Au moment où s'achève la rédaction de ce manuscrit, le LadHyX ayant déménagé, je lui souhaite de savoir recréer cette atmosphère ensoleillée, joyeuse et dynamique sous la verrière de ses nouveaux locaux ; je pense enfin (engagez-vous rengagez-vous, qui disaient) à tous ceux qui sont en cours de thèse : bon courage.

Table des matières

Introduction

Notre expérience courante, formée au contact d'objets macroscopiques, nous conduit naturellement à identifier un certain nombre de paramètres (température, pression, ...) afin de caractériser l'état d'un système ; des relations phénoménologiques entre ces grandeurs sont alors recherchées afin de pouvoir décrire les phénomènes observés. Ces lois sont inhérentes à l'échelle de notre observation : la structure microscopique du système étudié peut se révéler extrêmement complexe, mettant en jeu un grand nombre de particules, et gouvernée par des équations de nature différente de leur contrepartie macroscopique. Il est alors tout à fait remarquable que les lois macroscopiques semblent indifférentes aux détails de la structure fine de la matière, et puissent souvent être extraites par la seule considération de propriétés très générales comme des symétries ou des lois de conservations.

Paradoxalement, les trajectoires microscopiques sont en général exactement descriptibles dès que nous disposons des équations fondamentales qui régissent les interactions entre ces particules. Cependant la dérivation de lois macroscopiques à partir de la connaissance de la structure interne d'un système est un problème profondément difficile, d'autant plus que les relations macroscopiques ne présentent pas toujours certaines des symétries présentes au niveau des équations microscopiques. C'est le cas de la thermodynamique des systèmes à l'équilibre dont la micro-structure est conservative, alors que le système macroscopique relaxe vers un état d'équilibre de façon irréversible : le système est alors régi par un Hamiltonien, et la physique statistique propose une façon particulièrement élégante de décrire l'état d'équilibre par une mesure de Gibbs. Quand de tels systèmes conservatifs sont mis hors équilibre, par exemple parce qu'on les soumet à un gradient, leur description est encore possible par des modèles simples soumis à un bruit extérieur. Le problème consiste alors à déterminer si le système admet un état stationnaire et quelles sont ses propriétés.

D'autres préoccupations ont cependant conduit à étudier le comportement

macroscopique de systèmes dont justement, les équations fondamentales ne sont pas réversibles. C'est le cas, par exemple, d'un fluide turbulent pour lequel une description complète des champs de vitesse et de pression n'est plus possible, bien que leur dynamique soit entièrement contenue dans l'équation de Navier-Stokes. C'est aussi le cas de toute assemblée d'objets gouvernés par un comportement non linéaire, des réseaux de neurones aux colonies d'insectes. Nous nous intéresserons dans ce mémoire à des systèmes modèles dont la structure microscopique est gouvernée par des équations irréversibles, de façon purement déterministe, et incorpore un désordre intrinsèque. La définition d'une thermodynamique pour ces systèmes en est à ses balbutiements, et les quantités macroscopiques qui permettent de caractériser leurs états sont elles-mêmes mal définies.

Un modèle de chaos spatio-temporel

Les premiers modèles de chaos temporel ont été introduits afin d'illustrer la dépendance de certains systèmes dynamiques vis-à-vis d'un paramètre de contrôle. Bien qu'ils ne contiennent qu'un petit nombre de degrés de liberté, ces modèles ont été abondamment utilisés dans l'interprétation de phénomènes complexes comme ceux observés dans certaines expériences d'hydrodynamique. Par exemple, ces concepts sont ainsi bien adaptés à la description des rouleaux de convection apparaissant dans une cellule de Rayleigh-Bénard, mais seulement tant que le système est suffisament confiné. Il y a cependant peu de cas où l'espace peut-être éliminé, et il est donc nécessaire pour étendre ces idées de commencer par incorporer une extension spatiale.

Il convient donc de considérer un champ de *variables locales*, $\mathbf{X}_{\vec{r}}$, réparties en tout point d'un espace $\mathcal{L}$, et de définir une évolution déterministe pour ces variables, c'est à dire pour la configuration $\mathbf{X} = (\mathbf{X}_{\vec{r}})_{\vec{r}\in\mathcal{L}}$. C'est par exemple le cas d'un champ de vecteurs dont la dynamique est gouvernée par un système d'équations aux dérivées partielles : l'espace et le temps sont alors continus ($\mathcal{L} = \mathbb{R}^d$). Dans le cas des automates cellulaires, au contraire, l'espace est discret (c'est souvent le réseau hypercubique, $\mathcal{L} = \mathbb{Z}^d$), les variables locales sont binaires et évoluent par une dynamique où le temps lui-même est discret.

Nous nous intéressons à l'un des modèles parmi les plus simples de chaos spatio-temporel, où des itérations chaotiques sont simplement attachées aux sites d'un réseau discret et couplées entre elles par la dynamique. Les réseaux d'itérations couplées ont été introduits par Kaneko, qui les a présentés comme

un modèle de dynamique de réaction-diffusion et qui en a conduit les premières explorations numériques [10, 11, 14, 13, 12, 15, 8].

Définition

Le système est constitué de variables réelles $\mathbf{X}_{\vec{r}}$ disposées aux nœuds (ou sites) $\vec{r}$ d'un réseau $\mathcal{L}$ hypercubique de dimension d. Chaque variable locale prend ses valeurs sur un intervalle I, et la configuration instantanée $\mathbf{X}^t$ évolue dans l'espace des phases $\mathbf{I} = I^{\mathcal{L}}$. Le temps est discret, et le système est mis à jour de façon synchrone : tous les sites sont transformés simultanément par un opérateur de la forme

$$\mathbf{X}^{t+1} = \mathbf{\Delta}_g \circ \mathbf{S}_\mu \left(\mathbf{X}^t \right) . \tag{1}$$

L'opérateur $\mathbf{S}_\mu$ transforme chaque variable locale par une application non linéaire $S_\mu : I \to I$ dont μ est le paramètre de non-linéarité, tandis que $\mathbf{\Delta}_g$ couple dynamiquement chaque site à ses voisins.

Différentes applications de l'intervalle $I = [-1, 1]$ sont étudiées au cours de ce travail, et en particulier les applications unimodales de la forme

$$S_\mu(X) = 1 - \mu |X|^{1+\varepsilon} , \quad \text{avec } \mu \in [0, 2] , \quad \text{et } \varepsilon \geq 0 , \tag{2}$$

où μ mesure la non-linéarité de S_μ. Ces itérations ont joué un rôle important dans l'élucidation des propriétés du chaos temporel : en faisant varier le paramètre de contrôle μ, la dynamique ainsi définie présente une cascade sous-harmonique de comportements périodiques puis devient chaotique au delà d'un seuil μ_∞ [9]. Ces propriétés seront rappelées ultérieurement.

L'opérateur de couplage est habituellement défini par

$$[\mathbf{\Delta}_g(\mathbf{X})]_{\vec{r}} = (1 - 2dg)\mathbf{X}_{\vec{r}} + g \sum_{\vec{e} \in \mathcal{V}'} \mathbf{X}_{\vec{r}+\vec{e}} , \tag{3}$$

où g est la force du couplage et $\mathcal{V}'$ l'ensemble des $2d$ plus proches voisins du site $\vec{r} = \vec{0}$. Le paramètre g est pris dans l'intervalle $g \in [0, 1/2d]$ pour assurer que les coefficients qui interviennent dans la combinaison linéaire soient tous positifs. Cet opérateur est alors l'analogue dynamique d'une force d'interaction attractive (ferromagnétique) qui cherche à rapprocher les valeurs de sites voisins : il conduit toute configuration vers un état spatialement uniforme s'il est appliqué récursivement.

Observations

Deux paramètres

Le système ainsi défini a deux paramètres de contrôle : μ qui définit la dynamique de l'itération locale, et g qui détermine l'intensité du couplage. Nous nous intéresserons principalement au cas où l'application locale est chaotique (ce qui exige que μ soit suffisamment grand : $\mu \geq \mu_\infty$), et aux grandes valeurs de g. Cependant, la compréhension des comportements observés sous ces conditions nous conduira aussi à réfléchir aux systèmes pour lesquels le couplage est nul ou faible.

Chaos local

Quand l'application locale est chaotique, elle a tendance à accroître l'écart entre deux variables de valeurs voisines : elle s'oppose ainsi au couplage qui cherche, quant à lui, à synchroniser l'ensemble des sites du réseau. On observe alors que, même aux plus fortes valeurs du couplage g, le système n'atteint jamais une parfaite synchronisation (voir fig. 1) ; plus étonnant encore, la dynamique individuelle de chaque variable locale $\mathbf{X}^t_{\vec{r}}$ est chaotique : du point de vue des trajectoires individuelles, le couplage ne parvient donc pas à structurer le système.

Le «désordre» à l'œuvre dans le réseau peut être quantifié par la mesure des exposants de Lyapunov associés aux trajectoires des configurations $\mathbf{X}^t$ dans l'espace des phases : un exposant de Lyapunov positif correspond à une direction dans l'espace des phases selon laquelle deux trajectoires voisines s'écartent l'une de l'autre en moyenne. Dans les réseaux d'itérations couplées, le nombre de ces exposants est une quantité extensive, ce qui signifie que les trajectoires de deux configurations voisines divergent en moyenne selon un nombre extensif de directions dans l'espace des phases. Bien que cette propriété soit difficilement utilisable en tant que telle, elle indique assurément que ces systèmes présentent un chaos extrêmement fort.

Comportement macroscopique

La complexité de la trajectoire d'une configuration $\mathbf{X}^t$ dans l'espace des phases ne permet pas une description complète et incite alors à recourir à des méthodes statistiques. On en vient donc à mesurer la moyenne spatiale instantanée, $M^t = \langle \mathbf{X}_{\vec{r}} \rangle^t$, ou bien l'histogramme p^t des valeurs prises en chaque site

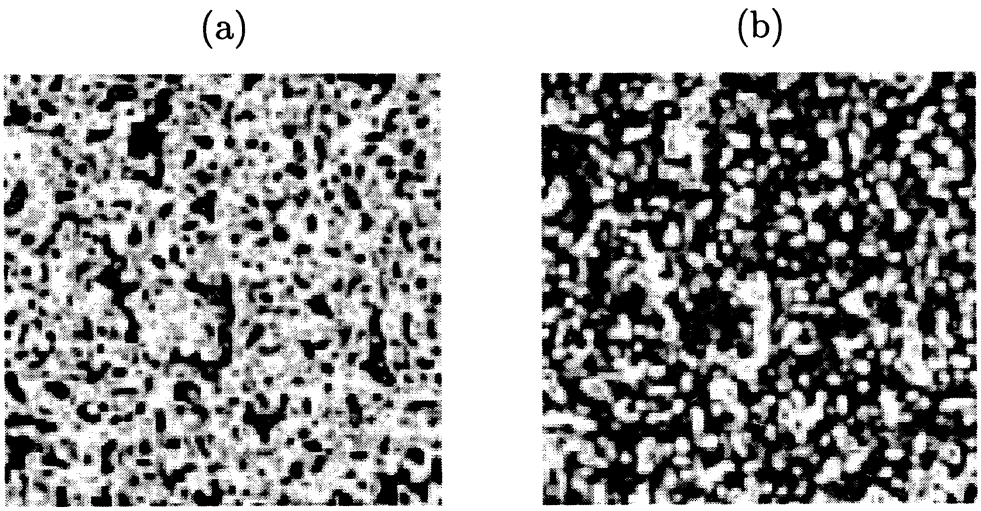

FIG. 1 – *(a-b) Deux images successives d'un réseau tridimensionnel d'applications logistiques fortement couplées ($g = 1/7$) et de coté $L = 128$. On voit bien que les sites ne sont pas synchronisés mais le système a pourtant une évolution globale de période 2 dans la mesure où toutes les images aux temps pairs (resp. impairs) ressemblent à (a) (resp. (b)). Cette évolution périodique n'existe cependant qu'à un niveau macroscopique : les petites structures (de l'ordre de quelques sites) qui subsistent d'un pas de temps à l'autre sont, en fait, en perpétuelle évolution. Elles ne constituent en aucun cas des structures gelées en espace, et il y a une perte de corrélation pour des configurations séparées d'un temps plus long.*

dans la configuration $\mathbf{X}^t$. Cette fonction de distribution est un quantificateur assez riche de l'état du système puisqu'elle permet par exemple de calculer tous les moments «locaux» c'est à dire ne faisant intervenir qu'un site (dont M^t est un cas particulier) : ce sont les quantités de la forme $\langle f(\mathbf{X}_{\vec{r}})\rangle^t$ pour toute fonction f. D'autres quantités en dérivent, comme la variance de p^t qui mesure l'étalement des valeurs prises par les variables locales sur tout l'espace, ou plus généralement tous les cumulants.

La caractérisation statistique de ces systèmes sur réseau ne peut cependant se suffire de quantificateurs locaux. La structure spatiale qui s'y établie est souvent évaluée par la mesure de la fonction de corrélation spatiale, $C(\vec{x}) = \langle \mathbf{X}_{\vec{r}} \mathbf{X}_{\vec{r}+\vec{x}} \rangle_c$, mais ce sont en fait toutes les fonctions de distribution des variables du réseau qu'il faudrait pouvoir prendre en compte, avec leurs moments ou leurs cumulants.

Nous nous intéresserons au *comportement collectif* de ces systèmes, c'est à dire à l'évolution des quantificateurs macroscopiques associée à la dynamique

sous-jacente d'une configuration dans l'espace des phases.

Couplage nul

Penchons-nous un instant sur le cas d'un système découplé. Puisque le couplage est nul, les aspects spatiaux disparaissent, et chaque variable locale est simplement itérée par $\mathbf{X}_{\vec{r}}^{t+1} = S_\mu(\mathbf{X}_{\vec{r}}^t)$. Le système se réduit alors à une collection de variables indépendantes qui évoluent par S_μ, et la dynamique de la distribution instantanée de ces variables est régie par l'opérateur de Perron-Frobenius [18]. Par exemple, dans le cas de l'application circonflexe ($\varepsilon = 0$), et pour $\mu = 2$, la dynamique de p^t ainsi définie admet la distribution uniforme sur l'intervalle I pour unique point fixe stable. Tous les exposants de Lyapunov sont alors égaux à l'exposant $\lambda_\mu > 0$, associé à l'itération locale chaotique S_μ, et le nombre d'exposants positifs est donc égal au nombre de sites. Nous reviendrons ultérieurement sur ce cas ainsi que sur celui des systèmes faiblement couplés qui lui ressemble.

Limite de couplage fort

Les comportements les plus remarquables apparaissent en effet quand le couplage est fort, et en particulier pour le couplage dit «démocratique» pour lequel des poids égaux sont attribués à tous les sites d'un voisinage dans la définition (3) de l'opérateur de couplage, soit $g = 1/(2d+1)$ [5]. Remarquons tout de suite que, dans ce cas, si l'itération locale est périodique ($\mu < \mu_\infty$), le couplage parvient alors à synchroniser tous les sites et leur valeur commune est gouvernée par la dynamique locale : $M^{t+1} = S_\mu(M^t)$; cette synchronisation n'est pas évidente *a priori* et nous y reviendrons. Nous nous concentrerons cependant sur le cas où les itérations locales sont chaotiques et fortement couplées.

Considérons un réseau d'applications logistiques couplées démocratiquement en dimension 3, de coté $L = 128$ et avec $\mu = 2$. La condition initiale du système est définie par un tirage aléatoire de chaque variable locale uniformément sur l'intervalle I. Après un transitoire relativement court (quelques dizaines de pas de temps), la dynamique de la distribution p^t rejoint une évolution périodique, de période 2, illustrée fig. 2.

L'ensemble des régimes asymptotiques ($t \to \infty$) atteints quand μ varie est représenté par le diagramme de bifurcations de la moyenne spatiale M^t (voir fig. 2). Quand μ décroît vers μ_∞, on observe les premiers pas d'une cascade

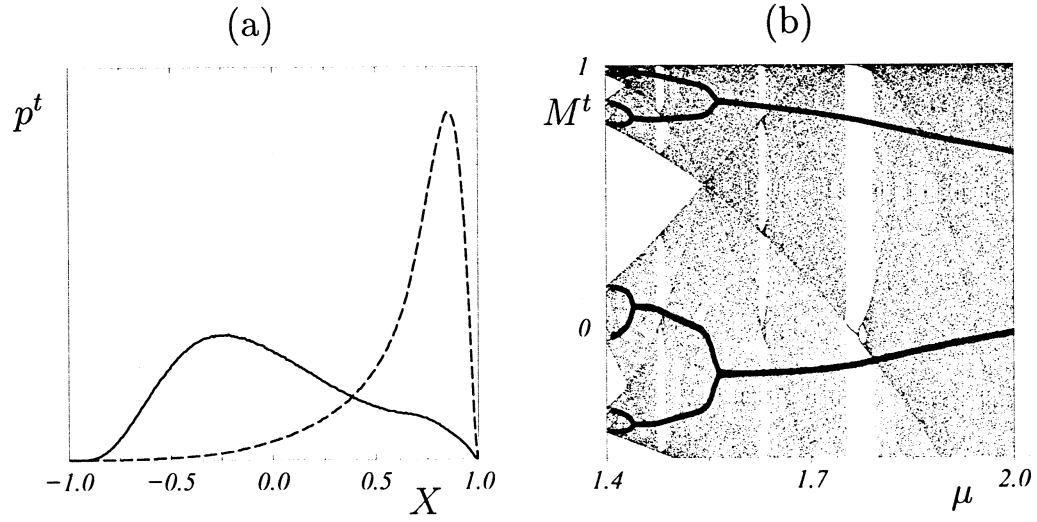

FIG. 2 – *Réseau tridimensionnel d'applications logistiques fortement couplées ($g = 0.2$) de coté $L = 128$: (a) Dynamique de période 2 de la distribution instantanée p^t au point $\mu = 2$. (b) Diagramme de bifurcation de la moyenne spatiale M^t en fonction du paramètre de non-linéarité, μ.*

sous-harmonique directe de comportements macroscopiques, mais les régimes de très grande périodicité sont difficilement accessibles numériquement.

Ces comportements persistent dans la limite thermodynamique ($L \to \infty$) où la distribution p^t converge vers une fonction régulière, et l'évolution de ces grandeurs macroscopiques ne dépend pas de la configuration initiale choisie. La fonction de corrélation converge elle aussi vers un régime asymptotique de même périodicité que les quantités macroscopiques à un site et ce sont en fait toutes les moyennes spatiales qui suivent la même évolution. C'est donc le *macro-état* du système, c'est à dire l'opérateur $\langle . \rangle^t$, moyenne spatiale au temps t, qui évolue de façon autonome.

L'observation de telles dynamiques macroscopiques est étonnante : le fort chaos local semble décorréler les variables du réseau, et pourtant l'observation de comportements périodiques indique l'existence d'une «synchronicité» entre toutes les variables locales. Cette synchronicité correspond à la mise en cohérence de tous les sites d'un réseau à un même instant : c'est un *ordre à longue distance*. C'est particulièrement flagrant quand l'itération locale n'a qu'une bande et que le comportement collectif est périodique comme c'est le cas fig. 2 pour $\mu = 2$. Il est remarquable que la dynamique microscopique chaotique des réseaux d'itérations couplées induise une évolution autonome des moyennes spatiales et ce phénomène à donc été appelé *comportement collectif non tri-*

vial [5], mais nous reviendrons sur cette terminologie pour lui donner un sens précis.

Notons pour finir que ces comportements collectifs non triviaux sont robustes, ils sont facilement observés pour toutes sortes d'itérations locales chaotiques, de couplages, et persistent même si la dynamique déterministe est perturbée par un bruit. Des dynamiques macroscopiques plus «exotiques» peuvent être observés en augmentant la dimension de l'espace : ainsi, en dimension $d = 4$, deux comportements macroscopiques (de période 2 et 4) coexistent à certaines valeurs de μ, et le système présente de l'hystérésis ; en dimension $d = 5$, des dynamiques macroscopiques quasi-périodiques peuvent être observées.

Il s'agit donc là d'un phénomène générique dont l'ingrédient essentiel semble être la mise à jour synchrone : tel que le système est défini, le temps discret n'admet pas de limite continue comme c'est le cas pour une dynamique de type Monte-Carlo. D'une certaine façon, la mise à jour synchrone revient à imposer que l'échelle de temps de la dynamique macroscopique soit la même que celle de la dynamique microscopique.

Approches mathématiques

L'étude des réseaux d'itérations couplées s'est principalement tournée vers les régimes de faible couplage. Une approche initiée par Bunimovich et Sinai [3] consiste à étendre aux réseaux d'itérations couplées le formalisme thermodynamique de Ruelle, Bowen et Sinai [28], tandis que les travaux de Keller et Künzle [16] traitent de l'opérateur de Perron-Frobenius associé à la dynamique d'une configuration dans l'espace des phases. Dans ces deux cas, la question porte en général sur l'existence et l'unicité d'une mesure absolument continue pour le système dynamique ainsi défini, ce qui correspond à un point fixe de la dynamique macroscopique.

L'étude de l'opérateur de Perron-Frobenius permet cependant de rendre compte de dynamiques collectives périodiques. En effet, dans le cas d'un ensemble de variables indépendantes itérées par S_μ, une propriété des opérateurs markoviens, la *périodicité asymptotique* [17, 18], appliquée à l'opérateur de Perron-Frobenius associé à S_μ permet de caractériser le chaos par bandes [29, 27]. Ceci se transpose dans le cas d'un réseau à la dynamique d'un ensemble de configurations. Certaines études en viennent alors à réduire le comportement collectif à la notion de périodicité asymptotique de la dyna-

mique de ces ensembles, ce qui revient à l'existence de bandes dans l'espace des phases [21, 20]. Cette périodicité asymptotique peut être démontrée pour certains systèmes, mais les techniques mises en œuvre ne permettent pas d'en quantifier la période, c'est à dire le nombre de bandes.

La caractérisation du comportement collectif par des dynamiques d'ensemble amène à deux remarques. D'une part sur la validité-même de cette description : la représentation du comportement d'une configuration par les propriétés d'un ensemble exige un saut conceptuel qui est loin d'être évident. Même dans le cas des systèmes à l'équilibre où l'introduction des mesures de Gibbs s'est révélée des plus profitable, l'interprétation n'en reste pas moins discutable et discutée [19, 25, 26]. De plus, dans notre cas, cette représentation semble inconsistante avec l'observation de dynamiques périodiques qui indique une brisure d'ergodicité, c'est à dire une perte de l'équivalence statistique des différents états atteints par la trajectoire d'une configuration.

Un argument en faveur de cette approche consiste à remarquer que quand la dynamique des observables macroscopiques est périodique, la trajectoire d'une configuration doit parcourir des sous-ensembles (probablement disjoints) de l'espace des phases. C'est certain. Mais la réciproque repose sur une hypothèse d'équivalence de toutes les configurations sur chacune de ces «bandes» et cette hypothèse est bien loin d'être évidente. En effet, en supposant que la périodicité asymptotique soit prouvée, et même, que sa période puisse être déterminée, — toute configuration parcourt des sous-ensembles disjoints de l'espace des phases — il reste encore à montrer que les éléments de chacun de ces sous-ensembles partagent les mêmes observables macroscopiques. Pour en revenir à l'analogie avec les bandes d'une itération simple, remarquons bien que l'existence de deux bandes, par exemple, ne renseigne pas sur les valeurs prises par X^t qui décrit une trajectoire chaotique. Comment donc la périodicité asymptotique du système dans l'espace des phases renseignerait-elle mieux sur la dynamique des observables macroscopiques ?

Nous développerons dans ce mémoire une autre approche, qui prend le contre-pied des méthodes canoniques pour lesquelles l'objet considéré est trop naturellement un ensemble de configurations, sans nécessairement s'interroger sur la signification d'une telle représentation. Il s'agira donc, non d'étudier la dynamique d'un ensemble, mais bien de caractériser l'évolution des grandeurs macroscopiques correspondant à la trajectoire *typique* d'une configuration dans l'espace des phases.

Plan du mémoire

Le premier chapitre de ce mémoire est consacré à la définition précise du comportement collectif non trivial, et à l'étude qualitative et quantitative des transitions qui interviennent quand le paramètre de couplage augmente. Au début du chapitre, je propose une exploration des mécanismes qui permettent que s'instaure une cohérence spatiale dans tout le réseau, puis je présente dans une lettre, une étude plus particulière des régimes transitoires pendant lesquels s'établit l'ordre à longue distance dans les systèmes fortement couplés ; cette approche permet alors de quantifier le seuil de couplage au delà duquel l'attracteur macroscopique est unique.

Le second chapitre aborde la question de la dépendance des comportements collectifs en fonction du paramètre de non-linéarité. Je montre que la dynamique du réseau est gouvernée par un groupe de renormalisation, de sorte que les comportements sélectionnés à grand couplage récupèrent les propriétés d'autosimilarité de l'itération locale, avec l'ajout d'une constante d'universalité liée à la mise à jour synchrone.

Avec le troisième chapitre, j'aborde la question de la modélisation de ces comportements collectifs à partir des équations microscopiques. Je montre comment la dynamique des quantités macroscopiques «en suivant» la trajectoire d'une configuration est régie par une hiérarchie d'équations agissant sur les fonctions de distribution des variables locales. Une méthode d'approximation systématique est présentée, qui permet d'extraire de cette hiérarchie un système fini d'équations gouvernant l'évolution des moments du réseau.

Le quatrième chapitre se tourne vers des approches de type «champ moyen», qui visent à isoler les ingrédients physiques minimaux nécessaires à l'observation de ces dynamiques. Je définis en deux étapes un modèle d'évolution pour la distribution instantanée p^t, qui couple un opérateur de Perron-Frobenius non linéaire à la dynamique des corrélations à courte portée.

Chapitre 1

Comportement collectif non trivial

Dans ce chapitre, je m'attacherai à montrer ce que recouvre le terme *comportement collectif non trivial*, en quoi le phénomène qu'il désigne diffère profondément des régimes de couplages faibles, et de quelle nature sont les transitions qui permettent de passer d'un système découplé à un système cohérent dans toute son étendue spatiale.

1.1 Nature du comportement collectif non trivial

Afin de mettre en évidence les spécificités des comportements collectifs observés pour les grandes valeurs de g, il est intéressant de montrer par contraste ce que l'on obtient en l'absence de couplage. Je commencerais par rappeler les propriétés des itérations unimodales avant d'aborder la question de la dynamique d'un ensemble de variables non couplées et sa description par l'opérateur de Perron-Frobenius.

1.1.1 Itérations de l'intervalle

Précisons la structure des régimes asymptotiques atteints par le système dynamique défini par une famille à un paramètre d'applications unimodales. La variable $X^t \in I = [-1, 1]$ évolue selon $X^{t+1} = S_\mu(X^t)$, où S_μ est de la forme

$$S_\mu(X) = 1 - \mu|X|^{1+\varepsilon} , \quad \text{avec } \mu \in [0, 2] , \quad \text{et } \varepsilon \geq 0 . \tag{1.1}$$

Cette expression recouvre en particulier les cas de l'application logistique ($\varepsilon = 1$) et de l'application circonflexe ($\varepsilon = 0$), mais toutes ces itérations unimodales présentent des comportements semblables quand μ varie.

Par exemple, le diagramme de bifurcation de l'application logistique est présenté fig. 1.1. Ces systèmes admettent un point fixe $X^*_\mu > 0$ qui est stable pour de faibles valeurs de μ (jusqu'au point μ_1), puis une cascade sous-harmonique (directe) de bifurcations : quand μ augmente, le régime de période 2^{n-1} se déstabilise au point μ_n où le système bifurque vers un comportement de période 2^n. Ces points μ_n s'accumulent vers une limite, notée μ_∞, au delà de laquelle le système devient chaotique, et qui vaut $\mu_\infty = 1.401\ldots$ pour l'application logistique. En ce qui concerne l'application circonflexe, la situation est identique, mais particulièrement dégénérée puisque le point fixe est stable jusqu'à $\mu_\infty = 1$ ce qui revient à dire que tous les points de bifurcations μ_n sont égaux à μ_∞.

À l'autre extrémité du diagramme de bifurcations, $\mu = 2$, la variable X^t parcours tout l'intervalle I dans son évolution. Pour toute valeur de μ, nous désignerons par I_μ l'intervalle $[1-\mu, 1] = S_\mu(I)$ qui est laissé invariant par S_μ et où se déroule la dynamique. Quand μ décroît, le système présente une cascade sous-harmonique (inverse) de régimes par bandes. Pour $\mu \in [\mu_\infty, \bar{\mu}_n]$, 2^n bandes peuvent être isolées : ce sont des intervalles disjoints deux à deux sur lesquels S_μ opère une permutation circulaire. En un certain sens, c'est alors la dynamique des intervalles qui est périodique de période 2^n. Nous noterons $I^{n,\sigma}_\mu$ ces bandes, avec la convention suivante : $I^{n,0}_\mu \ni 0$ est la bande «centrale», et l'indice $\sigma \in \{0, \cdots, 2^n - 1\}$ est défini par l'action de S_μ :

$$I^{n,\sigma}_\mu = S^\sigma_\mu \left(I^{n,0}_\mu \right) ,$$

de sorte que la permutation induite par S_μ sur les bandes se résume à l'incrémentation des indices, $\sigma \to (\sigma + 1)[2^n]$ (modulo 2^n). Dès que $\mu \leq \bar{\mu}_n$, presque toute condition initiale rejoint une trajectoire asymptotique chaotique qui parcourt périodiquement les bandes : nous dirons que ce sont des composantes ergodiques de S_μ. Toutes ces trajectoires parcourent les bandes dans l'ordre des σ croissant (modulo 2^n), mais avec une phase temporelle qui dépend de la condition initiale X^0 choisie.

Notons enfin que pour tout entier n, il existe un seuil $\bar{\mu}_n > \mu_\infty$ en deça duquel 2^n composantes ergodiques peuvent être isolées. Les points de jonction (ou de séparation) des bandes, $\bar{\mu}_n$, s'accumulent eux aussi vers μ_∞, et de façon semblable aux points μ_n [9, 6].

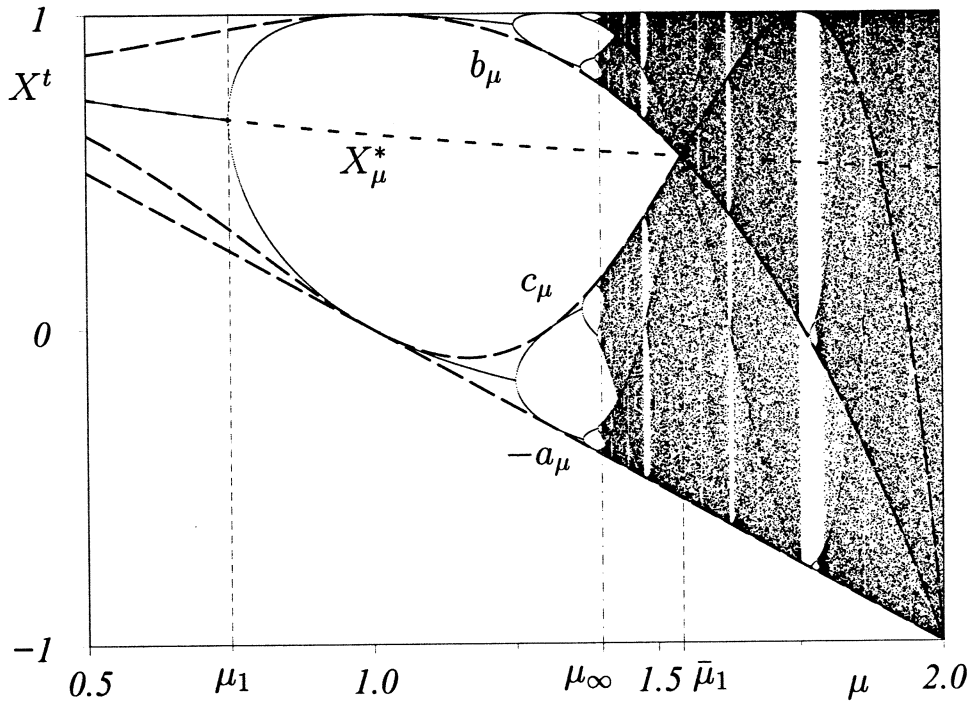

FIG. 1.1 – *Diagramme de bifurcations de l'application logistique sur l'intervalle* $\mu \in [1,2]$ *: le point fixe* X^*_μ *est indiqué en trait pointillé court et les courbes* $-a_\mu = 1 - \mu = S_\mu(1)$, $b_\mu = S_\mu(-a_\mu)$ *et* $c_\mu = S_\mu(b_\mu)$ *sont dessinées en traits pointillés long. Le point* $\bar{\mu}_1$ *où deux bandes se séparent correspond à l'intersection des courbes* b_μ *et* c_μ *(qui donc coïncident alors avec* X^*_μ*) : pour tout* $\mu \in [1, \bar{\mu}_1]$, $b_\mu \geq c_\mu$ *et* $a_\mu \geq c_\mu$, *de sorte que les intervalles* $[-a_\mu, c_\mu]$ *et* $[b_\mu, 1]$ *sont échangés par* S_μ*. Notons que ceci est valable de part et d'autre du point* μ_∞ *et pas seulement pour les régimes chaotiques (*$\mu > \mu_\infty$*) ou quand il y a exactement deux bandes (*$\mu \in [\bar{\mu}_2, \bar{\mu}_1]$*).*

Mentionnons que le diagramme de bifurcations de l'application logistique présente aussi de *fenêtres de périodicité*, c'est à dire des régions du paramètre μ au delà de μ_∞ où l'attracteur est tout de même périodique. Ces comportements sont «accidentels» dans la mesure ou, par exemple, ils disparaissent quand la dynamique est perturbée par l'adjonction d'un bruit. De ce fait ils n'ont pas d'influence sur les dynamiques couplées qui nous intéressent pour lesquelles le couplage avec les voisins perturbe fortement la dynamique locale, suffisamment en tout cas pour gommer de tels détails.

En effet, à cause de l'application de l'opérateur de couplage, les variables locales ne convergent jamais vraiment vers l'attracteur de S_μ et n'ont donc

pas accès à sa structure fine (fenêtres de périodicité, ergodicité, pics, ...). Par conséquent, l'ergodicité de l'itération locale n'a pas besoin d'être avérée, et la description grossière de S_μ par la dynamique des intervalles nous suffira : les bandes seront toujours considérées comme les composantes ergodiques de la dynamique d'une variable scalaire.

1.1.2 Périodicité asymptotique

Venons en à la dynamique d'un ensemble de variables scalaires non couplées, évoluant chacune par l'itération S_μ. Cet ensemble de variables est décrit par la distribution p^t de leur valeurs, et l'action de S_μ se traduit sur p^t par la relation

$$p^{t+1}(X) = \int p^t(Y)\delta(X - S_\mu(Y))dY \ , \quad \text{soit } p^{t+1} = \mathcal{P}_{S_\mu}(p^t) \ ,$$

qui définit l'opérateur de Perron-Frobenius associé à l'itération S_μ. Quand S_μ n'a qu'une bande, la distribution p^t converge vers un point fixe, et en particulier pour l'application circonflexe à $\mu = 2$ ce point fixe est simplement la distribution uniforme sur I.

Dès que S_μ a plusieurs bandes on peut observer des dynamiques collectives périodiques. Un tel comportement asymptotique de période 2 est présenté fig. 1.2 : la valeur de μ est choisie afin de s'assurer qu'il y a deux bandes sur lesquelles les sites puissent se répartir. Asymptotiquement p^t peut s'écrire sous la forme

$$p^t = (1 - \rho^t)p^0_{S_\mu} + \rho^t p^1_{S_\mu} \ . \tag{1.2}$$

où les distributions $p^0_{S_\mu}$ et $p^1_{S_\mu}$ sont échangées par $\mathcal{P}_{S_\mu}$, et donc $\rho^{t+1} = 1 - \rho^t$. La convergence en norme des distributions p^t vers une dynamique de ce type est appelée *périodicité asymptotique* [18].

En prenant une condition initiale où toutes les variables sont dans la même bande, on obtient un régime asymptotique dans lequel p^t oscille entre les deux *états purs* $p^0_{S_\mu}$ et $p^1_{S_\mu}$, tandis que ρ^t prend les deux valeurs extrêmes 0 et 1. En changeant la proportion initiale de variables dans l'une et l'autre bande, on peut générer toutes les dynamiques périodiques d'amplitude $0 \leq |1 - 2\rho^t| \leq 1$ avec toujours les mêmes états purs $p^0_{S_\mu}$ et $p^1_{S_\mu}$.

Remarquons que les deux distributions $p^0_{S_\mu}$ et $p^1_{S_\mu}$ sont les deux points atteints par la même dynamique de période 2. Nous les désignons cependant par le terme d'«états» pour insister sur l'existence de deux phases temporelles correspondant aux deux composantes ergodiques d'un même attracteur.

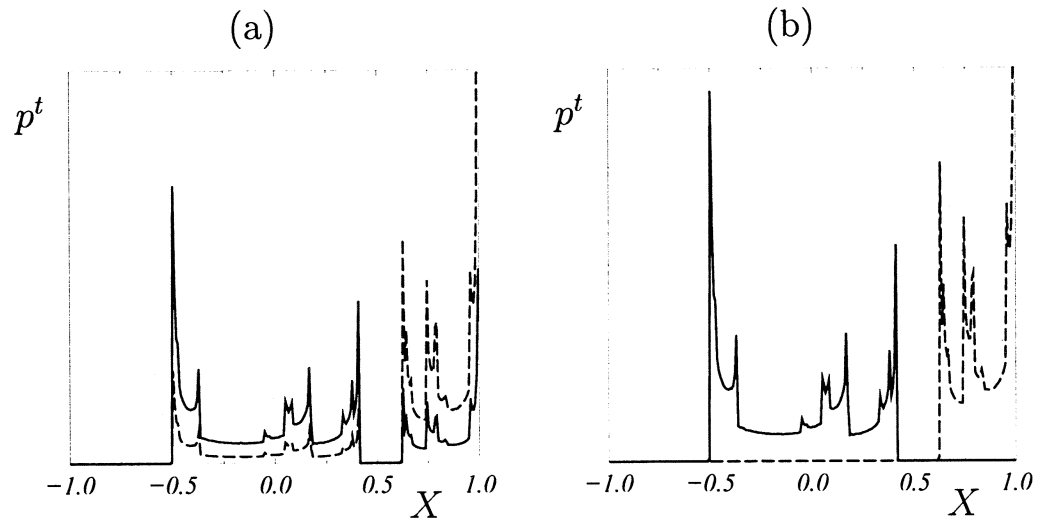

FIG. 1.2 – *États d'un ensemble de variables non couplées, itérées par l'application logistique dans le régime à deux bandes ($\mu = 1.5$). Les temps pairs et impairs sont représentés en traits continus et pointillés respectivement : (a) avec $\rho^0 = 0.75$ il y a un mélange des deux phases, (b) avec $\rho^0 = 1$ la dynamique de p^t décrit les deux états purs.*

Cette construction se généralise immédiatement au cas de périodes plus élevées : Une solution périodique extrémale pour $\mathcal{P}_{S_\mu}$ définit des états purs, et la linéarité de l'opérateur assure que tout élément de l'ensemble convexe généré par les états purs intervient dans une dynamique périodique. Il y a donc, en l'absence de couplage, un continuum d'attracteurs macroscopiques.

Remarquons enfin que cette situation présente une certaine analogie avec les systèmes conservatifs pour lesquels il y a un continuum de trajectoires classées par leur niveau d'énergie. Ici, les diverses amplitudes de la dynamique de ρ^t définissent des «niveaux de mélange» entre les états purs. Chaque variable décrit les bandes avec une phase temporelle dépendant de sa condition initiale, et le nombre de variables dans le bassin d'attraction d'une composante ergodique de S_μ est une quantité conservée du système.

Bien sûr les variables locales ont des trajectoires individuelles chaotiques, et au fond, la situation peut paraître extrêmement similaire aux dynamiques macroscopiques observées à fort couplage, telles que celles présentées fig. 2 : nous retrouvons bien les deux ingrédients, chaos local et comportement collectif périodique. Il est donc tentant de chercher à étendre ces résultats à la dynamique collective d'un système couplé, ce qui conduit à considérer l'évolution d'une

mesure, cette fois-ci, sur l'espace des phases. En l'absence de couplage, cette mesure est simplement le produit tensoriel

$$\mathbf{p}^t = \bigotimes_{\mathcal{L}} p^t = \prod_{\vec{r}\in\mathcal{L}} p^t(\mathbf{X}_{\vec{r}})$$

des fonctions de distribution locales. Dans ce cas simple, la dynamique de cette mesure est strictement équivalente à la dynamique de p^t. Quand on applique un couplage faible, l'état du système peut être encore représenté par une mesure d'ensemble, comme dans la physique des systèmes à l'équilibre.Cette mesure évolue par un opérateur de Perron-Frobenius qui agit sur les mesures de l'espace des phases, et non plus sur les mesures de l'intervalle. La fonction p^t est alors interprétée comme étant une distribution marginale associée à cette mesure : si la périodicité asymptotique de ce système peut être démontrée, il y a, là encore, un ensemble convexe d'états macroscopiques.

1.1.3 Origine du comportement collectif non trivial

Attracteur macroscopique

Dans le cas d'un système fortement couplé un tel continuum d'attracteurs macroscopiques n'est pas observé : le même comportement collectif est obtenu quel que soit la distribution $p^{t=0}$ selon laquelle sont tirées les conditions initiales. Hormis la forme des distributions, la différence essentielle entre le régime asymptotiquement périodique présenté fig. 1.2 et la dynamique fortement couplée de la fig. 2, c'est l'existence, pour le système non couplé, de deux composantes connexes au support de la distribution p^t : ces deux composantes sont le signe que cette distribution est une combinaison d'états. Au contraire, le système fortement couplé sélectionne en quelque sorte les états collectifs «purs». Cette propriété s'oppose donc au comportement linéaire de distributions itérées par l'opérateur de Perron-Frobenius, et indique *a contrario* le caractère fortement non linéaire de la dynamique macroscopique à grand couplage. Nous verrons au chapitre 3 et surtout au chapitre 4 que c'est paradoxalement l'opérateur de couplage qui détermine la partie non linéaire de la dynamique des macro-états. Nous verrons aussi que les systèmes faiblement couplés s'apparentent au système non couplé : une hypothèse de faible couplage est donc analogue à une non-linéarité faible de la dynamique macroscopique. Ce chapitre est concerné par l'origine de cette sélection d'états extrémaux dans les systèmes fortement couplés, et par la détermination de conditions sur

le couplage qui, éventuellement, pourraient assurer que seul ces états soient atteints.

Il est important de bien faire la différence entre la trajectoire d'une configuration et la dynamique collective induite par cette trajectoire. Du point vue microcanonique, des conditions initiales génériques sont définies par la mesure de Lebesgue sur $\mathbf{I}$ qui est la mesure produit $\otimes U_I$ des distributions uniformes sur l'intervalle I. En choisissant une condition initiale $\mathbf{X}^{t=0}$ selon cette mesure, on obtient une configuration «typique», mais on impose du même coup $p^0 = U_I$: toutes ces configurations déterminent la même condition initiale macroscopique et la même évolution pour leurs observables moyennées en espace. Le choix d'une condition initiale (microcanonique) où les variables locales ne sont pas distribuées selon U_I, correspond à une autre condition initiale macroscopique. Même si l'ensemble des configurations qui la réalise est de mesure nulle dans l'espace des phases, ces états n'en sont pas moins parfaitement observables et déterminent autant de trajectoires macroscopiques.

Dans le cas des systèmes non couplés ou faiblement couplés, on trouve un continuum de régimes macroscopiques en faisant ainsi varier les conditions initiales. Le comportement collectif non trivial diffère de cette situation par le fait que l'ensemble des *attracteurs macroscopiques* est discret. Il est d'ailleurs souvent unique, comme dans le cas des réseaux d'itérations couplées en dimension 2 ou 3, mais il peut aussi y avoir coexistence d'attracteurs macroscopiques et présence d'hystérésis, comme en dimension 4.

États collectifs purs

Il se produit donc à fort couplage une sélection d'un comportement collectif «pur». Cependant, la comparaison entre les régimes observés pour différents g n'est pas aisée, car on ne peut pas considérer le couplage comme une simple interaction entre des états purs indépendants du couplage. Par exemple, le comportement collectif présenté fig. 2 est obtenu pour $\mu = 2$, alors que la dynamique de p^t par l'opérateur de Perron-Frobenius «local» admet la distribution uniforme sur I pour point fixe : le système n'a qu'un état pur à $g = 0$, et deux états purs à $g = 0.2$, dont un seul est sélectionné par la dynamique.

Une situation simple peut être isolée quand l'itération locale a deux bandes et que le comportement collectif est de période 2, ce qui est le cas des réseaux bidimensionnels à certaines valeurs de μ. On observe alors que, quel que soit g, le système a exactement deux états purs dont les supports sont les bandes

de S_μ. Ces état purs sont représentés fig. 1.3 pour différentes valeurs de g dans le cas d'applications logistiques couplées. Ils ont été obtenus en imposant que toutes les variables locales soient dans la même bande à $t = 0$. On observe une transition à de faibles valeurs de g au delà de laquelle les états purs sont quasiment indépendants de g. Nous verrons cependant un peu plus loin que, dans ce cas, des états asymptotiques où les deux états purs coexistent peuvent être observés jusqu'à des valeurs de g de l'ordre de 0.1. Il y a donc deux phénomènes concurrents et relativement indépendants quand g augmente : l'existence de certains états purs, et leur sélection spatiale par la mise en cohérence de tous les sites du réseau.

Croissance de domaines

Plusieurs images d'un réseau d'applications logistiques couplées sont présentées fig. 1.4. Les valeurs initiales des sites sont prises uniformément sur l'intervalle I, et le système évolue par la dynamique définie par les paramètres, $\mu = 1.5$, et $g = 0.2$. Dans ce cas, le système admet un comportement collectif pur de période 2, représenté fig. 1.3-(d), que les variables locales cherchent à rejoindre ; seulement, selon les fluctuations des conditions initiales à une échelle mésoscopiques, ces variables atteignent leur régime asymptotique par bandes avec l'une ou l'autre phase temporelle : ceci conduit alors à la formation d'amas correspondants aux deux composantes ergodiques de l'attracteur macroscopique.

Le système est, en quelque sorte, spontanément diphasique, les deux «phases» correspondant aux deux phases temporelles du comportement collectif pur. Le couplage induit d'abord la mise en place de la dynamique collective à un niveau mésoscopique, puis joue un second rôle, en instaurant une compétition spatiale entre les deux états purs ; il y a alors un processus croissance de domaines qui démarre. Cependant, à cause de l'asymétrie des bandes, l'une des deux phases est vite prépondérante et absorbe l'autre. À l'issue de ce processus, tous les sites sont dans la même bande au même instant, et la dynamique collective parcourt périodiquement les états purs. C'est l'élimination de la phase minoritaire qui est responsable de l'unicité de l'attracteur macroscopique observé à grand couplage, c'est à dire du comportement collectif non trivial.

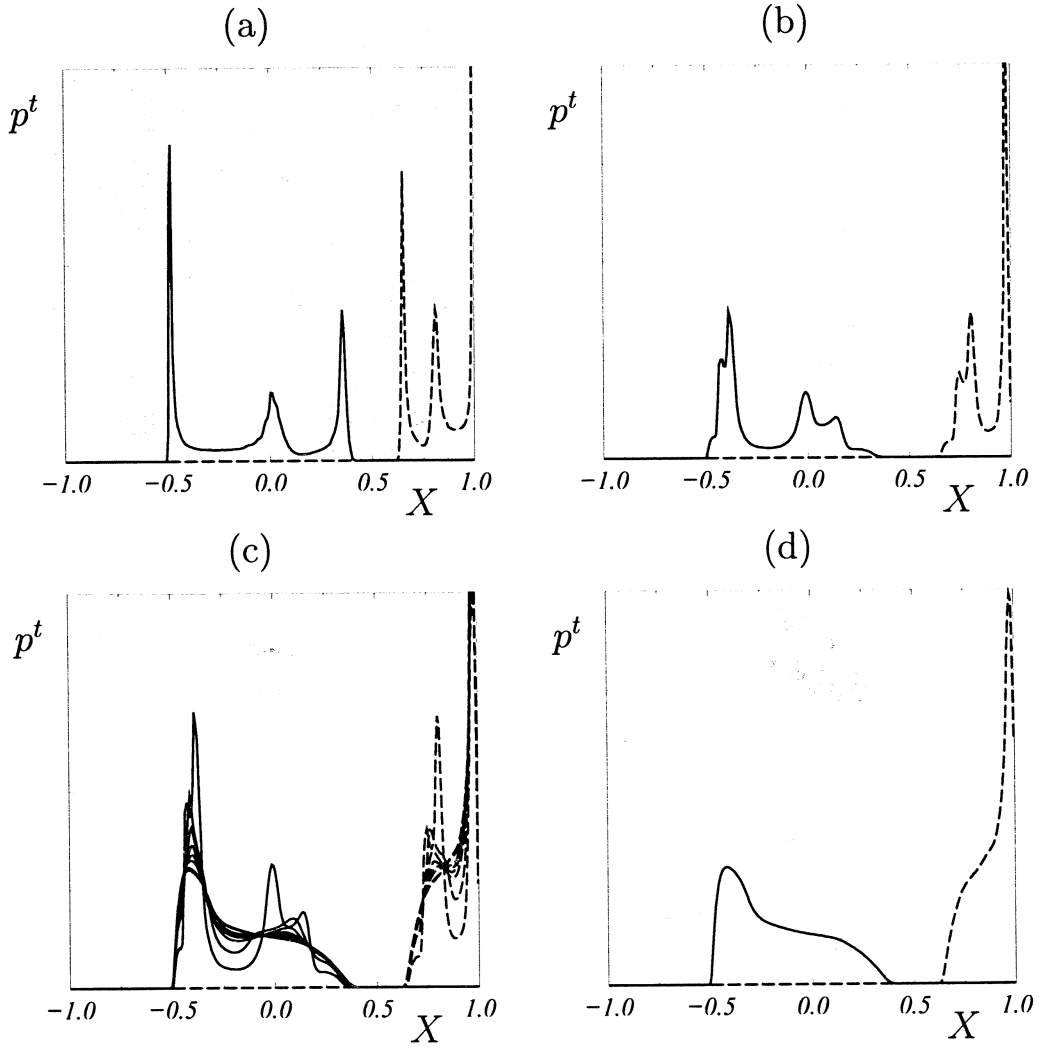

FIG. 1.3 – *États purs d'un réseau bidimensionnel d'applications logistiques couplées pour* $\mu = 1.5$. *Ces états sont obtenus en imposant que toutes les variables locales soient dans la même bande à* $t = 0$. *Les temps pairs et impairs sont représentés en trait continus et pointillés (resp.) : (a) pour* $g = 0.003$, *(b) pour* $g = 0.05$, *(c) pour plusieurs valeurs du couplage de* $g = 0.05$ *à* $g = 0.2$, *et (d) pour* $g = 0.2$.

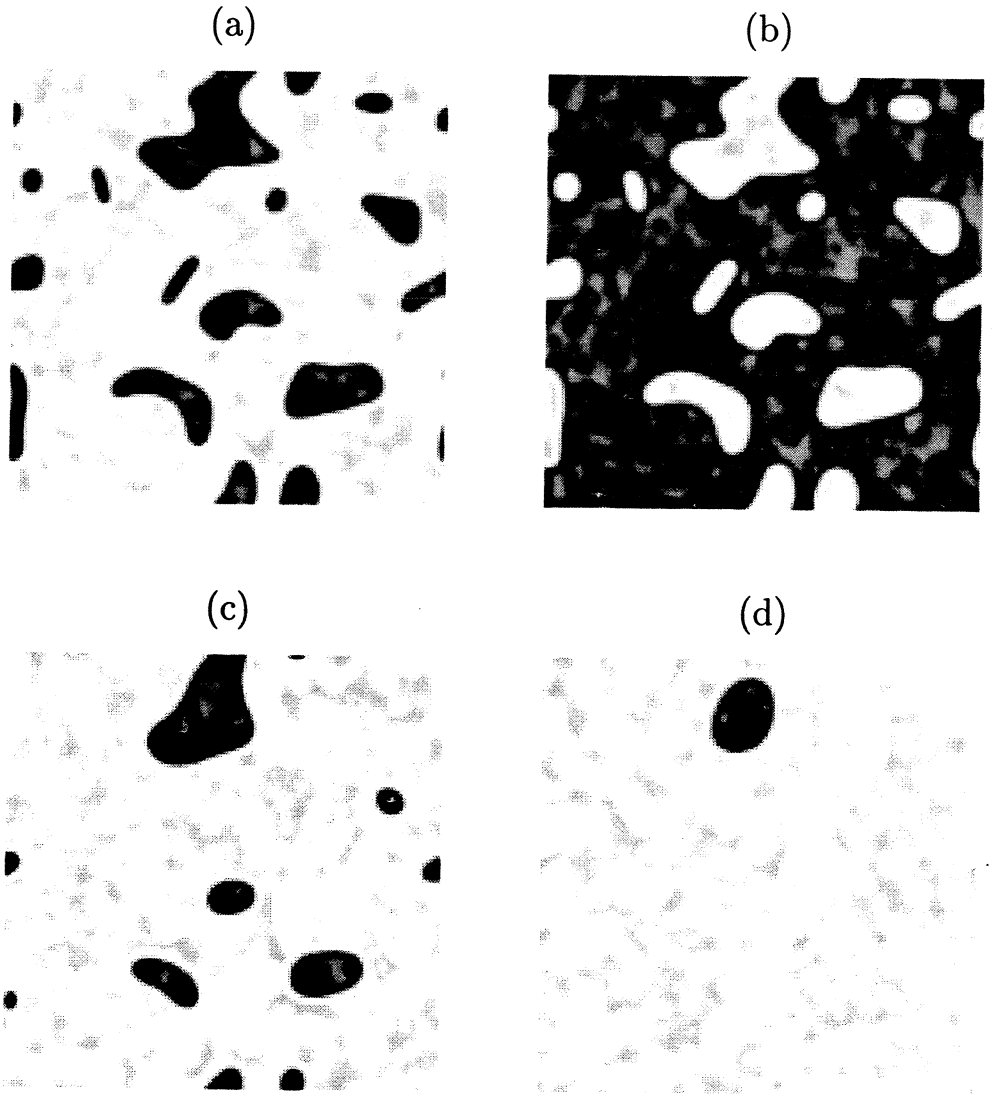

FIG. 1.4 – *Régime transitoire d'un réseau bidimensionnel d'applications logistiques couplées, de coté* $L = 128$, *pour* $\mu = 1.5$ *et* $g = 0.2$, *avec conditions aux limites périodiques. Pour définir la condition initiale, les variables locales sont indépendantes et distribuées uniformément sur* $[-1, 1]$. *(a-b) Deux instants successifs (*$t = 100$ *et* 101*) : les amas qui se forment suivent un comportement collectif pur, et la phase* σ *(en clair) est déjà nettement majoritaire. Les amas minoritaires sont éliminés : (c)* 100 *pas de temps plus tard, (d) à* $t = 500$.

1.2 Synchronisation par bandes

Afin d'isoler le processus de sélection des états purs qui est au cœur de la notion de comportement collectif, nous considérons le cas où l'itération locale a plusieurs bandes. Nous avons en effet remarqué que, pour les systèmes découplés, le support de la distribution p^t porte alors sur les différentes bandes, tandis qu'à fort couplage, tous les sites finissent par être dans la même bande au même instant indépendamment des conditions initiales macroscopiques. D'autre part, nous avons aussi observé que la proportion de variables dans chaque composante ergodique de la dynamique est une quantité conservée à $g = 0$. Ça n'est plus vrai quand le couplage diffusif est appliqué, et d'une certaine façon, «dissipe» ces taux de mélange entre les bandes. De telles quantités sont donc susceptibles de caractériser la «synchronisation» des variables locales évitant l'écueil de la dépendance des états purs par rapport à g.

1.2.1 États par bandes

Définition

Supposons que $\mu \leq \bar{\mu}_n$ de sorte que l'itération locale possède 2^n bandes, qui sont notées $I_\mu^{n,\sigma}$. Si a un instant donné tous les sites de la configuration $\mathbf{X}^t$ prennent leurs valeurs sur une même bande (disons $I_\mu^{n,\sigma}$), leurs images par l'itération locale S_μ sont envoyées sur $I_\mu^{n,\sigma+1}$, et après application du couplage diffusif, tous les sites sont encore sur $I_\mu^{n,\sigma+1}$. Ceci permet de définir des bandes généralisées $\mathbf{I}_\mu^{n,\sigma} = (I_\mu^{n,\sigma})^{\mathcal{L}}$, dans l'espace des phases : ce sont des intervalles qui sont échangées par la dynamique $\mathbf{\Delta}_g \circ \mathbf{S}_\mu$ dès que $\mu \leq \bar{\mu}_n$. Si donc la trajectoire d'une configuration $\mathbf{X}^t$ aboutit jamais à l'une de ces bandes, elle continue de les parcourir périodiquement : nous dirons alors que le système est dans un *état par bande* d'ordre n.

Contrairement aux itérations simples de l'intervalle, rien n'indique évidemment qu'un état par bandes soit atteint à partir de toute ou presque toute condition initiale, et ça n'est d'ailleurs pas vrai quand le couplage est nul ou faible. C'est pourtant toujours le cas du comportement collectif non trivial, et nous désignerons par *synchronisation non triviale* la propriété qu'un état par bandes soit atteint pour presque toute condition initiale (macroscopique).

Dans ce cas simple, présenté fig. 1.3, la synchronisation par bandes est équivalente au comportement collectif non trivial. Cependant, la propriété que le système soit dans un état par bandes n'induit aucune hypothèse ni sur la

périodicité exacte de la dynamique macroscopique qui peut être n'importe quel multiple de 2^n, voire quasi-périodique, voire chaotique, ni sur le nombre d'états purs. Il s'agit seulement un affaiblissement de la notion de comportement collectif non trivial qui rend compte de la déstructuration du chaos par bandes par le couplage.

Discrétisation des variables locales

Partant de conditions initiales non corrélées en espace et distribuées uniformément sur l'intervalle I, et en l'absence de couplage ($g = 0$), chaque variable locale $\mathbf{X}_{\vec{r}}^t$ évolue indépendamment de toute autre selon une dynamique chaotique propre déterminée par sa valeur initiale. Si l'itération locale possède plusieurs bandes, les variables locales évoluent périodiquement sur ces bandes avec des phases indépendantes, et on peut leur aisément attribuer des «spins» $\sigma_{\vec{r}}^t$ selon les bandes qu'elles occupent à l'instant t.

Afin d'étudier de la convergence (ou non) de systèmes couplés vers des états par bandes, nous devons pouvoir décrire des situations où tous les sites ne sont pas toujours sur la même bande et où certains d'entre eux peuvent éventuellement prendre leurs valeurs *entre* les bandes ; la définition d'une variable de spin requiert alors un petit peu plus de soin. Cependant, la dynamique de chaque variable locale a lieu sur l'intervalle $I_\mu = S_\mu(I)$ dès le premier pas d'itération, et il suffit donc de définir une partition de I_μ. Plutôt que les bandes elle-mêmes, qui ne recouvrent pas I_μ, il convient alors de considérer les bassins d'attraction qui leur correspondent.

Nous nous intéresserons en particulier au cas où l'itération locale a deux bandes. Le paramètre de non-linéarité μ est inférieur à $\bar{\mu}_1$ et les deux bandes de S_μ sont $I_\mu^{1,0}$ et $I_\mu^{1,1}$. Le point de séparation entre les deux bassins associés aux deux phases temporelles de la dynamique par bandes est bien sûr le point fixe instable $X_\mu^* > 0$ de S_μ : il n'y a pas d'inconvénient à le soustraire de I_μ, et ces bassins sont les intervalles

$$\tilde{I}_\mu^{1,0} = [1-\mu, X_\mu^*[\text{ et } \tilde{I}_\mu^{1,1} =]X_\mu^*, 1]\,,$$

qui, comme les bandes, sont échangés par S_μ. Ils ne constituent cependant pas des bandes dans la mesure où les valeurs trop proches de X_μ^* sont inaccessibles asymptotiquement. Tout sous-intervalle de la forme $[X_{min}, 1] \subset]X_\mu^*, 1]$ converge vers les bandes $I_\mu^{1,0}$ et $I_\mu^{1,1}$ quand il est itéré par S_μ, et pour cette raison, (presque) toute configuration du réseau dont les sites sont dans un même bassin, *e.g.* $\mathbf{X} \in \tilde{\mathbf{I}}_\mu^{1,1}$ converge vers un état par bandes quel que soit le couplage.

Avec cette définition, les spins sont «conservés» à couplage nul, c'est à dire que $\sigma_{\vec{r}}^{2t} = \sigma_{\vec{r}}^{0}$. Les états par bandes, au contraire, sont caractérisés par l'identité de tous les spins du réseau asymptotiquement, et dans ce cadre, la convergence vers un état par bande apparaît naturellement comme un phénomène de synchronisation des variables discrétisées $\sigma_{\vec{r}}^{t}$.

Notons enfin que la partition de I_μ en deux bassins, et l'existence d'une dynamique d'intervalles de période 2 est valable pour tout $\mu \in [\mu_1, \bar{\mu}_1]$ et pas seulement quand S_μ a exactement deux bandes, ou quand $\mu > \mu_\infty$. Si par exemple $\mu \in [\bar{\mu}_3, \bar{\mu}_2]$, de sorte qu'il y a quatre bandes, la question de la convergence vers un état par bandes d'ordre 2 peut s'analyser en deux étapes : d'abord la synchronisation à deux bandes (d'ordre 1) sur $I_\mu^{1,0}$ et $I_\mu^{1,1}$, puis sur les sous-bandes $I_\mu^{2,\sigma}$. Si $\mu < \mu_\infty$, les états par bandes sont toujours définis, mais si le système est dans un état par bandes maximal, par exemple, sur les bandes $I_\mu^{1,0}$ et $I_\mu^{1,1}$ et $\mu \in [\mu_1, \mu_2]$, la dynamique locale permet alors à l'ensemble du système de converger vers des états parfaitement synchrones : le réseau est alors uniforme et suit la dynamique périodique de S_μ.

Cette construction se généralise immédiatement au cas où il y a 2^n bandes ($\mu \in [\mu_n, \bar{\mu}_n]$) et permet de définir en chaque site un spin $\sigma_{\vec{r}}$ qui prend alors 2^n valeurs.

1.2.2 Attracteurs microscopiques et états Gibbsiens

Revenons au cas où l'itération locale a exactement deux bandes. Pour un réseau de N sites non couplés, les variables locales évoluent périodiquement sur les deux bandes ; le système a donc $\mathcal{N} = 2^N/2$ attracteurs correspondant à 2^N choix de phase pour l'ensemble des sites, modulo l'invariance par translation de l'axe des temps en régime asymptotique ($t \to \infty$). Dans une gamme de couplages très faibles, la situation est identique au cas découplé (limite anti-intégrable [1]), tous les arrangements spatiaux des spins sont autorisés par la dynamique, et le système a toujours $2^N/2$ attracteurs.

Quand le couplage augmente, certains motifs sont détruits et le réseau s'organise en petit amas de sites synchrones par bandes. C'est par exemple le cas des systèmes présentés fig. 1.5 pour lesquels $g = 0.05$ et $g = 0.08$ respectivement. La dynamique des variables au sein d'un amas est chaotique, mais la structure spatiale définie par $\sigma_{\vec{r}}^{t}$ est bloquée. En fait tout se passe comme si les sites avaient pris une extension spatiale : les variables indépendantes sont maintenant les cases d'un damier et, en supposant que les amas comportent

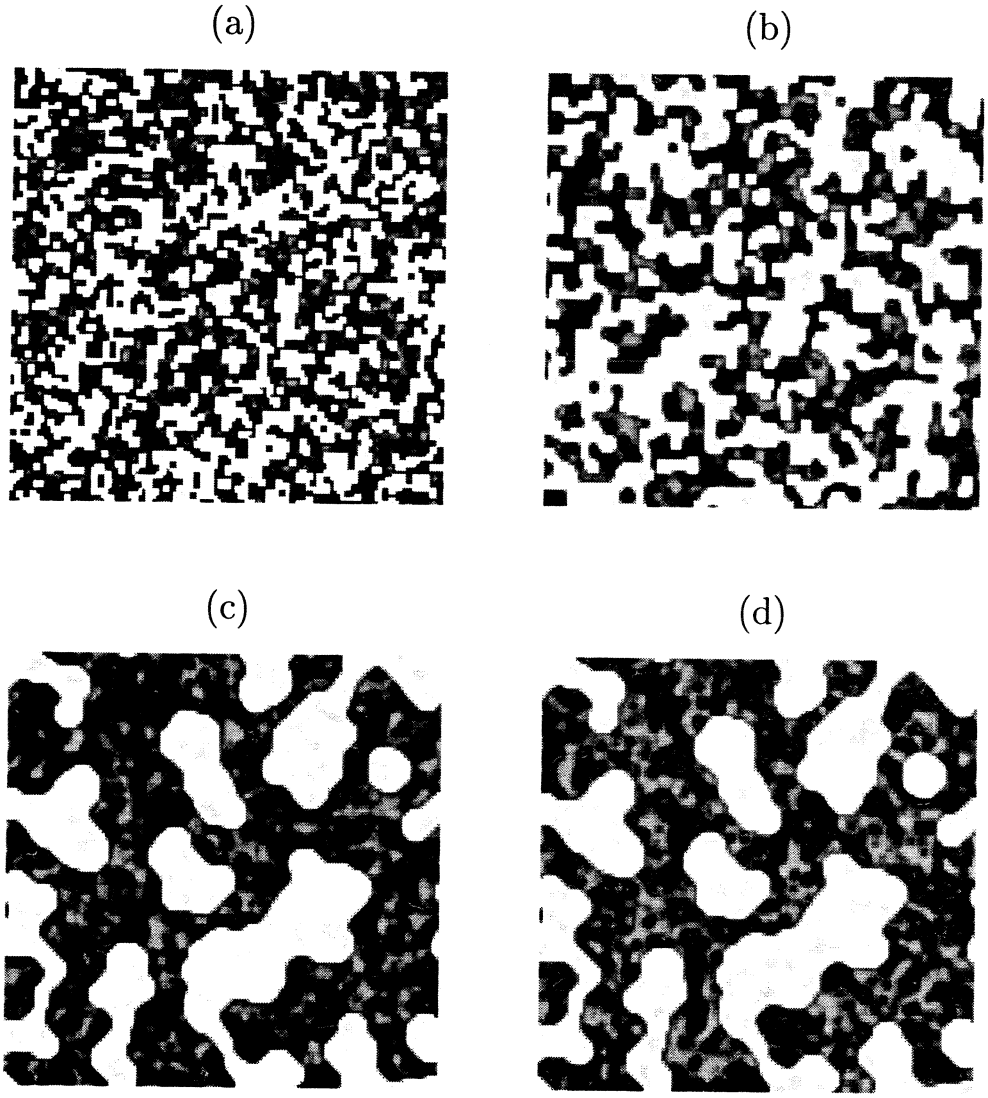

FIG. 1.5 – *États bloqués d'un réseau bidimensionnel d'applications logistiques couplées, de coté* $L = 128$, *pour* $\mu = 1.5$, *avec conditions aux limites périodiques, et pour une condition initiale prise indépendemment en chaque site et uniformément sur* $[-1, 1]$. *(a)* $g = 0.05$, *(b)* $g = 0.08$ *: à l'intérieur des amas, les variables locales suivent une dynamique par bandes, et les fronts qui séparent les deux phases ne se déplacent pas. (b-c) pour* $g = 0.09$, $t = 15000$ *et* 20000 *: les fronts ont convergés, ils n'évoluent plus, et les structures sont de taille suffisamment grande pour que soient visibles des états collectifs purs très proches de ceux qui sont sélectionnés aux plus grandes valeurs du couplage (voir par exemple fig. 1.4 pour* $g = 0.2$*).*

en moyenne ν sites, cela donne un nombre effectif de variables indépendantes de N/ν, soit $\mathcal{N} = 2^{N/\nu}/2$ attracteurs.

À cause de cette possible coexistence d'amas sur toute l'étendue du réseau, on peut s'attendre à ce qu'une représentation de ces systèmes par une mesure de Gibbs soit encore valable. En effet, une seule configuration peut alors réaliser physiquement un ensemble d'états dans toute son étendue spatiale. Au lieu de la mesure $\otimes p_{\vec{r}}$ qui décrit les couplages nuls, on s'attend alors à pouvoir représenter le système par une mesure de la forme $\otimes p_{\vec{R}}$ où la variable $\vec{R}$ varie plus lentement que $\vec{r}$ en espace.

Si le couplage augmente encore, il y a de moins en moins de configurations autorisées, ν augmente, et le nombre d'attracteurs diminue (voir fig. 1.5) ; On peut d'ailleurs observer plus facilement au sein de ces amas le comportement collectif «pur» qui aurait été obtenu en prenant tous les sites dans la même bande à $t = 0$.

Ces situations diffèrent encore profondément des régimes de fort couplage puiqu'ici encore $\ln \mathcal{N}$ est une quantité extensive tandis que dans le cas du comportement collectif non trivial le nombre de ces attracteurs est indépendant de la taille du système. Cette extensivité du nombre d'attracteurs autorise en effet un continuum d'états macroscopiques selon la proportion d'amas dans l'une ou l'autre phase.

1.2.3 Attracteurs macroscopiques

Venons-en aux comportements macroscopiques. La définition des variables discrétisées $\sigma^t_{\vec{r}} \in \{0, 1\}$ permet de s'affranchir des nuances liées à la dépendance des état collectifs purs par rapport au couplage. Le mélange entre les deux états est mesuré par la proportion $\rho^t = \langle \sigma^t_{\vec{r}} \rangle$ de sites à valeur dans la bande $\sigma = 1$.

La condition initiale macroscopique du système est définie par la répartition des variables entre les deux bandes avec la proportion $\rho^0 = \rho^{t=0}$. La façon dont sont distribuées ces variables sur chacune des bandes importe peu, mais afin de définir une procédure systématique, elles sont tirées selon les états purs du système non couplé : la distribution initiale p^0 vaut donc $p^0 = \rho^0 p^0_{S_\mu} + (1 - \rho^0) p^1_{S_\mu}$, et la configuration initiale est tirée selon la distribution $\otimes p^0$.

Des diagrammes de bifurcations de ρ^t en fonction de la proportion initiale ρ^0 sont présentés fig. 1.6 pour différentes valeurs de g. Pour $g = 0$, ρ^t prend les deux valeurs ρ^0 et $1 - \rho^0$ à tout temps : le taux de mélange est conservé. Quand le couplage augmente, le système franchit un premier seuil au-delà

duquel la phase minoritaire est éliminée dès qu'il y a un grand rapport de proportionnalité entre les deux phases : des états par bandes sont donc rejoints pour des conditions initiales trop déséquilibrées. Cette élimination s'interprète par le fait que la phase minoritaire ne peut pas créer des amas suffisamment grands pour résister au couplage[1]. Cependant, pour tous les régimes bloqués tels que ceux présentés précédemment, la proportion ρ^{2t} peut se figer à toute valeur non triviale, c'est à dire ni 0 ni 1 : tous les mélanges peuvent encore être atteints, même si les états par bandes commencent à dominer.

Remarquons que la proportion initiale ρ^* qui assure un mélange égal de deux phases n'est pas toujours 1/2, et qu'elle s'en éloigne lorsque le couplage augmente. Ceci s'explique par la considération du très court transitoire pendant lequel se forment les amas : à ce moment là, certaines variables sont redistribués par le couplage sur tout l'intervalle I_μ ; à cause de l'asymétrie des bandes, et de leurs bassins, ces variables sont alors capturées préférentiellement par l'une des composantes ergodiques de la dynamique macroscopique, ce qui induit un déséquilibre entre les phases. À ce sujet, il est intéressant d'observer que dans la limite asymptotique ($t \to \infty$), le temps est invariant par translation alors que ce n'est pas le cas aux temps courts. Les états ρ^t et $1 - \rho^t$ sont donc équivalents asymptotiquement, tandis que les proportions ρ^0 et $1 - \rho^0$ conduisent à des états différents.

La dépendance de ρ^t par rapport aux conditions initiales donne une idée du bassin d'attraction macroscopique des différents régimes collectifs. La taille de ces bassins est évidement liée à la complexité des attracteurs microscopiques, mais un mélange macroscopique donné peut être réalisé par une infinité de configurations spatiales. Afin de quantifier cette dépendance, nous pouvons par exemple mesurer la corrélation $\chi^t = \langle\langle(\rho^{2t} - \rho^0)^2\rangle\rangle$ où le double crochet, $\langle\langle\,.\,\rangle\rangle$ indique la moyenne uniforme sur les conditions initiales macroscopiques $\rho^0 \in [0, 1]$. Cette quantité est affichée fig. 1.6 en fonction de g. Ce diagramme permet de voir assez nettement les premières transitions traversées en partant de $g = 0$, mais ce qui se passe ensuite est moins net.

Remarquons pour finir que pour des valeurs de g non nulle, les états mélangés ne sont pas *stricto sensu* des combinaisons linéaires des états purs $p^0_{S_\mu}(g)$ et $p^1_{S_\mu}(g)$: quand des amas des deux phases coexistent, ils interagissent et les

1. En fait, les conditions initiales non corrélées en espace permettent d'envisager que sur un réseau infini, des amas de toutes tailles de la phase minoritaire soient produits. Cependant dans la limite thermodynamique, de tels amas occupent un volume nul du réseau, donc n'ont aucun effet sur les observables macroscopiques.

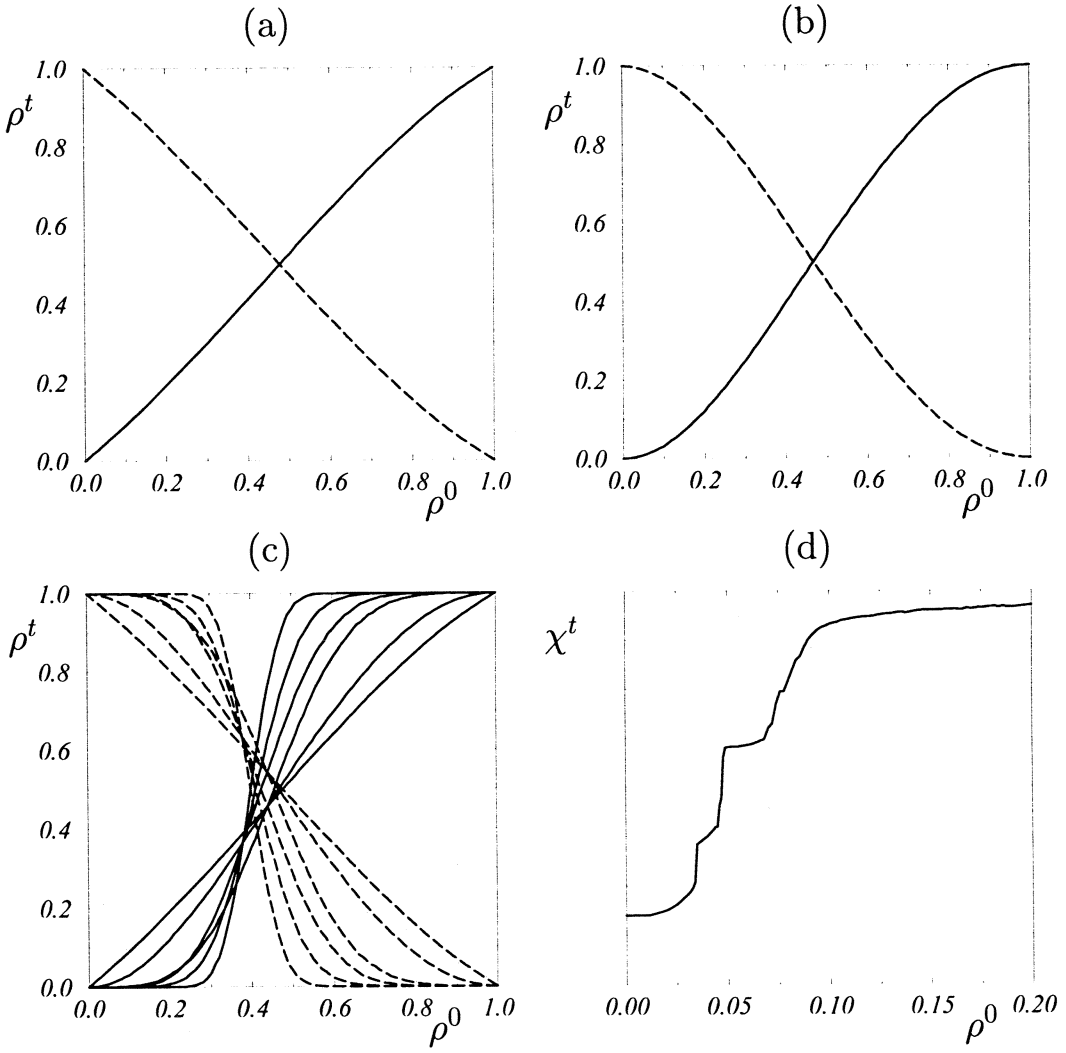

FIG. 1.6 – *Comportements asymptotiques de $\rho^t = \langle \sigma_{\vec{r}}^t \rangle$ en fonction de la condition initiale macroscopique définie par ρ^0, dans le cas d'un réseau d'applications logistiques faiblement couplées ($d = 2$, $L = 512$). Les temps pairs et impairs sont indiqués en traits continus et pointillés respectivement. La proportion ρ^t rejoint un régime stationnaire après un transitoire assez court : (a) $g = 0.03$: ρ^t rejoint une dynamique périodique non extrémale pour toute condition initiale mélangée. (b) $g = 0.04$ les courbes s'infléchissent aux extrémités, ce qui indique que les plus petits amas isolés de la phase minoritaire sont absorbés par la phase dominante. (c) Pour différentes valeurs entre $g = 0.03$ et $g = 0.09$. Pour $g = 0.2$, le système converge vers la solution stationnaire $\rho^t = 0$ ou 1, mais la durée du transitoire diverge quand on approche du mélange initial optimal ρ^* pour lequel les deux phases sont équilibrées dans la limite $t \to \infty$. (d) Mesure de la corrélation entre états macroscopiques, $\chi^t = \langle\langle (\rho^{2t} - \rho^0)^2 \rangle\rangle$, en fonction de g. On observe plusieurs transitions jusqu'aux environs de $g = 0.1$. Au delà de cette limite, le comportement par bandes est atteint pour toute condition initiale macroscopique, sauf ρ^* pour laquelle le régime transitoire diverge.*

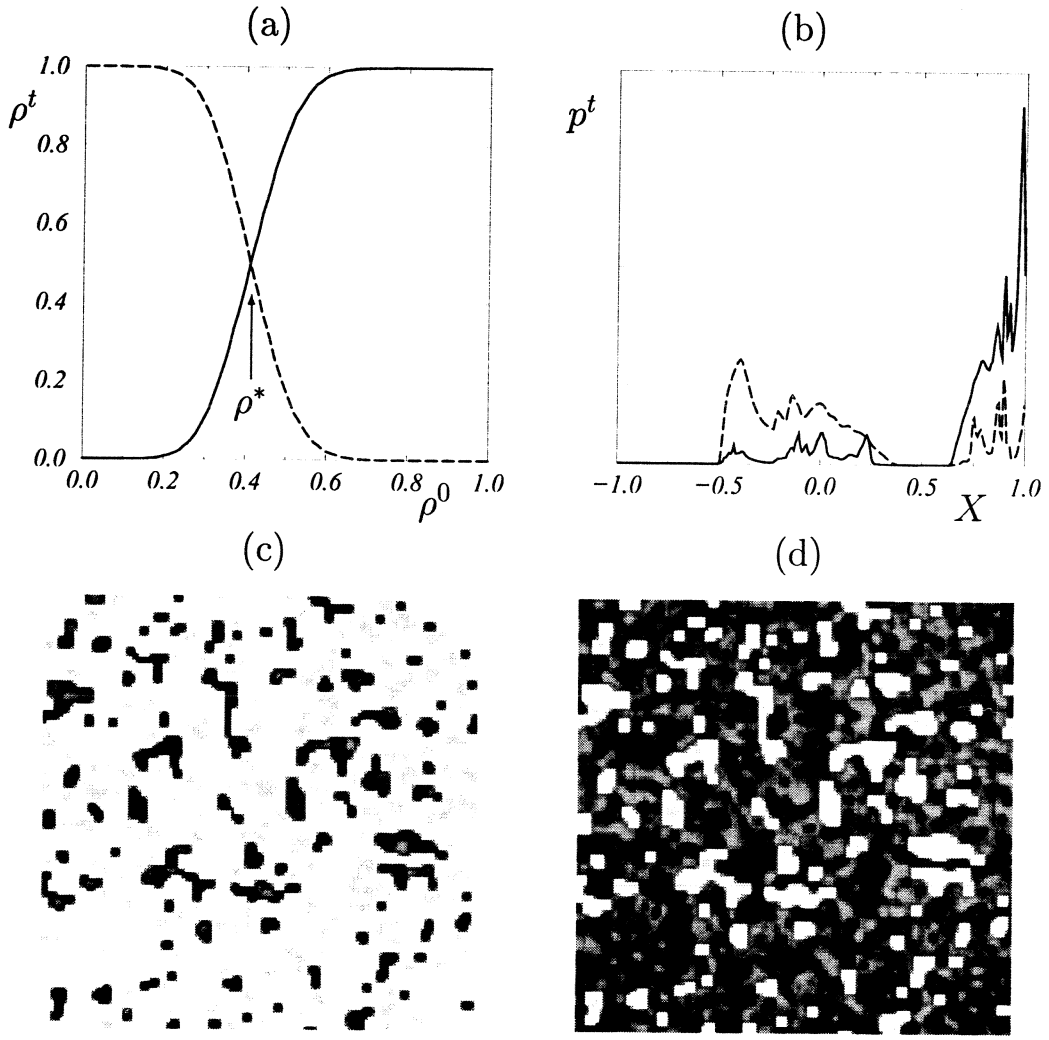

FIG. 1.7 – *Réseau bidimensionnel d'itérations logistiques faiblement couplées ($g = 0.08$) dans le régime à deux bandes ($\mu = 1.5$). Les temps pairs et impairs sont indiqués en traits continus et pointillés respectivement. (a) Comportements asymptotiques de $\rho^t = \langle \sigma^t_{\vec{r}} \rangle$ en fonction de la condition initiale macroscopique ρ^0 (mesurée pour un réseau de coté $L = 512$). Le système rejoint une dynamique d'état pur pour tout un intervalle de ρ^0 près des extrémités de l'intervalle $[0, 1]$. (b) Les valeurs de la distribution instantanée p^t pour le régime asymptotique mélangé obtenu en partant de $\rho^0 = 0.5$. La distribution p^t n'est plus à proprement parler une combinaison d'états purs (voir fig. 1.3) parce que les deux phases interagissent. Pourtant, il n'y a aucune variable dans l'intervalle entre les bandes, ce qui indique que les fronts entre les amas des deux phases sont très raides. (c-d) Deux images successives du réseau dans ce régime ($L = 128$, $\rho^0 = 0.5$, $t = 1000$ et 1001). Au temps pairs, la bande $\sigma = 1$ (en clair) est majoritaire.*

états purs sont hybridés (voir fig. 1.7).

1.3 Croissance de domaines

Nous avons pu mettre en évidence que l'existence de comportements collectifs cohérents à fort couplage, ou inversement d'états Gibbsiens à faible couplage, a son origine dans la mise en place spontanée d'une dynamique de croissance de domaines entre les différentes composantes ergodiques de la dynamique collective.

En augmentant le couplage g, le système traverse une succession de transitions associées au «dégel» de certains arrangements spatiaux. Plus le couplage augmente, plus des arrangements de grande taille, donc plus complexes, sont mis à l'épreuve, et le système traverse des points de transition de plus en plus nombreux. Une valeur de g au delà de laquelle aucune coexistence de phase n'est possible ne peut être que le point d'accumulation de tous ces points de transition : tous les sites sont alors dans la même composante ergodique de la dynamique collective, d'où la notation g_e pour un tel point.

D'autre part, près de chacun de ces points, la destruction d'amas qui sont en limite de stabilité peut mettre un temps relativement long à être initiée par les fluctuations de la dynamique locale. L'accumulation de points de transition vers le seuil g_e, accompagnée de la divergence des transitoires, indique que sur tout un intervalle de valeurs de g, ces mesures deviennent inaccessibles. L'approche de g_e par valeurs inférieures, si elle nous renseigne donc sur les mécanismes à l'œuvre, ne permet cependant pas d'estimer précisément la valeur de ce seuil. Ceci nous conduit à étudier la dynamique de croissance de domaines au-dessus du seuil pour chercher à le caractériser.

En effet, au delà de g_e, les deux seuls états asymptotiques sélectionnés par la dynamique sont des états par bandes. Quand il y a deux bandes disjointes ($\mu < \bar{\mu}_1$) le sites ne peuvent changer de phase que lorsqu'ils sont traversés par un front. La situation est alors analogue un système de spins ferromagnétiques à température nulle [2, 7, 22].

Il faut toutefois s'attendre dans notre cas à ce que cette dynamique se «ralentisse» quand g décroît vers g_e afin de permettre la transition vers des états gelés. Afin de quantifier ces effets, nous avons cherché à mesurer l'évolution de la fonction de corrélation «spin-spin», $\langle \sigma_{\vec{r}} \sigma_{\vec{r}+\vec{x}} \rangle_c$ et l'évolution de la persistance.

Cependant, l'étude de ces phénomènes de croissance de domaines requiert

que l'on puisse considérer des états où aucune des deux phases ne parvienne à dominer l'autre. Dans le cas de applications unimodales couplées que nous avons développé jusqu'à maintenant, à cause de l'asymétrie des bandes, cet équilibre entre les deux états ne perdure que pour une valeur précise de la proportion initiale, $\rho^0 = \rho^*$. Ceci exige de contrôler très finement ce paramètre puisque la proportion optimale ρ^* qui donne lieu à ces transitoires infinis dépend elle même du couplage.

Afin de résoudre cette difficulté, nous utilisons une application locale antisymétrique. Les deux états par bandes sont alors échangés par la symétrie $X \to -X$, pour tout g, ce qui impose $\rho^* = 0$. Une telle itération peut être définie comme suit :

$$\begin{array}{rcll} S_\mu(X) & = & \mu X & \text{si} \quad X \in [-1/3, 1/3] \\ & = & 2\mu/3 - \mu X & \text{si} \quad X \in [1/3, 1] \\ & = & -2\mu/3 - \mu X & \text{si} \quad X \in [-1, -1/3] \end{array} \tag{1.3}$$

où le paramètre μ prend ses valeurs sur l'intervalle $[-3, 3]$ pour laisser invariant l'intervalle I. Le point fixe $X = 0$ est stable tant que $|\mu| < 1$, et au delà, on observe des dynamiques par bandes. Il y a deux bandes pour $\mu \in [-2, -1]$, auxquelles correspondent deux intervalles invariants par S_μ pour $\mu \in [1, 2]$ (voir fig. 1.3). La situation $\mu < 0$ est donc analogue au cas des itérations unimodales, avec deux bandes qui définissent deux phases dynamiques, tandis que la situation opposée met en exergue l'analogie avec les systèmes de spin sur réseau, puisque ce sont bien des états collectifs purs invariants par la dynamique couplée qui sont observés. Le cas particulier où $\mu = 3$ avait d'ailleurs été introduit par Miller et Huse [24] pour motiver l'analogie avec les systèmes de spins, puis utilisée par P. Marcq *et al.* pour mesurer les exposants critiques associés aux transitions de phases que sont les points de bifurcations des régimes collectifs non triviaux [23].

Ce travail est maintenant développé dans la lettre qui suit, soumise à *Physical Review Letters*. Mentionnons seulement qu'elle fait référence au groupe de renormalisation et à la limite continue des réseaux d'itérations couplées : pour l'instant, ces deux questions ne sont pas nécessaires à la clarté de l'exposé et pourront être éludées. Elles seront développées dans le chapitre suivant et reliées à la problématique du comportement collectif non trivial.

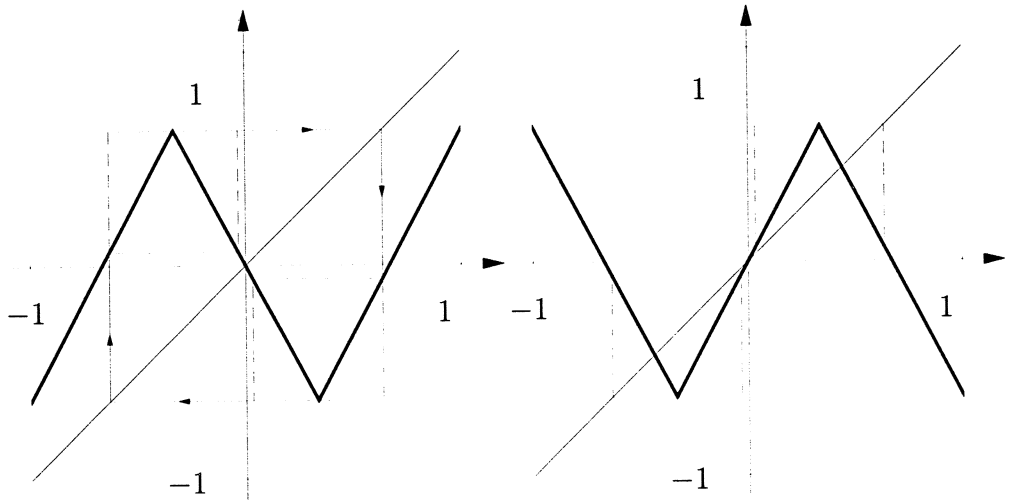

FIG. 1.8 – *Bandes (gauche) et intervalles invariants (droite) de l'itération (1.3) pour* $\mu = -1.9$ *et* $\mu = 1.9$ *(resp.).*

1.4 Phase Ordering and Onset of Collective Behavior

Article devant être soumis à *Physical Review Letters*

Phase Ordering and Onset of Collective Behavior in Chaotic Coupled Map Lattices

Anaël Lemaître[1,2] and Hugues Chaté[2,1]

[1] *LadHyX — Laboratoire d'Hydrodynamique, École Polytechnique, 91128 Palaiseau, France*

[2] *CEA — Service de Physique de l'État Condensé, Centre d'Études de Saclay, 91191 Gif-sur-Yvette, France*

Abstract

The phase ordering properties of lattices of band-chaotic maps coupled diffusively with some coupling strength g are studied in order to determine the limit value g_e beyond which multistability disappears and non-trivial collective behavior is observed. The persistence of equivalent discrete spin variables and the characteristic length of the patterns observed scale algebraically with time during phase ordering. The associated exponents vary continuously with g but remain proportional to each other, with a ratio close to that of the time-dependent Ginzburg-Landau equation. The corresponding individual values seem to be recovered in the space-continuous limit.

One of the most remarkable features distinguishing extensively-chaotic dynamical systems from most models studied in out-of-equilibrium statistical physics is that they generically exhibit non-trivial collective behavior (NTCB), i.e. long-range order emerging out of local chaos, accompanied by the temporal evolution of spatially-averaged quantities [1, 2, 3]. In particular, NTCB is easily observed on simple models of reaction-diffusion systems such as coupled map lattices (CMLs) in which (chaotic) nonlinear maps S of real variables X are coupled diffusively with some coupling strength g [3].

NTCB is often claimed to be a *macroscopic* attractor, well-defined in the infinite-size limit and reached for almost every initial condition, provided the local coupling between sites is "large enough". On the other hand, for small g values, such as those corresponding to the so-called "anti-integrable" limit which tries to extend zero-coupling behavior to small, but finite coupling

strengths, CMLs often exhibit multistability [4]. This is in particular the case if the local map shows banded chaos, because the interfaces separating clusters of sites in the different bands can be pinned. This multistability is "extensive": the number of (chaotic) attractors may then be argued to grow exponentially with the system size, in opposition to NTCB for which this number is small and size-independent.

In this Letter, we define and measure the limit coupling strength g_e separating the strong-coupling regime in which NTCB is observed from the weak-coupling, extensive multistability region. Using the discrete "spin" variables which can be defined whenever the one-body probability distribution functions (pdfs) of local (continuous) variables have disjoint supports, we study numerically the phase ordering process following uncorrelated initial conditions in cases where the spin variables take only two values. We find that the persistence probability $p(t)$ (i.e. the proportion of spins which have not changed sign up to time t) saturates in finite time to strictly positive values in the weak coupling regime whereas it decays algebraically to zero when $g > g_e$. The associated persistence exponent θ varies continuously with parameters, at odds with traditional models [5]. Moreover, data obtained on various two-dimensional CMLs is best accounted for by a relation of the form $\theta \sim (g - g_e)^w$, which we use to estimate g_e. We show further that this behavior is mostly due to the non-trivial scaling of the characteristic length $L(t) \sim t^\phi$ during the phase ordering process. Indeed, $\phi \neq \frac{1}{2}$, the expected value for a scalar, non-conserved order parameter [7], and is found to be proportional to θ, with the exponent ratio ϕ/θ approximately taking the value known for the time-dependent Ginzburg-Landau equation (TDGLE). We also provide evidence that, in the continuous-space limit, "normal" phase ordering behavior is recovered. Finally, we discuss the hierarchy of limit coupling values g_e^n which can be defined when the local map is unimodal and shows 2^n-band chaos, using recent results on renormalisation group (RG) ideas applied to CMLs [8].

Consider a d-dimensional hypercubic lattices $\mathcal{L}$ of coupled identical maps S_μ acting on real variables $(X_{\vec{r}})_{\vec{r}\in\mathcal{L}}$:

$$X_{\vec{r}}^{t+1} = (1 - 2dg)S_\mu(X_{\vec{r}}^t) + g\sum_{\vec{e}\in\mathcal{V}} S_\mu(X_{\vec{r}+\vec{e}}^t)\ , \qquad (1)$$

where $\mathcal{V}$ is the set of $2d$ nearest neighbors $\vec{e}$ of site $\vec{0}$. We first present results

obtained for the piecewise linear, odd, local map S_μ defined by:

$$S_\mu(X) = \begin{cases} \mu X & \text{if } X \in [-1/3, 1/3] \\ 2\mu/3 - \mu X & \text{if } X \in [1/3, 1] \\ -2\mu/3 - \mu X & \text{if } X \in [-1, -1/3] \end{cases} \tag{2}$$

which leaves the $I = [-1, 1]$ interval invariant. (For $\mu = 3$, this is the chaotic map introduced by Miller and Huse [9].) For $\mu \in [-2, -1]$, S_μ displays banded chaos, while for opposite μ values, these bands become invariant subintervals of I. At $\mu = 1.9$ in particular, S_μ possesses two symmetric such intervals $I^\pm = [\pm\mu(2-\mu)/3, \pm\mu/3]$, separated by a finite gap. For any value of g, the support of the pdf of X for the CML defined by (1-2) can be separated into two components thanks to the symmetry of the map. This allows the unambiguous definition of spin variables $\sigma_{\vec{r}} = \text{sign}(X_{\vec{r}})$. The deterministic nature of the system and the form of the coupling strictly forbids the nucleation of opposite-phase droplets in clusters: the analog spin system is at zero temperature.

For large g values, complete phase ordering occurs (Fig. 1a,b), and the system eventually reaches a regime in which all sites are situated in one of the two intervals $I^\pm$. For small g, initial conditions with sites in both intervals $I^\pm$ lead to spatially-blocked configurations where interfaces between clusters of each phase are strictly pinned, while chaos is present within clusters (Fig. 1c,d). [10]

To study the phase ordering process efficiently, uncorrelated initial conditions were generated as follows: exactly one half of the sites of a $d = 2$ lattice were chosen at random and assigned positive X values drawn according to the invariant distribution of S_μ on I^+, while the other sites were similarly assigned negative values. Large lattices with periodic boundary conditions were used, and the persistence $p(t)$ was measured. Fig. 2a shows the results of single runs for various values of g. For small g, $p(t)$ saturates at large times to strictly positive values, while it decays algebraically, for large g, on square lattices of linear size 2048 sites. The associated persistence exponent θ varies continuously with g, and its g-dependence is nicely accounted for by a functional form $\theta \sim (g - g_e)^w$ with $g_e \simeq 0.169(1)$ and $w \simeq 0.20(3)$ (Fig. 2b). We have, at this point, no theoretical justification of this fitting Ansatz. At any rate, it provides an operational definition of g_e yielding estimates consistent with those obtained using other, less accurate, methods [11].

The origin of this unusual behavior of the persistence exponent is largely explained by the evolution of the spatial structures formed during phase ordering. Usually, one expects the coarsening to be described by the algebraic growth of a

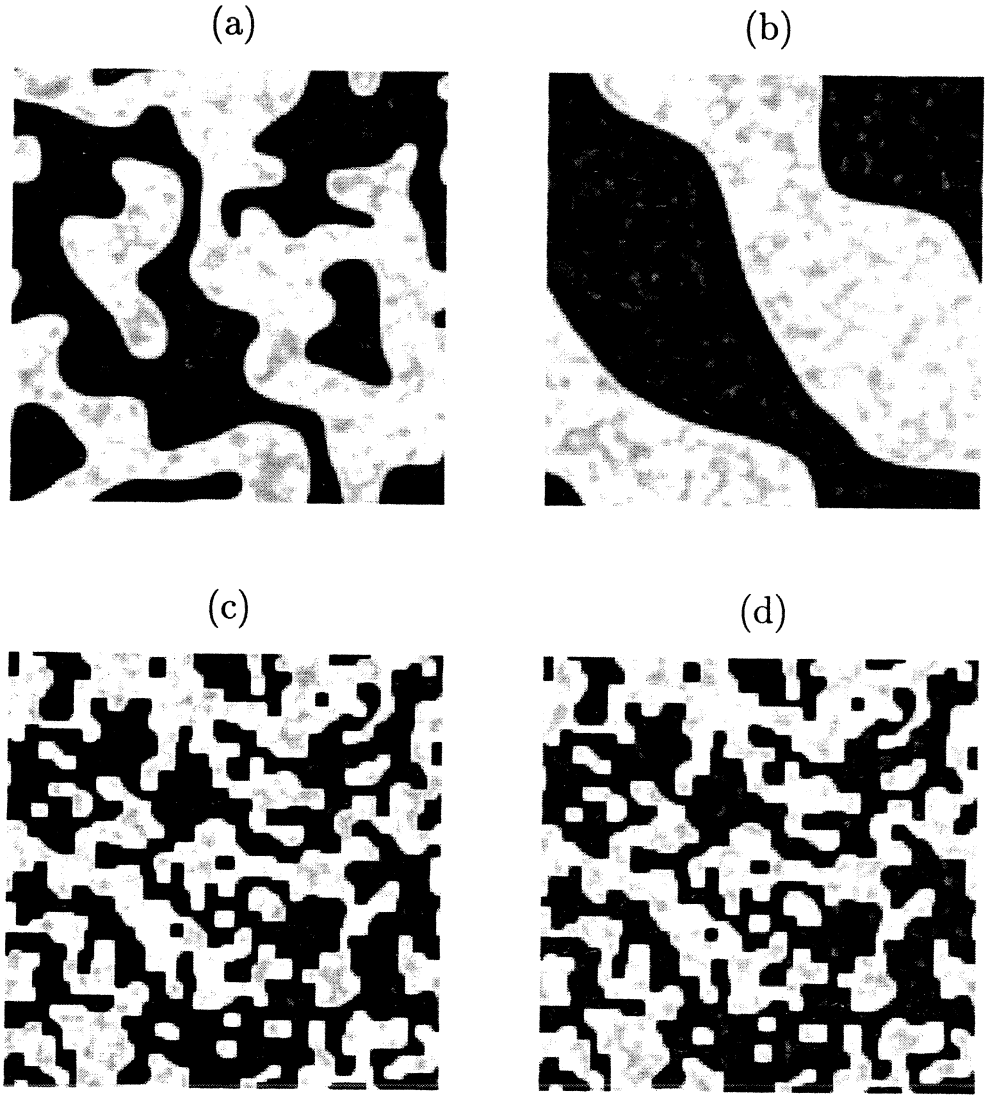

Figure 1: Snapshots of the $d = 2$ CML with local map (2). Lattice of 128^2 sites, grey scale from $X = -1$ (white) to $X = 1$ (black), uncorrelated initial conditions. (a,b): transient leading to complete ordering at $g = 0.2 > g_e$, $t = 100$ and 1000; (c,d): blocked state at $g = 0.15 < g_e$, $t = 1000$ and 2000.

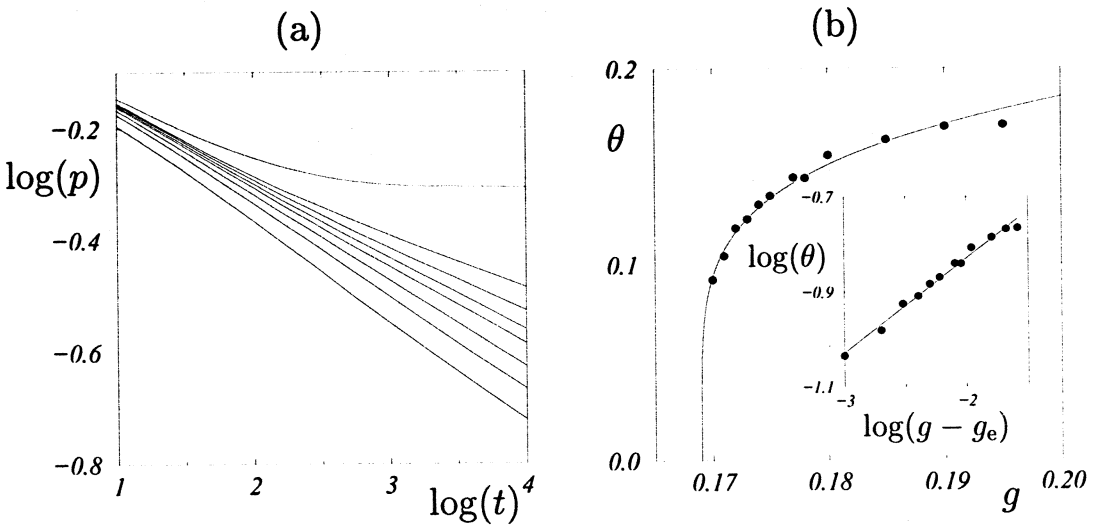

Figure 2: Phase ordering in the $d = 2$ CML with local map (2) at $\mu = 1.9$. (a): algebraic decay of the persistence probability $p(t)$ for, from top to bottom: $g = 0.16$ ($< g_e$: saturates to a finite level), 0.17, 0.172, 0.174, 0.176, 0.18, 0.185, and 0.195. (b): variation of persistence exponent θ with g. Solid line: fitting Ansatz $\theta \sim (g - g_e)^w$ with $g_e = 0.169(1)$ and $w = 0.20(3)$ Insert: $\log(\theta)$ vs. $\log(g - g_e)$.

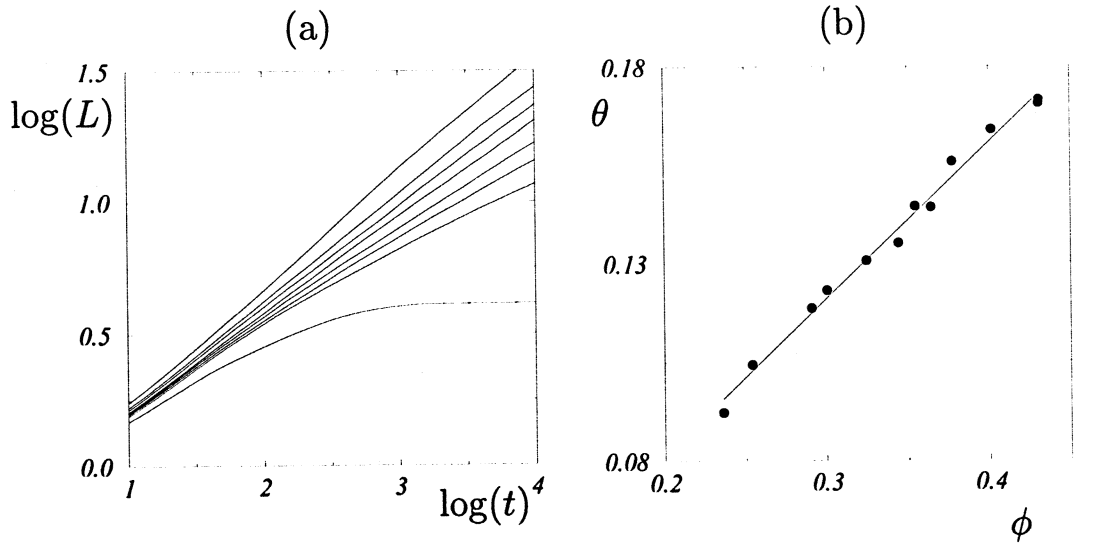

Figure 3: Same runs as in Fig. 2. (a) $\log(L)$ vs $\log(t)$ (bottom curve: $g = 0.16$, top curve $g = 0.195$); (b) $\theta(g)$ vs $\phi(g)$ for g values between 0.17 and 0.20; the solid line is the linear fit $\theta \simeq 0.396\phi - 0.002$.

single characteristic length $L(t) \sim t^{\phi}$ with $\phi = 1/2$ for a non-conserved, scalar order parameter [7]. In the CML studied above, the two-point correlation function $C(\vec{x},t) = \langle \sigma^t_{\vec{r}+\vec{x}} \sigma^t_{\vec{r}} \rangle$ was measured during phase ordering [12]. Length $L(t)$ was then evaluated to be the width at mid-height ($C(L(t),t) = 1/2$), determined by interpolation. This procedure was then validated by a collapse of all $C(||\vec{x}||/L(t),t)$ curves. Surprisingly, while the scaling behavior of $L(t)$ is observed, exponent ϕ departs from the expected $1/2$ value and varies continuously with g (Fig. 3). Again, we find a law of the form $\phi \sim (g - g_{\rm e})^w$ to be an acceptable Ansatz of our numerical results. The estimated values of $g_{\rm e}$ and w are consistent, within numerical accuracy, with those found when fitting $\theta(g)$. This is corroborated by studying directly $p(t)$ vs $L(t)$ (not shown), or by plotting θ vs ϕ which confirms that the two exponents are proportional to each other (Fig. 3d). Remarkably, the ratio θ/ϕ is found to have, within our numerical accuracy, the $d = 2$ TDGLE value: $\theta/\phi \simeq 0.40(2) \simeq 2\theta_{\rm GL} \simeq 0.40$ [13]. (We cannot, however, completely exclude the values corresponding to the Ising model, or the diffusion equation, since $\theta_{\rm Ising} \simeq 0.22$ [6], and $\theta_{\rm Diff.} \simeq 0.19$ [13].)

The same analysis was also performed on CMLs with a non-symmetric, unimodal, local map S_μ of the form:

$$S_\mu(X) = 1 - \mu|X|^{1+\varepsilon} \text{ with } \mu \in [0,2] \,, \tag{3}$$

in particular for $\varepsilon = 0$ (tent map) and $\varepsilon = 1$ (logistic map). For $\mu \in [\mu_\infty, 2]$, this map shows 2^n-band chaos and exhibits an inverse cascade of band-merging points $\bar{\mu}_n$ when $\mu \to \mu_\infty$. In the strong-coupling limit, the corresponding CMLs exhibit, depending on d, periodic or quasiperiodic NTCB with a period equal to, or a multiple of, that of the band-chaos of the local map [3, 8]. For $d = 2$ and 3, in particular, simple period-2^n NTCB occurs, with an infinite cascade of phase transition points $\mu^{\rm c}_n$ distinct from the band-merging points (Fig. 4a). When period-2 NTCB occurs in the two-band chaotic region of the map ($\mu \in [\bar{\mu}_2, \bar{\mu}_1] \approx [1.43, 1.54]$), two-state spin variables $\sigma^t_{\vec{r}} \in \{-1, 1\}$ can be defined, but the asymmetry of the two bands hinders the generation of "effectively" uncorrelated initial conditions. Indeed, an equal proportion of sites in each band quickly leads to complete phase ordering and saturation of $p(t)$, even in the strong-coupling regime. This happens because these initial conditions create, after a few timesteps, configurations with a fairly large unbalance between the two phases. Tuning the initial proportion ρ of sites in, say, the band containing $X = 0$, one can minimize such effects. We determined the

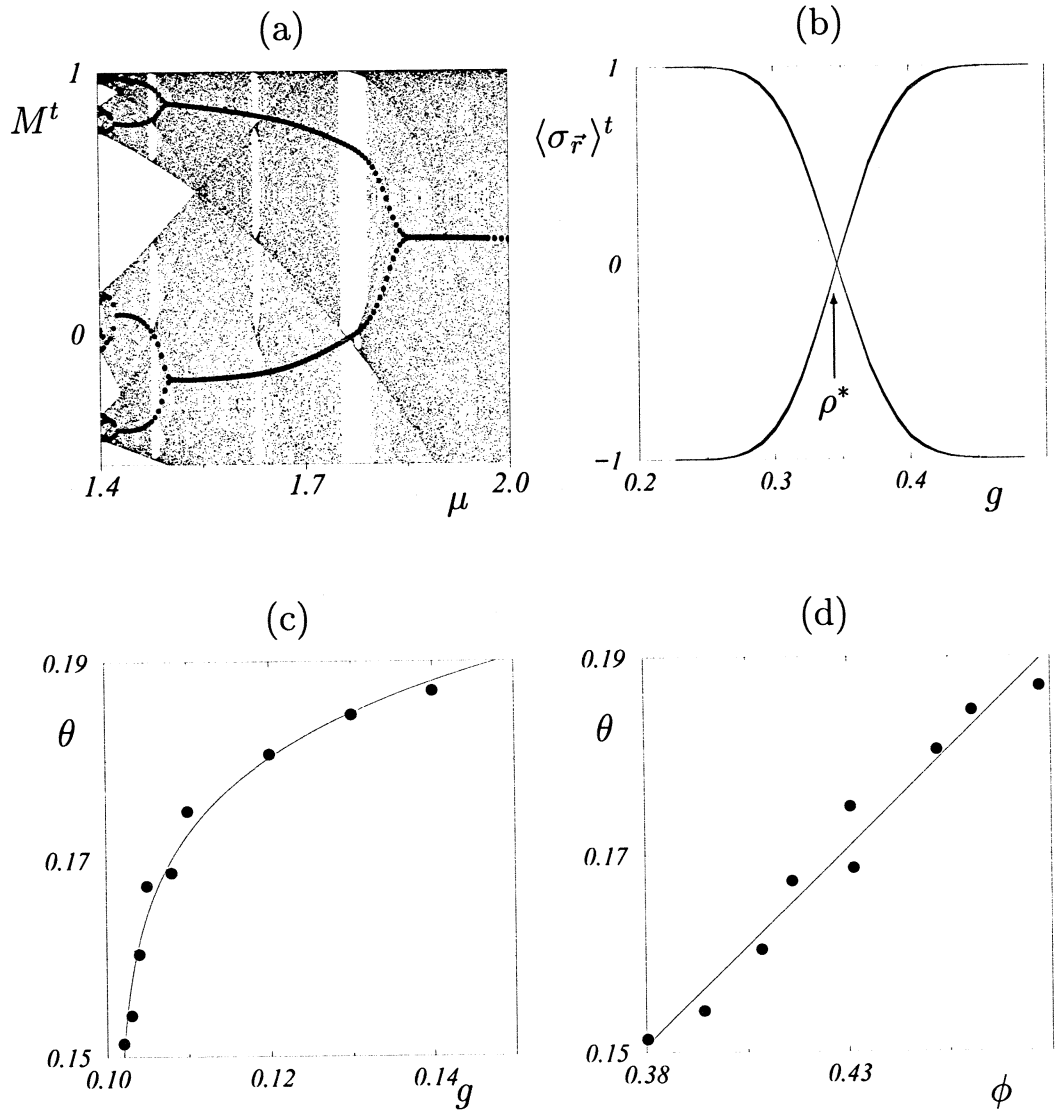

Figure 4: $d = 2$ lattice of coupled logistic maps for $g = 0.2$. (a) bifurcation diagram ($\langle X^t_{\vec{r}}\rangle_{\vec{r}}$, large dots) superimposed on that of single logistic map (small dots). (b): $\langle\sigma^t_{\vec{r}}\rangle_{\vec{r}}$ vs ρ plotted at 20 different timesteps between $t = 500$ and $t = 1000$ for $\mu_2^c < \mu = 1.5 < \bar{\mu}_2$. This "magnetization" remains constant only for $\rho = \rho^* \simeq 0.3465$, whereas it reflects the overall period-2 dynamics for all other ρ values. (c) $\theta(g)$ at $\mu = 1.5$ and $\rho = \rho^*(g)$ with log-log fit ($g_e \simeq 0.101$, $w \simeq 0.06$). (d) $\theta(g)$ vs $\phi(g)$; the solid line is the linear fit $\theta \simeq 0.40\phi - 0.002$.

optimal proportion ρ^* defined as the value for which the magnetization $\langle \sigma_{\vec{r}}^t \rangle$ remains constant (Fig. 4b). Clean scaling behavior of $L(t)$ and $p(t)$ is then observed with reasonable system sizes, as with the symmetric local map (2). Varying the coupling strength g, exponents ϕ and θ show the same behavior as above, decreasing continuously to zero at g_e. Fig. 4c shows the case of coupled logistic maps, for which the Ansatz $\theta, \phi \sim (g - g_e)^w$ is, again, valid, although not as good as in the case of local map (2). Note that the estimated value $w \simeq 0.06(2)$ is different from that measured for the CML with local map (2), but $\theta/\phi \simeq 0.48(4)$ is still rather close to the TDGLE value (Fig. 4d).

We now deal with the onset of more complex NTCB such as the period-2^n cycles mentioned above for which the study of the phase ordering in terms of two-state spin variables may not be legitimate.

Consider, for example, a CML with local map S_μ defined by (3) in a 4-band chaotic regime ($\mu \in [\bar{\mu}_3, \bar{\mu}_2]$) which exhibits period-4 NTCB. The "natural" spin variables to study phase ordering take four values, indexed by the 4-band chaotic cycle. However, these four bands can be grouped in two "meta-bands", since they arise from a band splitting bifurcation at $\bar{\mu}_2$, so that two-state spin variables can still be defined. Accordingly, two limit coupling strengths can be defined: g_e^1, marking the onset of complete phase ordering between the two meta-bands, and g_e^2 for ordering from initial conditions within one of the meta-bands. A priori, $g_e^2 \neq g_e^1$, and there might exist coupling strengths such that, e.g., pinned clusters exist within, but not between, the two meta-bands. The "true" onset of period-4 NTCB is then given by $g \geq \max(g_e^1, g_e^2)$. Similarly, for $\mu \in [\mu_\infty, \bar{\mu}_n]$, one can define n different μ-dependent limit coupling strengths $g_e^1, g_e^2, \ldots, g_e^n$, with $n \to \infty$ as $\mu \to \mu_\infty$. Using our recent work on renormalisation group arguments for CMLs [8], one can show that the threshold values of this infinite hierarchy are related to each other. Here, we only describe briefly these results, while a detailed derivation can be found in [8]. The RG structure of single map (3) induces the conjugacy between $(\mathbf{\Delta}_g^m \circ \mathbf{S}_\mu)^2$ and $\mathbf{\Delta}_g^{2m} \circ \mathbf{S}_{q(\mu)}$, where $\mathbf{S}_\mu$ transforms each variable $X_{\vec{r}}$ by S_μ, $\mathbf{\Delta}_g^m$ is the diffusive operator applied m times, and $q(\mu) = \mu^2$ for coupled tent maps. This relation can be shown to imply that $g_e^2(\mu, m) = g_e^1(q(\mu), 2m)$. Furthermore, using the fact that $g_e^n(\mu, m)$ decreases with m, one can prove that the maximum g_e for all n, μ, and m is $g_e^* = g_e^1(\bar{\mu}_1, 1)$. Thus, whenever $g \geq g_e^*$, complete ordering occurs for all bands.

The above results are at odds with the behavior of usual models studied in phase ordering problems [14]. But in both cases presented here, the exponent

ratio θ/ϕ seems to take the value expected for the TDGLE model. This "weak universality" is reminiscent of similar results found recently at the Ising-like critical points shown by the same models [15]. We note, moreover, that, when g is increased, ϕ approaches $1/2$ and θ reaches values close to $\theta_{\rm GL}$. We believe that this tendancy is mostly due to the lattice effects becoming less and less important (although strict pinning does not occur for $g > g_{\rm e}$). We have shown recently [8] that, in the continuous-space limit of CMLs, the weak coupling regime disappears ($g_{\rm e} \to 0$), together with any pinning effects. One can thus wonder whether, in this limit, one recovers more "conventional" phase ordering dynamics.

The continuous limit of CMLs such as those defined by (1-2) is reached when applying the coupling step of the dynamics more and more times per iteration, i.e. when taking the $m \to \infty$ limit of $\mathbf{\Delta}_g^m \circ \mathbf{S}_\mu$. In this limit, $\mathbf{\Delta}_g^m$ converges to a universal Gaussian kernel $\mathbf{\Delta}_\lambda^\infty = \exp(\frac{\lambda^2}{2}\nabla^2)$ with a coupling range $\lambda = \sqrt{2gm}\|\vec{e}\|$ where $\|\vec{e}\|$ is the lattice spacing, which can thus be chosen to scale like $1/\sqrt{m}$ so as to keep λ constant. We investigated the phase ordering properties of these CMLs with the symmetric local map (2) for increasing values of m. At a qualitative level, the scaling behavior of $L(t)$ and $p(t)$ is observed at all m values. Quantitatively, exponents θ and ϕ vary with m at fixed g. Increasing m, ϕ seems to converge to $1/2$, while $\theta \to \theta_{\rm GL}$: for $m = 1$ to 3, we find $\phi = 0.467$, 0.479, 0.505, and $\theta = 0.174$, 0.184, 0.196, from single runs on lattices of linear size 4096 sites.

Our work provides a quantitative method for determining the onset of NTCB in chaotic coupled map lattices. It also reveals that the phase-ordering properties of multiphase, chaotic CMLs are different from those of most models studied traditionally. More work is needed, especially at the analytical level, to clarify the origin of the non-universality observed and put our numerical results on firmer ground, since we cannot completely exclude a very slow, unobservable, crossover of the scaling behavior observed to that of a more traditional model. Different approaches can be suggested.

A continuous variation of the scaling exponent ϕ for the characteristic length of domains is not usually observed, but (at least) two exceptions are known. One is the case of coarsening from initial conditions with built-in long-range correlations [16], but then the persistence probability $p(t)$ does *not* decrease algebraically with time [17]. Another situation of possible relevance is the case of phase-ordering with an order-parameter-dependent mobility [18], for which, unfortunately, the behavior of the persistence is not known. At any

rate, the recovery of the "normal" scaling properties of the TDGLE in the space-continuous limit suggests that lattice effects are ultimately responsible for the non-trivial scaling properties recorded in discrete systems. This calls for a detailed study of interface dynamics in order to assess the effective role of discretization and anisotropy.

Finally, we believe our results are general and that similar behavior should be found in experiments on phase-ordering of pattern-forming systems, such as, e.g., electro-hydrodynamical convection in liquid crystals, or Rayleigh-Bénard convection [19].

We thank Ivan Dornic for many fruitful discussions and his keen interest in our work.

References

[1] H. Chaté, Int. J. Mod. Phys. B **12**, 299 (1998).

[2] J. A. C. Gallas et al., Physica A **180**, 19 (1992); J. Hemmingsson, Physica A **183**, 255 (1992); H. Chaté and P. Manneville, Europhys. Lett. **14**, 409 (1991); H. Chaté, L.-H. Tang, and G. Grinstein, Phys. Rev. Lett. **74**, 912 (1995).

[3] H. Chaté and P. Manneville, Prog. Theor. Phys. **87**, 1 (1992); Europhys. Lett. **17**, 291 (1992); H. Chaté and J. Losson, Physica D **103**, 51 (1997).

[4] R.S. MacKay and T.A. Sépulchre, Physica D **82**, 243 (1995); T.A. Sépulchre and R.S. MacKay, Nonlinearity **10**, 679 (1997); S. Aubry, Physica D **103**, 201 (1997).

[5] See, e.g.: I. Dornic and C. Godrèche, J. Phys. A **31**, 5413 (1998), and references therein.

[6] D. Stauffer, J. Phys. A **27**, 5029 (1994).

[7] P.C. Hohenberg and B.I. Halperin, Rev. Mod. Phys. **49**, 436 (1977).

[8] A. Lemaître and H. Chaté, Phys. Rev. Lett. **80**, 5528 (1998); preprint, 1998.

[9] J. Miller and D.A. Huse, Phys. Rev. E **48**, 2528 (1993).

[10] In CMLs, pinning can be strict (the "effective noise" arising from local chaos is bounded). It is *local*, and thus no finite-size effect is observed for large-enough systems.

[11] A. Lemaître, Ph.D. thesis, Ecole Polytechnique, 1998.

[12] The same analysis was also performed using the continuous variables $X_{\vec{r}}$, yielding similar, albeit noisier, results.

[13] S. Cueille and C. Sire, "Block persistence", cond-mat/9803014; S. H. Cornell, private communication.

[14] A.J. Bray, Adv. Phys. **43**, 357 (1994).

[15] P. Marcq, H. Chaté, and P. Manneville, Phys. Rev. Lett. **77**, 4003 (1996); Phys. Rev. E **55**, 2488 (1997).

[16] B. Derrida, C. Godrèche, and I. Yekutieli, Phys. Rev. A **44**, 6241 (1991).

[17] H. Nakanishi, H. Chaté, and I. Dornic, unpublished.

[18] C.L. Emmott and A.J. Bray, preprint cond-mat/9808308.

[19] M.C. Cross and D.I. Meiron, Phys. Rev. Lett. **75**, 2152 (1995).

Chapitre 2

Groupe de renormalisation et universalité

Afin de comprendre l'origine du comportement collectif non trivial, nous avons exploré la dépendance des états collectifs vis-à-vis du paramètre de couplage. Ce nouveau chapitre est concerné par les systèmes fortement couplés, et par la structure des différents comportements obtenus en faisant varier, cette fois-ci, le paramètre μ. En effet, sur un diagramme de bifurcations comme celui de la fig. 2 page 13, les régimes collectifs s'ordonnent comme les bandes en allant vers μ_∞, en suivant les premiers pas d'une cascade sous-harmonique. En dessous de μ_∞, l'analogue d'un état par bande est un état synchrone : pour des couplages suffisament forts, tous les sites se synchronisent et décrivent donc la même trajectoire périodique. Il y a donc, à fort couplage, une transition entre des comportement périodiques synchrones et les comportement collectifs non triviaux, autour de μ_∞. Quelle est la nature de cette transition ? Que se passe-t-il autour de ce point, dans des régimes de grande périodicité, à grand nombre de bandes ... ?

Le problème de la structure des régimes collectifs vers μ_∞ est double. C'est d'une part l'existence d'une similarité entre les différents états par bande, et d'autre part le comportement des seuils g_e dans cette limite. En effet, un scénario envisageable pourrait faire intervenir des états bloqués, comme ceux observés à couplage faible, entre des amas sur des petites bandes voisines, près de μ_∞ ; l'idée étant que le couplage doit alors avoir plus de difficultés à différencier ces états très proches. Dans ce cadre, le comportement collectif non trivial apparaîtrait comme un phénomène relativement fortuit, et pour passer des états cohérents de part et d'autre de μ_∞, il faudrait passer par des états de type «couplage faible».

En fait, la situation est toute autre : d'une certaine façon, le couplage se renforce vers μ_∞, en préservant la dynamique collective mais en interdisant toute coexistence de phases, de sorte qu'il y a une cascade sous-harmonique inverse infinie de comportements collectifs non triviaux à laquelle fait écho une cascade directe de régimes synchronisés. Dans cette limite, toutes les échelles de longueur spatiales divergent par rapport au pas du réseau, qui doit être amené à zéro pour des raisons de définition du comportement collectif. Le système est alors équivalent à un champ continu de variables itérées et le système traverse μ_∞ par des états extrêmement piqués et cohérents en espace.

Cette structure est mise en évidence dans les articles qui suivent par l'écriture d'une équation de groupe de renormalisation pour l'opérateur $\mathbf{\Delta}_g \circ \mathbf{S}_\mu$. C'est un résultat important puisqu'il étend au cas de systèmes à grand nombre de degrés de liberté les propriétés d'auto-similarité et d'universalité connues pour les itérations de l'intervalle, en les complétant par une universalité des échelles spatiales.

Je présente d'abord une lettre, publiée à *Physical Review Letters* qui décrit dans un cas simple comment peut s'écrire cette équation, puis un article qui montre plus précisément comment ceci s'inscrit dans la problématique du comportement collectif non trivial, et comment cette approche se généralise à toutes les itérations unimodales couplées.

2.1 Nonperturbative Renormalization Group for Chaotic Coupled Map Lattices

Article paru dans *Physical Review Letters*

2.2 Renormalization Group for Strongly Coupled Maps

Article devant être soumis à *Journal of Statistical Physics*

Nonperturbative Renormalization Group for Chaotic Coupled Map Lattices

Anaël Lemaître[1,2] and Hugues Chaté[2,1]
[1]*LadHyX, Laboratoire d'Hydrodynamique, Ecole Polytechnique, 91128 Palaiseau, France*
[2]*CEA, Service de Physique de l'Etat Condensé, Centre d'Etudes de Saclay, 91191 Gif-sur-Yvette, France*
(Received 26 January 1998)

A nonperturbative renormalization group is derived for chaotic coupled map lattices (CMLs) with diffusive coupling, leading to a natural space-continuous limit of these systems. We show that, under very general conditions, the universal properties of the local map are translated to the spatiotemporal level, demonstrating the self-similarity of the bifurcation diagrams of strongly coupled CMLs and the accompanying divergence of length scales. [S0031-9007(98)06460-6]

PACS numbers: 05.45.+b, 05.70.Ln, 64.60.Ak

The use of renormalization group (RG) ideas to unveil the universal features of the cascades of bifurcations of nonlinear dynamical systems with few degrees of freedom has played a major role in our understanding of (temporally) chaotic systems [1]. Simple maps of the real interval such as the logistic map have been the models of choice on which most theoretical advances were made [2–4]. No similarly general framework is available, however, for *spatiotemporal chaos* when the basic equations cannot be legitimately reduced to the interaction of a few modes. This holds even for simple models such as coupled map lattices (CMLs), i.e., discrete-time discrete-space dynamical systems in which maps, arranged at the nodes of a lattice, interact locally [5]. Literature dealing with the question of the extension of single-map RG to CMLs does exist [6], but it is restricted to perturbative treatments around the accumulation points of bifurcation cascades of the local map. Moreover, it usually considers the small coupling limit and small deviations from spatially homogeneous solutions in one or two space dimensions. One notable exception is the numerical work of van de Water and Bohr [7], who showed numerically that many quantities of interest do exhibit scaling properties related to those of the local map, even for rather large values of the coupling.

In this Letter, we introduce a nonperturbative renormalization group approach to CMLs with linear diffusive coupling which translates to the spatiotemporal level the universal features of the local maps involved. We show that, under broad conditions, the bifurcation diagrams of CMLs present the same self-similarity as that of their local maps, with the same coupling-independent accumulation point, around which length scales diverge with a universal scaling related to the diffusive coupling. Our work also leads to a definition of a "natural" continuous-space limit for CMLs which can be seen as a good starting point for analytical approaches of spatiotemporal chaos. We believe that these results are relevant to general reaction-diffusion systems. Our findings extend the scope of previous studies [6,7]. They are valid in chaotic regimes, are not restricted to the vicinity of accumulation points, and apply to large classes of solutions in all dimensions. They are demonstrated exactly for coupled tent maps, while they are valid asymptotically for more general local functions such as the logistic map.

For simplicity, we consider real variables X lying at the nodes of a d-dimensional hypercubic lattice $\mathcal{L}$. They are updated synchronously at discrete time steps by

$$\mathbf{X}^{t+1} = \mathbf{\Delta}_g \circ \mathbf{S}_\mu(\mathbf{X}^t), \tag{1}$$

where $\mathbf{X}^t = (\mathbf{X}^t_{\vec{r}})_{\vec{r}\in\mathcal{L}}$ represents the state of the lattice at time t, $\mathbf{S}_\mu$ transforms each variable by the local map S_μ, and $\mathbf{\Delta}_g$ is the diffusive coupling operator

$$[\mathbf{\Delta}_g(\mathbf{X})]_{\vec{r}} = (1 - 2dg)\mathbf{X}_{\vec{r}} + g\sum_{\vec{e}\in\mathcal{V}} \mathbf{X}_{\vec{r}+\vec{e}}, \tag{2}$$

with g the coupling strength and $\mathcal{V}$ the set of the $2d$ nearest neighbors of site $\vec{0}$. Without loss of generality, we consider the family of local maps

$$S_\mu(X) = 1 - \mu|X|^{1+\varepsilon} \quad \text{with } \mu \in [0,2] \text{ and } \varepsilon > 0, \tag{3}$$

which leave the $[-1,1]$ interval invariant and, in particular, the tent ($\varepsilon = 0$) and the logistic ($\varepsilon = 1$) maps.

We first present the collective behavior observed for strongly coupled, chaotic CMLs, and their self-similar bifurcation diagrams, and then define the strong coupling limit to which our study is especially relevant.

In the "chaotic region" of the local map ($\mu > \mu_\infty$ with $\mu_\infty = 1$ for the tent map, and $\mu_\infty = 1.401\ldots$ for the logistic map), and with the strong, "democratic," equal-weight coupling $g = 1/(2d + 1)$, the CMLs defined above are extensively chaotic (e.g., their Lyapunov dimension is proportional to their size). Almost all initial conditions flow to one of a few attractors which possess a well-defined infinite-size, infinite-time limit and can be characterized by the evolution of spatial averages. The corresponding dynamics has been termed nontrivial collective behavior (NTCB) [8] to emphasize the emergence of a macroscopic evolution in the presence of microscopic chaos. Figure 1 shows the bifurcation diagram

 0031-9007/98/80(25)/5528(4)$15.00

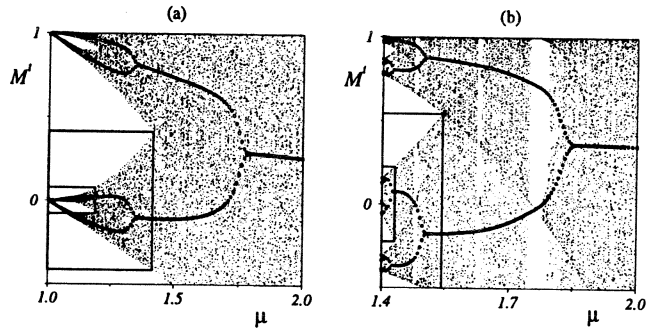

FIG. 1. Democratically coupled ($g = 0.2$) tent (a) and logistic (b) maps on a $d = 2$ lattice of linear size $L = 2048$ with periodic boundary conditions: Bifurcation diagram of $M' = \langle X \rangle'$ (filled circles) superimposed on that of the local map S_μ (small dots). The $[\mu_\infty, \bar{\mu}_1] \otimes I^1_{\bar{\mu}_1}$ and $[\mu_\infty, \bar{\mu}_2] \otimes I^2_{\bar{\mu}_2}$ regions are shown. For coupled tent maps, these regions transformed by the RG coincide with the bifurcation diagrams of $\Delta^2_g \circ \mathbf{S}_\mu$ and $\Delta^4_g \circ \mathbf{S}_\mu$, themselves indistinguishable from the whole figure. For the logistic maps, the agreement is poorer at such orders due to the inexactness of the RG for S_μ.

of the simplest spatial average, $M' \equiv \langle X \rangle'$, for $d = 2$ lattices of coupled tent and logistic maps. Decreasing μ at fixed g, periodic NTCB of period $1, 2, 4, 8, \ldots$ is observed. These collective period-doubling bifurcations are, in fact, Ising-like phase transitions [9]. The instantaneous distribution $p'(X)$ of site values, smooth and well defined in the infinite-size limit, follows the same collective behavior. Only periodic collective motion has been observed for $d = 2$ and 3 (Fig. 2b), while more complex NTCB (e.g., quasiperiodic) exists for $d > 3$. The bifurcation diagram of M' is reminiscent of the self-similar band structure of the local map, but the critical points μ^c_n of the phase transitions differ from the band-splitting points $\bar{\mu}_n$ of S_μ (Fig. 1). Approaching μ_∞, however, it rapidly becomes numerically impossible to resolve the particular

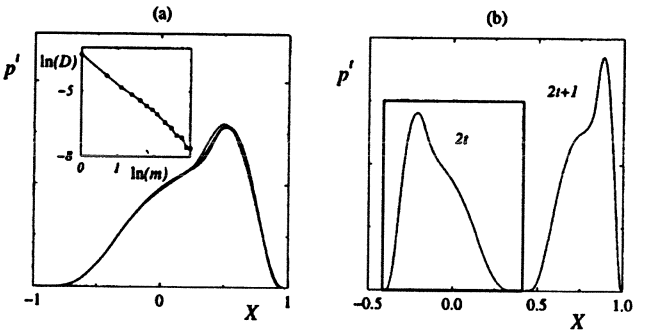

FIG. 2. Asymptotic (large t) single-site distributions p' for democratically coupled tent maps ($d = 2$, $L = 2048$). (a) Stationary states at $\mu = 2$ for $1 \le m \le 32$. For $m > 1$, the distributions cannot be separated on this graph; they converge to a universal distribution of the continuous limit. Inset: log-log plot of the distance $D^2 = \int dX\, (p_m - p_{32})^2$ vs m. (b) Period-2 collective cycle at $\mu = \bar{\mu}_1$ for $m = 1$; the distribution in the rectangle (even time steps) is transformed exactly by the RG onto that for $m = 2$ at $\mu = 2$ (a).

NTCB observed, because prohibitively large lattices, well as an increasing numerical resolution, are then r quired. If the periods observed are clearly rather large (least eight in Fig. 1), the uniqueness of attractors near μ cannot be ascertained, and no evidence of an infinite ca cade of phase transitions is available. The RG approa below clarifies these points.

The NTCB described above is observed for g $1/(2d + 1)$. As a matter of fact, it can be observed f all g values beyond a well-defined threshold, as argu below. Consider a CML with a local map S_μ in two-band chaos regime and the coarse-grained patter formed by considering only in which band each site li at large, even, time steps. For weak (and zero) couplin there exist "frozen" patterns of this type corresponding different chaotic attractors or ergodic components, eac with a finite basin of attraction [10]. Recent work [1 shows that there exists, at a given μ, a limit valu $g_e(\mu)$ beyond which no frozen pattern exists (excludir configurations whose basin of attraction is of the measu of zero in phase space). It is in this strong-coupling lim $g \ge g_e(\mu)$ that NTCB is observed. Generally, $g_e(\mu$ decreases weakly with μ [11], but, again, it is difficu to estimate near μ_∞. On the other hand, it is convenier to define $g^*_e = \max_\mu[g_e(\mu)]$, and to consider values of above g^*_e. For the $d = 2$ lattices of tent and logistic map considered above, $g^*_e \simeq 0.10$ [11].

We now briefly review how RG is defined for singl maps, before considering the case of CMLs. For clarity' sake, we use the tent map, for which the RG can b performed exactly. The invariant interval of S_μ is I^0_μ = $[1 - \mu, 1]$ for all $\mu \le \bar{\mu}_0 = 2$. The second iterate c the map, restricted to I^1_μ, the "central" band (containin $X = 0$) of the two-band region of S_μ is written

$$S^2_\mu|_{I^1_\mu} = h^{-1}_\mu \circ S_{q(\mu)}|_{I^0_{q(\mu)}} \circ h_\mu , \qquad (4$$

with $h_\mu(X) = X/(1 - \mu)$ and $q(\mu) = \mu^2$. Whenever $q(\mu) \le \bar{\mu}_0$, this relation may be interpreted in terms o an equivalent variable $X_1 = h_\mu(X) \in I^0_{q(\mu)}$ governed b the map $S_{q(\mu)}$. Therefore, for all $\mu \le \bar{\mu}_1 = q^{-1}(\bar{\mu}_0)$— here, $\bar{\mu}_1 = \sqrt{2}$—the invariant intervals of S^2_μ are I^1_μ = $h^{-1}_\mu(I^0_{q(\mu)})$ and $I^{1'}_\mu = S_\mu(I^1_\mu)$. Relation (4) is easily gen eralized to any iterate of S_μ. It insures that S_μ dis plays a self-similar cascade of band-splitting points $\bar{\mu}_n$ below which regimes with more than 2^n bands ar observed. When $n \to \infty$, $\bar{\mu}_n$ converges to μ_∞ and the in tervals shrink to zero with the so-called Feigenbaum con stants δ and α depending only on ε.

For more general maps ($\varepsilon > 0$), the RG equation (4 holds for some function q and some continuous bijec tion h_μ which cannot be derived exactly. Several ap proximations can be made. For example, expanding S^2_μ around $X = 0$ is the so-called one-parameter centered ap proximation of the RG. Higher-order, noncentered, mul tiparameter approximations are also possible [4]. The

all provide estimates of the points $\bar{\mu}_n$, which converge when $n \to \infty$ toward an effective accumulation point with Feigenbaum exponents close to the actual ones.

Let us now apply the same ideas to the CML defined above, and derive an expression for the second iterate $(\mathbf{\Delta}_g \circ \mathbf{S}_\mu)^2$ of the evolution operator. Take $\mu \leq \bar{\mu}_1$ to insure that the local map has at least two bands. Let $\mathbf{I}_\mu^1$ ($\mathbf{I}_\mu^{1'}$) denote the set of lattice configurations for which all variables $\mathbf{X}_i \in I_\mu^1$ ($I_\mu^{1'}$). Since $\mathbf{\Delta}_g$ keeps all such intervals invariant, $\mathbf{I}_\mu^1$ and $\mathbf{I}_\mu^{1'}$ are not only exchanged by the action of $\mathbf{S}_\mu$, but also by $\mathbf{\Delta}_g \circ \mathbf{S}_\mu$, and are thus invariant under $(\mathbf{\Delta}_g \circ \mathbf{S}_\mu)^2$: they constitute generalized bands in the phase space of the CML. For any $\mu \leq \mu_1$, the operator $(\mathbf{\Delta}_g \circ \mathbf{S}_\mu)^2$ restricted on the central band $\mathbf{I}_\mu^1$ can thus be written

$$(\mathbf{\Delta}_g \circ \mathbf{S}_\mu)^2|_{\mathbf{I}_\mu^1} = \mathbf{\Delta}_g \circ \mathbf{S}_\mu|_{\mathbf{I}_\mu^{1'}} \circ \mathbf{\Delta}_g \circ \mathbf{S}_\mu|_{\mathbf{I}_\mu^1}.$$

We now consider again tent maps, while the general case will be discussed later. In this case, $\mathbf{S}_\mu|_{\mathbf{I}_\mu^{1'}}$ is linear, since for all $X \in I_\mu^{1'}$, $S_\mu(X) = 1 - \mu X$. Therefore, it commutes with $\mathbf{\Delta}_g$ and we have

$$(\mathbf{\Delta}_g \circ \mathbf{S}_\mu)^2|_{\mathbf{I}_\mu^1} = \mathbf{\Delta}_g^2 \circ \mathbf{S}_\mu^2|_{\mathbf{I}_\mu^1}. \quad (5)$$

Using the RG equation (4) and the linearity of the operator $\mathbf{h}_\mu$ induced by h_μ on lattice configurations, we write

$$(\mathbf{\Delta}_g \circ \mathbf{S}_\mu)^2|_{\mathbf{I}_\mu^1} = \mathbf{h}_\mu^{-1} \circ \mathbf{\Delta}_g^2 \circ \mathbf{S}_{q(\mu)}|_{\mathbf{I}_{q(\mu)}^0} \circ \mathbf{h}_\mu.$$

This equation involves a CML in which the coupling operator is applied twice. It is easily extended to generalized CML of the form $\mathbf{\Delta}_g^m \circ \mathbf{S}_\mu$ where the coupling step is applied m times, yielding

$$(\mathbf{\Delta}_g^m \circ \mathbf{S}_\mu)^2|_{\mathbf{I}_\mu^1} = \mathbf{h}_\mu^{-1} \circ \mathbf{\Delta}_g^{2m} \circ \mathbf{S}_{q(\mu)} \circ \mathbf{h}_\mu, \quad (6)$$

which constitutes a RG equation for CMLs in the (m, μ) parameter space.

When $\mu \leq \bar{\mu}_n$, the local map has 2^n bands. If all the sites are, for example, taken inside I_μ^n, the central band of order n, then they lie at all times in one of the 2^n bands. In the following, we call this situation a *banded state of order n* [12]. We can thus write, generalizing (5)

$$(\mathbf{\Delta}_g^m \circ \mathbf{S}_\mu)^{2^n}|_{\mathbf{I}_\mu^n} = \mathbf{\Delta}_g^{2^n m} \circ \mathbf{S}_\mu^{2^n}|_{\mathbf{I}_\mu^n}. \quad (7)$$

This allows one to generalize (6) to banded states of order n.

More general maps ($\varepsilon > 0$) are not linear on $I_\mu^{1'}$, but they are invertible on this interval (the critical point $X = 0$ is in the other band). They can be approximated by a nonvanishing tangent and the calculations above can be repeated. For states of increasing periodicity ($\mu \leq \bar{\mu}_n$), the restrictions of S_μ on each of its 2^n bands but the central band $I_\mu^n \ni 0$, are better and better approximated by tangents, since the diameters of these intervals shrink with increasing n. Finally, since h_μ is generally linear, Eq. (6) holds as an approximation of the RG for CMLs exact for coupled tent maps.

RG equation (6) has been derived for the restriction of the evolution operator to $\mathbf{I}_\mu^1$ and $\mathbf{I}_\mu^{1'}$ and for $\mu \leq \bar{\mu}_1$ (banded states of the order of 1). *A priori,* banded states are only some of the many possible chaotic attractors of our CML for $\mu > \mu_\infty$. Suppose, however, that $g \geq g_e^*$ so that we are in the NTCB regime. If, furthermore, $\mu \leq \bar{\mu}_1$, almost all initial conditions eventually belong to $\mathbf{I}_\mu^1$ [13], and Eq. (6) can be applied once: for any $\mu \leq \bar{\mu}_1$, the behavior of the original CML is equivalent to that of $\mathbf{\Delta}_g^2 \circ \mathbf{S}_{\mu'}$ for $\mu' = q(\mu) \leq 2$. Without studying the collective behavior of $\mathbf{\Delta}_g^2 \circ \mathbf{S}_{\mu'}$ itself, it is already clear that if $\mathbf{\Delta}_g \circ \mathbf{S}_{\mu'}$ brings all sites into the same band, a second application of $\mathbf{\Delta}_g$ at each time step must "synchronize" the sites even more: $\mathbf{\Delta}_g^2$ is a "stronger" coupling than $\mathbf{\Delta}_g$. All generalized CMLs with $m \geq 1$ are in the strong-coupling regime whenever $g \geq g_e^*$. We can write, symbolically: $g_e^*(m+1) \leq g_e^*(m)$. Therefore, since $\mu' \leq \bar{\mu}_1$ when $\mu \leq \bar{\mu}_2$, then $\mathbf{\Delta}_g^2 \circ \mathbf{S}_{\mu'}$ reaches a banded state of the order of 1, corresponding to a banded state of the order of 2 for $\mathbf{\Delta}_g \circ \mathbf{S}_\mu$. Iterating this argument allows us to apply (6) recursively. This implies that the strongly coupled CML $\mathbf{\Delta}_g \circ \mathbf{S}_\mu$ reaches a banded state of the order of n from almost all initial conditions whenever $\mu \leq \bar{\mu}_n$. In particular, collective cycles of an arbitrarily large period must be reached for μ sufficiently close to μ_∞ and $g \geq g_e^*$. The actual collective dynamics exhibited though, depends on the behavior of the generalized CML $\mathbf{\Delta}_g^m \circ \mathbf{S}_\mu$.

We have performed numerical simulations of $\mathbf{\Delta}_g^m \circ \mathbf{S}_\mu$ for increasing m, for $d = 2$ and 3 lattices of coupled tent and logistic maps. In all cases, the asymptotic behavior observed for $m > 1$ is qualitatively the same as for $m = 1$ (Figs. 2a and 3a). Quantitative agreement is also very good, as one finds a fast convergence with m to a well-defined limit (insets of Figs. 2a and 3a). An immediate

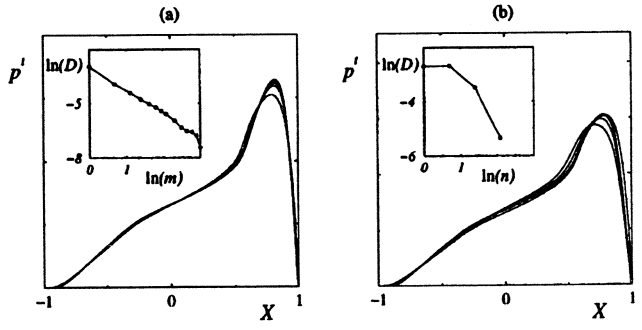

FIG. 3. (a) Same as Fig. 2 for coupled logistic maps. The convergence is to a nonuniversal distribution, because the RG for S_μ is not exact. (b) Central bands $I_{\bar{\mu}_n}^n$ of p' at $\mu = \bar{\mu}_n$ transformed by the RG for $n = 0, 1, \ldots, 5$ (period-2^n NTCB). Convergence to a universal distribution representative of the continuous limit. Inset of (b): log-log plot of $D^2 = \int dX\,(p_{2^n} - p_{32})^2$ vs 2^n.

consequence of this observation is the qualitative band-by-band self-similarity of the bifurcation diagram of these CMLs, parallel to that of their local map S_μ. Quantitative agreement improves rapidly with decreasing μ, and is already excellent at relatively small orders.

In fact, statistical properties of CMLs are not expected to depend strongly on the coupling operator, provided it remains local [6]. It is a classic calculation to show that $\mathbf{\Delta}_g^m$ converges, for large m, to $\mathbf{\Delta}_\lambda^\infty = \exp(\frac{\lambda^2}{2}\nabla^2)$, a coupling operator with Gaussian weights where $\lambda = 2\sqrt{gm}\|\vec{e}\|$ is the typical coupling range with $\|\vec{e}\|$ the lattice mesh size (usually set to 1). For an infinite lattice, $\|\vec{e}\|$ plays no role while λ determines the size of the smallest structures. To be meaningful, the large m limit must therefore be taken at fixed $\lambda = \lambda_0$ and, consequently, $\|\vec{e}\| \to 0$. This constitutes the correct continuous limit of CMLs, i.e., a "field map" where the field $\mathbf{X}_{\vec{r}}$ with $\vec{r} \in \mathbb{R}^d$ evolves under the operator $\mathbf{\Delta}_{\lambda_0}^\infty \circ \mathbf{S}_\mu$. The asymptotic state is then unique, since λ is the unit length, and one can observe only the strong-coupling regime. In other words, $\lim_{m\to\infty} g_e^*(m) = 0$. In the continuous limit, RG relation (6) reads

$$(\mathbf{\Delta}_{\lambda_0}^\infty \circ \mathbf{S}_\mu)^2 = \mathbf{h}_\mu^{-1} \circ \mathbf{\Delta}_{\lambda_0\sqrt{2}}^\infty \circ \mathbf{S}_{q(\mu)} \circ \mathbf{h}_\mu , \quad (8)$$

which implies that length scales are renormalized by a factor of $\beta = \sqrt{2}$, independently of the local map [14]. Space-independent quantities such as p^t, on the other hand, scale with the Feigenbaum constants of the local map.

RG relation (8) is approximate only insofar as the RG of S_μ is approximate. It does not predict the behavior of the continuous CML on the interval $[\bar{\mu}_1, \bar{\mu}_0]$, but implies that, whatever this behavior may be, it is reproduced on intervals $[\bar{\mu}_{n+1}, \bar{\mu}_n]$ with an added 2^n periodicity and a rescaling of lengths by β^n. This proves that the cascades of phase transitions are infinite and that every critical point μ_n^c observed in $[\bar{\mu}_{n+1}, \bar{\mu}_n]$ has counterparts in the higher-order μ intervals which converge with the exponent δ. Moreover, they must all share the same critical properties, since the characteristic divergence of the correlation length scales in the same way in $|\mu - \mu_n^c|$ for all n. Again, all the properties of the continuous limit are, of course, only exact for tent maps; for more general maps, they are quantitatively valid in the $n \to \infty$ limit, in parallel to the status of the RG for S_μ itself.

RG relation (6) implies that all CMLs $\mathbf{\Delta}_g^m \circ \mathbf{S}_\mu$ converge to their continuous limit as $\mu \to \mu_\infty$ and/or $m \to \infty$. The results derived above are expected to apply in this limit, which, in practice, is reached very fast (Figs. 2 and 3). However, one can argue further that the critical properties of the phase transition points, where the correlation length diverges, are not expected to depend on the details of the coupling, and thus should all be the same for *any* μ and m. This is in agreement with the direct measurement of the critical exponents for the first three period-doubling phase transitions of $d = 2$ lattices of coupled logistic maps [9].

Some of the conclusions reached in the present work are identical to those reached in [6], but they are neither restricted to the weak coupling limit, nor to weakly inhomogeneous solutions. They explain the numerical observations of [7], where banded states were studied at rather large coupling ($g \simeq 0.1$) for $d = 2$ lattices of logistic maps. We believe our work is also relevant to the globally coupled case and provides the framework for a rigorous RG approach of systems of coupled maps. Finally, we would like to suggest that the continuous-space limit defined above constitutes an interesting system by itself, perhaps more tractable than CMLs for studying NTCB and spatiotemporal chaos. Since then $g_e = 0$, this limit is not continuously related to the weak coupling regimes. This may explain the difficulties encountered when trying to extend weak coupling results to account for truly collective, strong-coupling behavior [15].

[1] See, e.g., *Universality in Chaos,* edited by P. Cvitanović (Adam Bilger, Boston, 1989), 2nd ed.

[2] M. J. Feigenbaum, J. Stat. Phys. **19**, 25 (1978); **21**, 669 (1979); Physica (Amsterdam) **7D**, 16 (1983); P. Coullet and J. Tresser, J. Phys. C **5**, 25 (1978).

[3] P. Collet and J. P. Eckmann, *Iterated Maps of the Interval as Dynamical Systems* (Birkhäuser, Boston, 1980).

[4] B. Derrida, A. Gervois, and Y. Pomeau, J. Phys. A **12**, 269 (1979).

[5] See, e.g., *Theory and Applications of Coupled Map Lattices,* edited by K. Kaneko (Wiley, New York, 1993).

[6] For a review, see S. P. Kuznetsov in [5] and references therein, in particular, S. P. Kuznetsov and A. S. Pikovsky, Physica (Amsterdam) **19D**, 384 (1986).

[7] W. van der Water and T. Bohr, Chaos **3**, 747 (1993).

[8] H. Chaté and P. Manneville, Prog. Theor. Phys. **87**, 1 (1992); Europhys. Lett. **17**, 291 (1992); H. Chaté and J. Losson, Physica (Amsterdam) **103D**, 51 (1997).

[9] P. Marcq, Ph.D. thesis, Université P. & M. Curie, 1996; P. Marcq, H. Chaté, and P. Manneville (to be published).

[10] For $g = 0$ (no coupling), there are $\mathcal{N} = 2^N/2$ such frozen patterns. For small $g > 0$, $\mathcal{N}$ is smaller, but $\mathcal{N} \sim \exp(N)$, with N being the number of sites in the lattice. For $g > g_e(\mu)$, $\mathcal{N}$ is small and *independent* of N [11].

[11] A. Lemaître and H. Chaté (to be published).

[12] The actual period could be larger than 2^n and/or combined with a quasiperiodic cycle.

[13] In fact, this usually happens for $g \leq g_e^*$.

[14] This explains, incidentally, why the numerical determination of the collective behavior is difficult in this region.

[15] See, e.g., J. Bricmont and A. Kupiainen, Commun. Math. Phys. **178**, 703 (1996); Physica (Amsterdam) **103D**, 18 (1997).

Renormalization Group for Strongly Coupled Maps

Anaël Lemaître[1,2] and Hugues Chaté[2,1]

[1] *LadHyX — Laboratoire d'Hydrodynamique, École Polytechnique, 91128 Palaiseau, France*

[2] *CEA — Service de Physique de l'État Condensé, Centre d'Études de Saclay, 91191 Gif-sur-Yvette, France*

Abstract

Systems of strongly-coupled chaotic maps generically exhibit collective behavior emerging out of extensive chaos. We show how the well-known renormalization group (RG) of unimodal maps can be extended to the coupled systems, and in particular to coupled map lattices (CMLs) with local diffusive coupling. The RG relation derived for CMLs is non-perturbative, i.e. not restricted to a particular class of configurations nor to some vanishingly small region of parameter space. After defining the strong-coupling limit in which the RG applies to almost all asymptotic solutions, we first present the simple case of coupled tent maps. We then turn to the general case of unimodal maps coupled by diffusive coupling operators satisfying basic properties, extending the formal approach developed by Collet and Eckmann [1] for single maps. We finally discuss and illustrate the general consequences of the RG: CMLs are shown to share universal properties in the space-continuous limit which emerges naturally as the group is iterated. We prove that the scaling properties of the local map carry to the coupled systems, with an additional scaling factor of lengthscales implied by the synchronous updating of these dynamical systems. This explains various scaling laws and self-similar features previously observed numerically.

1 Introduction

Renormalisation group (RG) ideas have been instrumental in unveiling the universal features of the cascades of bifurcations of nonlinear dynamical systems with few degrees of freedom [2]. Simple maps of the real interval such as the logistic map have been the models of choice on which most theoretical advances were made. [3, 1, 4, 6] These results have contributed greatly to our understanding of (temporally) chaotic systems.

Our current understanding of *spatiotemporal chaos* is, however, much less advanced, and no similarly general framework is available. As a matter of fact, even the term spatiotemporal chaos is somewhat ill-defined, loosely refering to situations where the basic equations cannot be legitimately reduced to the interaction of a few modes. Of all models of spatiotemporal chaos, coupled map lattices (CMLs) are among the most attractive. These discrete-time discrete-space dynamical systems in which maps, arranged at the nodes of a lattice, interact locally can be seen as the direct correspondents, at the spatiotemporal level, of the simple maps of the interval mentioned above. Existing literature on CMLs tend to be overwhelmingly descriptive, stressing the ability of these models to mimick nature, but lacking unifying, structuring results [7]. In particular, there is not, so far, any notion of universality akin to that at work within low-dimensional dynamical systems.

In this context, it has appeared natural to some researchers to try to extend single-map RG to CMLs, in the hope of uncovering some universal features of these systems, and more, generally, of spatiotemporal chaos. These works are, however, restricted to perturbative treatments around the accumulation points of bifurcation cascades of the local map and usually consider the limit of weak coupling between maps for configurations limited to small deviations from spatially-homogeneous solutions in one or two space dimensions [8, 9]. One notable exception is the numerical work of van de Water and Bohr [10], who showed numerically that many quantities of interest do exhibit scaling properties related to those of the local map, even for rather large values of the coupling.

Recently, we introduced a non-perturbative renormalization group approach to CMLs with linear diffusive coupling which translates to the spatiotemporal level the universal features of the local maps involved [11]. We showed that, under broad conditions, the bifurcation diagrams of CMLs present the same self-similarity as that of their local maps, with the same coupling-independent

accumulation point, around which lengthscales diverge with a universal scaling related to the diffusive coupling. Here, we give a more comprehensive exposition of these results, following in particular the approach of Collet and Eckmann of the RG for simple maps [1].

The paper is organized as follows.

In Section 2, we define the general CMLs we study, which consist of identical, chaotic, unimodal, local maps coupled by a local "diffusive" coupling operator. We then present a short description of their collective dynamics in the limit of strong coupling between maps, which are the regimes where our RG approach is most important since it then applies to almost all asymptotic solutions. This is followed by the introduction of the continuous-space limit of these CMLs, which plays a major role in the RG treatment.

Section 3 is devoted to a precise definition and a quantitative estimate of the strong-coupling limit mentioned above. Various degrees of collective dynamics are defined, and their relationship to the band structure of the local chaos explained.

Our extension of RG methods to CMLs is first presented in Section 4 for the case of coupled tent maps, where the RG is "exact" and explicit. The consequences of these results on various dynamical properties are also discussed.

In Section 5, we treat the case of coupled general unimodal maps. The approach of Collet and Eckmann is formally extended to CMLs, and approximations of their RG are introduced.

Section 6 is a conclusion where we summarize our results and discuss some general issues related to our findings.

2 Collective dynamics

We consider the discrete-time evolution of an infinite ensemble of (real) variables $\mathbf{X} = (\mathbf{X}_{\vec{r}})_{\vec{r}\in\mathcal{L}}$ for some index set $\mathcal{L}$. In the following, $\mathcal{L}$ will usually represent a regular lattice. But the case of globally-coupled maps will also be discussed, in particular in the conclusion. Each *local* variable takes its value on an interval I while the whole configuration $\mathbf{X}$ lies in the phase space $\mathbf{I} = I^{\mathcal{L}}$. The instantaneous configuration $\mathbf{X}^t$ is updated synchronously by

$$\mathbf{X}^{t+1} = \mathbf{\Delta} \circ \mathbf{S}\left(\mathbf{X}^t\right) , \tag{1}$$

where $\mathbf{S}$ transforms each variable $\mathbf{X}_{\vec{r}}^t$ by a non-linear local map S, and $\mathbf{\Delta}$ is a linear coupling operator [1]. Following classic works on single maps, we consider one-parameter families of non-linear local maps. Without loss of generality, such maps can be written under the form

$$S_\mu(X) = 1 - \mu|X|^{1+\varepsilon} \text{ with } \mu \in [0,2] \text{ and } \varepsilon \geq 0\,, \tag{2}$$

which leaves the interval $I = [-1,1]$ invariant. We will in particular consider, in the following, the tent ($\varepsilon = 0$) and the logistic ($\varepsilon = 1$) maps.

Such dynamical systems exhibit a rich phenomenology rooted in the opposition between the coupling, which drives the local variables towards complete synchronization, and the non-linearity of the map, which may produce chaos. The macroscopic behavior of such systems can be characterized by the evolution in time of $\mathcal{L}$-averaged quantities like the mean $M^t = \langle \mathbf{X}_{\vec{r}}^t \rangle$, higher-order moments, multi-point correlations, etc. In particular, single-point moments $\left\langle (\mathbf{X}_{\vec{r}}^t)^k \right\rangle$ of all orders are contained in the instantaneous distribution (pdf) of local values p^t. The collective dynamics can be related to emerging mesoscopic structures — formation of clusters, synchronization — and to the microscopic trajectories of local variables.

2.1 Coupled map lattices

2.1.1 Diffusive coupling: general properties

In the case of coupled map lattices, the local variables $\mathbf{X}_{\vec{r}}$ can be chosen to lie at the nodes of a d-dimensional hypercubic lattice: $\mathcal{L} = Z^d$, and $\mathbf{\Delta}$ to be a diffusive coupling operator. In the following, we consider operators $\mathbf{\Delta}$ which verify some basic properties [8]:

1. Linearity, homogeneity and symmetry, which allow to write,

$$[\mathbf{\Delta}(\mathbf{X})]_{\vec{r}_1} = \int \mathcal{D}\left(\vec{r}_1 - \vec{r}_2\right) \mathbf{X}_{\vec{r}_2} d\vec{\rho},$$

where the kernel $\mathcal{D}\left(\vec{r}_1 - \vec{r}_2\right)$ only depends on the vector difference between an image site $\vec{r}_1$ and an antecedent $\vec{r}_2$; spatial symmetry, $\mathcal{D}\left(\vec{\rho}\right) = \mathcal{D}\left(-\vec{\rho}\right)$ guarantees that the spectrum $\widetilde{\mathcal{D}}\left(\vec{k}\right)$ is real.

2. Normalization: $\int \mathcal{D}\left(\vec{\rho}\right) d\vec{\rho} = 1$ or $\widetilde{\mathcal{D}}\left(\vec{0}\right) = 1$ and non-negativity: $\mathcal{D}\left(\vec{\rho}\right) \geq 0$: it implies that the spectrum $\widetilde{\mathcal{D}}\left(\vec{k}\right)$ of $\mathbf{\Delta}$ lies in the unit circle. The

[1] this definition excludes the case of the so-called "inertial coupling" (see *e.g.* [7]) where the coupling operator involves $\mathbf{S}(\mathbf{X}^t)$ *and* $\mathbf{X}^t$ itself.

coupling operator has only one eigenvalue equal to 1 corresponding to the configurations where all sites are synchronized; the others are smaller than one, and therefore all volumes in the phase space shrink to the line $\mathbf{I}_{\text{syn}}$ of synchronized states when $\mathbf{\Delta}$ is applied repeatedly.

3. Locality: $\int \vec{\rho}^2 \mathcal{D}(\vec{\rho})\, d\vec{\rho} = \lambda_0^2 < \infty$ is a diffusion constant, and the *coupling length* λ_0 defines the range of the coupling. It is proportional to the lattice mesh size $\|\vec{e}\|$ (usually taken to 1): $\lambda_0 = c_0\|\vec{e}\|$.

These properties lead to the following form of the spectrum in the region of small wavenumbers:

$$\tilde{\mathcal{D}}\left(\vec{k}\right) = 1 - \frac{\lambda_0^2}{2}k^2 + \cdots . \tag{3}$$

The large-scale dynamics of coupled systems is expected to depend essentially on the coupling range λ_0 and not on the details of the coupling.

For numerical convenience, the diffusive coupling is usually taken to be the so-called *forward* coupling to nearest-neighbors:

$$[\mathbf{\Delta}_g(\mathbf{X})]_{\vec{r}} = (1 - 2dg)\mathbf{X}_{\vec{r}} + g\sum_{\vec{e}\in\mathcal{V}}\mathbf{X}_{\vec{r}+\vec{e}}\,. \tag{4}$$

where g is the *coupling strength*, and $\mathcal{V}$ denotes the set of the $2d$ nearest-neighbors of site $\vec{0}$. This operator verifies the properties (1-3) with $\lambda_0 = \sqrt{2g}\|\vec{e}\|$. Even though we do not consider this possibility in the following, our results also apply to the so-called *backward* coupling, defined implicitly through the relation

$$[\mathbf{\Delta}_g(\mathbf{X})]_{\vec{r}} = \mathbf{X}_{\vec{r}} + g\sum_{\vec{e}\in\mathcal{V}}\left([\mathbf{\Delta}_g(\mathbf{X})]_{\vec{r}+\vec{e}} - [\mathbf{\Delta}_g(\mathbf{X})]_{\vec{r}}\right).$$

2.1.2 Lattice dynamics

The behavior of the local map S_μ is well-known. Parameter space is divided into two parts. For small values of μ, the only attractors are periodic cycles of period 2^k, while chaotic behavior can be observed for $\mu > \mu_\infty$ (with $\mu_\infty = 1$ for the tent map, and $\mu_\infty = 1.401\ldots$ for the logistic map).

In the chaotic region of the local map and for the strong, "democratic", equal-weight coupling $g = 1/(2d+1)$, the CMLs defined above display *non-trivial collective behavior* (NTCB) [12]: almost all initial conditions flow towards one of a few attractors which possess a well-defined infinite-size, infinite-time limit (see Section 3 below and [13] for a quantitative assessment of this

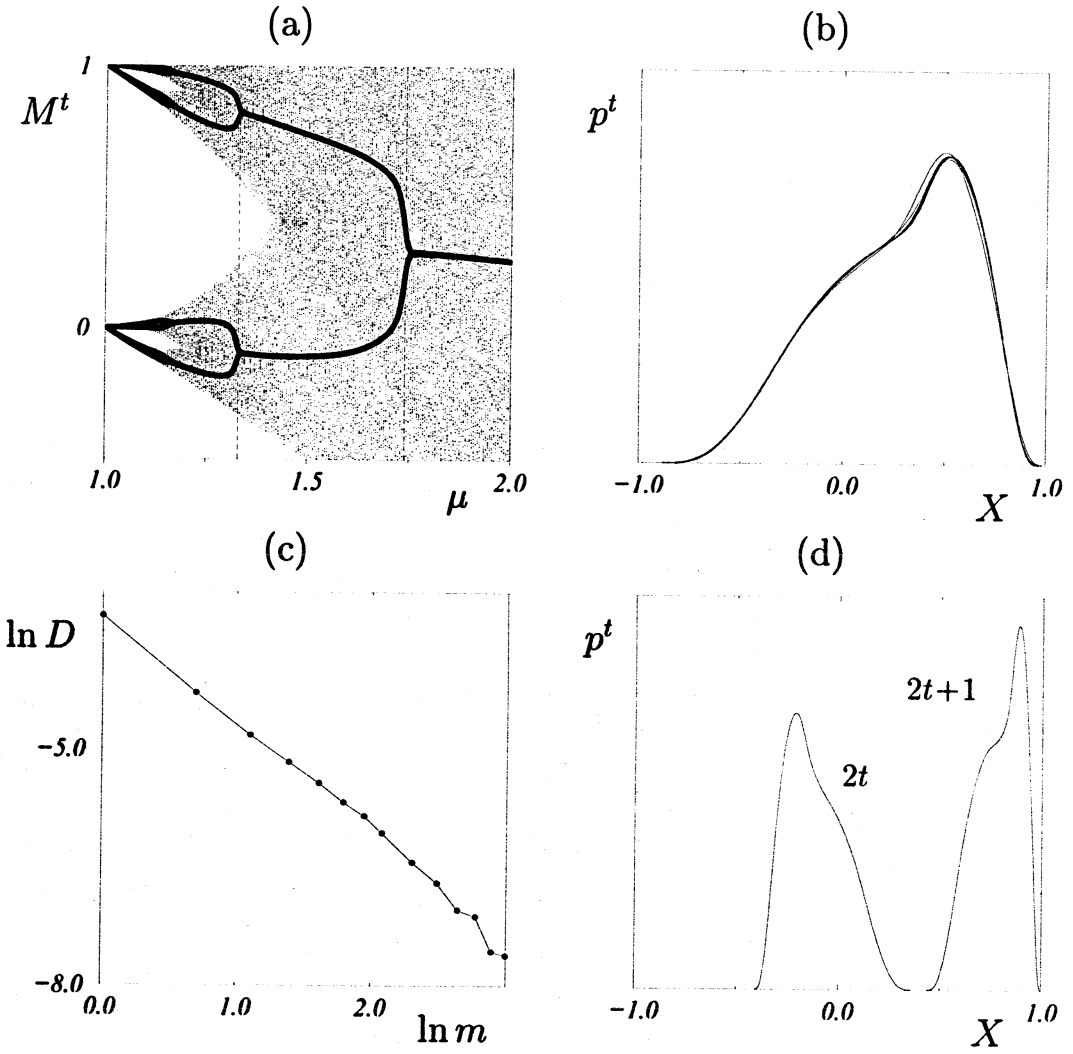

Figure 1: Democratically-coupled ($g = 0.2$) tent maps on a $d = 2$ lattice of linear size $L = 2048$ with periodic boundary conditions: (a) bifurcation diagram of $M^t = \langle \mathbf{X} \rangle^t$ (filled circles) superimposed on that of the local map S_μ (small dots). (b-d): Asymptotic (large t) single-site distributions p^t (b): stationary states at $\mu = 2$ for $1 \leq m \leq 32$. For $m > 1$, the distributions cannot be separated on this graph; they converge to a universal distribution of the continuous limit. (c): log-log plot of the distance $D^2 = \int \mathrm{d}X \, (p_m - p_{32})^2$ vs m. (d): period-2 collective cycle at $\mu = \bar{\mu}_1$ for $m = 1$.

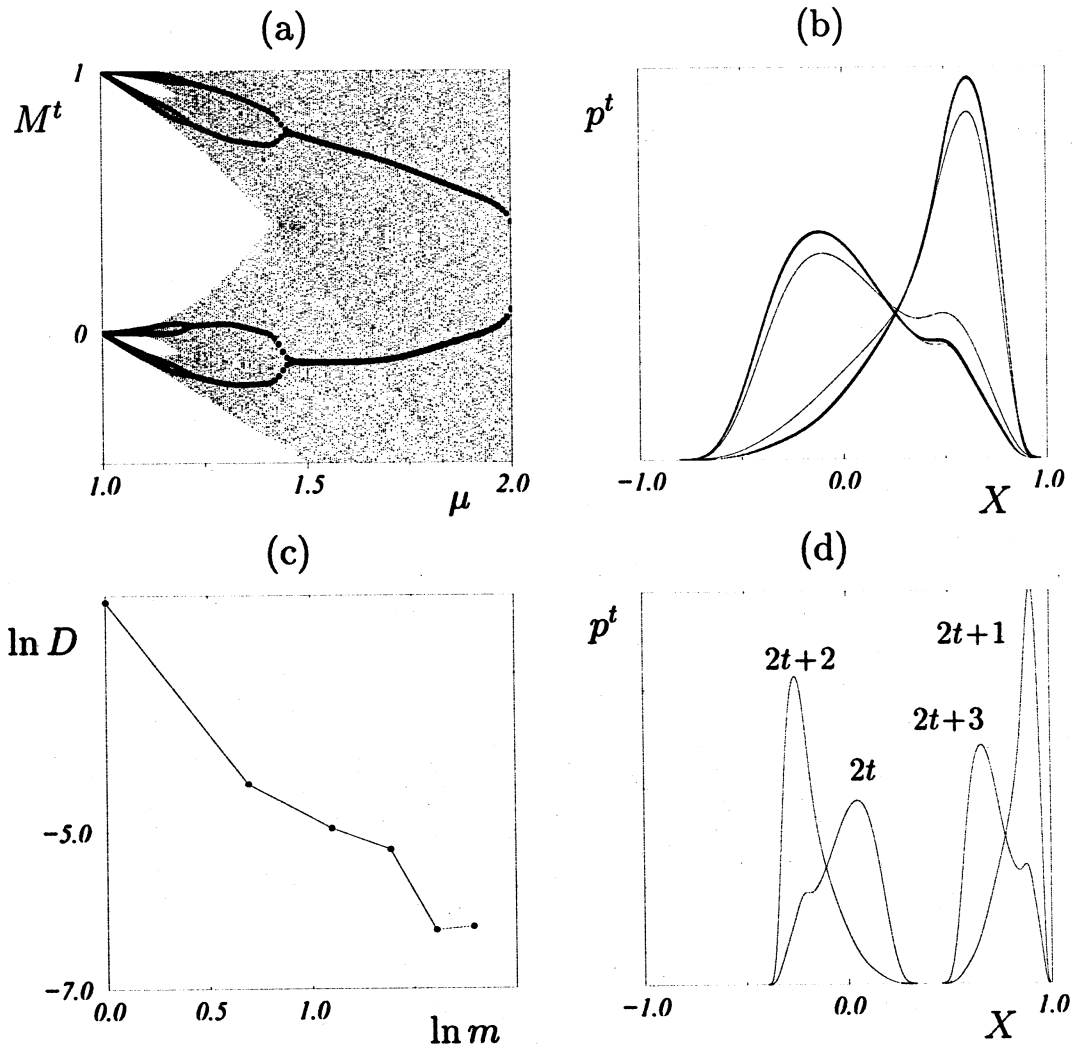

Figure 2: $d = 3$ lattice of democratically-coupled ($g = 1/7$) tent maps of linear size $L = 128$ with periodic boundary conditions: (a): bifurcation diagram of M^t (filled circles) superimposed on that of the local map (small dots). (b): Asymptotic period-2 collective cycle for the single-site distribution p^t at $\mu = 2$ for $1 \leq m \leq 8$. (c): log-log plot of the distance $D^2 = \int \mathrm{d}X\, (p_m - p_8)^2$ vs m. (d): Asymptotic period-4 collective cycle for the single-site distribution p^t at $\mu = \bar{\mu}_1$ for $m = 1$.

statement). In the asymptotic regime, spatial averages usually display a low-dimensional motion (periodic, quasiperiodic,...) while local trajectories are chaotic. (Chaos is in fact *extensive*, as seen, e.g., from the proportionality of the Kolmogorov-Sinai entropy to the volume of the system.) Figure 1 and 2 show the bifurcation diagrams of the spatial average $M^t = \langle \mathbf{X}_{\vec{r}}^t \rangle$ for two- and three-dimensional lattices of coupled tent maps. Decreasing μ at fixed g, one observes period-doubling of the collective behavior, reminiscent of the self-similar structure of bands of the local map. The instantaneous distribution p^t is smooth and well-defined in the infinite-size limit and follows the same collective behavior as M^t. These period-doubling macroscopic bifurcations are actually Ising-like phase transitions, and their critical points μ_n^c differ from the band-splitting points $\bar{\mu}_n$ of S_μ [14]. Approaching μ_∞, it rapidly becomes numerically impossible to resolve the particular NTCB since prohibitively large lattices as well as increasing numerical resolution are then required. In particular, near μ_∞ the uniqueness of the attractor cannot be ascertained, and no evidence of an infinite cascade of phase transitions is available.

Although only periodic motion have been observed in dimensions $d = 2$ and 3 (see figs. 1 and 2), more complex NTCB exist for $d > 3$. Four-dimensional CMLs display regions of the parameter μ where two periodic attractors coexist (*e.g.* period-2 and period-4 collective regimes for coupled tent maps). Five-dimensional CMLs display quasi-periodic collective behavior.

2.2 Continuous limit

2.2.1 Iterated couplings

A straightforward generalization of CMLs of the form $\mathbf{\Delta}_g \circ \mathbf{S}_\mu$ consists in applying several times the operator $\mathbf{\Delta}_g$ after each transformation $\mathbf{S}_\mu$: the evolution operator becomes $\mathbf{\Delta}_g^m \circ \mathbf{S}_\mu$ and involves the m-th neighborhood of each site. Although the importance of such systems is not evident at this stage, they play an essential role in the RG (see Section 4).

In the small wavenumber limit, the spectrum of $\mathbf{\Delta}_g^m$ reads,

$$\tilde{\mathcal{D}}_g^m\left(\vec{k}\right) = 1 - \frac{\lambda_0^2 m}{2} k^2 + \cdots .$$

For large m, the iterated operator $\mathbf{\Delta}_g^m$ is equivalent to the coupling operator with Gaussian kernel:

$$\mathbf{\Delta}_g^m \underset{m\to\infty}{\simeq} \mathbf{\Delta}_\lambda^\infty = \exp\left(\frac{\lambda^2}{2}\nabla^2\right),$$

where $\lambda = \lambda_0\sqrt{m} = c_0\sqrt{m}\|\vec{e}\|$ is the typical range of the coupling and $\|\vec{e}\|$ is the lattice mesh size. This coupling length λ fixes the size of small structures, therefore the length below which no spatial average can be performed: it is the relevant length scale for macroscopic dynamics. When $m \to \infty$, the coupling operator should keep a finite range: we call the limit $m \to \infty$, taken at fixed λ and $\|\vec{e}\| \propto 1/\sqrt{m} \to 0$, the *continuous limit* since it is a continuous-space limit of usual CMLs. In this limit, a d-dimensional field of variables $\mathbf{X} = (\mathbf{X}_{\vec{r}})_{\vec{r}\in\mathcal{L}}$, $\mathcal{L} = R^d$, evolves under the discrete-time dynamics $\mathbf{\Delta}_\lambda^\infty \circ \mathbf{S}_\mu$. No continuous-time limit is defined for such systems: they constitute a Poincaré-section version of the evolution of spatially extended systems.

The parameter λ plays a trivial role since it is the only length scale which remains after the limit $\|\vec{e}\| \to 0$ has been taken: changing λ amounts to a mere zoom over space. Therefore, the collective behavior of one-site macroscopic variables like M^t or p^t does not depend on λ, while correlation functions are simply rescaled by a change of λ. Note that the limit reached, $\mathbf{\Delta}_\lambda^\infty$, is "universal", since it is independent of the choice of the operator $\mathbf{\Delta}_g$, provided it satisfies properties (1-3).

2.2.2 Numerics

Careful numerical investigation of dynamics of the form $\mathbf{\Delta}_g^m \circ \mathbf{S}_\mu$ has been performed for $d = 2$ and 3 lattices of democratically-coupled logistic and tent maps for increasing values of m. In these cases, bifurcation diagrams for any m are not distinguishable from those displayed in Fig. 1 corresponding to the case $m = 1$. Asymptotic distributions in the fixed point regime of 2-dimensional lattice of size $L = 2048$ at $\mu = 2$ are given in Fig. 1: at fixed μ, they quickly converge with increasing m to a well-defined asymptotic pdf, as seen from the estimation of the distances $D(p_1, p_2) = \sqrt{\int (p_1 - p_2)^2}$ (see insert of Fig. 1). In these cases at least, the collective behavior is extremely weakly dependent on the details of the coupling, and the lattice behavior is qualitatively similar to the continuous limit.

In higher dimensions, the comparison of the usual CMLs ($m = 1$) with systems with increasing values of m, shows noticeable (qualitative) differences. For example, in dimension 4, the coexistence of macroscopic attractors seems to disappear for $m \simeq 8$ [15]. However, the numerical estimation of the collective behavior displayed in the continuous limit requires lattices with an increasing linear size, and consequently prohibitive number of sites. The pre-

cise evaluation of the continuous limit therefore seems to be beyond capability of current computers.

3 Conditions for non-trivial collective behavior

Non-trivial collective behavior is observed for strong enough coupling. If the coupling is weak, spatially-blocked clusters of various phases can coexist, leading to infinitely many possible macroscopic attractors. This is especially the case when the local map is in a band-chaos regime since then clusters of the different band "phases" are observed in space. The strong coupling limit, in this context, appears as the coupling strength beyond which no blocked interfaces between bands exist, so that all sites get "synchronized" in the same band from almost all initial conditions.

The NTCB regimes displayed in Section 2.1 assume that the strong coupling limit is realized. However, the existence of some limit value g_e^* of the coupling above which the strong coupling assumption is valid remains unclear and need to be studied quantitatively. In the following, we prove the existence of g_e^* and provide some quantitative numerical estimates of this quantity marking the onset of NTCB.

3.1 Bands

3.1.1 Banded chaos

We first review briefly the phenomenology displayed by unimodal maps. Some of their universal features like the order of occurrence of periods [5] or the internal similarity [6] depend only on the existence of a unique maximum and this property is usually referred to as structural universality.

When the parameter μ increases, the map S_μ undergoes a cascade of subharmonic bifurcations. We denote μ_n the value at which the period 2^{n-1} regime becomes unstable and above which the system enters period 2^n. These points accumulate at some critical value μ_∞ where the system enters the chaotic regime. Above this value, the local map displays banded chaos, possibly intermingled with parameter windows of periodic behavior.

At the other end of the inverse cascade, at the value $\bar{\mu}_0 = 2$, trajectories run over the whole interval $I = [-1, 1]$. When μ decreases, asymptotic trajectories run over one band $I^0_{S_\mu} = [1 - \mu, 1]$, the smallest invariant interval for

S_μ. This band splits at the value $\bar{\mu}_1$ into two bands $I^{1,0}_{S_\mu} \ni 0$ and $I^{1,1}_{S_\mu}$ which are non-intersecting invariant intervals for the iterated map S^2_μ, and ergodic components for S_μ:

$$I^{1,0}_{S_\mu} \cap I^{1,1}_{S_\mu} = \emptyset \ , \ S_\mu\left(I^{1,0}_{S_\mu}\right) \subset I^{1,1}_{S_\mu} \text{ and } S_\mu\left(I^{1,1}_{S_\mu}\right) \subset I^{1,0}_{S_\mu} \ .$$

Below $\bar{\mu}_1$, and for almost all initial condition, the system reaches an asymptotic trajectory which flips between the two bands: if X^t lies in the band $I^{1,0}_{S_\mu}$ at some even time, it will be found in $I^{1,0}_{S_\mu}$ (resp. $I^{1,1}_{S_\mu}$) at all following even (resp. odd) times.

Decreasing μ towards μ_∞, an inverse cascade of band splitting bifurcations occurs. We denote $\bar{\mu}_n$ the point below which the regime with 2^n bands takes place: for $\mu \in [\mu_\infty, \bar{\mu}_n]$, the iterated map $S^{2^n}_\mu$ admits 2^n ergodic components over which asymptotic trajectories of the variable X^t run periodically. Let us denote $I^{n,\sigma}_{S_\mu}, \sigma = 0, \cdots, 2^n - 1$ these 2^n bands with the following convention: take the "central" band $I^{n,0}_{S_\mu} \ni 0$, and order the bands such that

$$I^{n,\sigma}_{S_\mu} = S^\sigma_\mu\left(I^{n,0}_{S_\mu}\right) \ .$$

Therefore, the action of S_μ on these bands amounts to the permutation $\sigma \to (\sigma+1)[2^n]$ (modulo 2^n).

It is important to note that these intervals $I^{n,\sigma}_{S_\mu}$ are invariant under the map $S^{2^n}_\mu$ for all $\mu \in [\mu_\infty, \bar{\mu}_n]$, even though, approaching μ_∞, the system reaches regimes with more and more bands. For example, $I^0_{S_\mu}$ is the stable interval of S_μ for all μ, and below $\bar{\mu}_1$, the two bands $I^{1,0}_{S_\mu}$ and $I^{1,1}_{S_\mu}$ are subsets of $I^0_{S_\mu}$. Furthermore, if $\mu \leq \bar{\mu}_n \leq \bar{\mu}_1$, the map has 2^n bands, but $I^{1,0}_{S_\mu}$ and $I^{1,1}_{S_\mu}$ are still exchanged by S_μ and all even (resp. odd) bands lie on $I^{1,0}_{S_\mu}$ (resp. $I^{1,1}_{S_\mu}$):

$$I^{n,2\sigma}_{S_\mu} \subset I^{1,0}_{S_\mu}, \text{ and } I^{n,2\sigma+1}_{S_\mu} \subset I^{1,1}_{S_\mu} \ .$$

3.1.2 Banded states

Let us now consider the evolution of some configuration $\mathbf{X}^t$ under an operator of the form $\mathbf{\Delta}^m_g \circ \mathbf{S}_\mu$. Whenever $\mu \in [\mu_\infty, \bar{\mu}_n]$, the local map has (at least) 2^n bands: we denote $\mathbf{I}^{n,\sigma}_{S_\mu}$ the set of configurations for which all variables $\mathbf{X}_{\vec{r}}$ lie on the band $I^{n,\sigma}_{S_\mu}$:

$$\mathbf{I}^{n,\sigma}_{S_\mu} = \left(I^{n,\sigma}_{S_\mu}\right)^{\mathcal{L}} \ .$$

$\mathbf{S}_\mu$ operates a permutation on σ, and since the operator $\mathbf{\Delta}^m_g$ keeps intervals stable, $\mathbf{\Delta}^m_g \circ \mathbf{S}_\mu$ operates the same permutation $\sigma \to (\sigma+1)[2^n]$: these intervals $\mathbf{I}^{n,\sigma}_{S_\mu}$ constitute generalized bands in the phase space $\mathbf{I} = [-1,1]^{\mathcal{L}}$.

If the configuration $\mathbf{X}^t$ falls on some of these intervals at some time, it runs periodically over these 2^n bands at all following times. We call such at state of the system a *banded state of order n* (BSn). The fact that the system is in a BSn does not imply that it displays a period-2^n macroscopic regime: the actual collective behavior could be of higher (multiple) periodicity, or even quasiperiodic. For example, the $d = 3$ lattice of coupled tent maps shown in Fig. 2 displays a period-2 behavior for $\mu = \bar{\mu}_0$, and the two-dimensional lattice displays period-2 just above $\mu = \bar{\mu}_1$: these are banded states of order 0 since the local map has only one band.

3.2 Non-trivial synchronization

When the local map has several bands, the coupled map system operates a permutation on the bands $\mathbf{I}_{S_\mu}^{n,\sigma}$ in the phase space: if all sites of the lattice lie in the same band at some given time (say $t = t_0$), they run together periodically over the bands of the local map. Suppose now that not the whole lattice, but some region of the lattice $\ell \in \mathcal{L}$ only has all its sites in the same band $I_{S_\mu}^{n,\sigma}$ (with, say $\sigma = 0$) at t_0 while all other variables lie in another band (say $\sigma = 1$). Inside each of these domains, the variables follow a collective regime which resembles a BS at a mesoscopic scale. However, different situations can occur at the boundaries: one domain can invade the other, in which case the system converges towards a BS, or the fronts can be blocked and clusters of different phases can coexist on the same lattice.

These situations are illustrated in Figs. 3-4 using a two-dimensional lattice of coupled tent maps for $\mu = 1.4$, a case in which the local map has two bands. Starting from random initial conditions, mesoscopic regions start flowing towards the two-band attractor: some regions of the lattice try to follow a period-2 evolution with $\sigma = 0$ while the other regions converge to the same evolution with the phase $\sigma = 1$. During the first time steps of the dynamics, clusters are formed due the indetermination on σ.

For small coupling strengths (see Fig. 3), the boundaries between these domains form walls that the coupling cannot break: the walls are pinned to the lattice and clusters persist in the infinite-time limit. The pinning allows for the co-existence of clusters on the same lattice and all the possible patterns correspond to the "ergodic components" of the dynamical system.

For stronger values of the coupling, the domain wall structure is broken as illustrated in Fig. 4 for the same lattice but with $g = 0.2$. The comparison

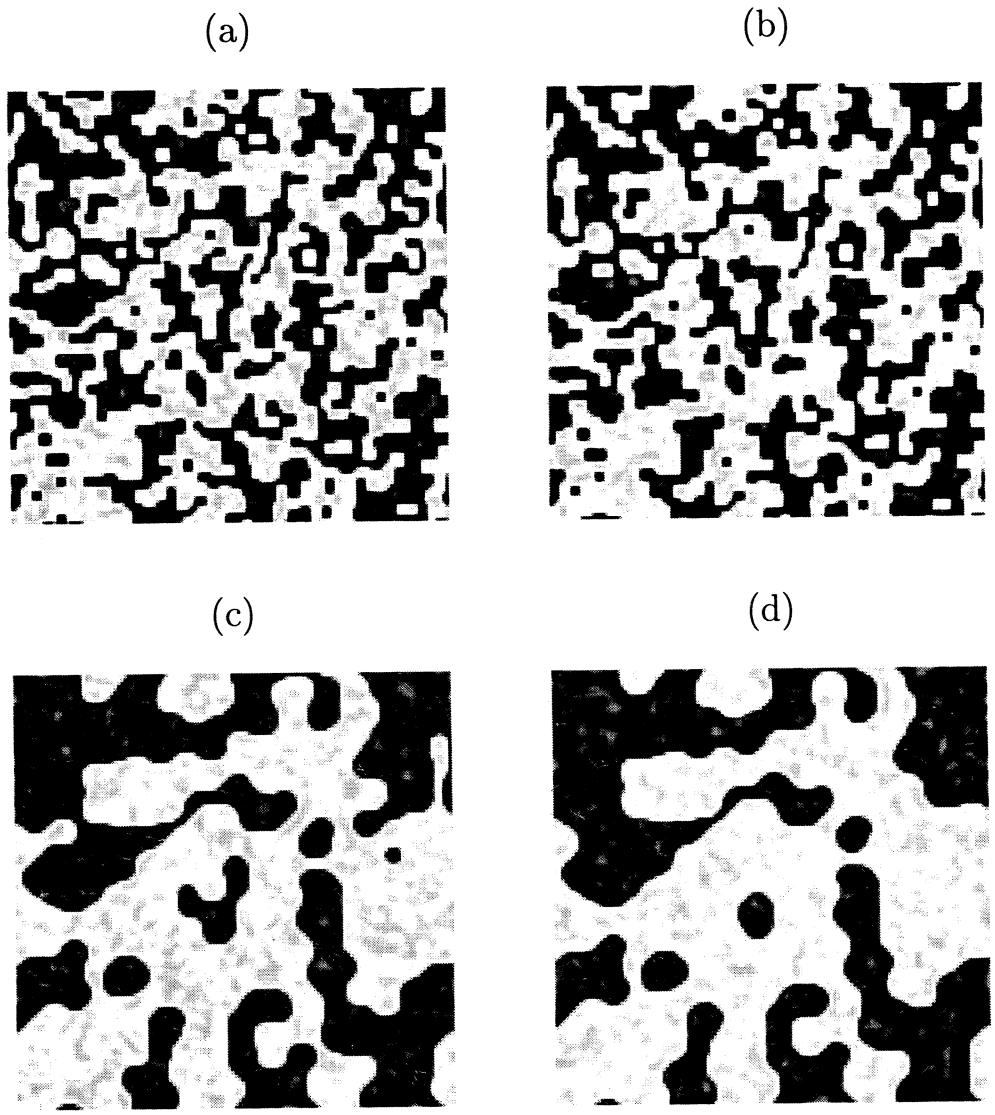

Figure 3: Snapshot of a 2-dimensional lattice of coupled tent maps of size $N = 128^2$ with periodic boundary conditions and $\mu = 1.4, g = 0.08$: (a) after a transient (b) 10000 time steps later. A few small clusters have been eliminated while the largest structures are blocked in the space and do not evolve any longer. Inside a cluster, the dynamics is similar to that of a banded state: the local variables evolve chaotically while the cluster as a whole follows a period-2 regime. (c-d) same for $g = 0.1$.

of the same lattice at different time-steps show that the smaller clusters are eliminated: except for exceptional initial conditions leading to a flat interface between the two phases, the system converges towards a banded state, and there is a unique attractor for the collective regime.

We call *non-trivial synchronization* (NTS) the property that the system reaches a BS from (almost) all initial conditions. Estimating quantitatively the value of the coupling marking the onset of NTS is a difficult task. We now briefly present how this can be achieved in the simple case of NTS to a BS1. More detailed results will be published elsewhere [13].

3.3 Estimating the onset of NTS: phase ordering of coarse-grained variables

Take some $\mu \in [\mu_\infty, \bar{\mu}_1]$, to insure that the local map has two bands, and consider first the uncoupled case ($g = 0$): each variable $\mathbf{X}_{\vec{r}}^t$ evolves independently under the local map S_μ, and its trajectory reaches the asymptotic regime where it flips between the bands $I_{S_\mu}^{1,0}$ and $I_{S_\mu}^{1,1}$. Depending on its initial value $\mathbf{X}_{\vec{r}}^0$ it falls in $I_{S_\mu}^{1,0}$ at even or odd times, and some phase variable $\sigma_{\vec{r}}^t \in \{0,1\}$ can be associated to each site. For a finite lattice of N sites, $\mathcal{N} = 2^N/2$ different patterns can be obtained, corresponding to different ergodic components for the dynamics of the configuration $\mathbf{X}^t$ in the phase space $\mathbf{I}$.

The coarse-grained variables $\sigma_{\vec{r}}^t$ are similar to Ising spins and the diffusive coupling operator $\mathbf{\Delta}_g^m$ plays the role of some ferromagnetic interaction with range $\lambda = \sqrt{2gm}\|\vec{e}\|$. When g increases, sites try to synchronize, and for strong enough coupling, isolated variables jump to the other phase (*e.g.* $\sigma_{\vec{r}}^t = 0$ surrounded by $\sigma_{\vec{r}+\vec{e}}^t = 1$). For a given $g > 0$, only clusters with a minimal transverse size survive: a continuous family of asymptotic states can be observed depending on the proportion of clusters in each phase, and the number of ergodic components is expected to scale like $\mathcal{N} \propto \exp(\alpha N)$ with the system size. Coefficient α is expected to decrease when g increases. For large values of the coupling, say $g > g_e^1(\mu, m)$, no cluster persists, all sites end up in one of the two phases and a BS1 is reached from almost all initial condition.

The direct estimation of $\mathcal{N}$ is impossible in practice, although one can easily get a flavor of the sequence of bifurcations marking the decrease of α when g is increased [16]. It is, in fact, easier to estimate $g > g_e^1(\mu, m)$ from the behavior of the probability of persistence of the coarse-grained variables, as explained now.

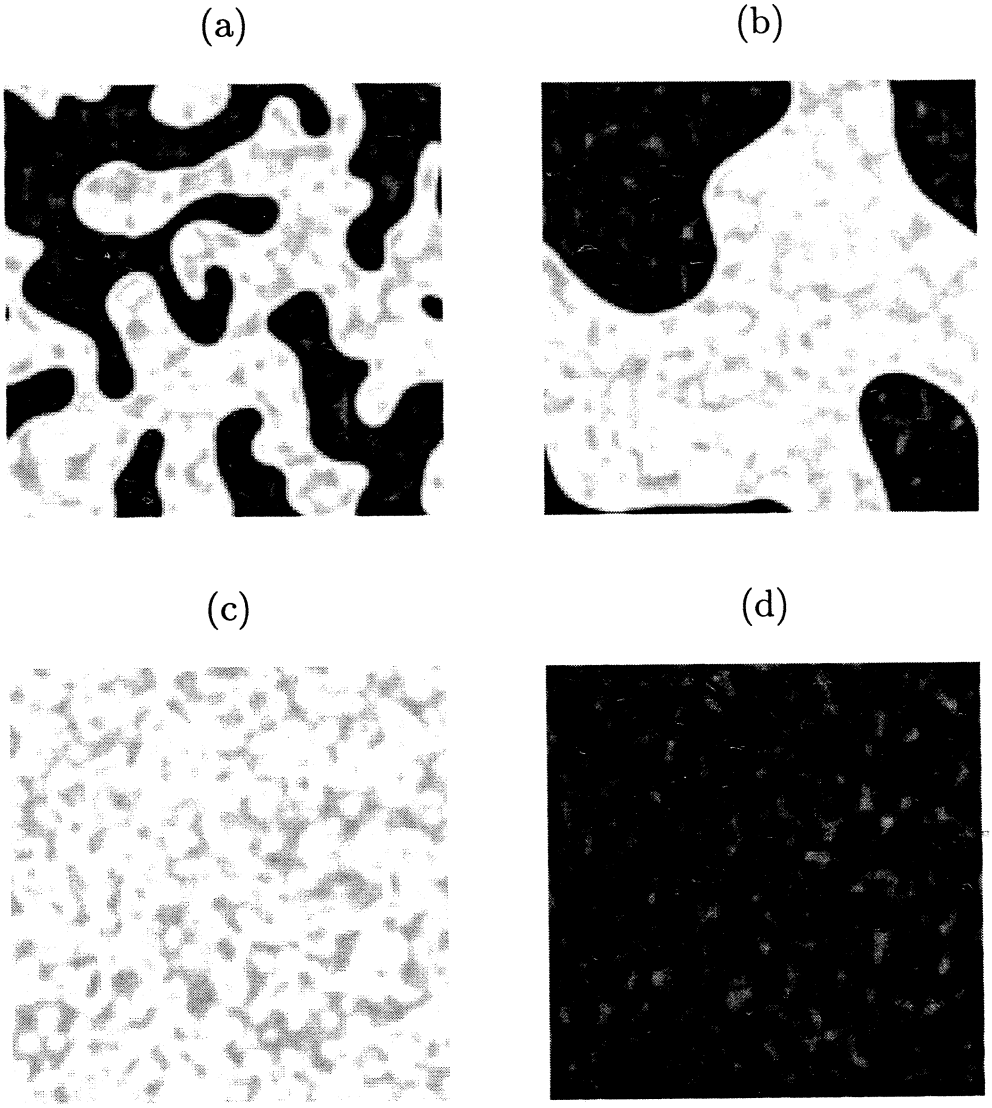

Figure 4: Snapshot of a 2-dimensional lattice of coupled tent maps of size $N = 128^2$ with periodic boundary conditions and $\mu = 1.4, g = 0.2$: (top) after a short transient (right) and 1000 time steps later (left). The fronts between the two phases propagate so that the small structures are eliminated. (bottom) 10000 and 10001 time steps later only one phase remains.

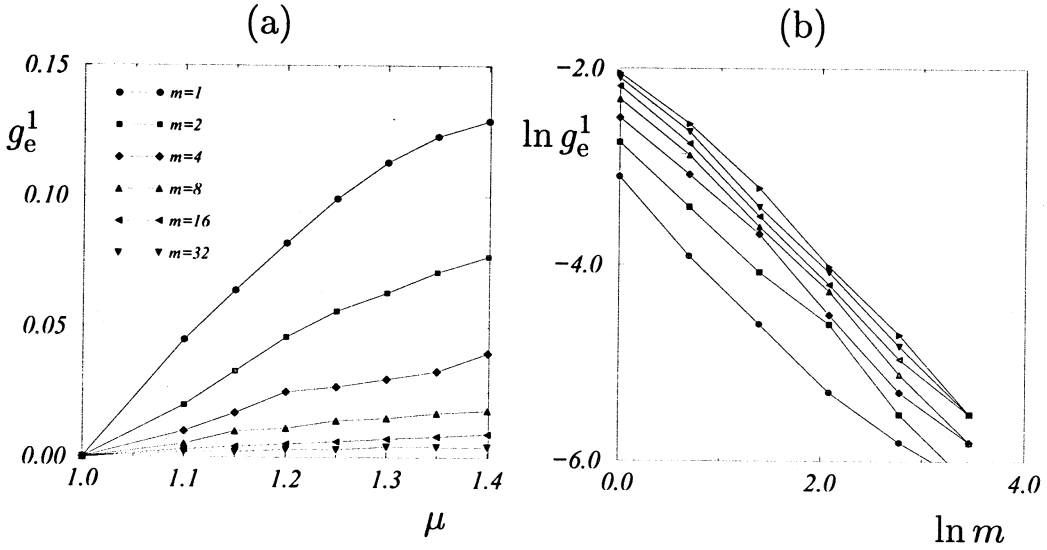

Figure 5: Values of $g_e^1(\mu, m)$ vs μ (a) and m (b) for 2-dimensional lattices of coupled tent maps ($L = 512$).

The persistence probability is defined as the fraction P^t of phase variables $\sigma_{\vec{r}}^t$ that have not changed their value since $t = 0$ (modulo the period, here two, of the local cycle):

$$P^t = P\left(\forall t' \leq t,\ \sigma_{\vec{r}}^{t'} = (-1)^{t'}\sigma_{\vec{r}}^0\right).$$

We have performed numerical investigations of the behavior of the persistence probability for $\mu \in [\mu_\infty, \bar{\mu}_1]$ and $m \geq 1$ aiming at estimating $g_e^1(\mu, m)$.

Starting from random initial conditions shared between the two bands, if no coupling is applied (g=0), $\sigma_{\vec{r}}^t = \sigma_{\vec{r}}^0$ for all sites, and $P^t = 1$ at all times. For small but non-zero coupling, the synchronization of phase variables with their neighbors is accounted for by a decay of P^t which saturates at some finite asymptotic value characterizing the pinning of different possible clusters. If g is large enough, however, the system converges towards a BS1, and P^t decreases algebraically to zero, similarly to the quench of an Ising model at zero temperature [17].

Results in the case of coupled tent maps are displayed in Fig. 5 which shows values of P^t obtained while increasing adiabatically the coupling. Such measurements allow for a rough evaluation of $g_e^1(\mu, m)$ as shown in Fig. 5-(b). Better estimates can be obtained by extrapolating the changes in the scaling behavior of P^t observed at large g to $g \to g_e^1(\mu, m)$.

The value of $g_e^1(\mu, m)$ decreases when $\mu \to \mu_\infty$: this is expected since in this limit the tendency of the local map to separate trajectories weakens

(decrease of the largest Lyapunov of the lattice) [2]. A immediate consequence of this observation is that there exists a maximal value for fixed m,

$$g_e^1(m) = \max_\mu \left[g_e^1(\mu, m) \right] = g_e^1(\bar{\mu}_1, m)$$

above which the system governed by $\mathbf{\Delta}_g^m \circ \mathbf{S}_\mu$ reaches a BS1 for all $\mu \in [\mu_\infty, \bar{\mu}_1]$ and for (almost) all initial conditions.

Similarly, $g_e^1(\mu, m)$ decreases when m increases, because then the coupling is "stronger". Therefore, there exists a maximal value

$$g_e^{1*} = \max_m \left[g_e^1(m) \right] = \max_{\mu,m} \left[g_e^1(\mu, m) \right] = g_e^1(\bar{\mu}_1, 1) \ ,$$

above which a BS1 is reached for all μ *and* m.

In fact, in the general case of coupled maps lattices (not necessarily tent maps), taking the limit $m \to \infty$ with the appropriate rescaling of the lattice mesh size $\|\vec{e}\| \propto 1/\sqrt{m} \to 0$ yields the continuous limit of the coupling operator. Since the coexistence of phases in the small coupling regime is made possible by the pinning of localized structures on lattice sites as illustrated in Fig. 3, we must expect this effect to disappear in the continuous limit:

$$g_e^1(\mu, m) \underset{m \to \infty}{\to} 0 \, .$$

Finally, these limit values correspond to the worst possible situation when the initial state is chosen to insure that the competition between bands continues at all times. In fact, if the local variables are taken randomly on the interval I at time $t = 0$, due the asymmetry between the basins of the two ergodic components of the local map, one phase predominates after a few timesteps. Then the minoritary phase is eliminated in a finite time on a macroscopic level.

3.4 Banded states when $\mu \to \mu_\infty$?

Consider $\mu \in [\bar{\mu}_2, \bar{\mu}_1]$: the local map has exactly two bands, and multistability of the two associated phases disappears at $g_e^1(\mu)$. For g above this value, the system flows towards a BS1 and asymptotically, all sites lie in the same band. If, however, $\mu \in [\bar{\mu}_3, \bar{\mu}_2]$, the local map has four bands, and local phase variables $\sigma_{\vec{r}}^t$ take their values in $\{0, 1, 2, 3\}$. The limit value $g_e^1(\mu)$ is still defined, and

[2] In fact, in the particular case of coupled tent maps which is illustrated, $g_e^1(\mu, m) \to 0$ when the parameter μ approaches μ_∞. This is not surprising since the local map presents marginal stability at $\mu_\infty = 1$: no divergence of nearby trajectories is opposed to even the smallest couplings; however this is only verified by coupled tent maps.

above it all sites fall into one of the two "meta-bands" $I_{S_\mu}^{1,0}$ or $I_{S_\mu}^{1,1}$: all $\sigma_{\vec{r}}^t$ are either even or odd.

Suppose now that the system is in a BS1, *i.e.* it flips between the intervals $\mathbf{I}_{S_\mu}^{1,0}$ and $\mathbf{I}_{S_\mu}^{1,1}$. Pinned clusters can be formed inside these bands, *e.g.* between the sub-intervals $I_{S_\mu}^{2,0}$ and $I_{S_\mu}^{2,2}$ of $I_{S_\mu}^{1,0}$: according to this new coarse-graining, an infinite number of attractors can be evidenced again. One can defined a limit value of the coupling, $g_{\mathrm{e}}^2(\mu, m)$, above which the system converges towards a BS2 starting from initial conditions *in* a BS1. Thus, for all $g > g_{\mathrm{e}}^{2*}(\mu, m)$ with

$$g_{\mathrm{e}}^{2*}(\mu, m) = \max(g_{\mathrm{e}}^1(\mu, m), g_{\mathrm{e}}^2(\mu, m)),$$

the system converges towards a BS2 starting from *any* initial condition.

One can this way define a whole hierarchy of limit coupling values $g_{\mathrm{e}}^n(\mu, m)$ above which a BSn is reached from any initial BS$n-1$. Thus the condition for NTS is defined by

$$g_{\mathrm{e}}^{n*}(\mu, m) = \max_{n' \leq n} g_{\mathrm{e}}^{n'}(\mu, m),$$

above a BSn is reached from any initial condition.

Understanding NTS in the limit $\mu \to \mu_\infty$ requires to evaluate all possible $g_{\mathrm{e}}^{n*}(\mu, m)$ in order to establish some general threshold $g_{\mathrm{e}}^*(\mu, m)$ above which NTS is observed at all orders.

It is not clear, at this stage, whether NTS persists in this limit and what occurs at the transition between the periodic $\mu < \mu_\infty$ and chaotic $\mu > \mu_\infty$ regimes of the local map: how behaves the series g_{e}^{n*} when $\mu \to \infty$. In fact, there are (naive) arguments against the existence of an infinite cascade of BS since the local chaos at work among the sites is sometimes represented as some effective noise: chaotic systems with external noise [18] show a truncated (finite) cascade of bifurcation because the refined structure of bands is broken by the noise near μ_∞. This would correspond to a situation in which, for a given $g > g_{\mathrm{e}}^{1*}$, although a BS1 can be reached for all μ, the smallest bands cannot be separated when μ goes sufficiently close to μ_∞ so that a banded state of maximal order cannot be reached and NTS is not achieved. The following presentation of RG arguments will clarify these issues.

4 Renormalization group for coupled tent maps

The sequence of periodic behavior observed on bifurcation diagrams like those displayed in Figs. 1 and 2 in strong-coupling regimes shows similarities with

the band structure of the local map. In particular, it is reminiscent of the band-splitting period of the single map. This simple observation raises the question of the existence of some self-similarity for these collective regimes. Since, as mentioned above, NTCB could be lost when approaching μ_∞, two different questions can be addressed: First, is their some universality displayed by asymptotic banded states, whatever the coupling, if necessary starting from adequate initial conditions? Second, what is the asymptotic regime reached from almost all initial conditions, and is there an infinite cascade of NTCB for sufficiently strong coupling?

The previous section intended to study the second question, but failed to give a general answer near μ_∞: this requires to evaluate all $g_e^n(\mu, m)$ or at least to provide some maximization of them. We now turn to the derivation of a RG equation for coupled maps which applies to all types of banded states and gives a precise answer to the first question. This, in turn, provides a complete description of the phase diagram of coupled map systems in this limit, therefore answers the second question.

This RG is first derived on the example of coupled tent maps in which case calculation can be carried out exactly while the more general case of unimodal maps is discussed afterwards.

4.1 Recalling RG for single maps

Let us first recall how the RG works in the case of the tent map. In this simple case, the RG stems from an conjugacy relation between the iterated map S_μ^2 in the two band regime with the same map $S_{\mu'}$ for some other value of the parameter μ'. This RG characterizes the self-similar structure of this dynamical system and provide scaling exponents in the limit $\mu \to \mu_\infty$ for *e.g.* the band-splitting points or the widths of the bands in this limit. One can write the RG in two ways.

Centered RG For any $\mu > 1$, the second iterate S_μ^2 of the tent map $S_\mu(X) = 1 - \mu|X|$, restricted to the interval $[-1/\mu, 1/\mu]$ reads

$$S_\mu^2\big|_{[-1/\mu,1/\mu]}(X) = 1 - \mu + \mu^2|X|\,.$$

This allows for a change of variable $X' = -X/a$, with $a = -S_\mu(1)$ (or $-a = 1 - \mu$): the variable X' is governed by the map $S_{\mu'}$ with $\mu' = \mu^2$ (see Fig. 6). Whenever $\mu' \leq \bar{\mu}_0$ (*i.e.* $\mu \leq \sqrt{2}$), the map $S_{\mu'}$ leaves the interval $I = [-1, 1]$

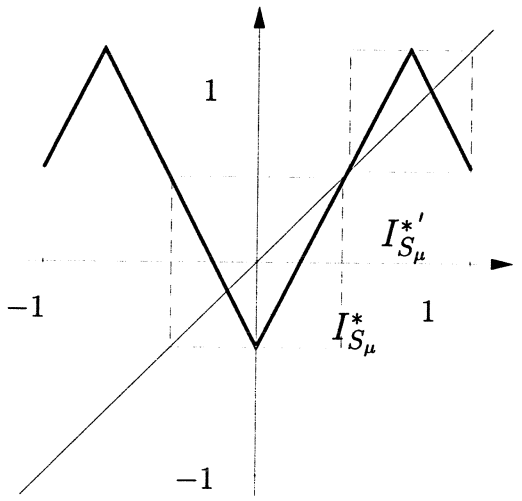

Figure 6: Iterated tent map S_μ^2 for $\mu = 1.4$, with indication of the intervals $I^*_{S_\mu}$ and $I^{*\prime}_{S_\mu}$.

stable; therefore X transformed by S_μ^2 cannot escape from the interval $I^*_{S_\mu} = [-a, a]$ *i.e.* this interval is stable under the map S_μ^2.

This equivalence is formalized as a conjugacy relation for the second iterate of the map S_μ^2 restricted to the interval $I^*_{S_\mu}$ in the two-band region of S_μ ($\mu \in [\mu_\infty, \bar{\mu}_1]$)

$$S_\mu^2\big|_{I^*_{S_\mu}} = h^{-1}_{S_\mu} \circ S_{\mu^2} \circ h_{S_\mu} \,, \tag{5}$$

with a linear transformation $h_{S_\mu}(X) = -X/a$. The map S_{μ^2} leaves the interval $I^0_{S_{\mu^2}}$ invariant, and the central band $I^{1,0}_{S_\mu} \subset I^*_{S_\mu}$ is obtained via

$$I^{1,0}_{S_\mu} = h^{-1}_{S_\mu}\left(I^0_{S_{\mu^2}}\right) ,$$

while the condition $\mu' \leq \bar{\mu}_0 = 2$ or $\mu \leq \sqrt{2}$ provides the value of the first band splitting point, $\bar{\mu}_1 = \sqrt{2}$.

Since this relation identifies the iterated map with the tent map itself, the process can be repeated. It shows that S_μ exhibits a self-similar cascade of band-splitting points $\bar{\mu}_n = \sqrt{\bar{\mu}_{n-1}}$ below which regimes with more than 2^n bands are observed. When $n \to \infty$, the points $\bar{\mu}_n = \sqrt[2^n]{2}$ converge to the fixed point $\mu_\infty = 1$ of $\sqrt{}$ and for large n, the points $\bar{\mu}_n$ converge to μ_∞ like $\bar{\mu}_n - \mu_\infty \sim \delta^{-n}$ which defines the Feigenbaum constant (or the *bifurcation velocity*), here $\delta = 2$.

Non-centered RG A conjugacy relation can also be written for S_μ^2 on the interval $I_{S_\mu}^{*\prime} = [2/\mu - 1, 1]$. This relation reads,

$$S_\mu^2\big|_{I_{S_\mu}^{*\prime}} = h_{S_\mu}^{\prime -1} \circ S_{\mu^2} \circ h_{S_\mu}^{\prime} \ , \tag{6}$$

for the same parameter $\mu' = \mu^2$ as in the centered version, while $h'_{S_\mu}(X) = (X - 1/\mu)/(1 - 1/\mu)$ and $I_{S_\mu}^{*\prime} = h_{S_\mu}^{\prime -1}([-1, 1])$. The band $I_{S_\mu}^{1,1}$ is obtained via

$$I_{S_\mu}^{1,1} = h_{S_\mu}^{\prime -1}\left(I_{S_{\mu^2}}^{0}\right) .$$

Equation (6) is a non-centered RG equation.

4.2 RG for coupled maps

Let us now consider coupled tent map dynamics governed in the general case by an operator of the form $\mathbf{\Delta}_g^m \circ \mathbf{S}_\mu$. In the spirit of the derivation of a RG for single maps, we are led now to study the iterated operator $\left(\mathbf{\Delta}_g^m \circ \mathbf{S}_\mu\right)^2$ restricted to one of the intervals $\mathbf{I}_{S_\mu}^*$ or $\mathbf{I}_{S_\mu}^{1,1}$ in the phase space $\mathbf{I}$. Such an approach requires the single assumption that the system is in a BS1 and concerns all values of the parameter $\mu \in [\mu_\infty, \bar{\mu}_1]$ to insure that the system remains in a BS1 at all times. This situation is encountered either because the coupling in sufficiently strong so that the system flows towards such a BS1 for almost all initial condition — $g \geq g_{\mathrm{e}}^1(\mu, m)$ —, or simply because adequate initial conditions have been chosen, whatever the coupling strength.

4.2.1 Centered RG

Commutation The iterated operator $\left(\mathbf{\Delta}_g^m \circ \mathbf{S}_\mu\right)^2$ restricted to the band $\mathbf{I}_{S_\mu}^*$ is simply written

$$\left(\mathbf{\Delta}_g^m \circ \mathbf{S}_\mu\right)^2\Big|_{\mathbf{I}_{S_\mu}^*} = \mathbf{\Delta}_g^m \circ \mathbf{S}_\mu\Big|_{\mathbf{I}_{S_\mu}^{1,1}} \circ \mathbf{\Delta}_g^m \circ \mathbf{S}_\mu\Big|_{\mathbf{I}_{S_\mu}^*} \ , \tag{7}$$

to emphasize that at the second application of S_μ only the restriction of the local map to $I_{S_\mu}^{1,1}$ is involved. This is an essential remark, because $I_{S_\mu}^{1,1} \subset [0, 1]$ and therefore S_μ is linear on the interval $I_{S_\mu}^{1,1}$ (in fact $S_\mu\big|_{I_{S_\mu}^{1,1}}(X) = 1 - \mu X$) [3], and consequently the operator

$$\mathbf{S}_\mu\Big|_{\mathbf{I}_{S_\mu}^{1,1}}(\mathbf{X}) = \mathbf{1} - \mu\mathbf{X}$$

[3] In other words, $0 \notin I_{S_\mu}^{1,1}$ precisely because the "central" band is $I_{S_\mu}^{1,0} \ni 0$ and $I_{S_\mu}^{1,0} \cap I_{S_\mu}^{1,1} = \emptyset$ and 0 is the point of non-linearity of the map.

commutes with $\mathbf{\Delta}_g^m$:

$$\mathbf{\Delta}_g^m \circ \mathbf{S}_\mu\Big|_{\mathbf{I}_{S_\mu}^{1,1}} = \mathbf{S}_\mu\Big|_{\mathbf{I}_{S_\mu}^{1,1}} \circ \mathbf{\Delta}_g^m \,. \tag{8}$$

This essential remark permits to write

$$\left(\mathbf{\Delta}_g^m \circ \mathbf{S}_\mu\right)^2\Big|_{\mathbf{I}_{S_\mu}^*} = \mathbf{\Delta}_g^{2m} \circ \mathbf{S}_\mu^2\Big|_{\mathbf{I}_{S_\mu}^*} \,, \tag{9}$$

where the iterated operator is expressed also in the form of coupled maps evolving under a iterated local map S_μ^2 and with a longer-range coupling.

Recalling now the centered RG (5) for the local map and linearity of h_{S_μ}, it comes

$$\left(\mathbf{\Delta}_g^m \circ \mathbf{S}_\mu\right)^2\Big|_{\mathbf{I}_{S_\mu}^*} = \mathbf{h}_{S_\mu}^{-1} \circ \mathbf{\Delta}_g^{2m} \circ \mathbf{S}_{\mu^2} \circ \mathbf{h}_{S_\mu} \,. \tag{10}$$

This relation states that in the two band regime, the dynamics under an operator $\mathbf{\Delta}_g^m \circ \mathbf{S}_\mu$ observed every other timestep is equivalent (conjugate) to another coupled system, $\mathbf{\Delta}_g^{m'} \circ \mathbf{S}_{\mu'}$, with a longer-range coupling $m' = 2m$, and parameter value $\mu' = \mu^2$. It is an *exact* RG equation for coupled tent maps in the space of parameters (μ, m).

In the case of globally coupled maps, iterating the coupling amounts to increasing the coupling strength:

$$\mathbf{\Delta}_g^m = \mathbf{\Delta}_{1-(1-g)^m} \,. \tag{11}$$

therefore the RG operates in the parameter space (μ, g) and $g' = 1 - (1-g)^2$. However, this is not true in the general case, and certainly not for CMLs: previous attempts to derive a RG for CMLs were looking towards a RG in this parameter space (μ, g). The calculation above shows that the RG is naturally written in the space (μ, m).

In the case of the continuous field operator $\mathbf{\Delta}_\lambda^\infty$, the RG can be derived either by performing a similar calculation or taking the continuous limit ($m \to \infty$ and $\|\vec{e}\| \propto 1/\sqrt{m} \to 0$) in equation (10):

$$\left(\mathbf{\Delta}_\lambda^\infty \circ \mathbf{S}_\mu\right)^2\Big|_{\mathbf{I}_{S_\mu}^*} = \mathbf{h}_{S_\mu}^{-1} \circ \mathbf{\Delta}_{\lambda\sqrt{2}}^\infty \circ \mathbf{S}_{\mu^2} \circ \mathbf{h}_{S_\mu} \,. \tag{12}$$

In this case, it operates in the parameter space (μ, λ) and maps λ onto $\lambda' = \lambda\sqrt{2}$.

4.2.2 Non-centered RG

A RG equation can also be derived on the band $\mathbf{I}_{S_\mu}^{1,1}$. However, if the operator $\left(\mathbf{\Delta}_g^m \circ \mathbf{S}_\mu\right)^2$ is restricted to this band, the commutation (8) leads to $\mathbf{\Delta}_g^m \circ (\mathbf{S}_\mu)^2 \circ \mathbf{\Delta}_g^m$. It is more appropriate in this case to consider the operator $\left(\mathbf{S}_\mu \circ \mathbf{\Delta}_g^m\right)^2$ which can be viewed as a coupled system observed just after the application of the map and not just after the coupling step. This does not change the dynamics of the mean M^t while the pdf are compared at intermediate time steps. For these operators the commutation yields:

$$\left(\mathbf{S}_\mu \circ \mathbf{\Delta}_g^m\right)^2 \Big|_{\mathbf{I}_{S_\mu}^{1,1}} = \mathbf{S}_\mu^2 \circ \mathbf{\Delta}_g^{2m} \Big|_{\mathbf{I}_{S_\mu}^{1,1}} . \tag{13}$$

Recalling the RG (6) for the local map and linearity of the transformation h'_μ, it comes

$$\left(\mathbf{S}_\mu \circ \mathbf{\Delta}_g^m\right)^2 \Big|_{\mathbf{I}_{S_\mu}^{1,1}} = \mathbf{h'}_{S_\mu}^{-1} \circ \mathbf{S}_{\mu^2} \circ \mathbf{\Delta}_g^{2m} \circ \mathbf{h'}_{S_\mu} . \tag{14}$$

It is worth noting that this RG does not take the same form on both bands. Previous approaches relied on a commutation between the operators $\mathbf{\Delta}_g$ and $\mathbf{S}_\mu$ under assumptions of weak coupling or as a perturbation approach of a synchronized state, disregarding the properties of the bands of the local map. Therefore they could not distinguish the bands on which it is possible to make this commutation from the central band where this is certainly not permitted. This distinction leads to the different expressions of the RG.

4.3 Universality

A RG is an extremely powerful tool, and its existence for coupled maps has numerous consequences. We now describe some of these consequences.

4.3.1 Validity

Universality emerges from the group structure of the conjugacy relation. Consequently, to insure the validity of universality results, it is necessary to make sure that this approach can be iterated: in the case of coupled maps it requires that the system reaches banded states of increasing order when $\mu \to \mu_\infty$. Although, this can be guaranteed by an appropriate choice of initial conditions, such as those restricted to smaller and smaller intervals, this procedure is not satisfying in all generality and the above assumption thus appears as a strong

impediment to the applicability of a RG approach to coupled maps. In fact, the RG itself provides a simple answer to this difficulty.

Let us first recall that the RG equation (10) relies on the single assumption that the system is in a BS1 for some $\mu \in [\mu_\infty, \bar{\mu}_1]$. Whenever $g > g_e^1(\mu, m)$ such a BS1 is reached from the most general initial conditions under the discrete-space dynamics $\mathbf{\Delta}_g^m \circ \mathbf{S}_\mu$. Let us consider such μ and g, and apply the RG (10) once: this establishes the conjugacy between $\left(\mathbf{\Delta}_g^m \circ \mathbf{S}_\mu\right)^2\Big|_{\mathbf{I}^*_{S_\mu}}$ and $\mathbf{\Delta}_g^{2m} \circ \mathbf{S}_{\mu^2}$. If moreover $\mu \in [\mu_\infty, \bar{\mu}_2]$, then $\mu^2 \in [\mu_\infty, \bar{\mu}_1]$ and $\mathbf{\Delta}_g^{2m} \circ \mathbf{S}_{\mu^2}$ reaches a BS1 whenever $g > g_e^1(\mu^2, 2m)$: this corresponds to a BS2 for $\mathbf{\Delta}_g^m \circ \mathbf{S}_\mu$ and is reached whenever $\mu \in [\mu_\infty, \bar{\mu}_2]$ and $g > g_e^2(\mu, m)$. This proves that the limit value $g_e^2(\mu, m)$ is simply expressed in terms of $g_e^1(\mu, m)$ by use of the RG:

$$g_e^2(\mu, m) = g_e^1\left(\mu^2, 2m\right) .$$

This argument is easily iterated and provides a complete description of the different regions where NTS is reached:

$$g_e^{n+1}(\mu, m) = g_e^1\left(\mu^{2^n}, 2^n m\right) .$$

In particular, since all $g_e^1(\mu, m)$ have a maximal value $g_e^1(m) = g_e^1(\bar{\mu}_1, m)$ for any fixed m, it shows that for all n and μ, $g_e^n(\mu, m) \leq g_e^1(m)$. Consequently, for any given m and $g > g_e^1(m)$, an infinite cascade of BSs is observed when $\mu \to \mu_\infty$. In particular, $g_e^1(\bar{\mu}_1, m)$ decreases with m, and the maximal value of all $g_e^1(m)$ is $g_e^1 = g_e^1(1)$. This guarantees the validity of the RG approach, which can indeed be applied recursively at all orders. Moreover, since $g_e^1(\mu, m) \to 0$ when $m \to \infty$, $g_e^1(\infty) = 0$ in the case of the continuous limit and a BS of maximal order is always reached.

Consider now some $g < g_e^1(m)$: since $g_e^1(\mu, m) \to 0$ when $\mu \to \mu_\infty$ (see Fig. 5), there exists a value $\mu_e^1(g, m)$ of the parameter μ for which

$$g = g_e^1\left(\mu_e^1(g, m), m\right) .$$

Since $g_e^1(\mu, m)$ is a increasing function of μ, a BS1 is reached by the system $\mathbf{\Delta}_g^m \circ \mathbf{S}_\mu$ for all $\mu < \mu_e^1(g, m)$. The same can be said of any critical curve $g_e^n(\mu, m)$ since all $g_e^n(\mu, m) \to 0$: there exists a value $\mu_e^1(g, m)$ such that $g = g_e^n(\mu_e^n(g, m), m)$. Below $\mu_e^n(g, m)$, a BSn is reached starting from any BS$(n-1)$. Therefore, below

$$\mu_e^{n*}(g, m) = \min_{n' \leq n} \mu_e^{n'}(g, m) ,$$

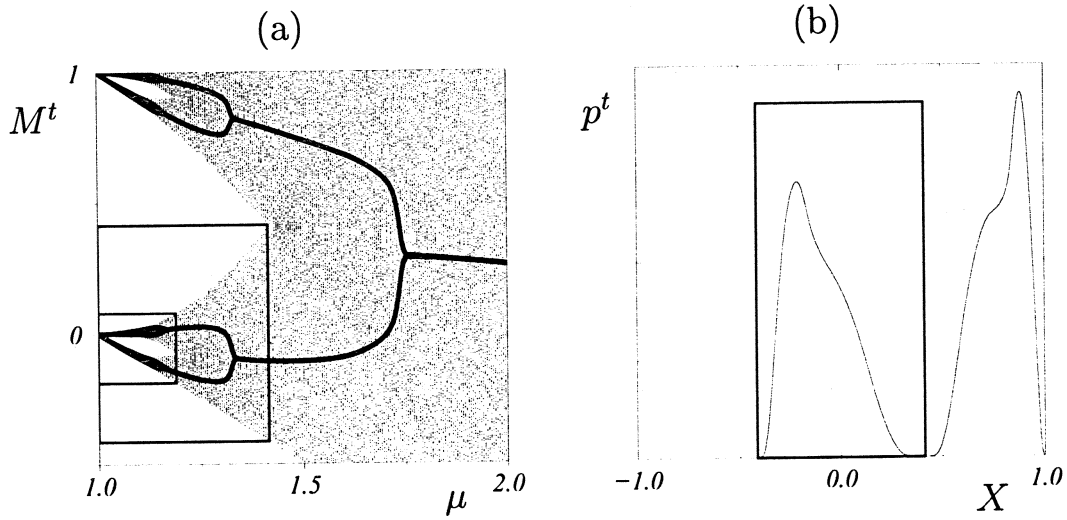

Figure 7: Democratically-coupled ($g = 0.2$) tent maps on a $d = 2$ lattice of linear size $L = 2048$ with periodic boundary conditions: (a) bifurcation diagram of $M^t = \langle \mathbf{X} \rangle^t$ (filled circles) superimposed on that of the local map S_μ (small dots). The $[\mu_\infty, \bar{\mu}_1] \otimes I^1_{\bar{\mu}_1}$ and $[\mu_\infty, \bar{\mu}_2] \otimes I^2_{\bar{\mu}_2}$ regions are shown. For coupled tent maps, these regions transformed by the RG coincide with the bifurcation diagrams of $\mathbf{\Delta}^2_g \circ \mathbf{S}_\mu$ and $\mathbf{\Delta}^4_g \circ \mathbf{S}_\mu$, themselves indistinguishable from the whole figure. (b): period-2 collective cycle at $\mu = \bar{\mu}_1$ for $m = 1$; the distribution in the rectangle (even time steps) is transformed exactly by the RG onto that for $m = 2$ at $\mu = 2$ displayed on Fig. 1-(b).

a BSn is reached from any initial condition. When $\mu \to \mu_\infty$, there always exists some μ sufficiently small to ensure that a BSn is reached. When μ decreases, the system passes first through regions of multistability, but after having crossed the maximal curve $g_e^{n*}1\ (\mu, m)$, it undergoes an full cascade of banded states. These results establish the relevance of the RG approach in all circumstances.

4.3.2 Scaling

An immediate consequence of the RG equation (10) is that CML $\mathbf{\Delta}_g \circ \mathbf{S}_{\bar{\mu}_1}$ in a banded state at $\bar{\mu}_1$ corresponds to the CML $\mathbf{\Delta}^2_g \circ \mathbf{S}_{\bar{\mu}_0}$ at $\bar{\mu}_0$. More precisely, for $g > g_e^{1*}$, the behavior of $\mathbf{\Delta}_g \circ \mathbf{S}_{\bar{\mu}_1}$ considered every other timestep (when the system lies on the central band) is equivalent to that of CML $\mathbf{\Delta}^2_g \circ \mathbf{S}_{\bar{\mu}_0}$ considered every timestep. Figure 7-(c) displays pdf p^t observed in the period-2 regime for a two-dimensional lattice of coupled tent maps. The pdf on the left lies on the central band, and transformed by the RG, it collapses with the

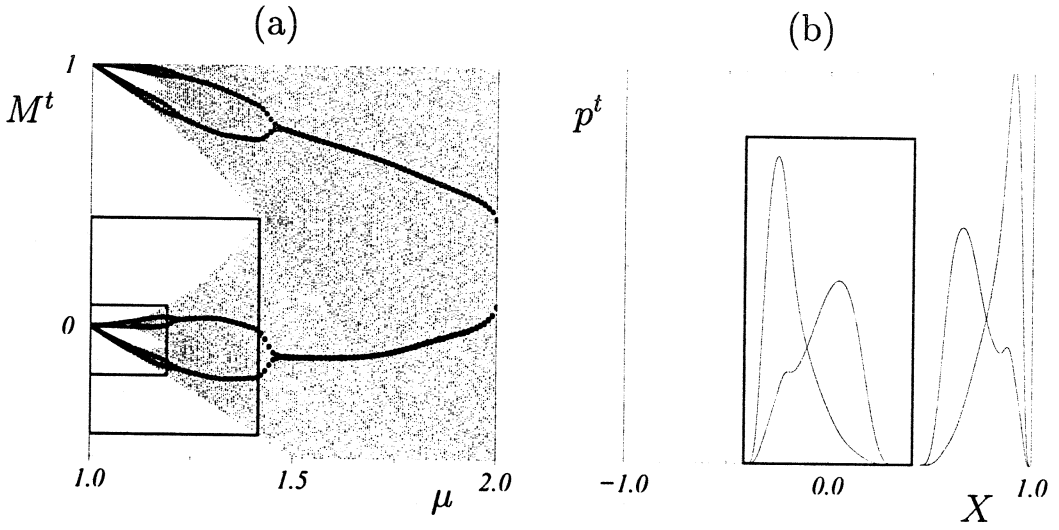

Figure 8: Democratically-coupled ($g = 0.2$) tent maps on a $d = 3$ lattice of linear size $L = 128$ with periodic boundary conditions: (a) bifurcation diagram of $M^t = \langle \mathbf{X} \rangle^t$ (filled circles) superimposed on that of the local map S_μ (small dots). The $[\mu_\infty, \bar{\mu}_1] \otimes I^1_{\bar{\mu}_1}$ and $[\mu_\infty, \bar{\mu}_2] \otimes I^2_{\bar{\mu}_2}$ regions are shown. For coupled tent maps, these regions transformed by the RG coincide with the bifurcation diagrams of $\mathbf{\Delta}^2_g \circ \mathbf{S}_\mu$ and $\mathbf{\Delta}^4_g \circ \mathbf{S}_\mu$, themselves indistinguishable from the whole figure. (b): period-4 collective cycle at $\mu = \bar{\mu}_1$ for $m = 1$; the distribution in the rectangle (even time steps) is transformed exactly by the RG onto that for $m = 2$ at $\mu = 2$ displayed on Fig. 2-(b).

pdf of Fig. 7-(b) corresponding to the fixed-point regime for $m = 2$ at $\bar{\mu}_0$.

The same comparison can be performed at all points $\bar{\mu}_n$ for $\mathbf{\Delta}_g \circ \mathbf{S}_{\bar{\mu}_n}$ and $\mathbf{\Delta}_g^{2^n} \circ \mathbf{S}_{\bar{\mu}_0}$ at $\bar{\mu}_0$. Since in two-dimensional lattices, for $\mu = \bar{\mu}_0$, a fixed-point regime is reached for all m, a period-2^n is reached at every $\bar{\mu}_n$. In the case of three-dimensional lattices, a period-2 collective regime is reached for all m at $\bar{\mu}_0$: consequently, period-2^{n+1} is reached at every band splitting point $\bar{\mu}_n$.

The RG does not predict the behavior displayed by $\mathbf{\Delta}_g^m \circ \mathbf{S}_\mu$ on the interval $[\bar{\mu}_1, \bar{\mu}_0]$; however, it relates the behavior of these systems on all other intervals $[\bar{\mu}_{n+1}, \bar{\mu}_n]$ of the parameter μ to the behavior observed on $[\bar{\mu}_1, \bar{\mu}_0]$. This approach is valid whatever the space dimension and the regimes observed for $\mu \in [\bar{\mu}_1, \bar{\mu}_0]$ (fixed-point, periodic, quasi-periodic,...). In higher dimensions, the behavior displayed $\mu \in [\bar{\mu}_1, \bar{\mu}_0]$ can change qualitatively for different (small) values of m, and there is no numerical evidence of what is the behavior displayed in the continuous limit. In these cases, the behavior observed on small-n bands also show qualitative changes ither than the period-doubling implied by the RG. However, in any case, the RG implies that there exists an infinite cascade of period doubling phase transitions for the collective behavior of these CMLs (the term "period doubling" being understood in a broad sense).

In the space-continuous limit governed by $\mathbf{\Delta}_\lambda^\infty \circ \mathbf{S}_\mu$, changing λ amounts to a mere rescaling of space: the system is invariant under the symmetry $\lambda \to \alpha\lambda$ and $\vec{r} \to \alpha\vec{r}$. Therefore, multiplying λ has no non-trivial effect on the collective behavior: quantities like the instantaneous pdf p^t are not affected at all while the correlation functions are simply rescaled in space. Therefore, the RG (12) implies that system $(\mathbf{\Delta}_\lambda^\infty \circ \mathbf{S}_\mu)^2$ has exactly the same behavior as $\mathbf{\Delta}_\lambda^\infty \circ \mathbf{S}_{\mu^2}$, but with all lengthscales multiplied by $\beta = \sqrt{2}$ and values reduced by a factor $a < 1$. In particular, the scaling laws displayed by $\mathbf{\Delta}_\lambda^\infty \circ \mathbf{S}_\mu$ are those of the local map with plus the divergence of lengthscales ruled by β. The existence of a phase transition point μ_1^c in the interval $[\bar{\mu}_1, \bar{\mu}_0]$ —and there must be one, since the behavior at $\bar{\mu}_1$ has twice the periodicity of the behavior at $\bar{\mu}_0$— implies, by similarity, the existence of an infinite cascade of phase transition points μ_n^c related by the RG.

In the case of usual discrete-space CMLs, iterating RG equation (5) shows that, near μ_∞, the system $\mathbf{\Delta}_g^m \circ \mathbf{S}_\mu$ is equivalent to a system on $[\bar{\mu}_1, \bar{\mu}_0]$ with a longer-range coupling $(\mathbf{\Delta}_g^{2^n m} \circ \mathbf{S}_{\mu'})$ *i.e.* it is closer to a continuous field map. Therefore, the scaling properties of CMLs are in fact governed by equation (12) and rely on the existence of a well-defined continuous limit for the

collective behavior. In particular, for the sub-harmonic cascades observed in 2 and 3 dimensions, the phase transitions at μ_n^c are critical points of Ising-like transitions [14], characterized by the divergence of the correlation length. The scaling properties observed in the critical region around these points are not expected to depend on the coupling range m. Therefore, points μ_n^c converge to μ_∞ with the Feigenbaum constant δ of the local map, and they are expected to show the same critical properties.

5 Renormalization group for coupled unimodal maps

Let us now turn to the more general case when the local map is given by equation (2) with $\varepsilon > 0$. We first review briefly how the RG applies to these maps, then, using as a guideline the exact calculation performed for the tent map, we study how the RG can be written in the general case of coupled unimodal maps.

5.1 Single maps

5.1.1 An example: the logistic map

Let us take the example of the logistic map, $S_\mu(X) = 1 - \mu X^2$, and write,

$$S_\mu^2(X) = 1 - \mu + 2\mu^2 X^2 - \mu^3 X^4 . \tag{15}$$

in this case, S_μ^2 is a polynomial of order 4. Clearly, if polynomial maps of the form

$$S_\mu(X) = 1 - \mu^{(1)} X^2 - \mu^{(2)} X^4 \cdots$$

are considered, with a more general definition for the parameter μ as the sequence $\mu = \left(\mu^{(1)}, \mu^{(2)}, \cdots\right)$, the RG transformation operates on these sequences μ: like in the case of the tent map (equation (5)), it relies on the existence of a conjugacy relation between S_μ^2 restricted to a band and a map $S_{\mu'}$ for another parameter value μ'.

Keeping only second order terms in the rhs of equation (15) provides the simplest approximation of the RG for the logistic map, $X' = X/(1-\mu)$ and $\mu' = 2\mu^2(1-\mu)$ which allows for an estimation of the Feigenbaum constants [6].

5.1.2 Doubling transformation

In order to tackle the general case of coupled unimodal maps, we now adopt a more formal point of view on the RG following [1].

Let us denote Ω the space of symmetric, unimodal maps S of the interval $[-1,1]$ with the *normalization condition* that the maximum (reached for $X = 0$) equals 1. For a given map $S \in \Omega$, the bounds of the invariant intervals are the iterates of $X = 0$. Let us define,

$$a = -S(1) \ , \ b = S(a) \ \text{and} \ c = S(b) \ .$$

The map S has two bands whenever $0 < a \leq b$ and $c \in I_S^* = [-a, a]$, because the intervals $I_S^{1,0} = [-a, c]$ and $I_S^{1,1} = [b, 1]$ are then exchanged by S, and $I_S^{1,0} \subset I_S^*$. The RG stems from the observation that I_S^* is stable by S^2, and the map $-S^2$ restricted to I_S^* is again unimodal with a maximum at $X = 0$. An appropriate linear change of variables transforms $S^2|_{I_S^*}$ into a normalized unimodal map $T[S] \in \Omega$:

$$S^2\Big|_{I_S^*} = h_S^{-1} \circ T[S] \circ h_S \ ,$$

with $h_S(X) = -X/a$. The *doubling transformation* T operates in the space Ω of such maps and the geometric properties of the operator T as a dynamical system acting in Ω determines the universal properties of the local map [4]. In the case of the tent map, $T[S_\mu] = S_{\mu^2}$.

Let us recall the main results of this approach. Transformation T has a fixed-point Φ and the derivative of T at the point Φ has a simple eigenvalue which is larger than one, which turns out to be the bifurcation velocity, δ. This fixed point verifies the relation $\Phi(X) = -\alpha\Phi \circ \Phi(-X/\alpha)$ which defines the *reduction parameter* $\alpha = -1/\Phi(1)$, characterizing the shrinking of the bands near μ_∞. The unstable manifold W_u of T is one-dimensional, and the stable manifold W_s has codimension-one.

Let us denote Σ_a the codimension-one surface $\Sigma_a = \{S : S(1) = -a\}$, and Φ_a^* the intersection of W_u with Σ_a. The inverse images of a surface Σ_a by the doubling transformation are denoted,

$$\Sigma_a^{(n)} = T^{-n}[\Sigma_a] \ ,$$

and $\Sigma_a^{(0)} = \Sigma_a$. When T^{-1} is iterated, these surfaces accumulate to the stable manifold at the transversal rate δ^{-1}.

A family of maps $\mu \to S_\mu$ can be regarded as a curve which crosses the stable manifold W_s at the point S_{μ_∞}. For the different maps considered, the point $\bar{\mu}_0 = 2$ corresponds to the case when the image set of the map is the whole interval $[-1, 1]$, *i.e.* $S_{\bar{\mu}_0}(1) = -1$, and therefore by definition, $S_{\bar{\mu}_0} \in \Sigma_1$. The band-splitting points $\bar{\mu}_n$ correspond to the same property for their images: $T^n[S_{\bar{\mu}_n}] \in \Sigma_1$ or equivalently, $S_{\bar{\mu}_n} \in \Sigma_1^{(n)}$. Therefore the maps $S_{\bar{\mu}_n}$ are the intersection of the curve $\mu \to S_\mu$ with the surfaces $\Sigma_1^{(n)}$. This shows that the points $\bar{\mu}_n$ converge to μ_∞ at the velocity δ. Moreover when $n \to \infty$, the sequence $T^n[S_{\bar{\mu}_n}]$ converges to the universal map Φ_1^* which lies on the unstable manifold W_u, while the sequence $T^n[S_{\mu_\infty}] \in W_s$ converges to Φ.

5.2 Maps on phase space

Let us now turn to the general case of coupled unimodal maps of the form $\mathbf{\Delta} \circ \mathbf{S}$. Multivariate maps have been studied in [19], where it is shown in some cases that a doubling transformation can be defined which guarantees the existence of universal properties. However, it is especially relevant to our problem to find a relation between this universality, the extension of the coupling and the universality of the single map.

In the case of coupled tent maps, the derivation of the self-similarity relation (10) relies on the possibility to let the operators $\mathbf{\Delta}$ and $\mathbf{S}$ commute in the expansion (7) of $(\mathbf{\Delta} \circ \mathbf{S})^2$. In the general case, the commutation relation (8) does not hold because the local map is not linear on the interval $I_S^{1,1}$; therefore, the iterated operator restricted to a stable interval cannot be written in the same form (linear coupling composed with a local non-linear map). However, the local map is invertible on $I_S^{1,1}$ precisely because the only point where it is locally non-invertible lies on the central band (by definition). Invertibility guarantees that the operators $\mathbf{\Delta} \circ \mathbf{S}$ and $\mathbf{S} \circ \mathbf{\Delta}$ restricted to $I_S^{1,1}$ are conjugate to each other. This conjugacy can be seen as an extension of the notion of commutation.

The invertibility property and the consequent conjugacy relation are at the core of the existence of a RG in the general case; it allows to write,

$$(\mathbf{\Delta} \circ \mathbf{S})^2 \Big|_{\mathbf{I}_S^*} = \left(\mathbf{\Delta} \circ \mathbf{S} \Big|_{\mathbf{I}_S^{1,1}} \circ \mathbf{\Delta} \circ \mathbf{S} \Big|_{\mathbf{I}_S^{1,1}}^{-1} \right) \circ \mathbf{S}^2 \Big|_{\mathbf{I}_S^*}$$

which resembles usual coupled maps systems with the local map $\mathbf{S}^2$ but with a non-linear transformation in place of the coupling operator. It appears at

this stage that the definition of coupling operators requires to be extended to the case of non-linear operators.

In order to tackle the most general case, it is therefore necessary to "embed" the usual linearly coupled maps in an enlarged space on which a doubling transformation can be defined: this leads to consider coupled maps of the form $\mathbf{Q} \circ \mathbf{S}$ where $\mathbf{Q}$ is a non-linear operator. The nonlinearity of $\mathbf{Q}$ could interfere with that of the local map, and it is necessary to specify the roles that must be given to these two operators: for this purpose, it is shown in the following that for very general unimodal maps on $\mathbf{I}$ there is a canonical representation in a coupled map form $\mathbf{Q} \circ \mathbf{S}$. This approach also requires to extend the definition of linear diffusive coupling operators (DCOs) to the case of non-linear operators. Finally, as expected, this framework provides a straightforward definition for the doubling transformation.

5.2.1 Canonical representation

Let us define some space $\boldsymbol{\Upsilon}$ of (continuously differentiable) normalized unimodal maps $\mathbf{X} \to \boldsymbol{\Psi}(\mathbf{X})$ on the phase space $\mathbf{I} = I^{\mathcal{L}}$ (For simplicity the index set $\mathcal{L}$ can be supposed finite). These maps are taken symmetric (for $X \to -X$), homogeneous and isotropic to respect the symmetries of the index set $\mathcal{L}$. Unimodality means that all partial maps

$$\mathbf{X}_{\vec{r}_2} \to [\boldsymbol{\Psi}(\mathbf{X})]_{\vec{r}_1}$$

are unimodal for all $\vec{r}_2, \vec{r}_1 \in \mathcal{L}$ (in particular, if there is no dependence induced by $\boldsymbol{\Psi}$ between the sites $\vec{r}_2$ and $\vec{r}_1$, this map is flat); the absolute maximum for $\boldsymbol{\Psi}$ is obtained at the configuration $\mathbf{X} = \mathbf{0}$, and the normalization condition reads

$$\boldsymbol{\Psi}(\mathbf{0}) = \mathbf{1}.$$

Let us denote $\mathbf{I}_{\text{syn}}$, the *synchronous manifold i.e.* the set of configurations where all sites are synchronized. The image of some synchronized state $\mathbf{X} \in \mathbf{I}_{\text{syn}}$ (*e.g.* $\mathbf{X}_{\vec{r}} = X$, for all $\vec{r} \in \mathcal{L}$) by a unimodal map $\boldsymbol{\Psi} \in \boldsymbol{\Upsilon}$ is again synchronized due to the assumption of homogeneity. We write $P[\boldsymbol{\Psi}](X)$ the common image value of all sites in $\boldsymbol{\Psi}[\mathbf{X}]$: $P[\boldsymbol{\Psi}]$ is a normalized, symmetric, unimodal map on $[-1,1]$ (*i.e.* $P[\boldsymbol{\Psi}] \in \Omega$) that we call the *reduced map* of $\boldsymbol{\Psi}$. In the case of linearly coupled maps, $\boldsymbol{\Psi} = \boldsymbol{\Delta} \circ \mathbf{S}$, the reduced map is $P[\boldsymbol{\Delta} \circ \mathbf{S}] = S$.

The reduced map is unimodal with its maximum at 0, and therefore it is invertible from the interval $I^+ = [0,1]$ to $I^0_{P[\Psi]} = [-a,1]$ (with $a = -P[\Psi](1)$); thus, the operator $\mathbf{P}[\Psi]$ transforms the interval $\mathbf{I}^+$ of configuration with only non-negative values to the whole invariant interval $\mathbf{I}^0_\Psi$ where the dynamics takes place. This allows to define

$$\mathbf{Q}[\Psi] \equiv \Psi \circ (\mathbf{P}[\Psi])^{-1}$$

on $\mathbf{I}^0_\Psi$, and to write, in all generality,

$$\Psi = \mathbf{Q}[\Psi] \circ \mathbf{P}[\Psi] \tag{16}$$

to emphasize the coupled map-like structure of unimodal maps in the general case. It is equivalent to take the inverse of the reduced map on $\mathbf{I}^- = -\mathbf{I}^+$ due to the symmetry $\mathbf{X} \to -\mathbf{X}$. If $\Psi = \Delta \circ \mathbf{S}$, then $\mathbf{Q}[\Psi] = \Delta$, $\mathbf{P}[\Psi] = \mathbf{S}$ and the decomposition (16) amounts to the definition of the map.

The reduced map $P[\Psi]$ can be seen as a mean-field version of Ψ: it accounts for the global transformation applied to a site when setting aside the effects of the other variables (precisely, these effects have been canceled out by taking all the sites synchronized). The operator $\mathbf{Q}[\Psi]$ accounts for the effects of other sites added to this mean-field transformation. It contains no local evolution by itself (its reduced map is the identity) or equivalently, it admits all synchronized states $\mathbf{X} \in \mathbf{I}_{\text{syn}}$ for fixed points. In this sense, $\mathbf{Q}[\Psi]$ is a pure coupling operator, although it is not linear in general.

For any given local map $S \in \Omega$, $\mathbf{S}$ is an uncoupled map on $\mathbf{I}$. Let us denote $\mathbf{\Omega}$ the space of such uncoupled maps. The canonical decomposition presented above shows that any map $\Psi \in \Upsilon$ can written as the composition of some $\mathbf{S} \in \mathbf{\Omega}$ with a "coupling" operator. This property can be written formally as $\Upsilon = \Upsilon' \circ \mathbf{\Omega}$, where Υ' denotes the space of coupling operators. Now, the definition of Υ should be completed by some assumptions, and clearly, these assumptions concern in fact the space Υ'.

Although the coupling operator $\mathbf{Q}[\Psi]$ already appears as a complicated object, this decomposition shows that under general assumption, there is a unique way to define a coupled map form for Ψ, and in particular a unique possible local map.

5.2.2 Non-linear coupling operators

We consider coupled map dynamics of the form $\Psi = \mathbf{Q} \circ \mathbf{S}$, where $\mathbf{Q} \in \Upsilon'$ is taken regular so that the differentiability of Ψ is determined solely by the

local map. The tangent operator for Ψ is defined by the functional derivative,

$$\frac{\delta \Psi [\mathbf{X}]_{\vec{r}_1}}{\delta \mathbf{X}_{\vec{r}_2}} = \frac{\delta \mathbf{Q} [\mathbf{X}]_{\vec{r}_1}}{\delta \mathbf{X}_{\vec{r}_2}} S' (\mathbf{X}_{\vec{r}_2}) ,$$

and the form of Ψ near a maximum is naturally characterized by the exponent ε of the local map as defined by (2).

Other requirements (analogous to properties (1-3)) for Ψ concern the operator $\mathbf{Q} \in \Upsilon'$. Roughly speaking, theses properties should insure that $\mathbf{Q}$ behaves as expected from a DCO in the most general case: basically, $\mathbf{Q}$ should drive all configurations towards the synchronous manifold, and make all volumes in the phase space shrink to the line $\mathbf{I}_{\text{syn}}$. In the case when the coupling operator $\mathbf{Q} = \mathbf{\Delta}$ is linear, properties (1-3) are expressed via the kernel

$$\mathcal{D} (\vec{r}_1 - \vec{r}_2) = \frac{\delta \mathbf{\Delta} [\mathbf{X}]_{\vec{r}_1}}{\delta \mathbf{X}_{\vec{r}_2}}$$

which is constant over $\mathbf{I}$ and only depends on the difference $\vec{r}_1 - \vec{r}_2$. For non-linear couplings, these properties should be reinterpreted in terms of the tangent operator $\delta \mathbf{Q} / \delta \mathbf{X}$.

However, the non-linear DCOs that are relevant to our problem can be given a simple description. Given a linear diffusive transformation $\mathbf{\Delta}$ with a kernel $\mathcal{D}$ and a coupling length λ, let us consider the operator $\mathbf{Q} = \mathbf{h}^{-1} \circ \mathbf{\Delta} \circ \mathbf{h}$ where h is some smooth change of variables. This operator is conjugate to $\mathbf{\Delta}$ and therefore has an action on phase space which resembles that of a linear DCO. It is homogeneous and accounts for the same lattice symmetries as $\mathbf{\Delta}$; it drives all configurations towards the synchronous manifold. Since h does not induce any correlation between sites (it is purely local), the interaction between sites is completely governed by $\mathbf{\Delta}$. In particular, the asymptotic behavior (long time) under $\mathbf{Q}$ is determined via $\mathbf{Q}^n = \mathbf{h}^{-1} \circ \mathbf{\Delta}^n \circ \mathbf{h}$, and is completely characterized by $\mathbf{\Delta}$ [4].

Finally, the composition of such non-linear diffusive coupling operators is also a diffusive coupling operator since it is nothing else than a (possibly

[4] In fact, the derivative of $\mathbf{Q}$ at any configuration $\mathbf{X}$ reads

$$\frac{\delta \mathbf{Q} [\mathbf{X}]_{\vec{r}_1}}{\delta \mathbf{X}_{\vec{r}_2}} = \frac{h' (\mathbf{X}_{\vec{r}_2})}{h' \left([\mathbf{h}^{-1} \circ \mathbf{\Delta} \circ \mathbf{h} (\mathbf{X})]_{\vec{r}_1} \right)} \mathcal{D} (\vec{r}_1 - \vec{r}_2)$$

and depends on $\mathbf{X}$, although it is constant on $\mathbf{I}_{\text{syn}}$ where it is equal to $\mathcal{D}$. The symmetry $\vec{r}_1, \vec{r}_2$, and the invariance by translation are not respected by this operator, but they recovered by considering its spatial average $\langle \delta \mathbf{Q} / \delta \mathbf{X} \rangle$. This tangent operator accounts for the dependence of an image site with respect to its antecedents. In all cases, $\delta \mathbf{Q} / \delta \mathbf{X}$ is non-negative since h' does not change sign, and the kernel $\mathcal{D}$ is non-negative. The range of

complicated) way to drive a system towards complete synchronization. Such an operator is in general written as

$$\mathbf{Q} = \mathbf{h}_1^{-1} \circ \mathbf{\Delta}_1 \circ \mathbf{h}_1 \circ \cdots \circ \mathbf{h}_N^{-1} \circ \mathbf{\Delta}_N \circ \mathbf{h}_N$$

for some invertible h_i's and linear couplings $\mathbf{\Delta}_i$'s. It means that when $\mathbf{Q}$ is applied, the system is driven towards synchronization by following the $\mathbf{\Delta}_i$'s in different systems of coordinates. In particular, the tangent operator of $\mathbf{Q}$ on $\mathbf{I}_{\rm syn}$ is $\mathbf{\Delta}_1 \circ \cdots \circ \mathbf{\Delta}_N$, which defines uniquely the diffusion constant by $\lambda^2 = \sum_i \lambda_i^2$. By construction, the space $\mathbf{\Upsilon}'$ of such operators is invariant by composition (which adds up the diffusion constants) and by applying some change of variable (which keeps the diffusion constant invariant).

All intervals are invariant by all $\mathbf{Q} \in \mathbf{\Upsilon}'$ and all volumes shrink. These operators drive all configurations to the synchronous manifold and they are characterized by their tangent operator at $\mathbf{I}_{\rm syn}$ which accounts for the strength of the coupling and its spatial extension.

5.3 Doubling transformation

5.3.1 Definition

The application of the doubling transformation to some map $\mathbf{\Psi} = \mathbf{Q} \circ \mathbf{S} \in \mathbf{\Upsilon}$ is now straightforward. When the reduced map is in a two-band regime, it exchanges the intervals $I_S^* = [-a, a]$ and $I_S^{1,1} = [b, 1]$. The coupling operator $\mathbf{Q}$ is nonlinear ($\in \mathbf{\Upsilon}'$) and therefore keeps intervals invariant: it guarantees that the two non-intersecting intervals $\mathbf{I}_S^* = [-a, a]^{\mathcal{L}}$ and $\mathbf{I}_S^{1,1} = [b, 1]^{\mathcal{L}}$ are exchanged by $\mathbf{\Psi}$ and stable by $\mathbf{\Psi}^2$. Thus $\mathbf{\Psi}^2$ can be restricted to $\mathbf{I}_S^*$, and reads,

$$\mathbf{\Psi}^2\Big|_{\mathbf{I}_S^*} = \mathbf{Q} \circ \mathbf{S}\Big|_{\mathbf{I}_S^{1,1}} \circ \mathbf{Q} \circ \mathbf{S}\Big|_{\mathbf{I}_S^*} .$$

Considering $\mathbf{\Psi}^2$ on $\mathbf{I}_{\rm syn}$ shows that its reduced map is S^2 and, using the invertibility of S on $\mathbf{I}_S^{1,1}$, provides its canonical representation:

$$\mathbf{\Psi}^2\Big|_{\mathbf{I}_S^*} = \left(\mathbf{Q} \circ \mathbf{S}\Big|_{\mathbf{I}_S^{1,1}} \circ \mathbf{Q} \circ \mathbf{S}\Big|_{\mathbf{I}_S^{1,1}}^{-1}\right) \circ \mathbf{S}^2\Big|_{\mathbf{I}_S^*} .$$

---

this dependence is measured on $\delta\mathbf{Q}/\delta\mathbf{X}$ by a quantity of the form

$$\int (\vec{r}_1 - \vec{r}_2)^2 \, \frac{\delta \mathbf{Q}\,[\mathbf{X}]_{\vec{r}_1}}{\delta \mathbf{X}_{\vec{r}_2}} d\vec{r}_1 d\vec{r}_2 \;, = \int \vec{\rho}^{\,2} \left\langle \frac{\delta \mathbf{Q}}{\delta \mathbf{X}} \right\rangle (\vec{\rho})\, d\vec{\rho}$$

which remains bounded provided that $|h'|$ verifies $m \leq |h'| \leq M$ for some $M, m > 0$. The assumption on bounds for $|h'|$ is stronger than just invertibility. It insures that the nonlinear coupling operator works in a normal diffusive manner at all points in phase space. It will be always verified in this work.

Applying the linear change of variable $\mathbf{h}_S(\mathbf{X}) = -\mathbf{X}/a$ yields

$$\Psi^2\big|_{\mathbf{I}_S^*} = \mathbf{h}_S^{-1} \circ \Theta[\Psi] \circ \mathbf{h}_S ,$$

which defines the doubling transformation in Υ:

$$\Theta[\Psi] \equiv \Theta'_S[\mathbf{Q}] \circ \mathbf{T}[\mathbf{S}] , \tag{17}$$

where $\mathbf{T}[\mathbf{S}]$ denotes the uncoupled map which transforms each local variable by $T[S]$ while

$$\Theta'_S[\mathbf{Q}] \equiv \mathbf{h}_S \circ \left(\mathbf{Q} \circ \left(\mathbf{S}\big|_{\mathbf{I}_S^{1,1}} \circ \mathbf{Q} \circ \mathbf{S}\big|_{\mathbf{I}_S^{1,1}}^{-1}\right)\right) \circ \mathbf{h}_S^{-1} \tag{18}$$

defines the action of the doubling transformation on the space Υ' of non-linear coupling operators.

Phase portrait for Θ We have shown that there a unique way to define the doubling transformation in the general case and that it must respect the RG of the local map. This property stems from the definition of the reduced map, *i.e.* the only possible local map under very general assumptions.

When the doubling transformation is applied to map Ψ, its reduced map is transformed by the local doubling transformation T on Ω (Θ and $\mathbf{P}$ commute) and when Ψ follows the flow of Θ in Υ, $\mathbf{P}[\Psi]$ follows the flow of T in Ω. Taking the local map in the stable (resp. unstable) manifold of the local RG shows that the manifolds $\Upsilon' \circ \mathbf{W}_s \subset \Upsilon$ (resp. $\Upsilon' \circ \mathbf{W}_u$) are invariant by Θ.

Similarly, the univoque definition of a diffusion constant for any DCO shows that under the doubling transformation, the diffusion constant doubles *i.e.* the coupling length is multiplied by $\beta = \sqrt{2}$. This property was already found for coupled tent maps, and appears to be directly related to the "synchronously updated" form of the evolution operator. It must also be accompanied by a decay of the lattice mesh size, $\|\vec{e}\|$: the lattice converges to a continuous limit.

The precise action of the doubling transformation on DCOs in the space Υ' is however complicated and "coupled" with the local RG. Iterating (18) shows that Θ'^n involves the different iterates of the local map under T. In some sense, the dynamical operator Θ' depends on the "time" n when iterated. However, when the iteration of the local map converges to some universal map, Θ' also converges and the existence of some limit behavior for the coupling operator arises from the properties of the asymptotic Θ'.

Let us consider the case when the local map is the fixed point Φ:

$$\Theta\left[\mathbf{Q}\circ\Phi\right]\equiv\Theta'_{\Phi}\left[\mathbf{Q}\right]\circ\Phi\,,$$

and associate the doubling transformation with the rescaling $\|\vec{e}\|\to\|\vec{e}\|/\beta$. The coupling length λ of the coupling operator is invariant under this transformation: due to the spatial rescaling, a fixed point coupling operator under Θ'_{Φ} should correspond to a continuous field of variables. Such an operator is denoted $\mathbf{Q}_{\lambda}$ to mention explicitly the dependence in the length-scale λ, and the fixed point is determined by the equation,

$$\mathbf{h}_{\Phi}\circ\left(\mathbf{Q}_{\lambda}\circ\left(\Phi\big|_{\mathbf{I}_{\Phi}^{1,1}}\circ\mathbf{Q}_{\lambda}\circ\Phi\big|_{\mathbf{I}_{\Phi}^{1,1}}^{-1}\right)\right)\circ\mathbf{h}_{\Phi}^{-1}=\mathbf{Q}_{\lambda\beta}\,.$$

In the case of coupled tent maps, this equation reduces to the equality,

$$\mathbf{Q}_{\lambda}^{2}=\mathbf{Q}_{\lambda\beta}$$

which is verified by $\mathbf{\Delta}_{\lambda}^{\infty}$. However, the convergence of the coupling operator to such a limit is not proven.

5.3.2 Qualitative universality

Limits of NTS The application of the doubling transformation relies on the assumption that the system is in a BS. The RG can be iterated provided that the system reaches BSs of increasing order when $\mu\to\mu_{\infty}$. Like in the case of coupled tent maps, the generality of this approach stems from the observation that taking $\mu\to\mu_{\infty}$ amounts to a strengthening of the coupling and guarantees that, for sufficiently strong coupling, there is an infinite sub-harmonic cascade of phase transitions. Let us now detail this argument. We consider a lattice of non-linearly coupled maps, $\Psi=\mathbf{Q}_{q}\circ\mathbf{S}_{\mu}$: this could represent a CML of the form $\mathbf{\Delta}_{g}^{m}\circ\mathbf{S}$, where the two parameters m and g of the original coupling operator are encoded by the "strength" q.

For $\mu\leq\bar{\mu}_{n}$, a BSn is reached from almost all initial conditions in a BS$(n-1)$ whenever the coupling strength is larger than the limit value $g_{\mathrm{e}}^{n}\left(\Psi\right)$. If moreover $\mu\leq\bar{\mu}_{n+1}$, the map $T\left[S_{\mu}\right]$ has 2^{n} bands, and the system $\Theta\left[\Psi\right]$ reaches a BSn for $g>g_{\mathrm{e}}^{n}\left(\Theta\left[\Psi\right]\right)$: this situation corresponds to a BS$(n+1)$ in the 2^{n+1}-band regime of S_{μ}, hence

$$g_{\mathrm{e}}^{n+1}\left(\Psi\right)=g_{\mathrm{e}}^{n}\left(\Theta\left[\Psi\right]\right)\,.$$

Let us denote $\mathbf{Q}_q^{(n)} \circ \mathbf{T}^n [\mathbf{S}_\mu]$ the successive images of $\mathbf{\Psi} = \mathbf{Q}_q \circ \mathbf{S}_\mu$ by the doubling transformation. From the definition (18) of doubling transformation $\mathbf{\Theta}'$ for DCOs, $\mathbf{Q}_q^{(n+1)}$ is a "stronger" coupling than $\mathbf{Q}_q^{(n)}$ in the sense that it makes the volume of the phase space shrink even more. Consequently, for any fixed local map S with at least two bands, the system $\mathbf{Q}_q^{(n)} \circ \mathbf{S}$ reaches banded states more easily with n increasing, hence $g_{\mathrm{e}}^1 \left(\mathbf{Q}_q^{(n)} \circ \mathbf{S} \right)$ decreases with n. Moreover, when $n \to \infty$, the coupling length diverges at a fixed mesh size (*i.e.* the ratio $\lambda / \|\vec{e}\|$ diverges like β^n): taking $\|\vec{e}\| \propto \beta^{-n}$ shows that for large n, $\mathbf{Q}_q^{(n)}$ corresponds to a coupling operator for a continuous field without even knowing precisely the behavior of $\mathbf{Q}_q^{(n)}$ in this limit. Therefore, the discretization of the lattice disappears, there is no possible pinning of clusters to allow for the co-existence of phases and $g_{\mathrm{e}}^1 \left(\mathbf{Q}_q^{(n)} \circ \mathbf{S} \right)$ is expected to vanish:

$$g_{\mathrm{e}}^1 \left(\mathbf{Q}_q^{(n)} \circ \mathbf{S} \right) \underset{n \to \infty}{\to} 0 . \tag{19}$$

If the system is considered *e.g.* at all $\bar{\mu}_n$, the property (19) added to the fact that the sequence $\mathbf{T}^n [\mathbf{S}_{\bar{\mu}_n}]$ converges to $\mathbf{\Phi}_1^*$ show that the sequence

$$g_{\mathrm{e}}^n \left(\mathbf{Q}_q \circ \mathbf{S}_{\bar{\mu}_n} \right) = g_{\mathrm{e}}^1 \left(\mathbf{Q}_q^{(n)} \circ \mathbf{T}^n [\mathbf{S}_{\bar{\mu}_n}] \right)$$

vanishes in the limit $n \to \infty$; in particular it is bounded above which shows that by an appropriate choice of the coupling strength q *i.e.* the strength and/or the extension of the DCO $\mathbf{\Delta}_g^m$, the sub-harmonic cascade of banded states is infinite. In this strong-coupling limit, coupled maps exhibit their universal behavior since the low-coupling regimes stem from the existence of a discrete lattice and depend on the fine details of the system *i.e.* the details of the chosen coupling operator.

Illustration The RG is illustrated in Fig. 9 on the case of democratically-coupled logistic maps on a 2-dimensional lattice. Period 2^n is observed at the points $\bar{\mu}_n$ *i.e.* for $\mathbf{\Psi} = \mathbf{\Delta}_g \circ \mathbf{S}_{\bar{\mu}_n}$: these regimes correspond to fixed points for $\mathbf{\Theta}^n [\mathbf{\Delta}_g \circ \mathbf{S}_{\bar{\mu}_n}]$. When n increases, the reduced map of these operators follows the local RG and therefore converges to the universal map Φ_1^*.

These distributions were evaluated by the direct simulation of $\mathbf{\Delta}_g \circ \mathbf{S}_{\bar{\mu}_n}$, and the measure of the pdfs when the system lies on the central band, followed by a simple rescaling. These pdfs p_n are displayed on Fig. 9-(c) where it is clear that they admit a well-defined limit when $n \to \infty$. This limit does not necessarily corresponds to the existence of a limit for the coupling operator iterated by

$\mathbf{\Theta}'$ and involving all $\mathbf{T}^n[\mathbf{S}_{\bar{\mu}_n}]$: it is the macroscopic motion produced by the operators of the form $\mathbf{Q}_q^{(n)} \circ \mathbf{\Phi}_1^*$ which admit a well-defined limit when $n \to \infty$.

5.4 Metric properties

In the case $\mathbf{\Psi} = \mathbf{\Delta} \circ \mathbf{S}_\mu$, for a family of unimodal maps, the bands shrink when the parameter μ approaches μ_∞, and the local map is better and better approximated by a tangent on each non-central band $I_{S_\mu}^{n,\sigma}$. The shrinking of these bands near μ_∞ allows to perform the commutation so that, in this limit, a doubling transformation defined by forcing the commutation accounts for the universal properties of the coupled dynamics.

5.4.1 Commuting doubling transformation

The observation that in the general case, a non-linear DCO is naturally characterized by the tangent operator on $\mathbf{I}_{\text{syn}}$ leads to define a *"commuting" doubling transformation* for which the commutation is performed *a priori*. Let us define

$$\mathbf{\Theta}_c[\mathbf{Q} \circ \mathbf{S}] \equiv \mathbf{Q}^2 \circ \mathbf{T}[\mathbf{S}] \,. \tag{20}$$

When the doubling transformations are iterated, the operator $\mathbf{\Theta}^n[\mathbf{\Psi}]$ shares strong similarities with $\mathbf{\Theta}_c^n[\mathbf{\Psi}] = \mathbf{Q}^{2^n} \circ \mathbf{T}^n[\mathbf{S}]$ although this comparison is only qualitative.

Phase portrait of $\mathbf{\Theta}_c$ Denoting

$$\mathbf{\Theta}_c[\mathbf{\Delta} \circ \mathbf{S}] \equiv \mathbf{\Theta}_c'[\mathbf{\Delta}] \circ \mathbf{T}[\mathbf{S}] \,,$$

and

$$\mathbf{\Theta}_c'[\mathbf{\Delta}] \equiv \mathbf{\Delta}^2$$

permits to separate $\mathbf{\Theta}_c$ into the local RG transformation T and the spatial RG transformation $\mathbf{\Theta}_c'$. This case is particularly simple since all linear coupling operators converge to $\mathbf{\Delta}_\lambda^\infty$ when iterated: there a unique family of stable fixed points which, in fact, are all equivalent to each other since λ plays no particular role. Under $\mathbf{\Theta}_c$, the local map converges to a universal map, while the coupling operator $\mathbf{\Delta}_g^m$ goes to some $\mathbf{\Delta}_\lambda^\infty$ like in the case of coupled tent maps.

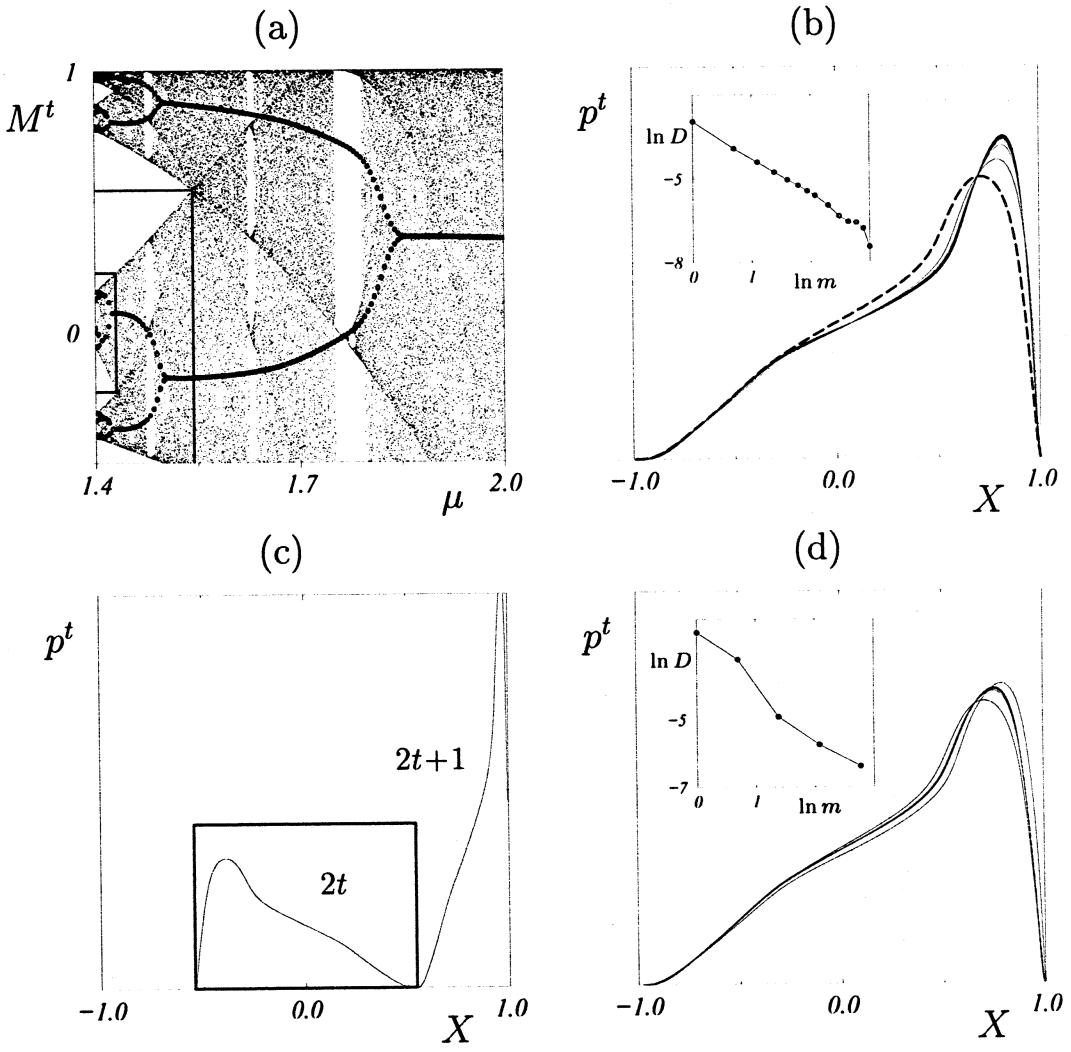

Figure 9: Two-dimensional lattice of democratically coupled ($g = 0.2$) logistic maps. (a): Bifurcation diagram of M^t (circle) compared with the bifurcation diagram of the single logistic map; the $[\mu_\infty, \bar{\mu}_1] \otimes I^1_{\bar{\mu}_1}$ and $[\mu_\infty, \bar{\mu}_2] \otimes I^2_{\bar{\mu}_2}$ regions are shown. (b-d): Asymptotic regime for the single-site pdf p^t. (b): stationary state at $\mu = 2$ for $1 \leq m \leq 32$: they converge towards the pdf for the continuous limit. (c): period-2 collective cycle at the first band-splitting point $\mu = \bar{\mu}_1$; the distribution in the rectangle corresponds to the times when all sites lie on the central band and is reported on (b) (dashed) after renormalization. (d): Period-2^n is found at all points $\bar{\mu}_n$ and the renormalized pdfs on the central band converge.

5.4.2 Asymptotic equivalence

Let us first estimate the commutator

$$[\mathbf{\Delta}, \mathbf{S}] = \mathbf{\Delta} \circ \mathbf{S} - \mathbf{S} \circ \mathbf{\Delta}$$

of $\mathbf{\Delta}$ and $\mathbf{S}$ applied to some configuration $\mathbf{X}$. For this purpose, each local variable is written

$$\mathbf{X}_{\vec{r}} = \langle \mathbf{X} \rangle + \mathbf{x}_{\vec{r}} \,,$$

where the field $\mathbf{x}$ has been introduced which measures the local departure from the mean-field $M = \langle \mathbf{X} \rangle$. A Taylor expansion of the local map around M reads,

$$S\left(\mathbf{X}_{\vec{r}}\right) = S\left(M\right) + \mathbf{x}_{\vec{r}} S'\left(M\right) + \frac{\left(\mathbf{x}_{\vec{r}}\right)^2}{2} S''\left(M\right) + \cdots$$

for the field $\mathbf{X}$ and for $\mathbf{\Delta}\left(\mathbf{X}\right) = \mathbf{M} + \mathbf{\Delta}\left(\mathbf{x}\right)$, it reads,

$$S\left(\left[\mathbf{\Delta}\left(\mathbf{X}\right)\right]_{\vec{r}}\right) = S\left(M\right) + \left[\mathbf{\Delta}\left(\mathbf{x}\right)\right]_{\vec{r}} S'\left(M\right) + \frac{\left(\left[\mathbf{\Delta}\left(\mathbf{x}\right)\right]\left(\vec{r}\right)\right)^2}{2} S''\left(M\right) + \cdots$$

Applying $\mathbf{\Delta}$ to the first of these equations, and performing the difference, only the second order terms remain and it comes

$$\left[\mathbf{\Delta}, \mathbf{S}\right]\left(\mathbf{X}\right) = \frac{1}{2}\left[\mathbf{\Delta}\left(\mathbf{x}^2\right) - \left[\mathbf{\Delta}\left(\mathbf{x}\right)\right]^2\right] S''\left(M\right) + \cdots$$

If moreover, the histogram of all sites in the configuration $\mathbf{X}$ lies on an interval $I_{\mathbf{X}}$ of width $\eta_{\mathbf{X}}$, the rhs of this equation is dominated by $\eta_{\mathbf{X}}^2 \max_{I_{\mathbf{X}}} |S''|/2$, and

$$\left\| \left[\mathbf{\Delta}, \mathbf{S}\right]\left(\mathbf{X}\right) \right\| = \mathrm{O}\left(\eta_{\mathbf{X}}^2 \max_{I_{\mathbf{X}}} |S''|\right) \,,$$

where the norm $\|\mathbf{X}\| = \max X_{\vec{r}}$ has been introduced.

This permits to estimate the error committed by performing the commutation in the doubling transformation. When the operator

$$\left(\mathbf{\Delta} \circ \mathbf{S}\right)^2 - \mathbf{\Delta}^2 \circ \mathbf{S}^2 = \mathbf{\Delta} \circ \left[\mathbf{S}, \mathbf{\Delta}\right] \circ \mathbf{S}$$

is applied to a configuration $\mathbf{X} \in \mathbf{I}_S^*$, the commutator is evaluated on the configuration $\mathbf{S}\left(\mathbf{X}\right)$. However, when $\mu \to \mu_\infty$, the bands shrink and become small compared to the interval I_S^*: the state $\mathbf{S}\left(\mathbf{X}\right)$ lies on an interval $I_{\mathbf{S}(\mathbf{X})} \subset I_S^{1,1}$ which is much smaller than the "meta-bands" I_S^* or $I_S^{1,1}$. In fact, if η_μ denotes the average width of the bands at μ, $\eta_\mu \to 0$ when $\mu \to \mu_\infty$ because the attractor converges to a Cantor set. Moreover the second derivative of S which

appears in the commutator involves only values in $I_S^{1,1}$, and $\max_{I_S^{1,1}} |S''| = \mathrm{O}(\varepsilon)$. This provides the estimate,

$$\left\| \left[(\Delta \circ \mathbf{S})^2 - \Delta^2 \circ \mathbf{S}^2 \right] (\mathbf{X}) \right\| = \mathrm{O}\left(\eta_\mu^2 \varepsilon\right)$$

This result should be compared to fluctuations of the local values in the configuration $\mathbf{X}$ itself, measured by $\|\mathbf{x}\| = \|\mathbf{X} - \mathbf{M}\|$ which is of order η_μ: it comes,

$$\frac{\left\| \left[(\Delta \circ \mathbf{S})^2 - \Delta^2 \circ \mathbf{S}^2 \right] (\mathbf{X}) \right\|}{\|\mathbf{X} - \mathbf{M}\|} = \mathrm{O}(\eta_\mu \varepsilon)$$

Therefore, after performing the linear change of variables $\mathbf{h}_S\ \mathbf{X} \to -\mathbf{X}/a_\mu$ ($a_\mu = 1 - \mu$), it comes,

$$\frac{\left\| \Theta \left[\Delta \circ \mathbf{S} \right] (\mathbf{X}) - \Theta_{\mathrm{c}} \left[\Delta \circ \mathbf{S} \right] (\mathbf{X}) \right\|}{\|\mathbf{X} - \mathbf{M}\|} = \mathrm{O}(\eta_\mu \varepsilon) \ .$$

This means that the perturbation induced by the commutation decays in either one of the two limits $\mu \to \mu_\infty$ or $\varepsilon \to 0$. In particular, for any fixed ε, the metric properties of the doubling transformation Θ depend on its description near μ_∞: Θ and Θ_{c} are tangent near the stable manifold and therefore, these properties are the same as those given by the "commuting" doubling transformation.

5.4.3 Scaling consequences & universality

The commuting doubling transformation associates the operator $\Delta_g \circ \mathbf{S}_{\bar{\mu}_n}$ to

$$\Theta_{\mathrm{c}}^n \left[\Delta_g \circ \mathbf{S}_{\bar{\mu}_n} \right] = \Delta^{2^n} \circ \mathbf{T}^n \left[\mathbf{S}_{\bar{\mu}_n} \right] .$$

In this case the existence of a limit when $n \to \infty$ arises directly from the existence of a well-defined collective behavior in the continuous limit and when the local map converges to a universal map: when $n \to \infty$, the operator $\Theta_{\mathrm{c}}^n \left[\Delta_g \circ \mathbf{S}_{\bar{\mu}_n} \right]$ converges to $\Delta_\lambda^\infty \circ \Phi_1^*$.

We studied this convergence numerically from a simulation of $\Delta^{2^n} \circ \mathbf{S}_{\bar{\mu}_n}^{2^n}$ followed by a simple rescaling of the pdfs on the central band. The fixed-point pdfs p_n^c observed for these systems are displayed Fig. 10-(a) for n varying from 1 to 32. They are then compared with the universal collective fixed-points p_n obtained from $\Theta^n \left[\Delta_g \circ \mathbf{S}_{\bar{\mu}_n} \right]$: p_{32} and p_{32}^c are displayed on Fig. 10-(b) and differ of less than a percent. However, these series of pdfs are not expected to have the same limit, and this appears when the distances $D(p_n - p_n^c)$ are plotted versus n (insert of Fig. 10-(b)). This excellent agreement indicates that

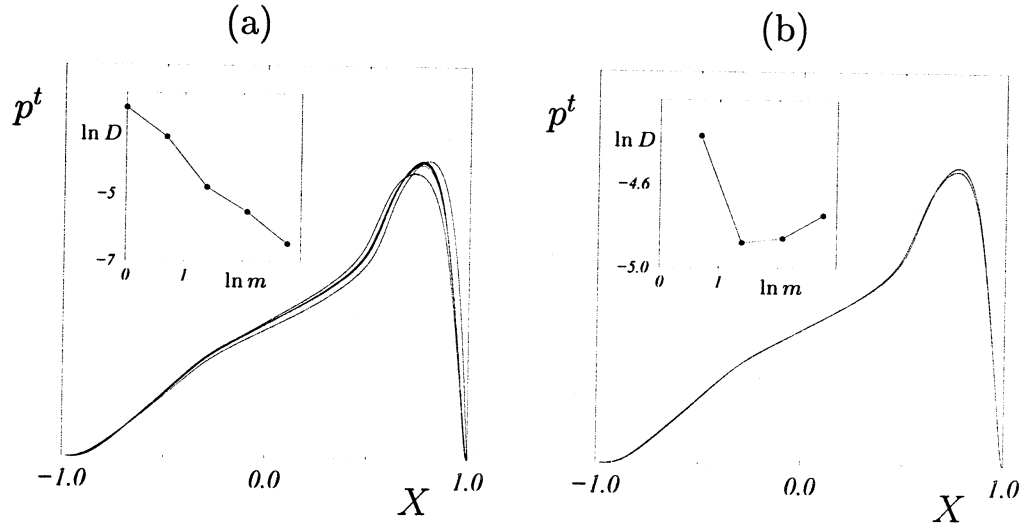

Figure 10: 2-dimensional lattice of democratically coupled ($g = 0.2$) logistic maps. (a): fixed point regimes displayed by the operators $\Theta_c^n [\Delta_g \circ \mathbf{S}_{\bar{\mu}_n}]$. (b) comparison of the universal collective behaviors obtained from the RG and the commuting RG.

the macroscopic motion induced by the operator $\Theta^n [\Delta_g \circ \mathbf{S}_{\bar{\mu}_n}]$ is essentially dominated by its expression near the synchronous manifold: in this limit, the space is continuous, the profile $\mathbf{X}_{\bar{r}}$ is smooth, and the largest weights in the coupling are attributed to the nearest sites.

In the case of the continuous field dynamics, $\Delta_\lambda^\infty \circ \mathbf{S}_\mu$, the commuting doubling transformation (20) reads,

$$\Theta_c [\Delta_\lambda^\infty \circ \mathbf{S}_\mu] = \Delta_{\lambda\sqrt{2}}^\infty \circ \mathbf{T} [\mathbf{S}_\mu] \ . \tag{21}$$

Thanks to the asymptotic equivalence, it characterizes the universal properties of coupled dynamics. In this case, the RG holds in its greatest generality since BSs of maximal order are always reached. Moreover, because λ does not affect the collective behavior of the single-site observables contained in p^t, equation (21) is strictly equivalent to the RG equation for the local map for these macroscopic quantities. In particular, the width w of these pdfs therefore scales with the reduction parameter α of the local map: $w \simeq (\mu - \mu_\infty)^\gamma$ with $\gamma = \ln\alpha / \ln\delta$. However, this "normal" behavior of the single-site observables is accompanied by an increase of the coupling length, since it is multiplied by $\beta = \sqrt{2}$ at each period doubling. The same dilatation applies to all length-scales and in particular to the coherence and correlation length: $\xi \simeq (\mu - \mu_\infty)^{\beta'}$ with $\beta' = \ln\beta / \ln\delta$. Let us mention finally that in this continuous limit, the

Lyapunov exponents are *not* expected to be related to the coupling length λ, and they all scale like their local counterpart: $\Lambda \simeq (\mu - \mu_\infty)^\nu$ with $\nu = \ln 2 / \ln \delta$. However, this does not indicate, as claimed in [10] the existence of a relation of the form $\xi \simeq \Lambda^{-1/2}$ in all generality: spatial lengthscales and Lyapunov exponents may vary differently on any interval $[\bar{\mu}_{n+1}, \bar{\mu}_n]$. This is quite obvious at the Ising-like phase transition points μ_n^c observed for $d = 2$ and $d = 3$, where the correlation length diverges while the largest Lyapunov exponent does not vanish [14].

For large n, if the map is observed, *e.g.*, at the band-splitting points, $\mathbf{\Theta}_c^n [\mathbf{\Delta}_\lambda^\infty \circ \mathbf{S}_{\bar{\mu}_n}]$ is equivalent to the universal coupled system $\mathbf{\Delta}_{\lambda\beta^n}^\infty \circ \mathbf{\Phi}_1^*$ with a diverging coupling length, while $\mathbf{\Theta}_c^n [\mathbf{\Delta}_\lambda^\infty \circ \mathbf{S}_{\mu_\infty}]$ is equivalent to $\mathbf{\Delta}_{\lambda\beta^n}^\infty \circ \mathbf{\Phi}$.

These results for the continuous field operator $\mathbf{\Delta}_\lambda^\infty \circ \mathbf{S}_\mu$ can be immediately translated to the case of discrete (usual) CMLs. In this case, the commuting doubling transformation (20) can be accompanied by a rescaling of the lattice mesh size to maintain a constant coupling length λ. This show that all the scalings properties of the local map are transmitted to the coupled system, with the additional exponent $\beta = \sqrt{2}$ characterizing the divergence of length-scales. Similarly, the shrinking of the widths of the pdfs on the central band is controlled by the exponent α. This provides a complete explanation of the results obtained numerically by [10].

For example, in the case of two- or three-dimensional lattices of coupled tent or logistic maps, the bifurcation points μ_n^c which are Ising-like phase transitions are related to each other by the RG like the band splitting points $\bar{\mu}_n$ and therefore follow the same universal behavior. The convergence $\mu_n^c \to \mu_\infty$ is characterized by the Feigenbaum constant δ of the local map. For the same reasons, the root mean square of the pdfs p^t shrinks like the widths of the bands. Finally, for large n, operator $\mathbf{\Delta}_g^m \circ \mathbf{S}_{\bar{\mu}_n}$ is equivalent to the universal operator $\mathbf{\Delta}_\lambda^\infty \circ \mathbf{\Phi}_1^*$. This is illustrated on Fig. 9 where the asymptotic renormalized pdfs on the central band at the points $\bar{\mu}_n$ are seen to converge.

6 Conclusion

Our work has shown how RG equations can be derived for coupled unimodal maps. Like in the case of maps of an interval, this RG relies on the following observation (which holds under some assumptions to be defined more precisely): given a normalized unimodal map $\mathbf{\Phi}$ on the phase space $\mathbf{I}$, the iterated map $\mathbf{\Phi}^2$ can be restricted to an interval, and, by an appropriate rescaling,

yield again a normalized unimodal map on $\mathbf{I}$. The transformation $\mathbf{\Theta}$, which associates this unimodal map to $\mathbf{\Phi}$, is called the doubling transformation and provides a natural framework for understanding the self-similarity properties of discrete-time spatially-extended dynamical systems.

RG for banded states In the case of coupled maps, $\mathbf{\Phi} = \mathbf{\Delta}_g^m \circ \mathbf{S}_\mu$ and the RG equations hold for configurations where all sites lie in the same band at every timestep (banded-states). The RG relies on the commutation properties of the coupling operator with the local map on bands where the local map in invertible. It takes a surprisingly simple form when applied to the case of coupled tent maps since,

$$\mathbf{\Theta}\left[\mathbf{\Delta}_g^m \circ \mathbf{S}_\mu\right] = \mathbf{\Delta}_g^{2m} \circ \mathbf{S}_{\mu^2}\,.$$

In this case the RG operates directly in the parameter space (μ, m): $(\mu, m) \to (\mu^2, 2m)$ where the transformation $\mu \to \mu^2$ corresponds to the RG for the tent map. This example provides a clear illustration of how the RG acts: the local map is transformed by its own (local) doubling transformation T while the coupling operator is iterated, implying the doubling of the diffusion constant, *i.e.* a multiplication of the coupling length λ by a factor $\beta = \sqrt{2}$.

The expression of the RG requires more care in the general case of coupled unimodal maps. It leads to embed the usual linearly coupled maps into the wider space $\mathbf{\Upsilon}$ of coupled maps of the form $\mathbf{Q} \circ \mathbf{S}$. The DCO $\mathbf{Q}$ may contain some nonlinearities, although it should operate like a linear DCO at least locally in phase space. With this enlarged definition, the doubling transformation operates on $\mathbf{\Upsilon}$ and can be specified by its action on the local map and on the DCO. It is striking that, in all cases, the local map S is always transformed by its own (local) doubling transformation T. Meanwhile, the (non-linear) DCO $\mathbf{Q}$ is transformed into a operator (which resembles $\mathbf{Q}^2$) with a doubled diffusion constant like in the case of linearly coupled tent maps.

Commuting doubling transformation Two remarks summarize this approach: Firstly, a RG relation can indeed be written in the general case, and it transforms the local map by the RG for maps on an interval. Secondly, the action of this RG on non-linear DCO resembles the iteration $\mathbf{Q} \to \mathbf{Q}^2$. This leads to define a commuting doubling transformation $\mathbf{\Theta}_c$ which is an approximation of the exact RG. It accounts qualitatively for the self-similarity

displayed by these systems. Moreover, the property that, near μ_∞, the bands shrink, allows to show that Θ share the universal properties of Θ_c.

No hypothesis on the behavior on $[\bar{\mu}_1, \bar{\mu}_0]$ The RG approach does not provides any description of the behavior on the interval of parameter $[\bar{\mu}_1, \bar{\mu}_0]$. This situation is similar to the case of single maps: depending on $\mu \in [\bar{\mu}_1, \bar{\mu}_0]$, the system can be ergodic or reach a periodic window. In the case of coupled maps, for a given coupling operator, a given dimension, a given local map and $\mu \in [\bar{\mu}_1, \bar{\mu}_0]$, the collective behavior can be periodic or quasi-periodic, can display some hysteresis,... and this is not predicted by the RG. However, the RG permits to relate the different regimes on all intervals $[\bar{\mu}_{n+1}, \bar{\mu}_n]$ to the behavior observed on $[\bar{\mu}_1, \bar{\mu}_0]$. Since no assumption is made about the particular collective dynamics in a given band nor about the local state of the lattice, the RG approach is very general and can be applied to CMLs in all dimensions, globally-coupled maps, etc. However, the universal collective behavior reached near μ_∞ is directly related to the continuous limit which remains essentially unexplored in higher dimensions.

Validity The single requirement needed to apply the doubling transformation is that the system is in a BS. The property that, for strong enough coupling, and from almost initial conditions, the system flows to a BS has been termed non-trivial synchronization (NTS), and is a weaker property than NTCB. However, the requirements on the coupled maps dynamics to insure that NTCB is reached are often not explicited. A usual assumption is that NTCB is achieved for sufficiently strong coupling strengths. Therefore, the study of the necessary conditions for NTS is of great interest since it allows both to state when the RG can be applied to generic asymptotic regimes, and also to shed some light on NTCB. By use of the RG itself, it is possible to show that, when $\mu \to \mu_\infty$, the coupling operator takes on a wider spatial extension and therefore appears to be stronger compared to the local map. This insures that a coupling operator that guarantees that NTS is reached in a two-band regime, also allows to reach NTS for any number of bands encountered when $\mu \to \mu_\infty$. Consequently, there must be an infinite sub-harmonic cascade of phase transitions, independently of the particular behavior observed on $[\bar{\mu}_1, \bar{\mu}_0]$.

Scaling properties Although the commuting doubling transformation is purely qualitative for the comparison of the regimes on the intervals $[\bar{\mu}_{n+1}, \bar{\mu}_n]$ and $[\bar{\mu}_1, \bar{\mu}_0]$, it becomes exact in the limit $\mu \to \mu_\infty$, when comparing the regimes on $[\bar{\mu}_{n+1}, \bar{\mu}_n]$ and $[\bar{\mu}_n, \bar{\mu}_{n-1}]$ for $n \to \infty$. Therefore, it is sufficient to study the universality properties displayed by Θ_c to characterize the universality properties of coupled maps. The commuting doubling transformation has the same simple form as in the case of the coupled tent maps: it associates the properties of the RG for the local map to the convergence of the coupling operator to the continuous limit, Δ_λ^∞. This insures that the scaling properties of the local map are preserved (this concerns the transition points, the rms of the asymptotic pdfs,...) and that lengthscales are multiplied by $\beta = \sqrt{2}$ at each step.

This work provides the basis of a rigorous approach to RG for coupled map systems. We have shown that the continuous limit plays an essential role since the operator Δ_λ^∞ is universal. It indicates surprisingly that the strong coupling limit of coupled maps, rather than corresponding to some particular, large value of the parameter g, is reached by considering continuously coupled maps. Thus, any weak coupling strategy appears as irrelevant when trying to account for non-trivial collective behavior [20]. Moreover, the continuous limit provides us with the natural framework within which a "zero temperature" expansion should be carried out and therefore seems to be a key ingredient when trying to understand the emergence of collective motion from local chaos.

References

[1] P. Collet and J.P. Eckmann, *Iterated Maps of the Interval as Dynamical Systems*, (Birkhäuser, Boston, 1980).

[2] See, e.g., P. Cvitanović, Ed., *Universality in Chaos*, 2nd. ed., (Adam Bilger, Boston, 1989).

[3] M.J. Feigenbaum, J. Stat. Phys. **19**, 25 (1978); **21**, 669 (1979); Physica D **7**, 16 (1983); P. Coullet and J. Tresser, J. Phys. C **5**, 25 (1978).

[4] P. Collet, J.P. Eckmann and O.E. Lanford III, Commun. Math. Phys. **76**:211-254 (1980).

[5] N. Metropolis, M.L. Stein and P.R. Stein, J. Comb. Theory A **15**, 25 (1973)

[6] B. Derrida, A. Gervois, and Y. Pomeau, J. Phys. A **12**, 269 (1979).

[7] See, e.g., K. Kaneko, Ed., *Theory and Applications of Coupled Map Lattices*, (Wiley, New York, 1993), and references therein.

[8] S.P. Kuznetsov and A.S. Pikovsky, Physica D **19**, 384 (1986).

[9] For a review, see: S.P. Kuznetsov, in [7] and references therein.

[10] W. van der Water and T. Bohr, Chaos **3**, 747 (1993).

[11] A. Lemaître and H. Chaté, Phys. Rev. Lett. **80**, 5528 (1998).

[12] H. Chaté and P. Manneville, Prog. Theor. Phys. **87**, 1 (1992); Europhys. Lett. **17**, 291 (1992); H. Chaté and J. Losson, Physica D **103**, 51 (1997).

[13] A. Lemaître and H. Chaté, "Phase-ordering and onset of collective behavior in chaotic coupled map lattices", preprint, 1998.

[14] P. Marcq, PhD Thesis, Université P. & M. Curie (1996); P. Marcq, H. Chaté, and P. Manneville, in preparation.

[15] A. Lemaître and H. Chaté, unpublished.

[16] A. Lemaître, PhD Dissertation, Ecole Polytechnique, 1998.

[17] I. Dornic and C. Godrèche, J. Phys. A **31**, 5413 (1998), and references therein; D. Stauffer, J. Phys. A **27**, 5029 (1994).

[18] J. P. Crutchfield and B. A. Huberman, Phys. Lett. **77 A**, 407 (1980); J. P. Crutchfield, M. Nauenberg and J. Rudnik, Phys. Rev. Lett. **46**, 933 (1981).

[19] P. Collet, J.P. Eckmann and H. Koch, Period Doubling Bifurcation for Families of Maps on R^n, *Commun. Math. Phys.* **76**:211-254 (1980).

[20] See, e.g.: J. Bricmont and A. Kupiainen, Comm. Math. Phys. **178**, 703 (1996); Physica D **103**, 18 (1997).

Chapitre 3

Dynamique des moments et équations hiérarchiques

Les deux premiers chapitres de ce mémoire m'ont permis de décrire assez précisément la structure des comportements collectifs non triviaux. Dans les deux chapitres qui suivent, j'aborde la question de de l'émergence des comportement collectifs purs à partir de la dynamique microscopique et de leur modélisation.

La première approche qui est développée porte sur la dynamique de quantités macroscopiques que sont les moyennes spatiales instantanées. Il est en effet possible dans le cas des applications logistiques couplées d'écrire une hiérarchie infinie d'équations pour la dynamique des moments des variables locales. Le problème revient alors à extraire de cette hiérarchie un nombre fini d'équations qui puissent rendre compte de la dynamique de la moyenne spatiale M^t et de sa dépendance vis-à-vis du paramètre μ telle qu'elle est présentée sur un diagramme de bifurcations. En fait, il n'est pas évident *a priori* qu'une telle approche locale marche, mais si c'est le cas, cela indique que la dynamique collective est déterminée par quelques aspects très généraux des équations locales.

Cette technique est maintenant présentée dans les deux articles qui suivent. Une présentation concise des résultats obtenus est d'abord proposée par l'intermédiaire d'une lettre parue dans *Physical Review Letters*. L'article qui suit donne une description plus détaillée des techniques mises en œuvre, et s'intéresse plus largement à la dynamique des distributions de blocs, c'est à dire des distributions des variables $\mathbf{X}_\ell = (\mathbf{X}_{\vec{r}})_{\vec{r}\in\ell}$ pour toutes les parties finies $\ell \subset \mathcal{L}$. Il montre en particulier comment une hiérarchie d'opérateurs de Perron-Frobenius marginaux agissant sur ces distributions peut rendre compte de la

dynamique autonome des quantités macroscopiques du réseau. La compréhension de cette structure s'est révélée essentielle pour définir une approximation de la dynamique des moments, mais est surtout intéressante en elle-même puisqu'elle renseigne sur la dynamique de l'opérateur $\langle . \rangle^t$ induite par la trajectoire d'une configuration typique. Cette approche se démarque donc du point de vue canonique usuel par le fait que l'objet considéré est bien la trajectoire macroscopique d'une configuration, et pas du tout d'un ensemble.

3.1 Cluster Expansion for Collective Behavior in Discrete-Space Dynamical Systems

Article paru dans *Physical Review Letters*

3.2 Hierarchical Equations for Collective Behavior in Chaotic Coupled Map Lattices

Article devant être soumis à *Physica D*

Cluster Expansion for Collective Behavior in Discrete-Space Dynamical Systems

Anaël Lemaître, Hugues Chaté, and Paul Manneville
LadHyX, Laboratoire d'Hydrodynamique, Ecole Polytechnique, 91128 Palaiseau, France
Commissariat à l'Energie Atomique, Service de Physique de l'Etat Condensé, Centre d'Etudes de Saclay, 91191 Gif-sur-Yvette, France
(Received 17 October 1995)

We introduce an approximation scheme for determining the evolution of spatially averaged quantities in large classes of extensively chaotic dynamical systems. The case of lattices of diffusively coupled logistic maps is presented. Results in two space dimensions show that the scheme succeeds in reproducing the nontrivial collective behavior observed in this system. [S0031-9007(96)00709-0]

PACS numbers: 05.45.+b, 02.60.–x, 05.70.Ln, 82.20.–w

When studying spatiotemporal chaos in out-of-equilibrium systems, it is generally difficult to estimate even the simplest statistical quantifiers, such as spatial averages, from the (local) evolution rule at the origin of the observed phenomena. This task is made harder for systems exhibiting nontrivial collective behavior, i.e., extensively chaotic regimes in which spatially averaged quantities evolve in time—most often regularly—in sharp contrast with equilibriumlike situations [1]. In this Letter, we introduce a general scheme to attack this problem for discrete-space dynamical systems and detail its implementation and significance in the case of coupled map lattices (CML).

Spatiotemporal chaos refers to physical situations more complex than (temporal) chaos but simpler than, say, fully developed turbulence. This intermediate situation is mainly due to the existence of basic scales arising, for example, from a symmetry-breaking instability, as in Rayleigh-Bénard convection or Taylor-Couette flow [2]. Discrete-space systems are of particular interest in this context because they can be thought of as *a priori* incorporating these basic scales. Even when chaos is extensive, i.e., when quantities measuring the degree of chaos in the system are proportional to the system size [3], there is no general method [4] to estimate statistical properties despite the existence of a well-defined, infinite-size, infinite-time, "thermodynamic" limit. In any case, conventional mean-field theory is unable to account for nontrivial collective behavior [1]. Our approach relies on an exact treatment of local correlations, applies *a priori* to many infinite-size, discrete-space dynamical systems in any space dimension d, and provides the dynamical evolution of spatially averaged quantities. Related to BBGKY-type cluster expansions [5], it allows for a self-consistent calculation of the statistical properties of many extensively chaotic systems including those showing nontrivial collective behavior. Here, we treat only the case of CML whose evolution can be put into a polynomial form. For simplicity, we present preliminary results on hypercubic lattices of logistic maps $S(X) = 1 - \mu X^2$ with "democratic" (equal-weight), nearest-neighbor coupling. Their evolution rule reads

$$X_i^{t+1} = 1 - \frac{\mu}{2d+1} \sum_{j \in \mathcal{V}_i} X_j^{t2}, \tag{1}$$

where $X_i \in [-1, 1]$, $\mu \in [0, 2]$, subscripts denote space, and $\mathcal{V}_i$ is the neighborhood of site i (including itself). These CML are known to exhibit strict synchronization for $\mu < \mu_\infty \simeq 1.401$: all sites in the lattice eventually take on the same value and follow the period-2^k cycle of the (uncoupled) logistic map. This is a "trivial" collective behavior. For $\mu > \mu_\infty$ and space dimension $d \geq 2$, CML (1) displays nontrivial collective behavior, in which the sites are not synchronized: in spite of strong, local, chaotic fluctuations, spatially averaged quantities are not statistically stationary in time, even in the "thermodynamic" limit. In general, the collective motion is *not* directly related to the behavior of the local map. A striking example for CML (1) is the collective quasiperiodic cycle reported for $d = 5$ and $\mu \simeq 1.71$ [1], which cannot be accounted for by a single-variable iteration such as the local map. For $d = 2$ and $d = 3$, CML (1) exhibits periodic collective behavior, but the period of these cycles do not correspond to that of the banded-chaos regimes exhibited by the logistic map for $\mu > \mu_\infty$ (see below). Predicting the collective motion from the local dynamical rule is thus a major challenge which is addressed here.

Taking spatial averages, the evolution rule (1) yields an infinite hierarchy of equations,

$$\begin{aligned}
\langle X_i \rangle^{t+1} &= 1 - \mu \langle X_i^2 \rangle^t, \\
\langle X_i^2 \rangle^{t+1} &= 1 - 2\mu \langle X_i^2 \rangle^t + \left(\frac{\mu}{2d+1}\right)^2 \sum_{j,k \in \mathcal{V}_i} \langle X_j^2 X_k^2 \rangle^t, \\
\langle X_i X_j \rangle^{t+1} &= \cdots, \\
\langle X_i X_j^2 \rangle^{t+1} &= \cdots,
\end{aligned} \tag{2}$$

where the indice i is retained only for clarity. Even though this hierarchy can always be written, here we treat only the (common) case where the solutions of the CML

 0031-9007/96/77(3)/486(4)$10.00

do not break the symmetries of the lattice and where, consequently, all points share the same statistical properties. Leaving this experimental point of view for a more theoretical one, the variables of (2) can be taken as the *moments* of a probability distribution function governed by the Perron-Frobenius operator. Hierarchy (2) then represents the action of this operator on the subset of probability densities which describe the ensemble of statistically equivalent systems displaying the same collective behavior [6]. In the following, this point of view is adopted, and we discuss our approximation in terms of moments rather than spatially averaged quantities.

A moment $\langle X_{i_1}^{\alpha_1} \cdots X_{i_n}^{\alpha_n} \rangle^t$ is characterized by its geometrical support $(i_1, \ldots, i_n)$ and the set of weights $(\alpha_1, \ldots, \alpha_n)$, $\alpha_j \geq 1$, associated to the points of the support. Due to the (assumed) statistical equivalence of all points, the symmetry properties of the lattice $\mathcal{L}$ (translations *and* rotations) can be used to classify moments. Hierarchy (2) is then rewritten in terms of classes of moments with integer multiplicative factors coming out of the reduction process. Hierarchy (2) is an infinite set of linear equations derived from the nonlinear evolution rule (1). Each class of moments on the left-hand side is expressed in terms of classes of wider geometrical support and/or higher total order $\alpha = \sum_{j=1}^{n} \alpha_j$. Keeping only a given set C of moments (defined by a set of supports and weights), the truncated hierarchy can be symbolically written $\vec{M}^{t+1} = \mathcal{F}(\vec{M}^t + \vec{N}^t)$, where $\vec{M}^t$ is the set of moment values corresponding to C, and $\vec{N}^t$ is the set of moment values on the left-hand side corresponding to moments which are not in C. A closure relation is written symbolically $\vec{N}^{t+1} = \mathcal{G}(\vec{M}^{t+1})$. We now describe a physically motivated truncation and closure scheme. It is twofold: a "geometrical" truncation—similar to BBGKY cluster expansion [5]—stopping the growth of supports and providing the closure, and an "analytical" truncation stopping the increase of the total order α of moments.

In extensively chaotic systems, spatial correlations decay fast—often exponentially—far enough from critical points [7]. In terms of moments, strict decorrelation is expressed by (possibly complicated) factorization relations involving moments of smaller geometrical support. These relations are implicitly and efficiently taken into account when *cumulants* are considered instead of moments. Decorrelation of one subset of $(i_1, \ldots, i_n)$ from the other points of the geometrical support is simply expressed by saying that cumulants with the same support vanish. To implement the approximation scheme, a criterion is needed to designate the supports for which the cumulants are to be canceled. A natural choice is to keep all cumulants such that the maximal distance between any two points of their support is less than some threshold distance $r_{\max}$. The analytical truncation is also based on cumulants. Numerical observations show that the cumulants decrease when their total order α increases (see Table I). This is related to the unimodal structure of the probability densities observed [8]. In practice, a maximum ord $\alpha_{\max}$ is chosen, and cumulants with higher total order a set to zero [9].

TABLE I. Values of single-variable moments and cumula for $\mu = 1.5725$ (period 2 collective behavior) for the latti defined in Fig. 1. Data are given for both the original CM (numerical simulation) and the result of the approximation f $\alpha_{\max} = 2$, $r_{\max} = 3$, and $n_{\max} = 30$.

	$\langle X \rangle$	$\langle X^2 \rangle$	$\langle X^2 \rangle_c$	$\langle X^3 \rangle$	$\langle X^3 \rangle$
CML	0.856	0.745	0.012	0.657	−0.00
	−0.171	0.091	0.062	−0.027	0.00
Approx.	0.881	0.794	0.017	0.730	0
	−0.165	0.076	0.048	−0.028	0

Hierarchy (2) is given in terms of moments, where both truncation steps involve cumulants. We thus need compute moments from cumulants (and vice versa). Th is achieved in practice by making recursive use of th relation [10]

$$\langle X_1^{\alpha_1} \cdots X_n^{\alpha_n} \rangle = \sum_{\beta_i \leq \alpha_i} \frac{\sum_{i=1}^{n} \beta_i}{\sum_{i=1}^{n} \alpha_i} \prod_{i=1}^{n} \binom{\alpha_i}{\beta_i} \times \langle X_1^{\alpha_1 - \beta_1} \cdots X_n^{\alpha_n - \beta_n} \rangle \langle X_1^{\beta_1} \cdots X_n^{\beta_n} \rangle_c . \quad (3$$

Let us summarize our approach so far. The two-ste truncation leaves a finite set C of nonzero cumulants. L us call $\mathcal{D}_C$ the set of all probability densities [9] whos only nonzero cumulants are inside C. The probabilit density $\mathbf{f}^t$ describing the system is approximated by $\mathbf{g}^t$, th unique element of $\mathcal{D}_C$ sharing the same cumulant value $\vec{C}^t$ over C. The image of $\mathbf{g}^t$ by the (truncated) hierarch belongs to $\mathcal{D}_C$. The truncation thus also provides a closur via relation (3).

Although the approximation is self-consistent, produc ing a time series of elements of $\mathcal{D}_C$, the situation is les satisfactory than it looks. Elements of $\mathcal{D}_C$ are "general ized Gaussian" distributions. In particular, they posses tails and therefore do not belong to $\mathcal{D}_I$, the set of proba bility densities with their support in $I = [-1, 1]^N$. Un der the action of the local map S, points outside $[-1, 1$ quickly diverge to infinity. Indeed, implementations a this stage lead to the divergence of moment values.

We now present a resummation scheme which force the probability densities produced by the approximation t belong to $\mathcal{D}_I$. We look for $\mathbf{h}^t$ in $\mathcal{D}_I$ approximating th functions $\mathbf{g}^t$ produced by the truncation. The "natural" solution—closely linked to the definition of cumulant in terms of the characteristic function (see below)—is t periodize $\mathbf{g}^t$ on I and multiply it by the indicator functio $\mathbb{1}_I$ of I [$\mathbb{1}_I(X) = 1$ if $X \in I$, $\mathbb{1}_I(X) = 0$ otherwise],

$$\mathbf{h}^t = \mathcal{P}_I(\mathbf{g}^t) \cdot \mathbb{1}_I ,$$

where $\mathcal{P}_I$ symbolizes the operator periodizing the densi ties [$\mathcal{P}_I(\mathbf{g}(\vec{X})) = \sum_{\vec{q} \in \mathbb{Z}^n} \mathbf{g}(\vec{X} + \vec{q}\Delta)$ where $\Delta = 2$ is the

length of I]. This amounts to "cutting" the tails of $\mathbf{g}^t$ outside of I and "pasting" each of them at the other end of the interval ($\mathbf{h}^t$ is the aliased approximation of $\mathbf{g}^t$ appropriate to fast Fourier transforms). If $\mathbf{g}^t$ is a good approximation of $\mathbf{f}^t$ (the "true" probability density belonging to $\mathcal{D}_I$), then its tails outside of I are small, and consequently $\mathbf{h}^t$ itself is a good approximation of $\mathbf{g}^t$ and $\mathbf{f}^t$. In other words, the coefficients $c_{\vec{n}}$ of the multidimensional Fourier series of the density $\mathbf{f}^t$ are approximated by

$$c_{\vec{n}} = \left\langle \exp\left(\frac{2i\pi\vec{n}\cdot\vec{X}}{\Delta}\right)\right\rangle = \tilde{\mathbf{g}}^t\left(\frac{2\pi\vec{n}}{\Delta}\right),$$

where $\tilde{\mathbf{g}}^t$ is the characteristic function of $\mathbf{g}^t$, given by the *finite* sum

$$\tilde{\mathbf{g}}^t(\vec{k}) = \exp\left\{\sum_{\langle X_1^{\alpha_1}\cdots X_n^{\alpha_n}\rangle_c \in C}\left[\prod_{j=1,\ldots,n}\frac{(ik_j)^{\alpha_j}}{\alpha_j!}\right]\langle X_1^{\alpha_1}\cdots X_n^{\alpha_n}\rangle_c^t\right\}.$$

All the moments of $\mathbf{h}^t$ are then given by

$$\langle X_{i_1}^{\alpha_1}\cdots X_{i_n}^{\alpha_n}\rangle^t = \sum_{\vec{n}} c_{\vec{n}} \prod_{j=1}^{n} \mathcal{A}(n_j,\alpha_j), \qquad (4)$$

with

$$\mathcal{A}(n_j,\alpha_j) = \int_I X_j^{\alpha_j}\exp\left(-\frac{2i\pi n_j X}{\Delta}\right)dX.$$

Since $\mathcal{A}(n_j,0) = 0$, for every moment or cumulant, the only vectors $\vec{n}$ involved in (4) are those of dimension n, where n is the number of points in the geometrical support [$\vec{n} = (n_1,\ldots,n_n)$]. Moreover, the Fourier series are truncated to $n_{\max}$ coefficients in each dimension ($n_j \in \{-n_{\max},\ldots,n_{\max}\}$), so that only a finite number of $c_{\vec{n}}$ have to be calculated. We note, to conclude this presentation of the scheme, that the moments of the function $\mathbf{h}^t \in \mathcal{D}_I$ are close to those of $\mathbf{g}^t$, but $\mathbf{h}^t$ possesses an infinite number of (small) nonzero cumulants.

In realistic cases, the calculations are too tedious to be done by hand. This is all the more acute as (1) we eventually want to apply the approximation to high-dimensional CML, and (2) we know that, even though correlations decay fast, the cutoff distance $r_{\max}$ may have to be chosen large in order to ensure a satisfactory level of decorrelation. Therefore, we have written a symbolic manipulation program in C++ to implement the scheme on a computer. While it is impossible to give a detailed account of the program here [10], we now describe its general structure. A first step calculates the set C of the cumulants kept and—implicitly—the equations giving the self-consistent evolution of densities in $\mathcal{D}_C$. Except for the data defining the CML (local map, lattice, coupling), the only parameters on input are $r_{\max}$, the cutoff distance, and $\alpha_{\max}$, the maximum total order of the moments or cumulants retained. Next comes the actual numerical simulation of the evolution of an initial probability density $\mathbf{h}^0 \in \mathcal{D}_I$. First, the truncated evolution rule is applied, yielding $\mathbf{g}^1 \in \mathcal{D}_C$. The resummation is then performed, calculating the coefficients $c_{\vec{n}}$ and then the moments of $\mathbf{h}^1 \in \mathcal{D}_I$. The process is iterated,

$$\cdots \mathbf{h}^t \in \mathcal{D}_I \overset{\text{rule}}{\rightarrow} \mathbf{g}^{t+1} \in \mathcal{D}_C \overset{\text{resummation}}{\rightarrow} \mathbf{h}^{t+1} \in \mathcal{D}_I \cdots,$$

building a time series of probability densities from which the evolution of various observables can be deduced.

We now present our first results, obtained for the $d = 2$ lattice of democratically coupled logistic maps. In this case, the nontrivial collective behavior observed for $\mu > \mu_\infty$ are periodic cycles of periods 1, 2, 4, 8, and 16 (Fig. 1). For almost every initial condition, instantaneous site values eventually end up all in the same "band," leading to statistically homogeneous spatial configurations. Droplets of one such state into another shrink and disappear. The observed bands have no direct relationship with those shown by the (chaotic) logistic map at the same μ value. Since they are just one-dimensional projections of the full CML state, they can (and often do) overlap. Moreover, the global bifurcation points are shifted with respect to the band-merging points, so that the collective period observed is different from the number of bands of the local map. This is not the only effect of the coupling: the dynamics of the CML is not "explained" by simply considering that of the local map, especially in the strong-coupling case of interest here. Except at the global bifurcation points where algebraic decay is observed [7], correlations decay exponentially, instantaneous distributions are unimodal, and cumulants

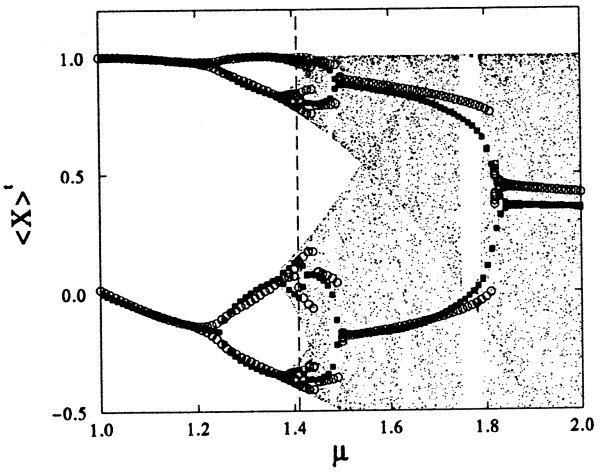

FIG. 1. Bifurcation diagram of $\langle X\rangle^t$ vs parameter μ for a $d = 2$ square lattice of democratically coupled logistic maps. Black squares: simulation of a lattice of $N = 1024^2$ sites with periodic boundary conditions and random initial conditions. Open circles: result of the approximation for $\alpha_{\max} = 2$, $r_{\max} = 3$, and $n_{\max} = 60$. The initial condition corresponds to a uniform distribution on the interval $[-0.5, 0.5]$; 10 iterations are shown after a transient of 50 time steps. Dots: single logistic map. The dashed line is at μ_∞.

decay fast with their total order (see Table I), so that the assumptions of our approach are satisfied.

We have performed our approximation scheme at maximal order $\alpha_{\max} = 2$ for various values of $r_{\max}$ and $n_{\max}$. Results are nearly identical as soon as $r_{\max} \geq 3$ and $n_{\max} \geq 20$, indicating the convergence of the scheme. The same attractor is reached for most initial conditions, and the nontrivial collective behavior observed for $\mu > \mu_\infty$ is recovered (Fig. 1), with only slight discrepancies with respect to the original CML: (1) the critical behavior near bifurcation points is not captured by the approximation, as expected from the presence of long-range correlations in these regions; (2) in the region $\mu \in [1.7; 2]$, the strong asymmetry of the distributions, not accounted for with $\alpha_{\max} = 2$, is at the origin of the small quantitative disagreement. The synchronized states observed for $\mu < \mu_\infty$ are also recovered. We note that even though the approximation at this stage might appear very simple—all probability distributions are (multidimensional) Gaussian functions for $\alpha_{\max} = 2$—the truncated hierarchy already involves 8 degrees of freedom and 25 intermediate variables.

The approximation is also very successful for the $d = 3$ case [10], but its success will have to be confirmed in the future when applied to even higher-dimensional systems. Preliminary results, to be detailed in [10], indicate that the main difficulty is controlling the *admissibility* of the approximated distributions [11] when $\alpha_{\max}$ must be chosen larger than 2. We nonetheless believe that our approach is very promising. At the very least, it sheds light on the problem of the origin of the particular type of collective dynamics arising in a given system when the local behavior is of a different type. Neglecting correlations beyond a "mesoscopic" scale of order $r_{\max}$, the collective motion is revealed. However, this does not solve the problem of the existence of nontrivial collective behavior in the infinite-size, infinite-time, "thermodynamic" limit: Even though, formally, systems of infinite size in their asymptotic state are treated, the approximation makes the assumption of spatial homogeneity and thus cannot account for (possible) fluctuations such as droplet excitations. Approximations of the type developed here do not prove the stability of the observed long-range order against intrinsic fluctuations, which should be studied in detail in another framework. Nevertheless, our results suggest an intermediate picture made of noisy mesoscopic units coupled together, a Langevin-like level of description at which the methods and results of statistical mechanics could be applied (as, e.g., in [12], in the case of cellular automata rules). Finally, we note that the approach presented here may be applied to other systems such as cellular automata [1], globally coupled maps and oscillators [13], and randomly connected networks [14], for which fascinating types of nontrivial collective behavior have also been reported.

[1] H. Chaté and P. Manneville, Europhys. Lett. **14**, 409 (1991); Prog. Theor. Phys. **87**, 1 (1992); J. A. C. Gallas *et al.*, Physica (Amsterdam) **180A**, 19 (1992).

[2] See, e.g., M. C. Cross and P. C. Hohenberg, Rev. Mod. Phys. **65**, 851 (1993).

[3] P. Manneville, in *Macroscopic Modeling of Turbulent Flows,* edited by O. Pironneau, Lecture Notes in Physics Vol. 230 (Springer, New York, 1985); P. C. Hohenberg and B. I. Shraiman, Physica (Amsterdam) **37D**, 109 (1989); D. A. Egolf and H. S. Greenside, Nature (London) **369**, 129 (1994).

[4] One notable exception is the case of one-dimensional systems, for which it is possible to derive systematic improvements of the simple mean-field theory. See, e.g., H. A. Gutowitz and J. D. Victor, Physica (Amsterdam) **28D**, 18 (1987); H. A. Gutowitz, Physica (Amsterdam) **45D**, 136 (1990). See also J. M. Houlrik, I. Webman, and M. H. Jensen, Phys. Rev. A **41**, 4210 (1990).

[5] See, e.g., G. Stell, in *Phase Transitions and Critical Phenomena,* edited by C. Domb and M. S. Green (Academic Press, New York, 1976), Vol. 5b.

[6] In this context, the notion of *asymptotic periodicity,* discussed in M. C. Mackey, Rev. Mod. Phys. **61**, 981 (1989), and recently extended to CML [J. Losson and M. C. Mackey, Phys. Rev. E **50**, 843 (1994); J. Losson, J. G. Milton, and M. C. Mackey, Physica (Amsterdam) **81D**, 177 (1995)], seems to be the appropriate mathematical framework to deal with nontrivial collective behavior from a probabilistic point of view [H. Chaté and J. Losson (to be published)].

[7] Ph. Marcq, H. Chaté, and P. Manneville, "Critical Properties of Lattices of Coupled Logistic Maps" (to be published).

[8] This is in agreement with the assumption of the statistical equivalence of all points in the lattice. The cumulants of a nonunimodal distribution do not decrease with order. Such a situation may be encountered when the system exhibits regular (e.g., "antiferromagnetic") patterns in space, or when macroscopic domains of different "phases" are present (e.g., near critical points), all cases where the above assumption is not legitimate.

[9] The term "probability density" is used to describe the truncated functions (later called $\mathbf{g}'$ and $\mathbf{h}'$) approximating the original density $\mathbf{f}'$. This is somewhat abusive insofar as these *functional approximations* are not, strictly speaking, probability densities, since they may be nonpositive. This point will be discussed at length in [10].

[10] A. Lemaître, H. Chaté, and P. Manneville (to be published).

[11] N. I. Akhiezer, *The Classical Moment Problem* (Hafner, New York, 1965).

[12] H. Chaté and L.-H. Tang (unpublished); H. Chaté, L.-H. Tang, and G. Grinstein, Phys. Rev. Lett. **74**, 912 (1995).

[13] K. Kaneko, Physica (Amsterdam) **86D**, 158 (1995), and references therein; N. Nakagawa and Y. Kuramoto, Prog. Theor. Phys. **89**, 313 (1993); Physica (Amsterdam) **75D**, 74 (1994); V. Hakim and W. J. Rappel, Phys. Rev. A **46**, 7347 (1992).

[14] N. Mousseau, Europhys. Lett. **33**, 509 (1996).

Hierarchical Equations for Collective Behavior in Chaotic Coupled Map Lattices

Anaël Lemaître,[1,2] Hugues Chaté,[2,1] and Paul Manneville[1,2]

[2] *LadHyX — Laboratoire d'Hydrodynamique, École Polytechnique, 91128 Palaiseau, France*

[1] *CEA — Service de Physique de l'État Condensé, Centre d'Études de Saclay, 91191 Gif-sur-Yvette, France*

Abstract

The emergence of non-trivial collective behaviour in extensively-chaotic dynamical systems is studied from a macroscopic point of view. An approximation scheme is introduced which relies on an exact treatment of the local correlations. For lattice of coupled chaotic polynomial maps, an infinite hierarchy of equations is derived for the dynamics of spatially-averaged quantities, which are then interpreted as the moments of isotropic and homogeneous distributions. The hierarchy is truncated and closed on phenomenological assumptions, yielding a finite-dimensional non-linear system. A resummation scheme further insures the admissibility of the set of moments/cumulants governed by the approximation. The procedure is applied to the case of lattices of diffusively-coupled logistic maps in two and three space dimensions. The results show that the scheme suceeds in reproducing the main features of the collective dynamics observed.

1 Introduction

The recent years have seen the development of studies of spatiotemporal chaos, an ill-defined term loosely referring to physical situations more complex than (temporal) chaos but simpler than fully developed turbulence. This intermediate situation is mainly due to the existence of basic scales arising, e.g., from an symmetry-breaking instability.

A more clearly-defined case is that when, in a large-enough system, chaos becomes *extensive*, i.e. quantities measuring the degree of chaos in the whole

system are proportional to the system size. When the extensivity of chaos is documented, for example by evaluation of the spectrum of Lyapunov exponents for different system sizes, one can confidently approach the infinite-size, "thermodynamic" limit where some (statistical) simplicity can be hoped to be found.

Models for spatiotemporal chaos are many degrees of freedom dynamical systems with local interactions. Of particular interest are discrete-space, discrete-time systems, or coupled map lattices (CMLs), because they can be thought of incorporating the above-mentioned basic scales in their discrete space-time. CMLs usually consist of simple maps of an interval $S : I \to I$ sitting at the sites $\vec{r}$ of a regular d-dimensional lattice $\mathcal{L}$. Each local variable $\mathbf{X}_{\vec{r}}$ takes its value on I while the whole configuration $\mathbf{X} = (\mathbf{X}_{\vec{r}})_{\vec{r}\in\mathcal{L}}$ lies in the phase space $\mathbf{I} = I^{\mathcal{L}}$. The instantaneous configuration $\mathbf{X}^t$ is updated synchronously by

$$\mathbf{X}^{t+1} = \mathbf{\Delta} \circ \mathbf{S}\left(\mathbf{X}^t\right) , \tag{1}$$

where $\mathbf{S}$ transforms each variable $\mathbf{X}^t_{\vec{r}}$ by the non-linear local map S, while $\mathbf{\Delta}$ is a linear coupling operator. Sites are locally coupled to each other, when $\mathbf{\Delta}$ only involves the neighbors of a site $\vec{r}$ at a finite range, and not the whole lattice. In the simple case of diffusive coupling, the evolution equation for a site may read

$$\forall \vec{r} \in \mathcal{L} \qquad \mathbf{X}^{t+1}_{\vec{r}} = (1 - 2dg)\, S\left(\mathbf{X}^t_{\vec{r}}\right) + g \sum_{\vec{e}\in\mathcal{V}'} S\left(\mathbf{X}^t_{\vec{r}+\vec{e}}\right) , \tag{2}$$

where $\mathcal{V}'$ denotes the set of the $2d$ nearest-neighbors of the site $\vec{0}$ (not including $\vec{0}$ itself), and g is the coupling parameter. For a d-dimensional hypercubic lattice with "democratic" coupling, the central site and its nearest neighbors possess equal weights, i.e. $g = 1/(2d+1)$; the evolution rule then becomes:

$$\forall \vec{r} \in \mathcal{L} \qquad \mathbf{X}^{t+1}_{\vec{r}} = \frac{1}{2d+1} \sum_{\vec{e}\in\mathcal{V}} S\left(\mathbf{X}^t_{\vec{r}+\vec{e}}\right) , \tag{3}$$

where $\mathcal{V}$ now includes the site $\vec{0}$.

Dynamical systems governed by (3) exhibit various types of behaviour depending on the local map S. In particular, the case where S is the logistic map $S(X) = 1 - \mu X^2$, has been studied extensively [12, 5].

The logistic map is a generic case of an application of the interval which exhibits temporal chaos [16, 7]. Its bifurcation diagram is displayed in Fig. 1. As is well known, a cascade of period doubling bifurcations is observed for

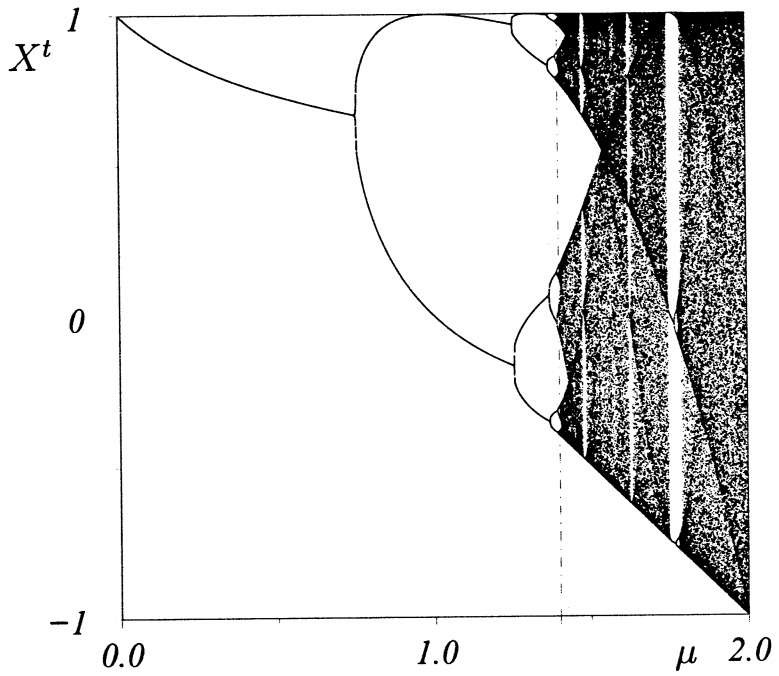

Figure 1: Bifurcation diagram of the logistic map.

values of the parameter μ smaller than $\mu_\infty = 1.40112\ldots$. Above this value, the system enters a banded-chaos regime with periodic windows. Banded chaos consists of a chaotic evolution within each band with an overall periodic cycle among the bands.

The case of a lattice of democratically-coupled logistic maps has been studied numerically in detail in [5]. In the periodic regime of the single logistic map, that is for $\mu < \mu_\infty$, exact synchronization of the sites is observed after a (rather short) transient and the global behaviour amounts to the evolution of a single logistic map. If $\mu > \mu_\infty$, however, the sites do not synchronize exactly and the instantaneous distributions of site values are broad (Fig. 2-(b-d)). In these regimes, the mean value of the sites, $\langle \mathbf{X} \rangle^t$, presents an asymptotic regular evolution. Fig. 2-(a) shows the case of a $d = 2$ square lattice. Two snapshots of this CML in a non-trivial collective behaviour are displayed in Fig. 3, corresponding to a "noisy" period-2 regime.

This *collective* behaviour is said *non-trivial* since there is no evidence of the global dynamics at the local (site) level: the trajectory of any particular site is "chaotic". Fluctuations around the collective dynamics are observed in

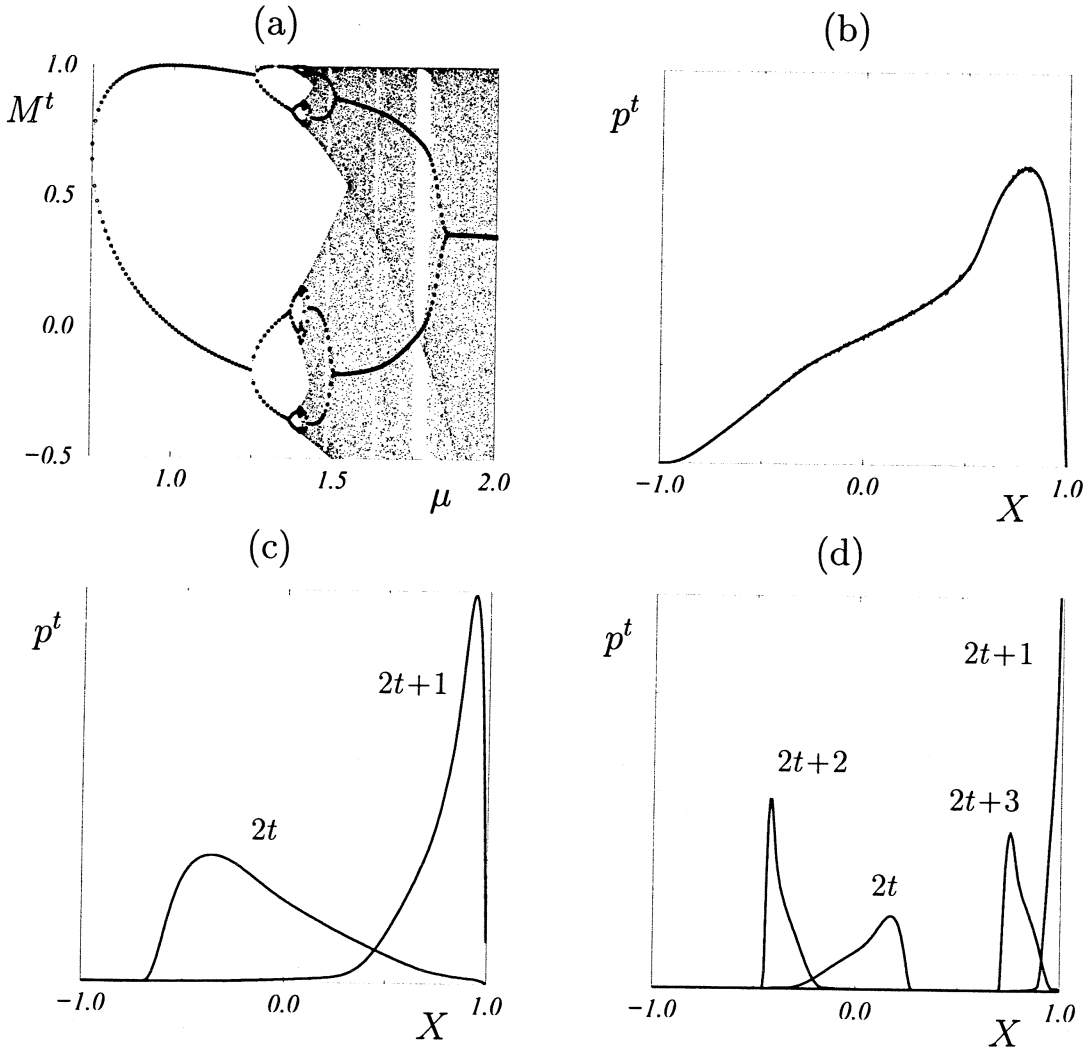

Figure 2: Democratically-coupled ($g = 0.2$) logistic maps on a $d = 2$ lattice of linear size $L = 2048$ with periodic boundary conditions: (a) bifurcation diagram of $M^t = \langle \mathbf{X} \rangle^t$ (filled circles) superimposed on that of the local map S_μ (small dots). (b-d): Asymptotic (large t) single-site distributions p^t (b): stationary states at $\mu = 2$. (c): period-2 collective cycle at $\mu = 1.7$. (d): period-4 collective cycle at $\mu = 1.45$.

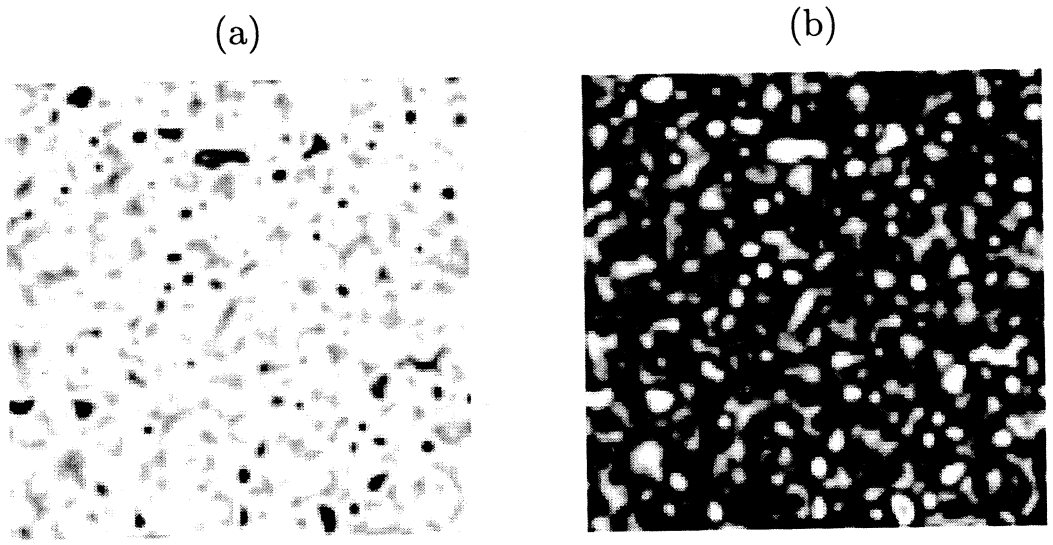

Figure 3: Two snapshots of the $2d$ CML with 128^2 sites, in noisy period-2 regime, at $\mu = 1.7$.

numerical experiments, but these fluctuations decrease like $1/\sqrt{N}$ – N being the number of sites in the lattice–, which insures the existence of a well-defined thermodynamic limit. Numerical experiments have shown that non-trivial collective behaviour (NTCB) is a robust regime attracting almost every initial condition. Studies of the bifurcation points between two types of NTCB have shown that they are "Ising-like", second-order phase transitions [17, 18].

Under the simplest mean-field (MF) approximation, the value $M^t = \langle \mathbf{X} \rangle^t$ is assigned to each site in Eq. (2), and the dynamics is then entirely governed by local map S itself. A different mean-field approximation can also be defined by assigning the mean value only to the neighbors of a site in the evolution equation. Using the general expression (2) to define the dynamics, this yields:

$$\forall \vec{r} \in \mathcal{L} \qquad \mathbf{X}_{\vec{r}}^{t+1} = g\, S\left(\mathbf{X}_{\vec{r}}^{t}\right) + (1-g)\left\langle \mathbf{S}\left(\mathbf{X}\right)\right\rangle^{t} .$$

This is the evolution equation for globally coupled maps: these systems, studied in particular by K. Kaneko [13], present in general a chaotic macroscopic motion and do not account for the behavior observed in locally coupled maps.

The failure of a simple mean field approach to explain NTCB shows the important role played by short-range correlations: for example, snapshots of an instantaneous configuration show a smooth landscape with small structures (bubbles) which correspond to the existence a spatial coherence at small scale. Therefore, these correlations must be properly taken into account at least up to

a mesoscopic scale in order to capture the emergence of a collective effect. Such ideas have been applied to the case of cellular automata (CA): local structure theory is an extension of MF that has been developped by H. Gutowitz for the study of one-dimensional CA [10]. However, the extension of these results to higher dimensions cannot be made systematic [9]. This method, which relies on a Bayesian extension of lattice distributions, provides an expression for correlations but does not simply apply to the case when the local variables lie on an interval.

2 Hierarchical expansion for collective behavior

The purpose of our study is to understand how a particular macroscopic behaviour arises from the local dynamics (3)[1]. Fig. 2 shows the evolution of single-site distribution functions p^t for a two-dimensional lattice of democratically coupled logistic maps. These distributions follow the periodic behaviour already observed for the mean-field $\langle \mathbf{X} \rangle^t$. Thus, all single point moments $\langle \mathbf{X}^\alpha \rangle^t$ follow the collective motion.

This study focusses on the evolution of spatially-averaged quantities following the evolution of a *single* microstate $\mathbf{X}^t$. Our approach stems from the naive observation that a hierarchy of equations is easily constructed in the case of coupled logistic maps ($S(X) = 1 - \mu X^2$) by taking spatial average of the evolution rule (3):

$$\left\{ \begin{array}{rcl} \langle \mathbf{X} \rangle^{t+1} & = & 1 - \mu \langle \mathbf{X}^2 \rangle^t \\ \langle \mathbf{X}^2 \rangle^{t+1} & = & 1 - 2\mu \langle \mathbf{X}^2 \rangle^t + \frac{\mu^2}{(2d+1)^2} \sum_{\vec{e},\vec{e}' \in \mathcal{V}} \left\langle \left(\mathbf{X}^t_{\vec{r}+\vec{e}} \right)^2 \left(\mathbf{X}^t_{\vec{r}+\vec{e}'} \right)^2 \right\rangle \\ \langle \mathbf{X}_{\vec{r}} \mathbf{X}_{\vec{r}'} \rangle^{t+1} & = & 1 - 2\mu \langle \mathbf{X}^2 \rangle^t + \frac{\mu^2}{(2d+1)^2} \sum_{\vec{e},\vec{e}' \in \mathcal{V}} \left\langle \left(\mathbf{X}^t_{\vec{r}+\vec{e}} \right)^2 \left(\mathbf{X}^t_{\vec{r}'+\vec{e}'} \right)^2 \right\rangle \\ \langle \mathbf{X}_{\vec{r}} \mathbf{X}^2_{\vec{r}'} \rangle^{t+1} & = & \cdots \end{array} \right. \tag{4}$$

The expression of spatial moments at time $t+1$ involve more complex moments at the preceding time, leading to a hierarchical structure of macroscopic equations.

In order to clarify the framework of this approach, we first introduce *block distributions*, i.e. distribution functions for lattice variables. Then, we see how

[1] and not to justify the existence of NTBC in the thermodynamic limit (see conclusion)

the macroscopic quantities measured on a single lattice configuration can be related to some particular block distributions because of the isotropy and homogeneity of the system. This enables us to represent the collective dynamics of the lattice by two hierarchies of equations: one written in terms of spatially averaged quantities and the other in terms of block distributions functions.

In the spirit of statistical thermodynamics, lattice dynamics are usually described by the temporal evolution of probability measures on the space of lattice configurations $\mathbf{I}$ [2], where these measures play the role of the canonical ensemble in usual thermodynamics. The evolution of such a measure μ^t is governed by the Perron-Frobenius operator (PFO) $\mathcal{P}_\Psi$ associated to the global map Ψ: $\mu^{t+1} = \mathcal{P}_\Psi[\mu^t]$. The associated pdf ρ^t evolves accordingly:

$$\begin{aligned} \forall \mathbf{X} \in \mathbf{I} \qquad \rho^{t+1}(\mathbf{X}) &= \int_{\mathbf{I}} \delta(\mathbf{X} - \Psi(\mathbf{X}'))\, \rho^t(\mathbf{X})\, d\mathbf{X}' \\ &\equiv \mathcal{P}_\Psi\left[\rho^t\right](\mathbf{X}), \end{aligned} \tag{5}$$

which expresses the conservation of probability and where the action of the PFO on probability densities is also denoted $\mathcal{P}_\Psi$.

2.1 Block probability densities

2.1.1 Definition

Let us first introduce a few notations. We call a *frame* a finite subset $\ell = \{\vec{r}_1, \ldots \vec{r}_{|\ell|}\}$ of $\mathcal{L}$, with cardinal $|\ell|$, and a *block*, or an *ℓ-vector*, the set of values $\mathbf{X}_{\vec{r}}$ assigned to each site $\vec{r} \in \ell$. Such blocks, denoted $\mathbf{X}_\ell$, take their value on the space $\mathbf{I}_\ell \equiv I^\ell$, where I is the interval of definition of the local variables. Given any finite subset $\ell' \subset \ell$, an ℓ'-vector may be defined by restricting an ℓ-vector $\mathbf{X} \in \mathbf{I}_\ell$. If ℓ'' denotes the complementary set of ℓ' in ℓ, ($\ell'' = \ell \backslash \ell'$), any ℓ-vector $\mathbf{X}_\ell$ is decomposed into two orthogonal parts by writing, $\mathbf{X}_\ell = \mathbf{X}_{\ell'} \oplus \mathbf{X}_{\ell''}$.

Probability densities on $\mathbf{I}_\ell$ are called *block probability densities*. We denote them $p_\ell(\mathbf{X})$. They verify the conditions:

$$\forall \mathbf{X} \in \mathbf{I}_\ell, \quad p_\ell(\mathbf{X}) \geq 0 \tag{6}$$

$$\int_{\mathbf{I}_\ell} p_\ell(\mathbf{X})\, d\mathbf{X} = 1, \tag{7}$$

with $d\mathbf{X} = \prod_{\vec{r} \in \ell} d\mathbf{X}_{\vec{r}}$. Moreover, given any finite subset $\ell' \subset \ell$, it is required

[2] In this article, the word *measure* stands for *probability measure i.e.* all measures are normalized

that the block pdf $p_{\ell'}$ can be expressed in terms of p_ℓ via the partial summation:

$$p_{\ell'}(\mathbf{X}) = \int_{\mathbf{I}_{\ell''}} p_\ell(\mathbf{X})\, d\mathbf{X}_{\ell''}, \tag{8}$$

with $\ell'' = \ell \setminus \ell'$. This is the Kolmogorov consistency condition (KCC), which expresses that $p_{\ell'}$ is a marginal distribution of p_ℓ.

2.1.2 Marginal pdfs for a measure on I

Given some pdf ρ on the phase space $\mathbf{I}$ and a $\ell \subset \mathcal{L}$, a block pdf on ℓ can be extracted from ρ: ρ_ℓ is the marginal distribution for ρ with respect to the block $\mathbf{X}_\ell = (\mathbf{X}_{\vec{r}})_{\vec{r}\in\ell}$. The pdf ρ_ℓ verify the properties (6-8) by construction.

For a given map $\mathbf{\Psi}$ on the phase space $\mathbf{I}$, the action of the associated Perron-Frobenius operator on the pdf ρ defines a dynamics for these block probability densities which is a restriction of Eq. (5) to finite subsets ℓ:

$$\rho_\ell^{t+1}(\mathbf{X}) = \int_{\mathbf{I}_{\mathcal{V}_\ell}} \delta\left(\mathbf{X} - \mathbf{\Psi}(\mathbf{X}')\right) \rho_{\mathcal{V}_\ell}^t(\mathbf{X}')\, d\mathbf{X}'. \tag{9}$$

It involves the neighborhood $\mathcal{V}_\ell$ of ℓ (including ℓ) although any superset ℓ' of $\mathcal{V}_\ell$ could be taken as well, since only the "parent" sites will appear in the Dirac delta functions by action of the global map $\mathbf{\Psi}$, the others being summed out because of the KCC.

For any given ℓ, Eq. (9) is not closed (like (5)), since a block probability defined on a (strict) superset of ℓ is involved. It cannot determine completely the dynamics of some ρ_ℓ for a given ℓ since larger and larger neighborhoods are involved along time.

2.2 Collective dynamics

Let us describe the physical observation of the lattice evolution as it is carried out during a numerical simulation: at each timestep, one configuration $\mathbf{X}^t$ of a lattice of $N = L^d$ sites is realized. The object under study is the dynamics of a single configuration $\mathbf{X}^t \in \mathbf{I}$. It is a microstate of the CML which evolves under the global map $\mathbf{\Psi}$: $\mathbf{X}^{t+1} = \mathbf{\Psi}(\mathbf{X}^t)$.

Since the dimensionality of the phase space is large, the trajectory of a configuration in $\mathbf{I}$ is not a useful object per se, and it is usually characterized by macroscopic *observables*. These observables are defined by (spatially) averaging over all the local variables in one instantaneous microstate. Such macroscopic quantities are, e.g., the mean $\langle \mathbf{X} \rangle^t$ of the field $\mathbf{X}_{\vec{r}}^t$, its variance,

the pair correlation function, or the instantaneous histogram p^t of local values. Previous numerical work have shown that these quantities and their dynamics are well-defined in the limit $L \to \infty$ of an infinite lattice [5].

The canonical approach which consists in studying the evolution of *ensembles* under Perron-Frobenius dynamics is a related but different mathematical problem. The observation of the collective dynamics displayed by an "infinite" lattice is in fact neither a microcanonical nor a canonical description. The object considered is the *macrostate* of the system defined by the operator $\langle . \rangle^t$, spatial average at time t, which determines the value of all macroscopic observables.

2.2.1 Macrostates

At any time t, the normalized histogram of values taken by the local variables can be identified with a single-valued pdf $p_1^t(X)$. In our case, such pdfs are represented from numerical data in Fig. 2, and can be identified with smooth functions provided N is sufficiently large. For a single-valued observable $\mathcal{O}(X)$, its spatial average at time t is defined as

$$\langle \mathcal{O} \rangle^t \equiv \frac{1}{N} \sum_{\vec{r} \in \mathcal{L}} \mathcal{O}\left(\mathbf{X}_{\vec{r}}^t\right) . \tag{10}$$

This average is also expressed via

$$\langle \mathcal{O} \rangle^t = \int_I p_1^t(X)\, \mathcal{O}(X)\, dX$$

which equates the spatial average at time t, $\langle . \rangle^t$, and the p_1^t-average, $\langle . \rangle_{p_1^t}$.

This definition of single-site macroscopic observables or distributions requires to sum over all sites in the lattice and therefore assumes that "all sites are equivalent" (translation invariance) [3]. Similarly, the definition of multivariable observables or pdfs relies on underlying symetries.

Let $\Omega_{\mathcal{L}}$ be the symmetry group of the lattice (point symmetries and translations), and let us consider some frame $\ell \subset \mathcal{L}$. When a symmetry transformation $\omega \in \Omega_{\mathcal{L}}$ is applied, any ℓ-vector $\mathbf{X}$ is transformed into the $\omega(\ell)$-vector $\omega(\mathbf{X})$ with the corresponding coordinates:

$$[\omega(\mathbf{X})]_{\omega(\vec{r})} \equiv \mathbf{X}_{\vec{r}} .$$

[3] The case of "frozen", arbitrary states which necessitates the introduction of mesoscopic variables will not be studied here

Suppose now that some function $\mathcal{O}_\ell$ on ℓ-vectors is given. Such a function corresponds to an $|\ell|$-point function $\mathcal{O}(\mathbf{X}_1, \ldots, \mathbf{X}_{|\ell|})$ provided that some ordering $\ell = \{\vec{r}_1, \ldots, \vec{r}_{|\ell|}\}$ of the sites in ℓ is prescribed. Then any symmetry operation $\omega \in \Omega_\mathcal{L}$ allows to define the corresponding function on $\omega(\ell)$-vectors: for all $\mathbf{X} \in \mathbf{I}_{\omega(\ell)}$, $\mathcal{O}_{\omega(\ell)}(\mathbf{X}) \equiv \mathcal{O}(\mathbf{X}_{\omega(\vec{r}_1)}, \ldots, \mathbf{X}_{(\vec{r}_{|\ell|})})$, or equivalently, $\mathcal{O}_{\omega(\ell)}(\mathbf{X}) \equiv \mathcal{O}_\ell(\omega^{-1}(\mathbf{X}))$. This defines an observable $\mathcal{O}_\ell$ on the whole class of equivalent frames, $\tilde{\ell} \equiv \{\omega(\ell),\ \omega \in \Omega_\mathcal{L}\}$, and this definition does not depend on the choice of the representing frame ℓ.

When $\mathcal{O}_\ell$ is evaluated on some instantaneous lattice configuration $\mathbf{X}^t \in \mathbf{I}$, $\mathcal{O}_\ell(\mathbf{X}^t)$ denotes the value taken by $\mathcal{O}_\ell$ on the restricted ℓ-vector $\mathbf{X}_\ell^t$ (instead of $\mathcal{O}_\ell(\mathbf{X}_\ell^t)$). The spatial average at time t of this observable is defined via

$$\langle \mathcal{O}_\ell \rangle^t = \left\langle \mathcal{O}_\ell\left(\mathbf{X}^t\right)\right\rangle \tag{11}$$

$$\equiv \frac{1}{|\Omega|_\mathcal{L}} \sum_{\omega \in \Omega_\mathcal{L}} \mathcal{O}_{\omega(\ell)}\left(\mathbf{X}^t\right). \tag{12}$$

Note that two notations are used concurrently to denote spatial averaging. The brackets $\langle . \rangle$ denote the action of $\frac{1}{|\Omega|_\mathcal{L}} \sum_{\omega \in \Omega_\mathcal{L}}$ applied to an observable $\mathcal{O}_\ell(\mathbf{X}^t)$ on all equivalent frames. The expression $\langle \mathcal{O}_\ell \rangle^t$, however, denotes the average at time t of the observable $\mathcal{O}_\ell$ to emphasize the underlying evolution of a microstate. The operator $\langle . \rangle^t$, (spatial average at time t) is the instantaneous macrostate of the system which defines how any macroscopic observable is evaluated when the trajectory $\mathbf{X}^t$ is followed.

The macrostate can be represented by probability distributions if spatial averages $\langle \mathcal{O}_\ell \rangle^t$ are expressed via

$$\langle \mathcal{O}_\ell \rangle^t = \int_{\mathbf{I}_\ell} p_\ell^t(\mathbf{X})\, \mathcal{O}_\ell(\mathbf{X})\, d\mathbf{X}. \tag{13}$$

The pdf p_ℓ is the normalized distribution

$$p_\ell^t(\mathbf{X}) = \frac{1}{|\Omega_\mathcal{L}|} \sum_{\omega \in \Omega_\mathcal{L}} \delta\left(\omega(\mathbf{X}) - \mathbf{X}_{\omega(\ell)}^t\right)$$

$$= \left\langle \delta\left(\mathbf{X} - \mathbf{X}_\ell^t\right)\right\rangle.$$

By construction, these statistics are $\Omega_\mathcal{L}$-invariant and form a complete structure of block distributions (for all ℓ): they are positive, normalized and verify the KCC. Since block pdfs p_ℓ are completely determined by their characteristic function,

$$\left\langle e^{i\mathbf{k}.\mathbf{X}}\right\rangle_{p_\ell^t} = \left\langle e^{i\mathbf{k}.\mathbf{X}_\ell}\right\rangle^t$$

there is a strict equivalence between the representation of a macrostate via the operator $\langle . \rangle^t$ or via the set of all pdfs p_ℓ^t, *i.e.* all $\langle . \rangle_{p_\ell^t}$.

Let us make a few remarks. First, by definition, an observable $\langle \mathcal{O}_\ell \rangle^t$ and/or the related pdf p_ℓ^t can be equivalently defined for any equivalent frame $\omega(\ell)$. Therefore, the natural index for p_ℓ or for an observable $\mathcal{O}_\ell$ is not a particular frame ℓ, but rather a whole equivalent class $\tilde{\ell}$. Secondly, the group $|\Omega_\mathcal{L}|$ is finite since the lattice is finite, but these statistics can be identified to smooth functions when the lattice size increase since $|\Omega_\mathcal{L}| \to \infty$. The group $\Omega_\mathcal{L}$ taken might be replaced by any subgroup Ω of the whole group of lattice symmetries which verifies this property. Finally, the selection of a group of symmetry $\Omega_\mathcal{L}$ or any subgroup, is not related to the actual existence of symmetries for the dynamics, it is only an "experimental choice". If some symmetry-breaking is at work in the system, it cannot be observed is the group $\Omega_\mathcal{L}$ is considered.

2.2.2 Hierarchical equations for collective dynamics

The microstate $\mathbf{X}^t$ corresponds to the microcanonical distribution $\delta(\mathbf{X} - \mathbf{X}^t)$ in $\mathbf{I}$ and the evaluation of p_ℓ^t involves all states $\omega(\mathbf{X}^t)$ *i.e.* all distributions $\delta(\mathbf{X} - \omega(\mathbf{X}^t))$ on the phase space. These block pdfs p_ℓ are the marginal distributions of the $\Omega_\mathcal{L}$-invariant measure $\langle \delta(\mathbf{X} - \mathbf{X}^t) \rangle$. Therefore, the evolution of these block pdfs is given by the marginal PFO:

$$p_\ell^{t+1}(\mathbf{X}) = \int_{\mathbf{I}_{\mathcal{V}_\ell}} \delta(\mathbf{X} - \Psi(\mathbf{Y})) \, p_{\mathcal{V}_\ell}^t(\mathbf{Y}) \, d\mathbf{Y} .$$

Let us denote formally this equation as

$$p_\ell^{t+1} = \mathcal{P}_\Psi \left(p_{\mathcal{V}_\ell}^t \right) \tag{14}$$

where the action of the marginal PFO (also denoted $\mathcal{P}_\Psi$) on a $\mathcal{V}_\ell$-block pdf yields an ℓ-block pdf. Of course, this equation (for any finite frame ℓ) holds in the thermodynamic limit where block pdfs are smooth functions.

The set of all these equations (for all frames) is closed: for example, iterating (14), $p_\ell^t = \mathcal{P}_\Psi^t \left(p_{\mathcal{V}_\ell^t}^0 \right)$ provides an expression for p_ℓ^t at all times in terms of the initial macrostate (*i.e.* given all $p_{\ell'}^0$). This system accounts for the evolution of the corresponding macrostate $\langle . \rangle^t$ from any initial macrostate hence describing the collective dynamics of CML's; any mention of the representing microstate has disappeared from these macroscopic equations.

However, each of these equations (for a given ℓ) is not closed since it involves a block pdf on a wider frame $\mathcal{V}_\ell$. In particular, if the dynamics of the single-site

pdf $p^t = p_1^t = p_{\{\vec{0}\}}^t$ is studied, writing Eq. (14) for the family of frames $\ell_n = \mathcal{V}_{\{\vec{0}\}}^n$ provides a hierarchy of equations that ressembles the BBGKY hierarchy, defined to study Liouville dynamics [6]. If the studied lattice is of infinite size, the hierarchy involves an infinite number of equations although only a finite number of these equations account for p^t at any finite time t.

2.3 Evolution of moments when the local map is polynomial

2.3.1 Power moments: definition and notations

Let us introduce some more notations. We call the power moments of a block pdf p_ℓ^t the quantities of the form

$$\mu_\ell^t(\alpha) = \left\langle \prod_{\vec{r}\in\ell} \left(\mathbf{X}_{\vec{r}}^t\right)^{\alpha_{\vec{r}}} \right\rangle$$

for some set of integer exponents α (*i.e.* an ℓ-vector with integer components). The convenient notation $(\mathbf{X}_\ell^t)^\alpha$ will be used for the monomial $\prod_{\vec{r}\in\ell}(\mathbf{X}_{\vec{r}}^t)^{\alpha_{\vec{r}}}$, so that $\mu_\ell^t(\alpha) = \langle(\mathbf{X}_\ell^t)^\alpha\rangle$. We call ℓ the *frame* of the moment $\mu_\ell^t(\alpha)$, and α (or sometimes $|\alpha| = \sum_{\vec{r}\in\ell}\alpha_{\vec{r}}$) its *degree*. Finally, it is assumed in this article that any block distribution function is uniquely determined by the values of all its (power) moments[4].

If some of the exponents $\alpha_{\vec{r}}$ cancel, the ℓ-vector α is decomposed into, $\alpha = \alpha_{\ell'} \oplus \mathbf{0}_{\ell''}$, and the moment $\mu_\ell^t(\alpha)$ reduces to $\mu_\ell^t(\alpha) = \mu_{\ell'}^t(\alpha_{\ell'})$, which is natural in monomial notation. Furthermore, under a symmetry operation ω, the frame ℓ is changed into $\omega(\ell)$ and the moments are transformed accordingly: $\mu_{\omega(\ell)}(\omega(\alpha)) = \mu_\ell(\alpha)$.

[4]In fact a given set of values for the power moments could be shared by differen distributions. The unicity of the representing distribution can be proved under some conditions. However, our aim here is to study the evolution of macroscopic variables given by hierarchical equations. These observables are the moments of pdfs and the evolution of these observables is accounted for by the evolution of their representing distributions. It will become clear later that the crucial question concerning approximations of these moments is the existence of a representing distribution (see sec. 4.1) and not its unicity.

2.3.2 Evolution equations

In general, for coupled maps of the form $\mathbf{\Psi} = \mathbf{\Delta}_g \circ \mathbf{S}_\mu$ [5], the evolution equation for power moments reads:

$$\begin{aligned} \mu_\ell^{t+1}(\alpha) &= \left\langle \prod_{\vec{r}\in\ell} \left(\mathbf{X}_{\vec{r}}^{t+1}\right)^{\alpha_{\vec{r}}} \right\rangle \\ &= \left\langle \prod_{\vec{r}\in\ell} \left((1-2dg)\, S\left(\mathbf{X}_{\vec{r}}^{t}\right) + g \sum_{\vec{e}\in\mathcal{V}} S\left(\mathbf{X}_{\vec{r}+\vec{e}}^{t}\right) \right)^{\alpha_{\vec{r}}} \right\rangle . \end{aligned}$$

If, in particular, the local map is polynomial of degree K, the expression inside the brackets expands as a polynomial in $\mathbf{X}_\ell^t$ of degree $K|\alpha|$ and the rhs can be written in the form

$$\mu_\ell^{t+1}(\alpha) = \sum_{\vec{e}\in\mathcal{V}_\ell} \sum_{\beta_{\vec{r}}=0}^{K|\alpha|} \Psi_{\alpha,\beta} \mu_{\mathcal{V}_\ell}^t(\beta) \tag{15}$$

where $\Psi_{\alpha,\beta}$ are coefficients depending on $\mathbf{\Psi}$.

We will focus in particular on the case of coupled logistic maps:

$$S(X) = 1 - \mu X^2 ,$$

where the interval of definition is $I = [-1, 1]$, and the parameter μ takes all values between 0 and 2. For simplicity, we are concerned by the case of democratically coupled maps, $g = 1/(2d+1)$ and Eq. (3) becomes

$$\mathbf{X}_{\vec{r}}^{t+1} = 1 - \frac{\mu}{2d+1} \sum_{\vec{e}\in\mathcal{V}} \left(\mathbf{X}_{\vec{r}+\vec{e}}^{t}\right)^2 ,$$

and the evolution of the moments comes out from the expansion of the expression:

$$\mu_\ell^{t+1}(\alpha) = \left\langle \prod_{\vec{r}\in\ell} \left(1 - \frac{\mu}{2d+1} \sum_{\vec{e}\in\mathcal{V}} \left(\mathbf{X}_{\vec{r}+\vec{e}}^{t}\right)^2\right)^{\alpha_{\vec{r}}} \right\rangle . \tag{16}$$

Some of these equations are given in Eq. (4). Like Eq. (14), which accounts for the evolution of block pdfs p_ℓ^t, this expression defines an infinite hierarchy of equations for power moments. Their structure is intimatelly related to that of equations (14): for a given ℓ, the Eq. (14) for p_ℓ^t accounts for the evolution of all moments with frame ℓ. Due to the KCC, this equation accounts also for the evolution of block pdfs on subframes of ℓ and for the corresponding moments.

[5] the notation μ, usual for the parameter of non-linearity is kept and should not be confounded with the also usual notation μ_ℓ^t for the moments

Conversely, the whole hierarchy of equations (15) for the power moments of frame ℓ for all $\alpha \in \mathbb{N}^\ell$ corresponds to the single Eq. (14) for the frame ℓ.

In the following, we show, in the case of coupled logistic maps, how both the hierarchies of pdfs and moments may be truncated and closed in order to derive a finite number of equations accounting for the global evolution of the CML.

3 Closing hierarchical equations

It is striking that the evolution of macroscopic observables and distributions characterizing NTCB, as illustrated in Fig. 2, present low-dimensional features: for coupled logistic maps, the macroscopic behavior is either periodic ($d = 2, 3$) possibly with coexistence of a few periodic attractors ($d = 4$) or quasiperiodic ($d = 5$) [5]. This observation indicates that a small number of "relevant" degrees of freedom are actually at work in these regimes while all others are enslaved. Finding them is a difficult and important task.

The exponential decay of spatial correlations generally observed in these regimes argues in favor of a local origin of NTCB since distant sites may be considered uncorrelated. In fact, the collective behavior is already observable at a mesoscopic scale [5]Therefore, it should be possible to account for the collective dynamics with only a few equations extracted form the hierarchical equations which account for the dynamics of short-range correlations, i.e. for all frames with a bounded diameter.

Let us give a flavor of how some approximation scheme can be defined at a practical level. The fast decay of spatial correlations far away from bifurcation points allows to conjecture the independence of sites far apart from each other. This leads to factorization relations: in the simplest case of two variables, if $\mathbf{X}^t_{\vec{r}}$ and $\mathbf{X}^t_{\vec{r}'}$ are supposed independent because the distance between the sites $\vec{r}$ and $\vec{r}'$ is large, the pair pdf $p_{\{\vec{r},\vec{r}'\}}$ is identified with $p_{\{\vec{r}\}} \otimes p_{\{\vec{r}'\}} = p_1 \otimes p_1$. When dealing with many sites in a complex geometry, this procedure is generalized by cancelling either cluster functions, or cumulants of the distribution. Therefore, before developping this closure scheme in greater details, it is now time to introduce these objects.

3.1 Cumulants

Let us consider the block pdf p_ℓ for a given frame ℓ, and some set of random variables $\mathbf{X}_\ell$ distributed according to p_ℓ (*e.g.* the restricted blocks of a microstate $\mathbf{X}$). The moment generating function

$$M_\ell(\xi) = \left\langle e^{\xi.\mathbf{X}} \right\rangle_{p_\ell} = \left\langle e^{\xi.\mathbf{X}_\ell} \right\rangle$$

is defined for all $\xi \in \mathbb{C}^\ell$ and its Taylor expansion involves the power moments of the pdf p_ℓ:

$$M_\ell(\xi) = \sum_{\alpha=0}^{\infty} \frac{\xi^\alpha}{\alpha!} \mu_\ell(\alpha) \ , \tag{17}$$

with the convenient vector notation, $\xi^\alpha \equiv \prod_{\vec{r}} \xi_{\vec{r}}^{\alpha_{\vec{r}}}$ and $\alpha! \equiv \prod_{\vec{r}} \alpha_{\vec{r}}!$. Of course, the characteristic function of the distribution, $C_\ell(\mathbf{k}) = M_\ell(i\mathbf{k})$ is also the Fourier transform of p_ℓ.

Similarly, the Taylor expansion of the cumulant function $K_\ell = \ln M_\ell$ involves the cumulants (or half-invariants) of the distribution p_ℓ:

$$M_\ell(\xi) = \exp\left[\sum_{\alpha} \frac{\xi^\alpha}{\alpha!} \kappa_\ell(\alpha)\right] \tag{18}$$

where the sum $\sum_\alpha$ is taken over all values of $\alpha \in \mathbb{N}^\ell$ and the cumulant of degree $\alpha = \mathbf{0}$ cancels (normalization). The cumulant $\kappa_\ell(\alpha)$ corresponding to the moment $\mu_\ell(\alpha) = \langle \mathbf{X}_\ell^\alpha \rangle_{p_\ell}$ is also denoted $\langle \mathbf{X}_\ell^\alpha \rangle_c$ and the bracket $\langle . \rangle_c$ is sometimes called the cumulant average. Note that the $\Omega_{\mathcal{L}}$-invariance of moments implies the same symmetry property for cumulants.

Expanding formally these Taylor series, it is straighforward to see that a moment $\mu_\ell(\alpha)$ is a function of the cumulants of lower degree, and conversely. For a single-variable distribution (dropping the subscript $\ell = \{\vec{r}\}$), the first equations of the cumulant expansion are

$$\left\{ \begin{array}{rcl} \langle \mathbf{X} \rangle_c & = & \langle \mathbf{X} \rangle \\ \langle \mathbf{X}^2 \rangle_c & = & \langle \mathbf{X}^2 \rangle - \langle \mathbf{X} \rangle^2 \\ \langle \mathbf{X}^3 \rangle_c & = & \langle \mathbf{X}^3 \rangle - 3 \langle \mathbf{X} \rangle \langle \mathbf{X}^2 \rangle + 2 \langle \mathbf{X} \rangle^3 \end{array} \right. \tag{19}$$

The first two cumulants are the mean value and the variance. The following ones measure the distance of the distribution to a Gaussian: usual quantities constructed from the cumulants are the skewness and kurtosis defined respectively by $\gamma_3 = \kappa_3/\kappa_2^{3/2}$ and $\gamma_4 = \kappa_4/\kappa_2^2$, with $\kappa_\alpha = \langle \mathbf{X}^\alpha \rangle_c$.

For a given ℓ, there is a one-to-one correspondance between the set of all moments $\mu_\ell(\alpha)$ with $\alpha' \leq \alpha$ (*i.e* $\alpha'_{\vec{r}} \leq \alpha_{\vec{r}}$ for all $\vec{r} \in \ell$) and the corresponding

set of cumulants. In the following, these sets are denoted $\mathfrak{M}_\ell(\alpha)$ and $\mathfrak{K}_\ell(\alpha)$ respectively. Symbolically, we can write: [6]

$$\mathfrak{K}_\ell(\alpha) = \ln \mathfrak{M}_\ell(\alpha) \quad \text{and} \quad \mathfrak{M}_\ell(\alpha) = \exp \mathfrak{K}_\ell(\alpha) \ .$$

Any set of moments $\mathfrak{M}$ which contains all moments of degree smaller than any of its element,

$$\forall \mu_\ell(\alpha) \in \mathfrak{M}, \quad \forall \beta \leq \alpha, \quad \mu_\ell(\beta) \in \mathfrak{M}$$

will be said complete. There is a univoque relation between a complete set of moments and the corresponding complete set of cumulants, $\mathfrak{K} = \ln \mathfrak{M}$.

For the implementation of our approximation scheme we perform numerically these transformations. Since formal expressions obtained by expanding the exponential are difficult to handle, we have derived another relation that allows for efficient recursive calculations. This relation reads:

$$\mu_\ell(\alpha) = \sum_{\beta \leq \alpha} \frac{|\beta|}{|\alpha|} \binom{\alpha}{\beta} \kappa_\ell(\beta)\, \mu_\ell(\alpha - \beta) \ , \tag{20}$$

with,

$$\binom{\alpha}{\beta} = \prod_{\vec{r}} \binom{\alpha_{\vec{r}}}{\beta_{\vec{r}}} .$$

A proof is given in Appendix A.

The essential property of the cumulants is that they simply account for any level of decorrelation within a set of variables. If, for example, the variables $\mathbf{X}_\ell$ can be divided into two statistically independent groups, $\mathbf{X}_\ell = \mathbf{X}_{\ell'} \oplus \mathbf{X}_{\ell''}$, then the pdf p_ℓ factorizes:

$$p_\ell(\mathbf{X}) = p_{\ell'}(\mathbf{X})\, p_{\ell''}(\mathbf{X}_{\ell''})$$

[6] A formal expression can be obtained by considering the term of degree $\alpha = \mathbf{1}$ in the definition of moments and expanding the exponential in (18). It comes,

$$\mu_\ell(\mathbf{1}_\ell) = \sum_{\varpi \in \Pi(\ell)} \prod_{\ell' \in \varpi} \kappa_{\ell'}(\mathbf{1}_{\ell'})$$

where the sum is carried out over all partitions of the set ℓ. This formulation may be used to obtained an expression for the moments at any degree. The inverse relation reads,

$$\kappa_\ell(\mathbf{1}) = \sum_{\varpi \in \Pi(\ell)} (|\varpi| - 1)!\, (-1)^{|\varpi|} \prod_{\ell' \in \varpi} \mu_{\ell'}(\mathbf{1}) \ .$$

An interesting proof of this relation can be found in [19].

and the moment generating function factorizes as

$$M_\ell(\xi) = M_{\ell'}(\xi_{\ell'})\, M_{\ell''}(\xi_{\ell''})$$

where $\xi_{\ell'}$ (resp. $\xi_{\ell''}$) is the projection of ξ on the set of ℓ-vectors (resp. ℓ'-vectors). Therefore, the cumulant generating function reads

$$K_\ell(\xi) = K_{\ell'}(\xi_{\ell'}) + K_{\ell''}(\xi_{\ell''}) ,$$

which proves that any cumulant involving variables from the two groups vanishes.

The cumulant expansion may be rearranged as a cluster expansion of the cumulant function. [14] The functions K_ℓ are expressed as a sum:

$$K_\ell(\xi) = \sum_{\ell' \subset \ell} K'_{\ell'}(\xi_{\ell'}) ,$$

where the function $K'_{\ell'}$ is the part of the Taylor expansion (18) which involves the cumulants of the variables $(\mathbf{X}_{\vec{r}})_{\vec{r} \in \ell'}$ exactly:

$$K'_{\ell'}(\xi) = \sum_{\alpha_{\ell'} > 0} \frac{\vec{\xi}^{\alpha_{\ell'}}}{\alpha_{\ell'}!} \kappa_{\ell'}(\alpha_{\ell'}) .$$

This decomposition is related to the expansion of the block pdf p_ℓ itself in Ursell functions defined via the relation,

$$p_\ell = \sum_{\varpi \in \Pi(\ell)} \bigotimes_{\ell' \in \varpi} u_{\ell'} , \tag{21}$$

where $\Pi(\ell)$ is the set of all partitions of the subset ℓ and the tensorial notation $(A_a \otimes B_b)(\mathbf{X}) \equiv A_a(\mathbf{X}_a)\, B_b(\mathbf{X}_b)$ has been introduced for non intersecting frames $a, b \in \mathcal{L}$. Given three sites $\vec{r}_1, \vec{r}_2, \vec{r}_3$, these relations read,

$$\begin{aligned}
p_{\{\vec{r}_1\}}(X_1) &= u_{\{\vec{r}_1\}}(X_1) \\
p_{\{\vec{r}_1,\vec{r}_2\}}(X_1, X_2) &= u_{\{\vec{r}_1\}}(X_1)\, u_{\{\vec{r}_2\}}(X_2) + u_{\{\vec{r}_1,\vec{r}_2\}}(X_1, X_2) \\
p_{\{\vec{r}_1,\vec{r}_2,\vec{r}_3\}}(X_1, X_2, X_3) &= u_{\{\vec{r}_1\}}(X_1)\, u_{\{\vec{r}_2\}}(X_2)\, u_{\{\vec{r}_3\}}(X_3) + u_{\{\vec{r}_1\}}(X_1)\, u_{\{\vec{r}_2,\vec{r}_3\}}(X_2, X_3) \\
&\quad + u_{\{\vec{r}_2\}}(X_2)\, u_{\{\vec{r}_1,\vec{r}_3\}}(X_1, X_3) + u_{\{\vec{r}_3\}}(X_3)\, u_{\{\vec{r}_1,\vec{r}_2\}}(X_1, X_2) \\
&\quad + u_{\{\vec{r}_1,\vec{r}_2,\vec{r}_3\}}(X_1, X_2, X_3) \\
&\cdots
\end{aligned}$$

These functions play, for the whole pdf p_ℓ, the role played by cumulants for the moments. Like in the case of cumulants, if $\mathbf{X}_\ell$ can be divided into two statistically independent groups, $\mathbf{X}_\ell = \mathbf{X}_{\ell'} \oplus \mathbf{X}_{\ell''}$, then the function u_ℓ vanishes.

3.2 Truncation & closure scheme

3.2.1 Truncation

In the following, the dynamics of the spatial mean field is studied as determined by equations (16) or (4). Since these equations are in infinite number, a few of them must be kept, which hopefully allows to account for the collective dynamics observed. Of course different choices are possible. Any finite set of these equations (a truncated hierarchy) expresses the evolution of a finite number of moments (in the lhs) in terms of a another set of moments with wider frames and higher degrees. We call the moments appearing in the rhs of a truncated hierarchy are called the *core moments* and the set of core moments is denoted $\mathcal{M}_0$. The truncated hierarchy provides an exact expression for these moments at time $t+1$ from the values at time t of a larger set of moments denoted $\mathcal{M}_0 \oplus \mathcal{M}^*$. This relation is written formally

$$\mathcal{M}_0^{t+1} = \mathcal{H}_0 \left(\mathcal{M}_0^t \oplus \mathcal{M}^{*\,t} \right) . \tag{22}$$

Of course, some moments in the lhs $\mathcal{M}_0$ do not appear in the rhs (see eq. (15)) but this is not really important. It is however essential that due to the hierarchical structure of these equations, there are always moments $\mathcal{M}^*$ in the rhs that cannot be evaluated via the truncated hierarchy: this system is not closed.

Due to the relation between the moments and the block pdfs, such a truncated hierarchy corresponds also to a truncation of the hierarchy of marginal PFO equation for block distributions. If $\mathcal{F}_0$ denotes all the frames which are involved in the core moments, the set of Eq. (14) (for block pdfs) for all $\ell \in \mathcal{F}_0$ contains $\mathcal{H}_0$: it corresponds to an infinite hierarchy of equations for power moments of all degrees.

The selection of a finite number of frames is a *geometrical truncation.* It corresponds to the truncation of the hierarchy for block pdfs. Another step, limiting the degree of the core moments, is needed in order to define a truncated hierarchy. We call it the *analytical truncation.* The moments $\mathcal{M}^*$ may thus be decomposed into two sets: the moments $\mathcal{M}_\mathcal{V}^*$ which correspond to no frame in $\mathcal{F}_0$ and are excluded from $\mathcal{M}_0$ due to the geometrical closure; on the other hand, the remaining moments $\mathcal{M}_0^*$, whose frame belong to the set of core frames $\mathcal{F}_0$, but with no correponding equation in the truncated hierarchy. This decomposition is written, $\mathcal{M}^* = \mathcal{M}_0^* \oplus \mathcal{M}_\mathcal{V}^*$.

3.2.2 Closure

In order to define approximate dynamical equations for the moments $\mathcal{M}_0$, it is necessary to define a closed system. This requires to prescribe an estimation of $\mathcal{M}^{*\,t}$ from the partial information contained in the moments $\mathcal{M}_0^t$. The closure relation may thus be written

$$\mathcal{M}_0^t \oplus \mathcal{M}^{*\,t} = \mathfrak{C}\left(\mathcal{M}_0^t\right) ,$$

which provides a closed dynamics for the core moments

$$\mathcal{M}_0^{t+1} = \mathcal{H}_0\left(\mathfrak{C}\left(\mathcal{M}_0^t\right)\right) .$$

The estimation of the moments $\mathcal{M}^{*\,t}$ relies on assumptions on the structure of block pdfs, correlations,...: it is an inference problem.

The exponential decay of correlations in a two-dimensional lattice of democratically coupled logistic maps is illustrated in Fig. 4. This observation sets the basis of the local origin of collective behavior and permits to make an assumption of independence when sites are far apart. Beyond some threshold, D_{max}, local variables are supposed independent and therefore any frame with diameter larger than D_{max} is assigned vanishing cumulants. The definition of D_{max} defines a criterion for the geometrical truncation; all block pdfs of wider frame are obtained via factorization relations which provide the corresponding geometrical closure.

Fig. 4 shows also the decay of cumulant values with increasing degree. This decay is a consequence of the unimodal structure of the site distribution: the average and the variance give the main information about the pdfs, and the lack of symmetry may be accounted for by considering cumulants of higher degree. The definition of a maximal degree for non-vanishing cumulants defines an analytical truncation and provides the necessary relations for the closure.

These two assumptions define a truncation and closure scheme for the moments. It is in particular required that the set of moments $\mathcal{M}_0^t$ should be complete to insure that all cumulants $\mathcal{K}_0^t$ corresponding to $\mathcal{M}_0^t$ can be evaluated: $\mathcal{K}_0^t = \ln \mathcal{M}_0^t$. The same property should be required for the sets $\mathcal{M}_0^t \oplus \mathcal{M}_0^{*t}$ of moments with frames in $\mathcal{F}_0^t$, and also for $\mathcal{M}_0^t \oplus \mathcal{M}^{*,t}$. The analytical closure reads,

$$\mathcal{M}_0^t \oplus \mathcal{M}_0^{*t} \simeq \exp\left(\ln\left(\mathcal{M}_0^t\right) \oplus \mathbf{0}\right) , \tag{23}$$

since the cumulants $\mathcal{K}_0^*$ are set to zero. Similarly, the geometrical closure

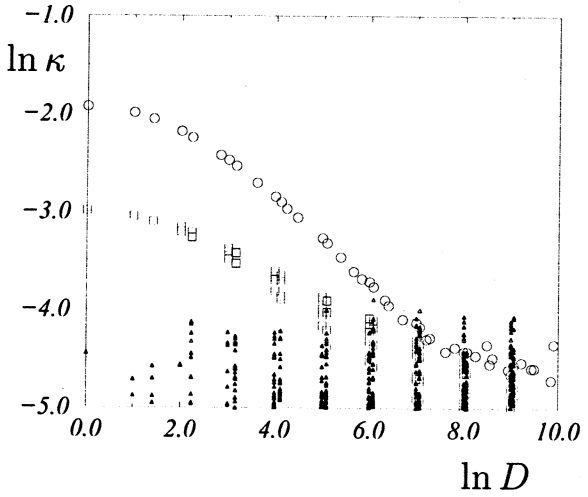

Figure 4: Log diagram of the value of cumulants, versus the diameter D of their support. Cumulants are measured during a numerical simulation at $\mu = 1.6$, in the period-2 regime, and for the higher branch. Second, third and fourth order cumulants are represented by circles, squares and triangles (resp.). The correlation function is given by second order cumulants.

consists in setting cumulants with wide frames to zero:

$$\mathfrak{M}_0^t \oplus \mathfrak{M}^{*t} \simeq \exp\left(\ln\left(\mathfrak{M}_0^t \oplus \mathfrak{M}_0^{*t}\right) \oplus \mathbf{0}\right) . \tag{24}$$

The three equations (22), (23), and (24) form a closed, nonlinear, finite-dimensional system,

$$\mathfrak{M}_0^{t+1} \simeq \mathfrak{H}_0\left(\exp\left(\ln\left(\mathfrak{M}_0^t\right) \oplus \mathbf{0}\right)\right) . \tag{25}$$

4 Resummation

4.1 Admissible values for the moments: the moment problem

4.1.1 Apparent pdf for a closure scheme

Any choice of truncation of the hierarchy attempts to represent a block distribution on a subset ℓ by a finite number of its cumulants. In fact, the closure assumptions not only concern the cumulants $\mathfrak{K}^*$ which appear explicitly in the hierarchical equations, but all cumulants for all frames and all degrees. The only non-vanishing cumulants are those in $\mathfrak{K}_0$. This defines an approximation

$\bar{p}_\ell$ of any block pdf p_ℓ via its Fourier transform, $\bar{C}_\ell^t$:

$$\bar{C}_\ell^t(\mathbf{k}) = \exp\left[\sum_\alpha{}' \frac{(i\mathbf{k})^\alpha}{\alpha_{\vec{r}}!}\kappa_\ell(\alpha)\right], \tag{26}$$

where the sum is finite. We call $\bar{p}$ the apparent macrostate of the system.

Let us now consider a cumulant expansion of the lattice distributions at second order. Only pair correlations within some distance are non vanishing. The Taylor expansion of the cumulant function is truncated at the second order and all block pdfs are Gaussian. In particular, the 1-site distribution has for characteristic function,

$$\bar{C}_\ell^t(\mathbf{k}) = \exp\left[ik\langle\mathbf{X}\rangle^t - \frac{1}{2}k^2\left\langle\mathbf{X}^2\right\rangle^t\right].$$

This has dramatic consequences when the closed system (25) is iterated. The truncated hierarchy $\mathfrak{H}_0$ corresponds to the action of the local polynomial map $S_\mu(X) = 1 - \mu X^2$, for some coupling strength. The Gaussian form of the approximate distribution implies that apparently some sites take their values outside the interval I. By action of the local map, these values will produce larger values, hence leading to the divergence of the whole system. In order to avoid such divergences, the moments $\mathfrak{M}^*$ produced by the closure scheme and transformed by $\mathfrak{H}_0$ should always correspond to a distribution of variables lying on the interval I.

4.1.2 Admissibility

The closure of the hierarchy is an inference problem: the few moments in $\mathfrak{M}_0$ give some information about the lattice pdf and the question is, how can this partial knowledge be extended in order to give "reasonable" values to the remaining moments appearing in the rhs of the truncated hierarchy? The observation above shows that it is essential to guarantee that the moments are *admissible*, *i.e.* that they indeed correspond to some probability distribution on $\mathbf{I}_\ell$:

$$\exists ?\, p_\ell :\ \mu_\ell(\alpha) = \int_{\mathbf{I}_\ell} \mathbf{X}^\alpha p_\ell(\mathbf{X})\, d\mathbf{X}.$$

The question of admissibility for a set of values is a complicated problem usually refered to as "the moment problem", and which has been widely studied [1]. In our case, the pdfs of interest are multi-dimensional in the sense that they involve many variables: in order to be admissible, the moments must

belong to some convex set. [3] However, the verification of this mathematical criterion is too complex to provide any tractable method in practice.

In fact, an inference method gives a direct expression of the pdf itself: "the maximum entropy method" [2]. Moreover, it would be most satisfying from a physical point of view since it provides the least informative expression for a pdf, given the values of some of its moments. The other moments could then be calculated directly from the distribution. However, it requires the evaluation of Lagrange's parameters from the moments that are known, by solving a number of non-algebraic equations. Such a closure can be written formally, but at present, it is too complicated to even simulate numerically the coresponding closed system in order to see whether it accounts for the collective behaviour observed in CMLs.

The formal expression of the moment problem gives a better understanding of the geometry of the closure problem, which is essential in order to define appropriate approximations of hierarchical equations. Although it does not provide (yet) any efficient closure method, it leads to believe that a partial verification of the values taken by the moments could be sufficient to maintain the apparent pdf in a proper functional space. In the case of the second order truncations presented above, the infinite tails appearing in the approximated distributions seem to be the main cause of the divergence observed in the truncated system: we therefore assume that controlling these tails provides "sufficient" admissibility of the pdfs.

We now present a workable resummation scheme which controls the Gaussian tails of second order approximations.

4.2 Resummation scheme

The purpose of the resummation scheme is to guarantee that the moments $\mathcal{M}^*$ correspond to apparent block pdfs $\hat{p}_\ell$ whose support lie on the intervals $\mathbf{I}_\ell$. If $\hat{p}_\ell$ verifies this property, it can be expanded in a Fourier series:

$$\hat{C}^t_\ell(\mathbf{X}) = \frac{1}{|I|^N} \sum_{\mathbf{n}} \hat{\mathbf{c}}^t_\ell(\mathbf{n}) \exp\left[-\frac{2i\pi}{T}\mathbf{n}.\mathbf{X}\right], \tag{27}$$

where $|I|$ is the length of the interval I, where the Fourier coefficients are given by the values of the characteristic function at the points $\mathbf{k} = 2\pi\mathbf{n}/|I|$:

$$\hat{\mathbf{c}}^t_\ell(\mathbf{n}) = \left\langle \exp\left[\frac{2i\pi}{|I|}\mathbf{n}.\mathbf{X}_\ell\right]\right\rangle . \tag{28}$$

These Fourier coefficients must verify the properties, $\hat{\mathbf{c}}^t_{\emptyset} = 1$, and

$$\hat{\mathbf{c}}^t_{\ell}(\mathbf{n}_{\ell'} \oplus \mathbf{0}) = c^t_{\ell'}(\mathbf{n}_{\ell'}) .$$

Their invariance under any element ω of the group $\Omega_{\mathcal{L}}$ follows immediately from their definition, [7] $\hat{\mathbf{c}}^t_{\ell}(\mathbf{n}) = \hat{\mathbf{c}}^t_{\omega(\ell)}(\omega(\mathbf{n}))$.

The closure assumption and the cumulant expansion (18) provide a natural expression for these coefficients in terms of the (finite number of) core cumulants $\mathfrak{K}^t_0$:

$$\hat{\mathbf{c}}^t_{\ell}(\mathbf{n}) = \exp\left[\sum_{\alpha_1 \cdots \alpha_n}{}' \frac{(i\mathbf{k})^{\alpha}}{\alpha!} \kappa_{\ell}(\alpha)\right] , \tag{29}$$

with $\mathbf{k} = 2i\mathbf{n}\pi/|I|$.

The approximated distribution $\bar{p}_{\ell}$ is, in this case, completely defined by equations (27) and (26) and presents infinite tails. The resummed distribution $\hat{p}^t_{\ell}$ is then given by the expansion (27), with the Fourier coefficients defined by Eq. (29) for a finite number of cumulants. This procedure is equivalent to periodizing $\bar{p}_{\ell}$, before taking its restriction on $\mathbf{I}_{\ell}$, which yields a normalized distribution:

$$\hat{p}^t_{\ell} \equiv \mathbf{P}_I\left[\bar{p}_{\ell}{}^t\right] . \mathbb{1}_{\mathbf{I}_{\ell}} ,$$

where $\mathbb{1}_{\mathbf{I}_{\ell}}$ is the characteristic function of the d-dimensional interval $\mathbf{I}_{\ell}$, and $\mathbf{P}_I$ symbolizes the operator periodizing the density:

$$\mathbf{P}_I[p_{\ell}](\mathbf{X}) \equiv \sum_{\mathbf{q} \in \mathbb{Z}^{\ell}} p_{\ell}(\mathbf{X} + |I|\mathbf{q}) .$$

The explicit expression of the Fourier coefficients allows for the evaluation of all the moments of any variable $\mathbf{X}^t_{\ell}$ by integration of the probability $\hat{p}_{\ell}$:

$$\hat{\mu}_{\ell}(\alpha) = \int_{\mathbf{I}_{\ell}} \mathbf{X}^{\alpha} \hat{p}_{\ell}(\mathbf{X}) \, d\mathbf{X} .$$

Expanding $\hat{p}_{\ell}$ in Fourier series yields,

$$\hat{\mu}_{\ell}(\beta) = \sum_{\mathbf{n}} \hat{\mathbf{c}}^t_{\ell}(\mathbf{n}) \prod_{\vec{r} \in \ell} \mathcal{A}(\beta_{\vec{r}}, n_{\vec{r}}) , \tag{30}$$

with the coefficients,

$$\mathcal{A}(\alpha, n) = \frac{1}{|I|} \int_I x^{\alpha} e^{-2i\pi n x/|I|} \, dx .$$

[7] They also verify $c^*_{\ell}(\mathbf{n}) = c_{\ell}(-\mathbf{n})$.

During numerical simulations of the reduced system, a finite number of Fourier terms is kept in Eq. (30), by demanding that all $n_{\tilde{r}}$ range in $\{-N_{max}, \ldots, N_{max}\}$.

The interest of this definition of the resummation lies in the fact that it provides an expression for the pdf which is normalized (7) and verifies (8). Another resummation could be defined by simply cutting the tails of the approximated pdf: $\hat{p}_\ell^t \propto \bar{p}_\ell{}^t \,.\, \mathbb{1}_{\mathbf{I}_\ell}$. This could be done with a better definition of the Fourier transform by taking the Fourier series for an interval J, wider than I, and replacing $|I|$ by $|J|$. Then the resummation would be performed as defined above. The problem in such an approach is that the pdf $\bar{p}_\ell{}^t \; \mathbb{1}_{\mathbf{I}_\ell}$ is not normalized, and the partial pdfs cannot be obtained via equations like $c_\ell^t(\mathbf{n}_{\ell'} \oplus \mathbf{0}) = c_{\ell'}^t(\mathbf{n}_{\ell'})$ but must be calculated from a wider pdf through summations (8). The partial distributions of such a resummed pdf do not share the same expression for their Fourier coefficients in terms of the core cumulants.

The resummation is therefore defined by periodization, and permits to evaluate the moments $\mathcal{M}_0^t + \mathcal{M}_0^{*t}$, through the resummation scheme,

$$\mathcal{M}_0^t \overset{\ln}{\longmapsto} \mathcal{K}_0^t \overset{(29)}{\longmapsto} \hat{\mathbf{c}}_0^t \overset{(30)}{\longmapsto} \mathcal{M}_0^t + \mathcal{M}_0^{*t}$$

where $\hat{\mathbf{c}}_0^t$ is the set of Fourier coefficients correponding to the core pdfs (it is a finite set for any N_{max}). Of course, after the resummation, the cumulants $\mathcal{K}_0^{*t}$ do not vanish although they are small.

The lattice symmetries drastically reduce the number of the coefficients necessary to define a set of functions p_ℓ^t. Only the coefficients corresponding to the frames in $\mathcal{F}_0$ are involved in the resummation scheme. The number of these coefficients is controlled by the number of selected frames, and by truncation of the Fourier expansion.

5 Numerical results

5.1 Implementation

We have applied the approximation scheme to the case of democratically-coupled logistic maps for different dimensions d of the lattice and different choices of truncation and closure.

The numerical implementation of the approximation is performed in the C++ language. It proceeds in two steps.

Firstly, the hierarchical equations for the dynamics of the spatial mean are expanded formally to yield the truncated hierarchy. The truncation is defined

by the maximal diameter D_{max} for core frames, and by the maximal degree A_{max} of core moments $\mathfrak{M}_0$. Lattice symetries are used to reduced the number of variables. The relations involved in the resummation scheme are also evaluated formally for a given range N_{max} of the Fourier transform. These relations define a formal, nonlinear, multidimensional dynamical system for $\mathfrak{M}_0^t$.

Secondly, this system is iterated numerically to observe the effective dynamics defined for the core moments $\mathfrak{M}_0^t$ in the approximations scheme. Initial conditions for $\mathfrak{M}_0$ correspond to the moments of spatially uncorrelated local variables uniformly distributed on some interval $[a,b] \subset I$. Due to the independence of local variables, the moments factorize,

$$\langle \mathbf{X}^{\alpha} \rangle = \prod_{i \in \ell} \langle \mathbf{X}_{\vec{r}}^{\alpha_{\vec{r}}} \rangle_{U_a^b} ,$$

where U_a^b stands for the uniform distribution on $[a,b]$, and

$$\begin{aligned} \langle X^{\alpha} \rangle_{p_0} &= \frac{1}{b-a} \int_a^b X^{\alpha} dX \\ &= \frac{b^{\alpha+1} - a^{\alpha+1}}{(\alpha+1)(b-a)} . \end{aligned}$$

This defines the values of the moments $\mathfrak{M}_0^{t=0}$ at any order. In order to characterize the asymptotic behaviour displayed by the reduced system, bifurcation diagrams when μ varies are evaluated. Fast convergence of the system to a well-defined attractor from a large set of initial conditions is observed. A transient of the order of 100 timesteps is discarded and $\langle \mathbf{X} \rangle^t$ is plotted during a few timesteps. The result is then compared to the bifurcation diagrams obtained by simulation of (large but finite) CMLs with periodic boundary conditions.

5.2 Second order truncations in two dimensions

In this section, we focus on one of the simplest CMLs showing NTCB: the $d = 2$ square lattice of logistic maps coupled democratically to their nearest neighbors. Given the choice $A_{max} = 2$, the approximated distribution functions ${\bar{p}_\ell}^t$ are Gaussian and account for pair correlations. Specifying the parameter D_{max} finishes to define the truncation completely. The only moments to appear in Eq. (15) involve at most two sites *i.e.* they are of the form $\left\langle \mathbf{X}_{\vec{r}_1}^{\alpha_{\vec{r}_1}} \mathbf{X}_{\vec{r}_2}^{\alpha_{\vec{r}_2}} \right\rangle$. Their frames, are simply characterized by the euclidian distance $D(\vec{r}_1, \vec{r}_2)$. Sites are supposed independent whenever $D(\vec{r}_1, \vec{r}_2) > D_{max}$. Setting cumulants to zero amounts to the factorization of the pair pdf: $p_{\{\vec{r}_1,\vec{r}_2\}} = p_{\{\vec{r}_1\}} \otimes p_{\{\vec{r}_2\}}$.

5.2.1 Simple example

With the choice $D_{max} = 2$, 5 core moments are obtained: $\langle \mathbf{X} \rangle$, $\langle \mathbf{X}^2 \rangle$, $\langle \mathbf{X}_{\vec{r}_1} \mathbf{X}_{\vec{r}_2} \rangle$, $\langle \mathbf{X}_{\vec{r}_1} \mathbf{X}_{\vec{r}_3} \rangle$, $\langle \mathbf{X}_{\vec{r}_2} \mathbf{X}_{\vec{r}_4} \rangle$, for configurations of the sites as drawn below:

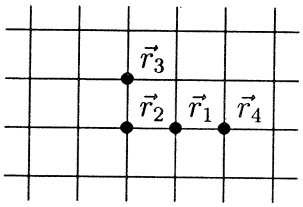

The hierarchical equations for these core moments involve 16 more moments, 8 of them are in $\mathfrak{M}_0^*$ (they have core frames): these are $\left\langle \mathbf{X}_{\vec{r}_1} \mathbf{X}_{\vec{r}_2}^2 \right\rangle$, $\left\langle \mathbf{X}_{\vec{r}_1} \mathbf{X}_{\vec{r}_3}^2 \right\rangle$, $\left\langle \mathbf{X}_{\vec{r}_2} \mathbf{X}_{\vec{r}_4}^2 \right\rangle$, $\left\langle \mathbf{X}_{\vec{r}_1}^2 \mathbf{X}_{\vec{r}_2}^2 \right\rangle$, $\left\langle \mathbf{X}_{\vec{r}_1}^2 \mathbf{X}_{\vec{r}_3}^2 \right\rangle$, $\left\langle \mathbf{X}_{\vec{r}_2}^2 \mathbf{X}_{\vec{r}_4}^2 \right\rangle$, $\langle \mathbf{X}^3 \rangle$, and $\langle \mathbf{X}^4 \rangle$. The remaining 8 moments (in $\mathfrak{M}_{\mathcal{V}}^*$) can be reduced to 3 since all frames of diameter larger than 2 are equivalent: these moments can be represented by $\langle \mathbf{X}_{\vec{r}_3} \mathbf{X}_{\vec{r}_4} \rangle$, $\left\langle \mathbf{X}_{\vec{r}_3} \mathbf{X}_{\vec{r}_4}^2 \right\rangle$, and $\left\langle \mathbf{X}_{\vec{r}_3}^2 \mathbf{X}_{\vec{r}_4}^2 \right\rangle$.

Fig. 5 shows the bifurcation diagram obtained for this 5-dimensional truncated system. At this order, it already accounts qualitatively for most of the features of the collective behaviour observed in the original system. Cycles of periods 1 to 8 are found in the synchronized and in the NTCB regimes. In the synchronized regimes, the decay of all cumulants (but $\langle \mathbf{X} \rangle_c = \langle \mathbf{X} \rangle$) is observed, corresponding to the convergence of the pdf to a Dirac delta function. In the collective regimes, the cumulants retain non-zero values in the asymptotic state. The values of the bifurcation points are larger than those observed in the CML. Morever, the evolution of the truncated hierarchy is difficult to control in the region $\mu \approx \mu_\infty$: for some values of the parameter, and/or some initial conditions the system may escape and yield divergences.

For our further study of the properties of the reduced system, let us begin with a slightly larger truncation, defined by $D_{max} = 3$. In this case, there are 8 equations which involve 25 moments. A bifurcation diagram is displayed in Fig. 5.2.1 for this approximation: the same observations as before can be made, existence of periodic behaviour, and difficulties of convergence of the system when μ approaches μ_∞. The values of the bifurcation points, however, are much closer to those of the original CML (dots).

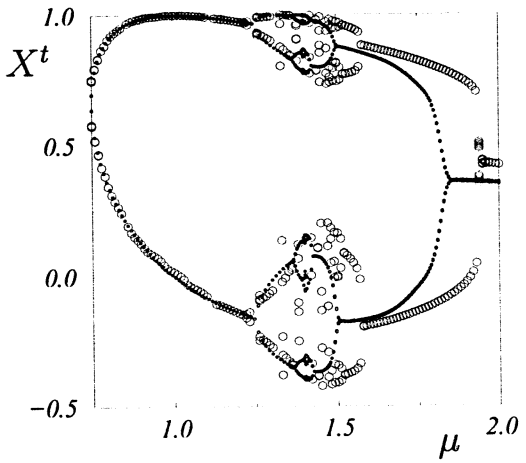

Figure 5: Bifurcation diagram of the reduced system at order 2, in dimension 2. $d = 2$, $A_{max} = 2$, $D_{max} = 2$, $N_{max} = 30$

5.2.2 Transient control for $\mu \approx \mu_\infty$

A quick look at the evolution of the reduced system with $D_{max} = 3$ for values of μ near μ_∞ sheds light on what is happening in this region. In the synchronized regime, the distribution tends towards a Dirac peak at the asymptotic common value of all sites in $\mathcal{L}$. When entering the NTCB regime ($\mu \approx \mu_\infty$), the distributions are sharply — but not strictly — peaked around values similar to those observed in synchronized regime. This corresponds to the destabilization of synchronized states leading to NTCB.

However, as already mentioned in section 4.1, the closure and resummation scheme do not preserve strictly the admissibility of the distribution: the values of the approximated moments are close to the actual one, but may be non-admissible. This is the case in particular when the distributions are sharply peaked (around μ_∞): the cumulant $\langle \mathbf{X}^2 \rangle_c$ is close to zero, and its approximation can take negative values. The system diverges if it is not controlled. "Missing" points in this region correspond to values of the parameter for which divergence occured. It must be noted also that in this region, the system is always close to a bifurcation point, and the cumulant expansion is not expected to be valid.

These problems, however, only take place during the transient, when the system explores large areas of its phase space. If the system is close to the expected periodic trajectory, the moments keep appropriate values and no

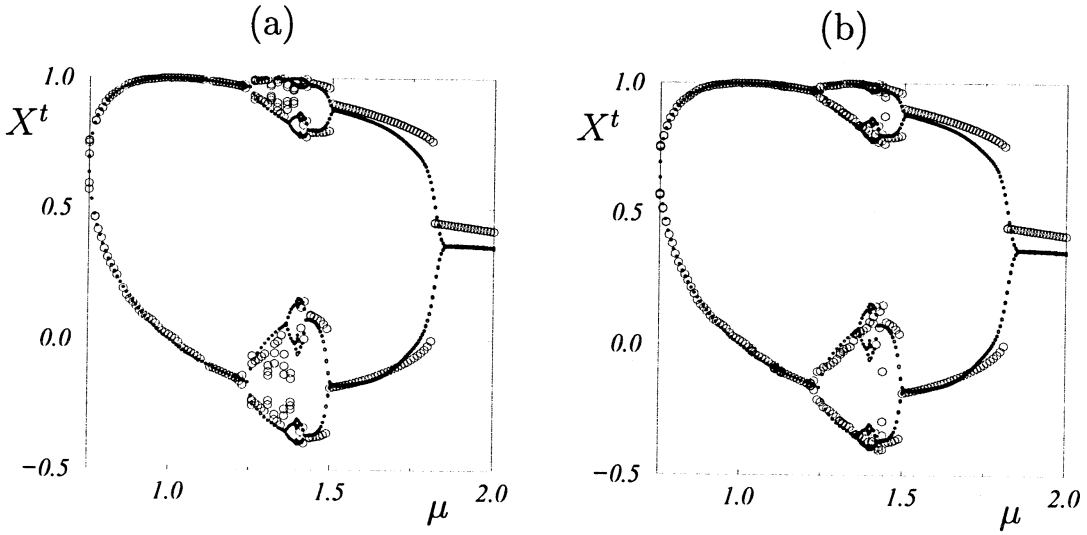

Figure 6: (a) Bifurcation diagram of the reduced system at order 2, in dimension 2: $d = 2$, $A_{max} = 2$, $D_{max} = 3$, $N_{max} = 30$. (b) same with control of the transient

divergence is observed. A control of the trajectories is thus applied during the transient: when $\langle \mathbf{X}^2 \rangle_c$ is small and negative, it is forced to a positive value of the same order. This can be done in different manners, the simplest of which is to change the sign of $\langle \mathbf{X}^2 \rangle_c$. It might seem a bit rough, but a small number of such "kicks" helps find the way to an attractor. It is checked afterwards that following this procedure during only a few steps is sufficient to put the system in the suitable basin of attraction. Fig. 5.2.2 shows the bifurcation diagram obtained when applying this control procedure to the case $D_{max} = 3$. Attracting regimes are easily found near μ_∞.

5.2.3 Bifurcation points

Before discussing the effects of the distance of truncation D_{max}, and of the parameter N_{max} of the Fourier expansion, let us now study in more details the nature of the bifurcations observed in the reduced system.

In the synchronised region, $\mu < \mu_\infty$, the CML follows the evolution of a single logistic map. For collective regimes, the collective behavior presents a subharmonic bifurcation cascade from $\mu = 2$ decreasing. For the reduced system, in the region $\mu < \mu_\infty$, the convergence towards a synchronized regime is observed: all cumulants decrease to zero but the first one $\langle \mathbf{X} \rangle_c = \langle \mathbf{X} \rangle$. The small fluctuations observed in this region on the bifurcation diagrams are due

to a lack of convergence. The reduced systems are heavy to simulate and the synchronized regimes do not present much interest once the convergence towards a synchronized state is evidenced.

We now focus on the NTCB region. The transition point between collective period-2^{n-1} and period-2^{n-1} is denoted μ_n^c.A closer look at the bifurcation points μ_1^c and μ_2^c reveals discontinuities typical of subcritical bifurcations: for the truncated system, two regimes may coexist for the same μ. In a small range of μ, it is possible to reach either of the two regimes by simply changing the interval $[a, b]$ of initial conditions. The bifurcation diagram of Fig. 5.2.2 was initialized with the uniform distribution on the interval [-0.5,0.5]. This hysteresis loop is evaluated by applying adiabatic variations to the parameter μ. The period-2 regime can be maintained up to $\mu_{21} = 1.818 > \mu_{12}^0$, while varying μ in the other direction — from period-1, decreasing — the reduced system maintains the fixed-point regime down to $\mu \approx 1.45$ where it enters a period-2 regime.

As already mentioned, our approximation is not expected to account for the transients, but for the existence of periodic regimes governed by a low-dimensional evolution as determined by the moments of a low order. The finite-dimensional truncated systems cannot provide a description of the whole infinite-dimensional phase space $\mathbf{I} = \mathcal{L}^I$ and of the structure of the basins. In this sense, it is a local approach which provides a local approximated decription of the asymptotic states; therefore, it accounts for the existence of these states and for necessary conditions of unstability.

The approximation does not capture the mechanisms that make low period regimes unstable. In fact when μ approaches the critical point μ_{12}, the correlation length diverges, and the fixed point distributions becomes more and more bimodal. Such multimodal pdfs with long range correlations certainly do not fulfill the requirements of the approximation scheme.

It is however interesting that these truncated systems can capture multistability which is a important feature of higher-dimensional CMLs.

5.2.4 Effect of N_{max}

Figures 5.2.4 and 5.2.2 display the bifurcation diagrams of reduced systems with $D_{max} = 3$ for different values of the resummation parameter, respectively, $N_{max} = 20$, 30, and 60. For small values of N_{max}, the period-8 behaviour is not captured by the approximation: the Fourier transform does not account

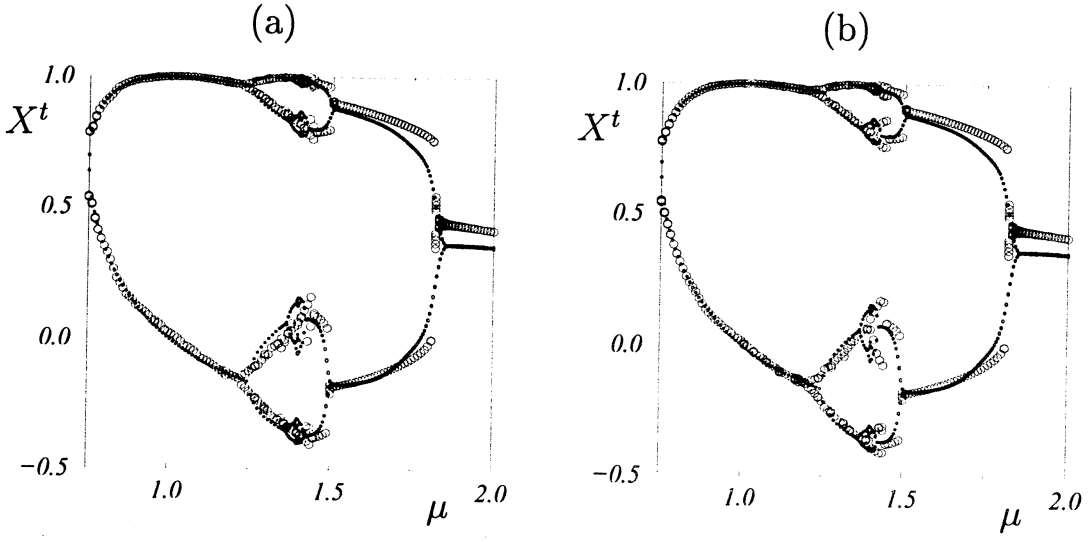

Figure 7: Bifurcation diagrams of the reduced system at order 2, in dimension 2. $d = 2$, $A_{max} = 2$, $D_{max} = 3$, $N_{max} = 20$ (a) and $N_{max} = 60$ (b), with control of the transient

for fine details of the distribution, which are "filtered out" by the resummation process. Increasing N_{max} yields a more precise description, in particular when the pdf is very localised.

Nevertheless, varying N_{max} does not change significantly the values obtained for the bifurcation points when they exist. These values for $D_{max} = 3$, and for different truncations of the Fourier series are reproduced in the following table:

Bifurcation points	Numerical data	$N_{max}(D_{max} = 3)$			
		10	20	30	60
μ_1^c		1.818	1.818	1.818	1.818
μ_2^c	1.4819	1.52	1.50	1.50	1.50

5.2.5 Varying D_{max}

We now evaluate the effect of the cut-off distance D_{max} on the approximation. The following table displays approximate values of the bifurcation points for the reduced systems, taken from the diagrams above, and compared to the numerical values extrapolated for a lattice of infinite size [17]:

Bifurcation points	Numerical data	D_{max}			
		2	3	6	10
μ_1^c			1.818	1.802	1.802
μ_2^c	1.4819	1.58	1.50	1.47	1.47

When D_{max} increases, the values of the bifurcation points for the reduced systems decrease, and converge towards a value close to the expected one. The limit values are different from the bifurcation points exhibited by the original CML. The size of the hysteresis loop decreases when increasing D_{max}.

5.2.6 Coarse-graining

A coarse-graining can be defined by changing the definition of the distance which characterizes frames. For example, the "information distance" D_I,

$$D_I(i,j) = \sum_{r=1}^{d} |i_r - j_r|$$

can be used instead of the euclidian distance D_E. This reduces the number of core moments, whihc is displayed in the following table for different values of D_{max}, with and without coarse-graining.

Core moments	D_{max}			
	2	3	6	10
D_E	5	8	20	45
D_I	4	5	8	12

The bifurcation diagrams of the coarse-grained reduced systems ressemble the diagrams presented in the sections above; the same difficulties are encountered. The position of the bifurcation points for these systems, with different values of D_{max} is displayed below:

Bifurcation points	Numerical data	$D_{max}(N_{max} = 30)$		
		3	6	10
μ_1^c	1.7979	1.77	1.71	1.71
μ_2^c	1.4819	1.49	1.45	1.45

Again, a convergence of the values of the bifurcation is observed with D_{max} increasing. It is surprising that the values obtained with the coarse-grained approximation are closer to the actual one than the values we obtained with the reduced systems above. In fact, the distance D_I seems more adequate for CML's since it really accounts for the path followed by information between the lattice sites.

5.3 Higher dimensions

The bifurcation diagram obtained from lattices of coupled logistic maps in dimension $d = 3$ is displayed figure [8]. In dimension 3, NTCB similar to that of

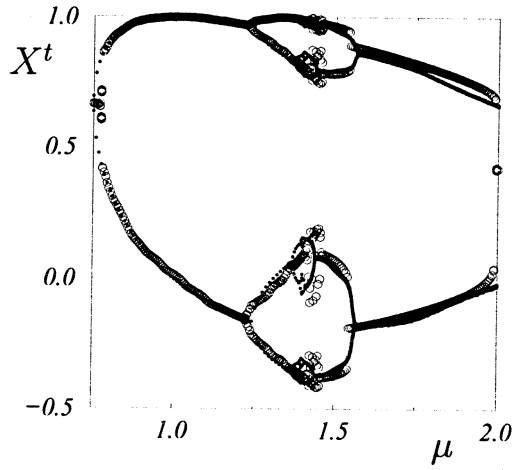

Figure 8: Dots: the bifurcation diagram of the three-dimensional CML. Circles: Adiabatic (μ increasing) bifurcation diagram of the reduced system at order 2, in dimension 3. $d = 3$, $A_{max} = 2$, $D_{max} = 3$, $N_{max} = 30$, with control of the transient

the two-dimensional case is found, but with different values for the bifurcation points. The procedure does not differ from the two-dimensional case detailed above: the approximated distributions are still resummed Gaussian, and the problems encountered are quite similar. The only effect of the dimension is to change the weights in hierarchical equations. All the moments involved in the hierarchy at this order involve at most two sites, and, therefore, are "one-dimensional" moments: they do not contain information about the dimension by themselves, as it could be the case for three-site moments in dimension 2, four-site moments in dimension 3, etc.

The reduced system again succeeds in reproducing some features of the collective regimes observed for these lattices. Again, the transients must be controlled when $\mu \approx \mu_\infty$, and the system presents hysteresis and multistability. The bifurcation diagrams displayed here have been obtained by increasing adiabatically the parameter, starting from the synchronized regime. Around μ_∞, the expected periodic evolution corresponding to the collective regime is found.

When μ approaches the limit value 2, the reduced system reaches a fixed point regime. This is not observed in the numerical simulations of a finite-size CML but there is some numerical evidence that when $\mu \sim 2$, the CML is actually "close" to a (virtual) bifurcation point because of the high value for

the correlation length [15].

In dimension 4 however, NTCB leads to more complex behaviour and the CML presents multistability and hysteresis [5]. This feature is not captured by the reduced system. We believe that such phenomena, induced by the spatial dimension, must be due to more complex correlations than the pair correlations retained in the approximation.

5.4 Higher orders

In higher order truncations, the hierarchy involves moments with more complex frames than the two-site Gaussian distributions kept at order two. Simulations have been carried out, for truncated hierarchies closed by cancelling cumulants only. The dynamics thus defined yield uncontrolled divergences due to the Gibbs phenomenon: the higher-order terms in the Taylor expansion of the cumulant function correspond to an oscillatory part of the distribution that would be resummed by the following terms in an infinite Taylor series. At a finite order, these oscillations yield uncontrolled errors in the approximation of the distribution function, which eventually take the reduced system out of the region of functional space where the truncation is valid.

6 Conclusion

6.1 Summary of the approach

The present work has proposed an approach of the problem of hte emergence of collective behavior out of locally-chaotic dynamics in CMLs. Hierarchical equations (4) were obtained as a macroscopic version of the local evolution Eq. (3) for coupled logistic maps. They were simply produced by recursively applying the linear operator $\langle . \rangle$. This hierarchy can be seen as the "most natural" expression for the collective dynamics of the lattice. It involves spatial averages of more and more complex observables. Isotropy and homogeneity then allowed us to interpret the macroscopic quantities appearing in this hierarchy as the moments of block distributions which are invariant under the group $\Omega_{\mathcal{L}}$ of lattice symmetries. Hierarchical equations were also written for a family of block distributions defined on embedded frames.

Keeping in mind these two macroscopic descriptions of the lattice dynamics, we looked for an approximation of the evolution operator. Indeed, the low-dimensional character of the observed collective regimes indicates that a

small number of equations can account for the asymptotic evolution of the lattice. Therefore, from the intuitive idea that the first moments of a distribution contain most of the global information, we were led to describe the collective dynamics by a small set of evolution equations for some of the simplest moments of the lattice distribution. This set of equations provides a linear expression of the moments $\mathcal{M}_0$ in the lhs in terms of a wider set of moments $\mathcal{M}_0 \oplus \mathcal{M}^*$ which appear in the rhs.

Considering any finite truncation of the hierarchy (4), we were confronted to a closure problem since the truncated system did not provide any value for the moments $\mathcal{M}^*$ which therefore must be obtained by an estimation relying on physical hypotheses. We based these assumptions on two aspects of the lattice distributions taken from numerical data: the exponential decay of site correlations (far from the bifurcation points) and the unimodal structure of the distribution itself. This was translated into setting all the cumulants corresponding to $\mathcal{M}^*$ to zero, leading to a factorization of the $\mathcal{M}^*$ moments in terms of those belonging to $\mathcal{M}_0$.

We noted that, while the site variables lie on the compact interval $I = [-1, 1]$, the approximated distribution has infinite tails which produce uncontrolled divergences when applying the polynomial map. We then developed a resummation scheme in order to ensure that at each timestep the moments take on admissible values.

The whole scheme yields finite-dimensional approximations, which we then studied numerically. Results in two and three space dimensions are remarkably good, even though they were obtained at teh somewhat crude second order of the approximation, for which only two-point moments are retained.

6.2 Limitations

Hierarchy (4) defines an infinite-dimensional linear operator for the moments $\mu_\ell^t(\alpha)$ of a lattice configuration. This operator is related to the PFO defined for the lattice pdfs. Our approach provides a finite-dimensional non-linear approximation of this evolution operator: a linear part is extracted from the original hierarchy and non-linearities are induced by the closure and the resummation.

Since it is finite-dimensional, the reduced system cannot be expected to account for the global geometry of the phase space (the space of admissible moments). In fact, by two assumptions (unimodality and spatial decorrelation), we limited our study to some particular distributions, hence to a subset

of the phase space. The interest of this approach stems from the fact that the numerically-observed asymptotic regimes are approximated by elements of this subspace.

This explains why the reduced system cannot properly account for the transients regimes during which the system explores large areas of the phase space before it is caught by an attractor. This allows for the existence in the reduced system of attracting regimes that are never reached by the CML.

A more difficult problem to deal with is the control of the approximation when higher-degree terms are kept in the cumulant expansion. In particular, the term $\langle X^3 \rangle_c$ introduces a fast variation of the complex phase in the characteristic function due to the factor

$$\exp\left(\frac{(ik)^3}{3!}\langle X^3\rangle_c\right).$$

For an actual distribution, with nonzero cumulants, this term is controlled (resummed) by the following terms in the expansion. In fact, a major limitation at these orders arises from the fact that the numerical calculations become extremely heavy. The higher degree terms make it more difficult to maintain or to check the admissibility of obtained moments. Consider, for example, a truncation of the hierarchy for a two-dimensional lattice, where the moments kept have less than 3 points, degree and diameter at most 3; The hierarchy involves 305 moments, which is reasonable, but the resummation for $N_{max} = 30$ demands the evaluation of nearly 3×10^6 Fourier coefficients, after all symmetry reductions.

6.3 Geometrical considerations

We already mentioned that, in the reduced system, the non-linearities come out of the closure while the hierarchical equations provide a linear system. This closure relies on geometrical aspects based on the structure of the space where the moments take their values.

From the beginning of this study, we have stressed the difference between the evolution of a microstate given by the local dynamics and the Perron-Frobenius approach, leading to linear dynamics in an infinite-dimensional space. However, we noticed that the evolution of one lattice can be represented by the action of the PFO restricted to a particular subspace of $\mathcal{D}$. The selection of attractors in CML's from the underlying Perron-Frobenius dynamics is in fact essentially due to geometrical considerations.

Let us illustrate this on an example. We consider the evolution of macrostates under the PFO and, for simplicity, we assume that the asymptotic states of this system is characterized by two measures[8] λ_1 and λ_2. These measures verify

$$\mathcal{P}_\Psi[\lambda_1] = \lambda_2 \quad \text{and} \quad \mathcal{P}_\Psi[\lambda_2] = \lambda_1$$

and for any given pdf ρ at long times

$$\mathcal{P}_\Psi^T[\rho] \sim R_1^T[\rho]\,\lambda_1 + R_2^T[\rho]\,\lambda_2\,,$$

where $R_1^T[\rho]$ and $R_2^T[\rho]$ are positive reals and verify

$$R_1^T[\rho] + R_2^T[\rho] = 1\,.$$

Excluding the trivial case $R_1^t \equiv R_2^t = 1/2$ for all t and ρ, this means that the system converges towards a period-2 evolution. In this case, it is possible to construct two initial conditions ρ_1 and ρ_2 such that for even times

$$\mathcal{P}_\Psi^{2T}[\rho_1] \sim \lambda_1 \quad \text{and} \quad \mathcal{P}_\Psi^{2T}[\rho_2] \sim \lambda_2\,.$$

Let us then consider any convex combination $\alpha_1\rho_1 + \alpha_2\rho_2$ (with $\alpha_1, \alpha_2 \geq 0$ and $\alpha_1 + \alpha_2 = 1$). It is a macrostate (the space $\mathcal{D}$ is convex) and because of the linearity of the PFO it converge at even times towards the state $\alpha_1\lambda_1 + \alpha_2\lambda_2$. This means that the attractor is a convex continuum of macrostates: this remark can be extended to more general cases of AP.Although the Perron-Frobenius approach can explain the periodicity, the collective behaviour exhibited by a CML shows convergence towards a discrete set of attractor, and no observation allow us to believe that intermediate (convex combined) states are reached.

How does this selection takes place? The PFO is defined on the convex set of lattice pdfs (macrostates) and is linear on this space. Any actual CML (microstate) is represented by a microcanonical distribution. Although the evolution of these states is also governed by the linear PFO, the problem is reduced to a set which is not convex: given two microstates, c_1 and c_2, their corresponding microcanonical ensembles are $\delta(c - c_i)$ and the pdf $\alpha_1\delta(c - c_1) + \alpha_2\delta(c - c_2)$ is not a microcanonical ensemble hence does not correspond to any microstate. Therefore, it is the restriction of the PFO to an invariant non-convex set which accounts for the evolution of a single lattice.

[8]This corresponds to asymptotic periodicity(AP) ([4]) if the distributions have disjoint supports

Two ingredients are therefore necessary if we want to understand the emergence of collective effects in CML from the point of view of pdf dynamics. One of these is the underlying linear dynamics depending on the chosen local map and represented by the PFO, the second one is the geometry of the phase space which is non-convex and contains the non-linear mechanisms leading to the selection of attractors.

6.4 Admissibility

Although we obtained a good understanding of the "geometry" of the closure problem, this does not provide us –so far– with an inference method that would guarantee the admissibility of the full set of moments appearing in the truncated hierarchy. We are currently looking for such methods allowing to prescribe reasonable values to the moments while maintaining admissibility.

One of these methods could rely on Bayesian extension of block distributions. It consist in using conditional probabilities to characterize the independence of variables. Suppose, for example, that we want to evaluate the probability distribution $p_\ell(\mathbf{X})$ for a given block ℓ in which at least two sites are far apart and can be considered independent (typically, this means that the distance between these sites is larger than the cut-off distance D_{max}). Let us denote i' and i'' these sites, $\ell'' = \ell \setminus \{i'\}$, $\ell''' = \ell \setminus \{i''\}$ and $\ell' = \ell \setminus \{i', i''\}$. Using conditionnal (Bayesian) probabilities, we write

$$p_\ell(\mathbf{X}) = p_{i'|\ell''}(\mathbf{X})\, p_{\ell''}(\mathbf{X}_{\ell''}) ,$$

where

$$p_{i'|\ell''}(\mathbf{X}) = p(\mathbf{X}_{i'} | \mathbf{X}_{\vec{r}+\vec{e}},\ j \in \ell,\ j \neq i')$$

is the conditional probability of $\mathbf{X}_{\vec{r}}$ for given values of the other sites (in ℓ''). The assumed independence of the variables $\mathbf{X}_{i'}$ and $\mathbf{X}_{i''}$ implies that the function $p_{i'|\ell''}$ does not depend on the value taken by $\mathbf{X}_{i''}$:

$$\begin{aligned} p_{i'|\ell''}(\mathbf{X}) &= p_{i'|\ell'}(\mathbf{X}_{\ell'''}) \\ &= \frac{p_{\ell'''}(\mathbf{X}'''_\ell)}{p_{\ell'}(\mathbf{X}_{\ell'})} . \end{aligned}$$

Finally, the block distribution p_ℓ reads

$$p_\ell(\mathbf{X}) = \frac{p_{\ell''}(\mathbf{X}_{\ell''})\, p_{\ell'''}(\mathbf{X}_{\ell'''})}{p_{\ell'}(\mathbf{X}_{\ell'})} .$$

This equation provides an expression of the block distribution p_ℓ in terms of block pdfs defined on smaller blocks. Therefore, it allows to close a hierarchy where blocks with a large diameter have been truncated.

Although it provides a distribution function which is clearly positive, two difficulties arise. The first one is technical: the closed system involving pdfs which can be written with this procedure is extremely difficult to handle numerically because the size of blocks increases very fast with the diameter increasing. The second problem, more serious, is that admissibility is not naturally preserved with this method: although the positiveness of the distribution is insured, its normalization is not as soon as $d \geq 2$.

6.5 Long range order

Our method allows for the construction of an approximated operator which accounts for the collective behaviour observed in CML's. It is a macroscopic approach which relies on the hierarchical expansion of the evolution equations for spatially-averaged quantities: it treats directly of an infinite lattice, that is, it describes the thermodynamic limit.

However, since it is finite-dimensional, the reduced system cannot provide a global description of the phase space which is infinite-dimensional; such a global description should be necessary to account for the different basins of attraction that may exist, hence to characterize global stability.

In fact our method relies on some properties which are verified for the observed asymptotic states (and far from the bifurcation points). The approximated operator acts on a subspace of distributions which approaches these observed asymptotic regimes; therefore it can give insights about the existence and (in some sense) local stability of these regimes.

Although this procedure allows for a direct treatment of the thermodynamic limit, a strong restriction comes out from the assumption of unimodality: it does not allow a proper description of a general perturbation of the asymptotic distribution; therefore it cannot account for stability/instability of the thermodynamic limit with respect to general perturbations. However, small variations of the values of the core moments $\mathfrak{M}_0$ are eliminated by the approximated operator: inside their space of definition, the asymptotic regimes are stable.

6.6 Extensions

Closure of hierarchical equations arise naturally in non-linear systems as soon as the evolution of macroscopic quantities is considered. In this study, we described how this closure must be formulated in terms of physical considerations (decay of correlations) and in term of the mathematical structure of the space of lattice pdfs, that is admissibility. How can the geometry of the closure problem be characterized? Are there necessary conditions that guarantee admissibility? We believe these geometrical aspects are essential for the understanding of the closure problems, not only for topological reasons, but because they play a central role in the emergence of collective behaviour and the selection of a macroscopic attractor.

Future work will try to apply these ideas to other lattice systems, such as cellular automata, for which NTCB was also reported[11, 8, 5].

References

[1] N. I. Akhiezer. *The Classical Moment Problem.* Hafner, New York, 1965.

[2] R. Balian. Statistical mechanics and the maximum entropy method. To be Published in "From statistical physics to statistical inference and back", P. Grassberger and J.P. Nadal, eds.

[3] G. Cassier. Problème des moments sur un compact de $\mathbb{R}^n$ et décomposition de pôlynomes à plusieurs variables. *Journal of Functional Analysis*, 58:254–266, 1984.

[4] H. Chaté and J. Losson. Non trivial collective behavior in coupled map lattices: A transfert operator perspective. preprint.

[5] H. Chaté and P. Manneville. Collective behaviors in spatially extended systems with local interactions and synchronous updating. *Prog. Theor. Phys.*, **87**(1):1–60, 1992.

[6] E. G. D. Cohen. On the generalization of the Boltzman equation to the general order in the density. *Physica*, 28:1025–1044, 1962.

[7] M. Feigenbaum. Universal behavior in nonlinear systems. *Physica D*, **7**:16, 1983.

[8] J.A.C Gallas, P. Grassberger, H.J. Hermann, and P. Ueberholz. Noisy collective behavior in cellular automata. *Physica A*, **180**:19–41, 1992.

[9] H. A. Gutowitz and J. D. Victor. Local structure theory in more than one dimension. *Complex Systems*, 1:57–68, 1987.

[10] H. A. Gutowitz, J. D. Victor, and B. W. Knight. Local structure theory for cellular automata. *Physica D*, 1986.

[11] Jan Hemmingsson and Hans J. Herrmmann. On oscillations in cellular automata. *Europhys. Lett.*, **23**:15–19, 1993.

[12] K. Kaneko. Pattern dynamics in spatio-temporal chaos. *Physica D*, **34**:1–41, 1989.

[13] K. Kaneko. Mean field fluctuations in globally coupled maps. *Physica D*, 55:368–384, 1992.

[14] R. Kubo. Generalized cumulant expansion method. *Journal of the Physical Society of Japan*, 17:1100–1120, 1962.

[15] A. Lemaître and H. Chaté. Nonperturbative renormalization group for chaotic coupled map lattices. *Phys. Rev. Lett.*, **80**(25):5528–5531, 1998.

[16] E. N. Lorenz. Deterministic non-periodic flow. *J. Atmos. Sci.*, 20:130–141, 1963.

[17] P. Marcq, H. Chaté, and P. Manneville. Universal critical behavior in two-dimensional coupled map lattices. *Phys. Rev. Lett.*, **77**:4003–4007, 1996.

[18] P. Marcq, H. Chaté, and P. Manneville. Universality in ising-like phase transitions of lattices of coupled chaotic maps. *Phys. Rev. E*, **55**:2606–2627, 1997.

[19] T. P. Speed. Cumulants and partition lattices. *Australian Journal of Statistics*, 25:378–388, 1983.

A Recursive relations

In this Appendix, we detail how the recursive relation (20) can be extracted from the definitions of moments and cumulants. This equation reads,

$$\mu_\ell(\alpha) = \sum_{\beta \leq \alpha} \frac{|\beta|}{|\alpha|} \binom{\alpha}{\beta} \kappa_\ell(\beta)\, \mu_\ell(\alpha - \beta)$$

Deriving the formal expansion (17) of the moment generating function, with respect to any cumulant $\kappa_\ell(\beta)$, it comes

$$\frac{\partial M_\ell(\xi)}{\partial \kappa_\ell(\beta)} = \sum_{\alpha=0}^{\infty} \frac{\xi^\alpha}{\alpha!} \frac{\partial \mu_\ell(\alpha)}{\partial \kappa_\ell(\beta)}$$

while the same operation performed on Eq. (18) yields

$$\begin{aligned} \frac{\partial M_\ell(\xi)}{\partial \kappa_\ell(\beta)} &= \frac{\vec{\xi}^\beta}{\beta!} M_\ell(\xi) \\ &= \sum_{\vec{\gamma}=0}^{\infty} \frac{\xi^{\beta+\vec{\gamma}}}{\beta!\, \vec{\gamma}!}\, \mu_\ell(\gamma)\ . \end{aligned}$$

Comparing the two series yields the equality:

$$\frac{\partial \mu_\ell(\alpha)}{\partial \kappa_\ell(\beta)} = \binom{\alpha}{\beta}\, \mu_\ell(\alpha - \beta)$$

which holds for any $\beta \leq \alpha$ while the derivative vanishes otherwise. This reminds us that a moment is a function of the cumulants of lower degree and conversely: from the definition of the cumulants, $\mu_\ell(\alpha)$ is a polynomial expression of the variables $\kappa_\ell(\beta)$ for all $\beta \leq \alpha$.

Let us now consider

$$\begin{aligned} P_\kappa(\alpha) &\equiv \mu_\ell(\alpha) - \sum_{\gamma \leq \alpha} \mathcal{A}(\alpha, \gamma) \binom{\alpha}{\gamma} \kappa_\ell(\gamma)\, \mu_\ell(\alpha - \gamma) \\ &= P\left[\kappa_\ell(\beta),\ \beta \leq \alpha\right]. \end{aligned}$$

For any choice of the coefficients $\mathcal{A}(\alpha, \beta)$, this quantity is a polynomial expression of the cumulants of degree smaller than α with no constant term. We will show that these coefficients can be chosen so that all the derivatives of P_κ cancel. In this case, the polynom must be constant, and since there is no constant term, P_κ vanishes: this provides the recurrence relation (20).

Deriving P_κ with respect to $\kappa_\ell(\beta)$ yields,

$$\frac{\partial P_\kappa(\alpha)}{\partial \kappa_\ell(\beta)} = \binom{\alpha}{\beta}\mu_\ell(\alpha-\beta) - \mathcal{A}(\alpha,\beta)\binom{\alpha}{\beta}\mu_\ell(\alpha-\beta) - \sum_{\beta\le\alpha-\gamma}\mathcal{A}(\alpha,\gamma)\binom{\alpha}{\gamma}\binom{\alpha-\vec{\gamma}}{\beta}\kappa_\ell(\gamma)\,\mu_\ell(\alpha-\vec{\gamma}-\beta)\,.$$

Using the identity

$$\binom{\alpha}{\beta}\binom{\alpha-\beta}{\gamma} = \binom{\alpha}{\gamma}\binom{\alpha-\gamma}{\beta}, \tag{31}$$

it comes

$$\frac{\partial P_\kappa(\alpha)}{\partial \kappa_\ell(\beta)} = \binom{\alpha}{\beta}\Bigg[(1-\mathcal{A}(\alpha,\beta))\,\mu_\ell(\alpha-\beta) - \sum_{\gamma\le\alpha-\beta}\mathcal{A}(\alpha,\gamma)\binom{\alpha-\beta}{\gamma}\kappa_\ell(\gamma)\,\mu_\ell(\alpha-\vec{\gamma}-\beta)\Bigg].$$

Let us now assume that the ratio $\mathcal{A}(\alpha,\gamma)/\mathcal{A}(\alpha-\beta,\gamma) \equiv \mathcal{B}(\alpha,\beta)$ is a function of α and β only, which means that the function $\mathcal{A}$ factorizes: $\mathcal{A}(\alpha,\gamma) \equiv f(\alpha)\,g(\vec{\gamma})$. The later expression becomes:

$$\frac{\partial P_\kappa(\alpha)}{\partial \kappa_\ell(\beta)} = \binom{\alpha}{\beta}\Big[(1-\mathcal{A}(\alpha,\beta)-\mathcal{B}(\alpha,\beta))\,\mu_\ell(\alpha-\beta) + \mathcal{B}(\alpha,\beta)\,P_\kappa(\alpha-\beta)\Big].$$

We choose the coefficients $\mathcal{A}(\alpha,\gamma)$ so that the quantities $1-\mathcal{A}-\mathcal{B}$ cancel:

$$\frac{1}{f(\alpha)} - g(\beta) - \frac{1}{f(\alpha-\beta)} = 0$$

for all α and $\beta \le \alpha$. This is solved for

$$\frac{1}{f(\alpha)} \equiv g(\alpha) \equiv |\alpha|\,,$$

or

$$\mathcal{A}(\alpha,\beta) = \frac{|\beta|}{|\alpha|}.$$

We are now in a position to make our recurrence. The first step of the recurrence ($|\alpha| = 0$) is trivial. If for all $\beta \neq \mathbf{0}$, $\beta \le \alpha$, the polynom $P_\kappa(\alpha-\beta)$ vanish, then all the derivatives of $P_\kappa(\alpha)$ are zero, and $P_\kappa(\alpha) \equiv 0$. This proves that the polynoms $P_\kappa(\alpha)$ defined with the above choice of the coefficients $\mathcal{A}(\alpha,\beta)$ vanishes, and Eq. (20) holds.

This relation can easily be extended to the averages. For any given set of exponents $\alpha = \alpha_\ell$, and for all $\ell' \subset \mathcal{L}$, the quantities $\nu_{\ell'}^{\alpha} = \nu_{\ell'}(\alpha_{\ell'})$ and $\mu_{\ell'}^{\alpha} = \mu_{\ell'}(\alpha_{\ell'})$ have the same algebraic relationship than the quantities $\kappa_{\ell'}^{\mathbf{1}} = \kappa_{\ell'}(\mathbf{1}_{\ell'})$ and $\mu_{\ell'}^{\mathbf{1}}$. The recurrence relation (20) for $\kappa_{\ell'}^{\mathbf{1}}$ must therefore be verified by $\nu_{\ell'}^{\alpha}$. It reads:

$$\mu_{\ell}^{\mathbf{1}} = \sum_{\beta \leq \mathbf{1}} \frac{|\beta|}{|\mathbf{1}_\ell|} \kappa_{\ell}^{\beta} \mu_{\ell}^{\mathbf{1}-\beta}$$

where $|\mathbf{1}_\ell|$ is the number of sites in ℓ, or equivalently,

$$\mu_{\ell}^{\mathbf{1}} = \sum_{\ell' \subset \ell} \frac{|\ell|'}{|\ell|} \kappa_{\ell'}^{\mathbf{1}} \mu_{\ell \backslash \ell'}^{\mathbf{1}}$$

where $\ell \backslash \ell'$ is the complementary set of ℓ' in ℓ. Hence,

$$\mu_{\ell}(\alpha) = \sum_{\ell' \subset \ell} \frac{|\ell|'}{|\ell|} \nu_{\ell'}(\alpha_{\ell'}) \mu_{\ell \backslash \ell'}\left(\alpha_{\ell \backslash \ell'}\right)$$

Chapitre 4

Petits modèles

La troncature et fermeture des équations hiérarchiques a l'avantage de proposer une méthode systématique d'approximation du comportement collectif. Elle a cependant le défaut d'être relativement opaque, et permet mal d'isoler les ingrédients minimaux nécessaires à l'instauration d'une dynamique collective. Pourtant, elle confirme que ces comportements peuvent être caractérisés par «ce qui se passe entre des sites voisins», ce qui suggère qu'une meilleure compréhension du phénomène puisse venir de modèles locaux.

Ce nouveau chapitre est consacré à ces «petits modèles», qui tentent d'extraire des équation locales les ingrédients essentiels à la dynamique collective d'un réseau. Ces modèles sont développés dans l'esprit d'une approche de champ moyen : la question posée est d'une certaine façon, comment un site voit-il le monde ? Dans le champ moyen usuel, la moyenne spatiale suffit à résumer l'effet de l'ensemble du réseau sur chaque site. Il remarquable qu'un modèle aussi «dépouillé» puisse rendre compte de l'existence de transitions de phases dans des systèmes magnétiques.

Dans le cas qui nous occupe, cette approche ne fonctionne pas, et il faut donc chercher les ingrédients physiques qui manquent. L'idée essentielle de ces modèles, c'est que le champ moyen local $m_{\vec{r}}$ que perçoit un site ne peut plus être une grandeur uniforme, mais doit pouvoir fluctuer : c'est donc une variable aléatoire. Alors, les fluctuations de cette variable et sa corrélation avec le champ $\mathbf{X}_{\vec{r}}$ sont déterminées par les corrélations spatiales à courte portée. En outre, afin de définir cette variable, il suffit de remarquer que le bruit ambiant dans le système est mesuré par la distribution p^t elle-même : ce champ moyen est donc construit à partir de p^t, et de façon à respecter les contraintes fixées par les corrélations spatiales. Cette approche est développée dans la première des deux lettres qui suivent, publiée à *Europhysics Letters*. À ce stade, il

manque une modélisation de la dynamique des corrélations qui sont imposées au modèle comme des contraintes extérieures et sont donc stationnaires. Cependant, ceci permet de définir un opérateur d'évolution non linéaire pour p^t qui rend remarquablement bien compte de comportements observés dans les réseaux d'itérations couplées.

La seconde lettre, soumise à *Europhysics Letters* montre alors comment le système peut être fermé en incorporant la dynamique des corrélations. Le couplage agit de façon relativement simple sur les fonctions de corrélations, et il faut donc ici modéliser la déstructuration de la cohérence spatiale par l'application locale chaotique. Cette dernière approche se fonde alors sur la remarque que ces effets peuvent s'écrire simplement en considérant la limite continue des itérations couplées, qui présente des comportements collectifs semblables à ceux des systèmes discret, au moins en petite dimension, et pour laquelle la fonction de corrélation peut être approchée par une Gaussienne.

4.1 Conditional mean-field for chaotic coupled map lattices

Article paru dans *Europhysics Letters*

4.2 Macroscopic model for collective behavior of chaotic coupled map lattices

Article devant être soumis à *Europhysics Letters*

EUROPHYSICS LETTERS 15 August 1997

Europhys. Lett., **39** (4), pp. 377-382 (1997)

Conditional mean field for chaotic coupled map lattices

A. LEMAÎTRE, H. CHATÉ and P. MANNEVILLE

Laboratoire d'Hydrodynamique, Ecole Polytechnique - 91128 Palaiseau, France
CEA -Service de Physique de l'Etat Condensé, Centre d'Etudes de Saclay
91191 Gif-sur-Yvette, France

(received 20 May 1997; accepted in final form 16 July 1997)

PACS. 05.45+b – Theory and models of chaotic systems.
PACS. 05.70Ln – Nonequilibrium thermodynamics, irreversible processes.
PACS. 64.60C – Order-disorder transformations, statistical mechanics of model systems.

Abstract. – A conditional mean-field approach to strongly chaotic coupled map lattices is presented. It focusses on the time evolution of the one-body probability distribution function $p(X)$ of instantaneous site values. The local environment of a site is modelled in terms of an effective number of independent neighbours, while keeping the Perron-Frobenius operator to account for the action of the local map. This approximation is shown to produce distributions $p(X)$ in agreement with empirical observations of non-trivial collective behaviour, and captures the essence of their dynamics.

Coupled map lattices (CMLs) constitute perhaps the most popular type of spatially extended dynamical systems for studying the generic properties and elementary mechanisms of spatiotemporal chaos [1]. These discrete-time, discrete-space models exhibit a rich phenomenology, in some instances very reminiscent of far-from-equilibrium physical situations. Yet, even for these "simple" systems, analytical methods [2], [3] for tackling their chaotic regimes are scarce and generally restricted to cases of limited physical relevance, such as very weak coupling coefficients and/or expanding piecewise linear maps. Unsurprisingly, simple mean-field approximations are also of limited use, since they neglect one of the essential features of spatiotemporal chaos, spatial correlations.

The situation is probably at its worst when spatiotemporal chaos takes the form of *non-trivial collective behaviour* (NTCB). This generic phenomenon of high-dimensional systems is characterized by the emergence of a temporal evolution of spatially averaged quantities out of local chaotic fluctuations [4]. Since natural extensions of the mean field can only be satisfactorily defined in one space dimension, where block probabilities factorize unambiguously [5], extensions of the simple mean-field approximation are notably difficult to derive for NTCB, which appears in space dimensions $d \geq 2$. Cluster-type expansions can be defined, but their practical implementation rapidly becomes intractable [6].

In this letter, a new type of approximation is introduced and shown to account remarkably well for the simple NTCB regimes of usual CMLs. More specifically, we consider real variables

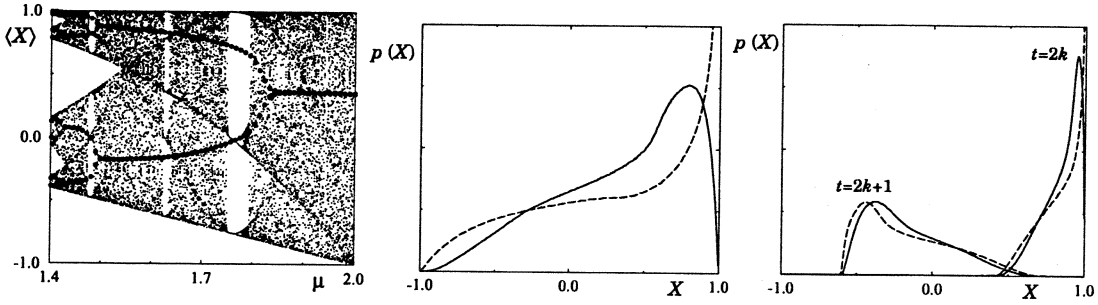

Fig. 1. – Non-trivial collective behaviour in democratically coupled logistic maps on a two-dimensional lattice of size $L = 1024$ with periodic boundary conditions ($g = 0.2$). Left: bifurcation diagram of the instantaneous spatial average M^t (filled circles) and bifurcation diagram of the single logistic map (small dots). Middle: asymptotic single-site pdf $p(X)$ in the stationary regime at $\mu = 2$ (solid line) and its iterate by the PFO $\mathcal{P}_S$ (dashed line). Right: same as middle panel, but in the collective period-2 regime at $\mu = 1.6$; up to statistical fluctuations, the two solid-line pdfs are iterates of each other during the CML evolution. The left dashed-line pdf is the iterate of the right solid-line pdf under the action of $\mathcal{P}_S$ (and vice-versa).

X_i at the nodes of d-dimensional hypercubic lattices updated synchronously *via*

$$X_i^{t+\frac{1}{2}} = S\left(X_i^t\right) \tag{1}$$

$$X_i^{t+1} = (1-2dg)X_i^{t+\frac{1}{2}} + g\sum_{j\in\mathcal{V}_i} X_j^{t+\frac{1}{2}}\,, \tag{2}$$

where S is a chaotic map, g is the (diffusive) coupling strength, and $\mathcal{V}_i$ denotes the set of the $2d$ nearest neighbours of site i.

Although our method is very general, for clarity's sake, it is applied only to lattices of logistic maps $S(X) = 1 - \mu X^2$, with $X \in [-1, 1]$ and $\mu \in [0, 2]$ in the following. In the band regime of the logistic map [7], $\mu > \mu_\infty \simeq 1.41...$, and for strong enough coupling (*e.g.* "democratic" coupling $g = 1/(2d+1)$), the above CML exhibits NTCB [4]. Figure 1 (left) illustrates the $d = 2$, $g = 0.2$ case by showing the bifurcation diagram of the instantaneous spatial average $M^t \equiv \langle X\rangle^t$ superimposed on that of the (uncoupled) logistic map. In this case, only periodic collective motion is observed. These regimes are reached from almost every initial condition. All sites evolve chaotically, and their instantaneous distributions $p(X)$ are wide, smooth, and follow the same collective behaviour (fig. 1, middle and right).

Under the simplest mean-field approximation, the spatial average M^t is governed just by the local map S: $M^{t+1} = S(M^t)$. While this obviously fails to account for the collective motion, a similarity can nevertheless be seen, in this simple example, between the NTCB of the CML and the band structure of the uncoupled map: varying μ from 2 to μ_∞, and neglecting the periodicity windows, the logistic map exhibits banded chaos, with an increasing number of bands (1, 2, 4, 8, ...). In this work, we start from this naive remark and present an approximation of the CML (1-2) in terms of the evolution of a *ensemble* of variables with an appropriate modelling of the coupling.

Let us first consider the case of uncoupled variables evolving under the action of the map S. When the number of such variables tends to infinity, this problem reduces to the evolution of a probability distribution function (pdf):

$$p^{t+1}(Y) = \int p^t(X)\,\delta\left(Y - S(X)\right)\mathrm{d}X \equiv \mathcal{P}_S\left[p^t\right]\,, \tag{3}$$

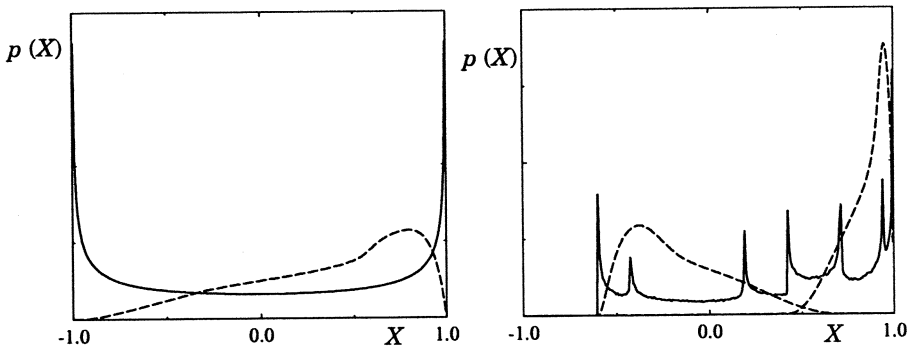

Fig. 2. – Asymptotic pdfs for the single logistic map (solid line) superimposed on the instantaneous distributions $p(X)$ produced by the CML of fig. 1 (dashed line). Left: $\mu = 2$. Right: $\mu = 1.6$.

where $\mathcal{P}_S$ is the Perron-Frobenius operator (PFO) associated to the map S.

In a banded chaos regime with q bands $\{B_i\}_{i=1}^q$, there exists a $\mathcal{P}_S$-invariant family $\mathcal{F} = \{\rho^i\}_{i=1}^q$ of disjoint distributions ρ^i of support B_i. At long times, p^t is a convex linear combination $\sum \lambda_i \rho_i$ of these *pure states*, and the action of the PFO on this decomposition is a permutation of the weights λ_i: $\mathcal{P}_S$ is said to be *asymptotically periodic* [8]. In the case of the logistic map, these pure states are not known exactly, except for $\mu = 2$. Numerical simulations reveal a very intricate structure with sharp peaks, in contrast to the smooth distributions of the CML (fig. 2).

In spite of this striking —and general— discrepancy, the PFO of the uncoupled map is essential to understanding the dynamics of the CML. After all, eq. (1) does correspond to the action of $\mathcal{P}_S$ on $p(X)$. And indeed, in the collective period-2 regime of our example, the PFO roughly transforms the two asymptotic distributions into one another (fig. 1, right), while the spatial correlations bring the corrections necessary to produce the regular cycle, and do not let the system evolve toward the uncoupled asymptotic distribution of fig. 2 (note that, in this case, the uncoupled map is still in a one-band regime). In other words, the periodicity of the CML is already contained in the local map, at least in its global features.

In the following, we numerically implement —without attempting to model— the action of the PFO on $p(X)$, and we focus on the spatial structure of the "typical" neighbourhood of a site. The object that evolves under our approximation is the pdf $p(X)$ of an infinite CML. In order to close equation (2) at first order, we must estimate the distribution of the *local* average at the site i, $M_i \equiv (1/2d)\sum_{j\in\mathcal{V}_i} X_j$, which depends on X_i.

Consider a "central" site with value X. Adopting a conditional approach, we want to estimate $m = m|_X$, the typical value of the local average around this site, and $y = y|_X$, the typical value taken by any of its neighbours. Due to invariance under lattice symmetries, the stochastic variables verify $\langle m|X\rangle = \langle y|X\rangle$, where the notation $\langle\,.\,|X\rangle$ indicates the conditional average taken for a fixed value of X.

Two limit cases can be considered: if all sites are synchronized, $y|_X = X$; if they are uncorrelated, $y|_X = x$, where x denotes a random variable independent of X and distributed according to p. In intermediate cases, the typical value $y|_X$ depends on p and X. This is the situation of interest in chaotic CMLs, since two-point correlations usually decay fast but are not zero. In particular, correlations are strong at very short distances, indicating the relative smoothness of the system's spatial profile. The corresponding "shoulder" of the two-point correlation function at small distances can be interpreted as the existence of a certain degree of

synchronization between nearby sites. Our central assumption is to approximate this situation by linearly interpolating between complete synchronization and complete independence of neighbouring sites. We thus write

$$y|_X = \alpha\, \widetilde{X} + (1-\alpha)\, X\,, \tag{4}$$

where $\alpha \in [0,1]$ and $\widetilde{X}$ and X are independent random variables distributed according to p. The *local* mean field then reads: $\langle m|X\rangle = \langle y|X\rangle = \alpha M + (1-\alpha)X$, a relation well verified by numerical simulations of CMLs such as those described above. This shows that $(1-\alpha)$ expresses the "screening" of the mean field M due to local correlations. Indeed, $(1-\alpha)$ is nothing but the correlation coefficient between neighbours since, letting X vary, we have $\langle mX\rangle_{\rm c} = \langle yX\rangle_{\rm c} = (1-\alpha)\langle X^2\rangle_{\rm c}$, where the subscript "c" denotes cumulants. Consequently, $(1-\alpha)$ is a macroscopic quantity which accounts for the mutual dependence of sites at short range and is invariant under linear transformations of the lattice variables.

Next, we want to express $m|_X$ in terms of $y|_X$. However, the fluctuations of the local average $\langle m^2\rangle_{\rm c}$ do not depend solely on the correlations between the neighbours and the central site, as the neighbours are themselves correlated with one another. If two neighbours (of the same central site) are represented by variables $y|_X = \alpha\, \widetilde{X} + (1-\alpha)\, X$ and $y'|_X = \alpha\, \widetilde{X}' + (1-\alpha)\, X$, with $\widetilde{X}$ and $\widetilde{X}'$ independent, their conditional correlation $\langle yy'|X\rangle_{\rm c}$ vanishes, even though $\langle yy'\rangle_{\rm c} = (1-\alpha)^2\langle X^2\rangle_{\rm c} \neq 0$: y and y' are correlated; but their dependence comes out through X only: they are independent in a Bayesian sense. To account for the correlations between neighbours of a common central site, we write m as a sum of N *effective* Bayes-independent variables $y_j|_X$:

$$m|_X \equiv \frac{1}{N}\sum_{j=1}^{N} y_j|_X\,,$$

where the number N is not necessarily equal to the actual number of neighbours in the lattice. As a matter of fact, extending the notion of a sum of independent variables, it is even possible to deal with non-integer N's. This allows the modelling of the coupling in terms of synchronized and independent neighbours in arbitrary proportions. This amounts to considering the system as living on a tree structure of connectivity N. Equation (2) is then "replaced" by

$$\widetilde{X}_i^{t+1} = (1-N\tilde{g})\widetilde{X}_i^{t+\frac{1}{2}} + \tilde{g}\sum_{j=1}^{N}\widetilde{X}_j^{t+\frac{1}{2}}\,, \tag{5}$$

where $\tilde{g} = 2d\alpha g/N$ and the N effective independent neighbours $\widetilde{X}_j$ are distributed according to p.

At this stage, our approximation involves two free parameters, α and N. They express the local structure of correlations in the CML and are related to the cumulants $\langle Xm\rangle_{\rm c}$, $\langle X^2\rangle_{\rm c}$, and $\langle m^2\rangle_{\rm c}$:

$$\langle Xm\rangle_{\rm c} = (1-\alpha)\langle X^2\rangle_{\rm c}\,, \tag{6}$$

$$\langle m^2\rangle_{\rm c} = [(1-\alpha)^2 + \alpha^2/N]\langle X^2\rangle_{\rm c}\,. \tag{7}$$

A priori, in NTCB regimes, these quantities evolve in time. In fact, α and N being ratios of second-order cumulants, they are relatively independent of the underlying collective motion (this is also true for the mutual information between neighbouring sites [9]), at least in simple cases such as the lattices of coupled logistic maps described above (see fig. 3 (left), which shows the numerical values of α and N as defined by eqs. (6) and (7)). These observations lead us to our final assumption of *geometrical stationarity*: α and N are taken as fixed parameters.

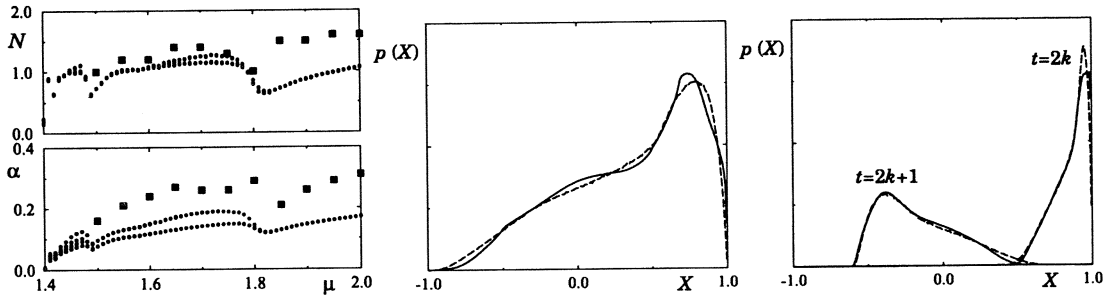

Fig. 3. – Left: α and N measured on the CML of fig. 1 at all timesteps in the asymptotic regime for different values of the parameter μ (small symbols), and best-fit values for the approximation, *i.e.* values of α and N for which the distance between the empirical pdfs and those produced by the approximation scheme is minimal (squares). Middle: asymptotic pdf $p(X)$ produced by the approximation for $\mu = 2$ and best-fit values of α and N (solid line); same for the original CML (dashed line). Right: same but for the collective period-2 regime at $\mu = 1.6$.

The dynamical evolution of $p(X)$ within our approximation is now complete: eq. (1) is replaced by the action of the PFO of the local map (eq. (3)), and eq. (2) by the action of a complex convolution operator $\Delta_{\tilde{g},N}$ (see eq. (5)):

$$\cdots p^t \xrightarrow{\mathcal{P}_S} p^{t+\frac{1}{2}} \xrightarrow{\Delta_{\tilde{g},N}} p^{t+1} \cdots .$$

The convolution operator $\Delta_{\tilde{g},N}$ is defined by

$$\Delta_{\tilde{g},N}[p](X') = \int p(X)\, p_N\left(\frac{X' - (1 - N\tilde{g})X}{N\tilde{g}}\right) \mathrm{d}X\,, \tag{8}$$

where p_N is the distribution of the average $(1/N)\sum_{j=1}^{N} \tilde{X}_j$ over the N effective independent neighbours $\tilde{X}_j$ distributed according to p:

$$p_N(Y) \equiv \int \left(\prod_{j=1}^{N} p(\tilde{X}_j)\mathrm{d}\tilde{X}_j\right) \delta\left(Y - \frac{1}{N}\sum_{j=1}^{N} \tilde{X}_j\right) . \tag{9}$$

The computation of this convolution integral can be performed for non-integer N *via* Fourier transform.

We will now describe the results of our approximation as applied to the two-dimensional lattice of democratically coupled logistic maps used throughout the text. First, we note that, for realistic values of α and N, eqs. (3), (8) and (9) usually converge rapidly to the same attractor for various initial distributions.

For $\mu = 2$, the CML is in a stationary state (fig. 1). For a large range of parameters including the numerically observed values of α and N (approximately $N \in [1,4]$ and $\alpha \in [0.15, 0.32]$), $p^t(X)$ converges, under the approximation, to a stationary pdf strikingly similar to the original one. For $\mu = 1.6$, the approximation easily captures the collective motion, again for a rather large range of parameter values ($N \in [1,3]$ and $\alpha \in [0.21, 0.26]$). In both cases, the agreement between the empirical and approximated pdfs is excellent and the results are remarkably robust, see fig. 3, middle and right, where the parameter values yielding the best agreement were used.

Similarly good results were obtained for the same CML and $d = 3$, as well as for coupled tent maps. However, it is more difficult, and sometimes impossible, to capture the larger-period

cycles of the CML and the more complex collective evolutions observed for $d > 3$. We believe that this is due to the non-stationarity of α and N in these cases. This indicates the direction towards which the present work should be extended: the *dynamics* of the effective parameters α and N should be self-consistently incorporated. We are currently working on various schemes toward this end, as well as on an extension to cellular automata.

At the present stage, the two parameters α and N have to be chosen somewhat arbitrarily, but their physical significance is clear: α measures correlations between neighbouring sites, while N can be seen as the mean effective number of Bayes-independent neighbours of a given site. This approximation yields robust and reliable results, reproducing the dynamics of non-trivial distributions. The basic ideas underlying our approach shed some light on "fully developed" spatiotemporal chaos and, in particular, on the macroscopic motion displayed by synchronously updated systems in the strong-coupling limit. They confirm [10], [6] the local origin of the non-trivial collective behaviour observed in CMLs, and detail the "regularizing" role of the coupling. In some sense, the geometry can be seen to correct the action of the Perron-Frobenius operator on one-site pdfs so as to make them drift towards a new operating point associated with the collective regime.

REFERENCES

[1] See, *e.g.*, KANEKO K. (Editor), *Theory and Applications of Coupled Map Lattices* (Wiley, New York) (1993).

[2] BUNIMOVICH L. A. and SINAI YA. G., *Nonlinearity*, **1** (1988) 491.

[3] KELLER G. and KÜNZLE M., *Ergod. Theor. Dyn. Sys.*, **12** (1992) 297.

[4] CHATÉ H. and MANNEVILLE P., *Europhys. Lett.*, **17** (1992) 291; *Prog. Theor. Phys.*, **87** (1992) 1.

[5] GUTOWITZ H. A. and VICTOR J. D., *Physica D*, **28** (1987) 18; GUTOWITZ H. A., *Physica D*, **45** (1990) 136; HOULRIK J. M., WEBMAN I. and JENSEN M. H., *Phys. Rev. A*, **41** (1990) 4210.

[6] LEMAÎTRE A., CHATÉ H. and MANNEVILLE P., *Phys. Rev. Lett.*, **77** (1996) 486; preprint (1997).

[7] FEIGENBAUM M., *Physica D*, **7** (1983) 16.

[8] LASOTA A. and MACKEY M. C., *Probabilistic Properties of Deterministic Systems* (Cambridge University Press, Cambridge) (1985).

[9] MANNEVILLE P., in 1996 Annual Report of CNCPST, Paris (available upon request at http://www.cncpst.jussieu.fr).

[10] CHATÉ H., TANG L.-H. and GRINSTEIN G., *Phys. Rev. Lett.*, **74** (1995) 912.

Macroscopic model for collective behavior of chaotic coupled map lattices

Anaël Lemaître[1,2] and Hugues Chaté[2,1]

[1] *LadHyX — Laboratoire d'Hydrodynamique, École Polytechnique, 91128 Palaiseau, France*

[2] *CEA — Service de Physique de l'État Condensé, Centre d'Études de Saclay, 91191 Gif-sur-Yvette, France*

Abstract

We present a simple model for the collective behavior exhibited by chaotic coupled map lattices (CMLs) in any space dimension which takes into account local mean-field fluctuations and short-range correlations. This reduces the dynamics of CMLs to the evolution of a one-body distribution function coupled to a coherence length. Quantitatively good results are obtained, especially in the case of coupled tent maps, even though no free parameter is available.

The emergence of collective behavior in large dynamical systems made of coupled chaotic units is now well documented [1, 2, 3, 4, 5]. Whether the connections are local or global, on a lattice or on a random network, one often observes that quantities averaged over the whole collection of individual units evolve in time, usually in some regular fashion, while strong chaos is present at the microscopic level, and no synchronisation occurs between sites. This constitutes some of the main features of non-trivial collective behavior (NTCB). To them one must add the sometimes implicit requirement that the collective behavior observed is a true macroscopic attractor, i.e. that it has a well-defined infinite-size/time limit, and that almost any initial condition leads to it. (The uniqueness of the collective motion is usually granted if the coupling between units is strong enough, with the weak-coupling regime being characterized by multistability.)

In lattice dynamical systems such as coupled map lattices (CMLs), NTCB can be seen as long-range order accompanied by the temporal evolution of

spatially-averaged quantities. Whereas globally- or randomly-coupled systems are somewhat easier to handle, being closer to some infinite-dimension limit, the case of lattice systems with local interactions is notably hard to approach analytically, especially if one is interested in the strong coupling case where there is no hope of extending zero-coupling results (like in the so-called anti-integrable limit [6]). In particular, one of the outstanding problems concerning NTCB in lattice systems is that of the prediction of the collective motion from the local dynamical rules. In this letter, we present a model accounting for NTCB in lattices of coupled chaotic maps at the macroscopic level.

Specifically, we consider the discrete-time dynamics of a set of variables $\mathbf{X} = (\mathbf{X}_{\vec{r}})_{\vec{r}\in\mathcal{L}}$ lying at the nodes of a d-dimensional hypercubic lattice $\mathcal{L}$. The nodes are updated synchronously at discrete timesteps which involve two stages: firstly, the operator $\mathbf{S}_\mu$, applied to $\mathbf{X}^t$ transforms each local variable $\mathbf{X}^t_{\vec{r}}$ by a non-linear local map S_μ, yielding an intermediate configuration $\mathbf{X}^{t+\frac{1}{2}}$. Secondly, $\mathbf{X}^{t+\frac{1}{2}}$ is transformed by a diffusive coupling operator $\mathbf{\Delta}_g$,

$$[\mathbf{\Delta}_g(\mathbf{X})]_{\vec{r}} = (1-2dg)\mathbf{X}_{\vec{r}} + g\sum_{\vec{e}\in\mathcal{V}}\mathbf{X}_{\vec{r}+\vec{e}}\,. \tag{1}$$

where g is the coupling strength, and $\mathcal{V}$ denotes the set of the $2d$ nearest-neighbors of site $\vec{0}$. The CML dynamics is thus simply written $\mathbf{X}^{t+1} = \mathbf{\Delta}_g \circ \mathbf{S}_\mu(\mathbf{X}^t)$.

In the following, we consider unimodal maps $S_\mu(X) = 1 - \mu|X|^{1+\varepsilon}$ with $\mu \in [0,2]$, which leave the interval $I = [-1,1]$ invariant, and in particular we deal with the $\varepsilon = 0$ case (tent map). For $\mu > \mu_\infty$ ($= 1$ for the tent map), and for strong enough coupling, CMLs $\mathbf{\Delta}_g \circ \mathbf{S}_\mu$ exhibit NTCB [3, 8]. The bifurcation diagram of the instantaneous spatial average $M^t \equiv \langle\mathbf{X}\rangle^t$ is displayed in Fig. 1 for $g = 0.2$ in dimensions 2 and 3. All sites evolve chaotically and are statistically equivalent. In fact, the instantaneous one-body distribution p^t is smooth, wide, and follows the same collective behavior as its mean M^t. Only periodic regimes are observed in these cases, but quasiperiodic dynamics appears in higher space dimensions, indicating that the collective motion may have no direct equivalent at the microscopic level.

In [7], we developed a conditional mean-field approximation yielding an effective evolution for p^t. We first recall this approach. Applying operator $\mathbf{S}_\mu$ to an infinite lattice, p^t is transformed by $\mathcal{P}_{S_\mu}$, the Perron-Frobenius operator (PFO) associated to the local map:

$$p^{t+\frac{1}{2}}(X) = \mathcal{P}_{S_\mu}[p^t] \equiv \int p^t(Y)\delta(X - S_\mu(Y))\,dY\,.$$

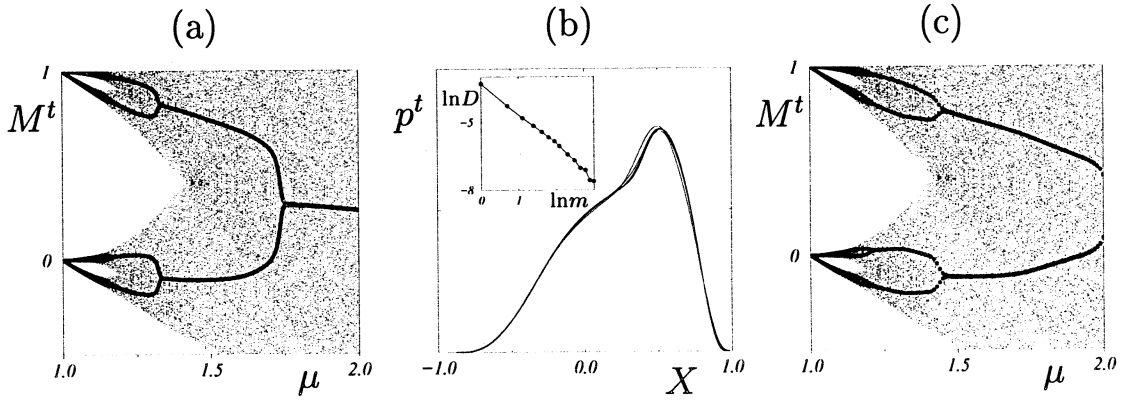

Figure 1: Non-trivial collective behaviour in lattices of coupled tent maps ($g = 1/(2d+1)$) with periodic boundary conditions. (a): $d = 2$ bifurcation diagram of the instantaneous spatial average M^t (filled circles) and bifurcation diagram of the single tent map (small dots). (b): asymptotic single-site pdf p in the stationary regime of $\mathbf{\Delta}_g^m \circ \mathbf{S}_\mu$ at $\mu = 2$, for m varying from 1 to 32; the distance $D = \int (p_m - p_{32})^2$ (insert) shows evidence of convergence with m. (c): same as (b) for $d = 3$.

When $\mathbf{\Delta}_g$ is applied to $\mathbf{X}^{t+\frac{1}{2}}$, the resulting local pdf p^{t+1} depends on the joint pdf of $\mathbf{X}_{\vec{r}}^{t+\frac{1}{2}}$ and the *local mean field* $\mathbf{m}_{\vec{r}}^{t+\frac{1}{2}} = \sum_{\vec{e}\in\mathcal{V}} \mathbf{X}_{\vec{r}+\vec{e}}^{t+\frac{1}{2}}$ at intermediate time. Neglecting these short-range correlations lead to simple mean-field approximations unable to account for NTCB [3, 7]. On the other hand, it is known that keeping only short-range correlations is often sufficient to account for the collective motion [9, 10]. In [7], we proposed that the local mean-field $\mathbf{m}_{\vec{r}}$ around a "typical" site with value X should be represented by a fluctuating variable $m = m_{|X}$ correlated with X. This led us to write the local mean-field at intermediate times, $m^{t+\frac{1}{2}}$, as a sum involving $X^{t+\frac{1}{2}}$ and N effective uncorrelated variables $\widetilde{X}_j^{t+\frac{1}{2}}$ distributed according to $p^{t+\frac{1}{2}}$. In this framework, physical space disappears and the CML is reduced to an ensemble of variables X_i governed by S_μ and by the following coupling

$$X_i^{t+1} = (1-G)X_i^{t+\frac{1}{2}} + \frac{G}{N}\sum_{j=1}^{N} \widetilde{X}_j^{t+\frac{1}{2}},$$

where G is an effective coupling strength a priori different from $2dg$. From the point of view of the pdf $p^{t+\frac{1}{2}}$, this amounts to apply the convolution operator $\Delta_{G,N}$, defined by:

$$\Delta_{G,N}[p](X) = \frac{1}{1-G}\int p\left(\frac{X-GY}{1-G}\right) p_N(Y)\, dY$$

where p_N is the distribution of the average of N independent variables distributed according to p. The computation of p_N is done *via* Fourier transform,

$\hat{p}_N(\xi) = (\hat{p}(\xi/N))^N$, and can be performed for any $N \geq 1$, not necessarily integer. Parameters G and N can be shown to be related to correlations and fluctuations in the original CML via the relations

$$\frac{\langle X^{t+1} X^{t+\frac{1}{2}} \rangle_c}{\langle X^2 \rangle_c^{t+\frac{1}{2}}} = 1 - G \quad \text{and} \quad \frac{\langle X^2 \rangle_c^{t+1}}{\langle X^2 \rangle_c^{t+\frac{1}{2}}} = (1-G)^2 + \frac{G^2}{N}, \tag{2}$$

with $\langle XY \rangle_c = \langle XY \rangle - \langle X \rangle \langle Y \rangle$ and where $\langle \, . \, \rangle$ denotes the ensemble p-average. Indeed, the corresponding quantities in the CML are spatial correlations like $\langle [\mathbf{\Delta}_g(\mathbf{X})]_{\vec{r}} \, \mathbf{X}_{\vec{r}} \rangle_c^{t+\frac{1}{2}}, \ldots$ where the brackets indicate the spatial average. Since $\mathbf{\Delta}_g$ is a linear operator, they are simple combinations of the correlations at time $t + \frac{1}{2}$ in a typical neighborhood.

At this stage, the approximation cannot provide any description of the dynamics of the correlations, and G and N, were assumed, in [7], to be stationary with numerical values chosen somewhat arbitrarily, but in a range suggested by numerical estimates of the above-mentioned correlations. Surprisingly, it accounted well for the shape and dynamics of p^t observed in CMLs, and this for a wide range of N and G, at least for not too large collective periodic cycles. Now, we go further and present a new model without any free parameter which insures that the large-period collective cycles observed when $\mu \to \mu_\infty$ are better accounted for.

To this aim, we need to incorporate the dynamics of correlations in the model. Consider the correlation function $C(\vec{x}) = \langle \mathbf{X}_{\vec{r}} \mathbf{X}_{\vec{r}+\vec{x}} \rangle_c$ and its Fourier transform, the structure function: $\hat{C}(\vec{k}) = |\hat{\mathbf{x}}_{\vec{k}}|^2$ where $\hat{\mathbf{x}}_{\vec{k}}$ is the spatial Fourier transform of the centered field $\mathbf{x}_{\vec{r}} = \mathbf{X}_{\vec{r}} - \langle \mathbf{X}_{\vec{r}} \rangle$. Their dynamical evolution, for usual CMLs, leads to write hierarchical equations which cannot be easily handled [10]. However, this dynamics takes a particularly simple form in the continuous-space limit defined in [8]. This limit is reached by applying the coupling operator an increasing number of times per iteration, i.e. when considering CMLs of the form $\mathbf{\Delta}_g^m \circ \mathbf{S}_\mu$. When $m \to \infty$, $\mathbf{\Delta}_g^m$ converges to a diffusive operator with a Gaussian kernel, $\mathbf{\Delta}_\lambda^\infty = \exp(\frac{1}{2}\lambda^2 \nabla^2)$. Its coupling range $\lambda = \sqrt{2gm}\|\vec{e}\|$ diverges with m but $\|\vec{e}\|$, the lattice spacing, can be chosen to scale like $1/\sqrt{m}$ so as to keep λ constant. Operator $\mathbf{\Delta}_\lambda^\infty$ is universal in the sense that all $\mathbf{\Delta}_g^m$ converge to it provided $\mathbf{\Delta}_g$ satisfies very general constraints [8].

In space dimensions $d = 2$ and 3, $\mathbf{\Delta}_\lambda^\infty \circ \mathbf{S}_\mu$ present the same periodic behavior as usual discrete-space CMLs. For example, the pdf p^t for a two-dimensional lattice of coupled tent maps in a fixed point collective regime

is displayed in Fig. 1b for increasing values of m. Fast convergence towards a well-defined $m \to \infty$ limit is observed, corresponding to a fixed point of operator $\mathbf{\Delta}_\lambda^\infty \circ \mathbf{S}_\mu$. For $d = 2$ and 3, the bifurcation diagrams obtained at different m are hardly distinguishable from those of Fig. 1a,c, although the bifurcation points tend to be shifted to the right as m increases. Moreover, CMLs $\mathbf{\Delta}_g^m \circ \mathbf{S}_\mu$ verify a renormalisation group (RG) equation which shows that, in any dimension, the system near μ_∞ is conjugate to another with a larger m [8]. Thus, a faithful model of this continuous limit will also be valid for usual discrete-space CMLs.

In the continuous limit, the diffusive coupling operator insures that the field $\mathbf{X}_{\vec{r}}$ is continuous and smooth in space at all times: therefore, the correlation function is Gaussian at short range (Porod's law). We can thus write, neglecting long-range correlations,

$$C(\vec{x}) = \left\langle \mathbf{X}^2 \right\rangle_c \exp\left(-\frac{x^2}{2\Lambda^2}\right) \quad \text{and} \quad \hat{C}(\vec{k}) = \left\langle \mathbf{X}^2 \right\rangle_c \left(\Lambda\sqrt{2\pi}\right)^d \exp\left(-\frac{\Lambda^2}{2}k^2\right). \tag{3}$$

with $\langle \mathbf{X}^2 \rangle_c$ the variance of p and Λ the *coherence length* of the field. The spatial order induced by the coupling is thus completely encoded by a single scalar, the coherence length Λ, while the distribution p^t, an infinite-dimensional object, potentially bears all the complexity of the observed NTCB.

We now define an effective coupled dynamics for the system (p^t, Λ^t). When the local map is applied, p^t is transformed by $\mathcal{P}_{S_\mu}$. The coherence length decreases because of the divergence of nearby trajectories induced by the local chaos. The evolution of p^t during the coupling stage requires to evaluate the instantaneous parameters G and N, which in turn are related to short-range correlations at times $t+\frac{1}{2}$ and $t+1$ via relation (2). The effect of the coupling on Λ is straightforward and permits to estimate these parameters: applying $\mathbf{\Delta}_\lambda^\infty$ in Fourier space, the structure function verifies $\hat{C}^{t+1}(\vec{k}) = \exp(-\lambda^2 k^2)\, \hat{C}^{t+\frac{1}{2}}(\vec{k})$. The coupling operator respects the Gaussian form (3) and simply increases Λ^2 by a constant term: $(\Lambda^{t+1})^2 = (\Lambda^{t+\frac{1}{2}})^2 + 2\lambda^2$. Moreover, identifying the prefactors yields a relation which fixes the dynamics of the variance $\langle \mathbf{X}^2 \rangle_c$ under the coupling operator. The direct calculation of the correlation $\langle \mathbf{X}_{\vec{r}}^{t+1} \mathbf{X}_{\vec{r}}^{t+\frac{1}{2}} \rangle_c$ provides a similar equation. Finally, we have

$$\frac{\langle \mathbf{X}_{\vec{r}}^{t+1} \mathbf{X}_{\vec{r}}^{t+\frac{1}{2}} \rangle_c}{\langle \mathbf{X}^2 \rangle_c^{t+\frac{1}{2}}} = \left(1 + \frac{\lambda^2}{(\Lambda^{t+\frac{1}{2}})^2}\right)^{-\frac{d}{2}} \quad \text{and} \quad \frac{\langle \mathbf{X}^2 \rangle_c^{t+1}}{\langle \mathbf{X}^2 \rangle_c^{t+\frac{1}{2}}} = \left(1 + \frac{2\lambda^2}{(\Lambda^{t+\frac{1}{2}})^2}\right)^{-\frac{d}{2}}. \tag{4}$$

These relations determine the effective parameters $G(\Lambda/\lambda)$ and $N(\Lambda/\lambda)$ of the convolution operator of the approximation: $\Delta_{G,N} \equiv \Delta_{\Lambda/\lambda}$.

We now have to estimate how the coherence length is changed when $\mathbf{S}_\mu$ is applied to the continuous field $\mathbf{X}_{\vec{r}}$. For this purpose, the correlation function is written

$$C(\vec{x}) = \langle \mathbf{X}^2 \rangle_c \left(1 - \frac{1}{2} \frac{\langle (\mathbf{X}_{\vec{r}+\vec{x}} - \mathbf{X}_{\vec{r}})^2 \rangle}{\langle \mathbf{X}^2 \rangle_c} \right)$$

to introduce explicitly the difference $\mathbf{X}_{\vec{r}+\vec{x}} - \mathbf{X}_{\vec{r}}$. Applying S_μ to $\mathbf{X}^t_{\vec{r}}$, it comes, for small $\vec{x}$:

$$\left\langle (\mathbf{X}_{\vec{r}+\vec{x}} - \mathbf{X}_{\vec{r}})^2 \right\rangle^{t+\frac{1}{2}} \simeq \left\langle \left(S'_\mu(\mathbf{X}_{\vec{r}}) \right)^2 (\mathbf{X}_{\vec{r}+\vec{x}} - \mathbf{X}_{\vec{r}})^2 \right\rangle^t = \mu^2 \left\langle (\mathbf{X}_{\vec{r}+\vec{x}} - \mathbf{X}_{\vec{r}})^2 \right\rangle^t ,$$

since, for the tent map, $S'_\mu(X) = \pm\mu$ everywhere. Finally, expanding $C(\vec{x})$ as $C(\vec{x}) \simeq \langle \mathbf{X}^2 \rangle_c (1 - \frac{1}{2}\frac{\vec{x}^2}{\Lambda^2})$ near $\vec{x} = \vec{0}$ yields, for the coherence length

$$\frac{\Lambda^{t+\frac{1}{2}}}{\Lambda^t} \simeq \frac{1}{\mu} \sqrt{\frac{\langle \mathbf{X}^2 \rangle_c^{t+\frac{1}{2}}}{\langle \mathbf{X}^2 \rangle_c^t}} = \frac{1}{\mu} \sqrt{\frac{\langle \mathbf{S}_\mu(\mathbf{X})^2 \rangle_c^t}{\langle \mathbf{X}^2 \rangle_c^t}} \equiv D(p^t) \,. \tag{5}$$

This relation couples the dynamics of Λ^t with p^t. Coefficient $D(p^t) \leq 1$ opposes the divergence of nearby trajectories measured by μ to the overall dilatation of the pdf p^t, measured by the ratio of standard deviations. In particular, if the pdf p^t lies on an interval which does not contain 0 (e.g. every other timestep when the local map has two bands), the local map is linear, $D(p^t) = 1$ and Λ is unchanged; on the contrary, $D(p^t) < 1$ when the pdf p^t crosses the inversion/folding point 0, *i.e.*, when the chaotic map "destructurates" the spatial organization induced by the coupling. The effective dynamics of p and Λ is now fully defined by

$$p^{t+1} = \Delta_{\Lambda^{t+\frac{1}{2}}/\lambda} \circ \mathcal{P}_{S_\mu} \left(p^t \right) , \quad \text{with} \quad \Lambda^{t+\frac{1}{2}} = D(p^t)\, \Lambda^t \quad \text{and} \quad \Lambda^{t+1} = \Lambda^{t+\frac{1}{2}} + 2\lambda^2 .$$

This model of the collective behavior of coupled tent maps in the continuous limit is self-consistent, without free parameters. Operator $\Delta_{\Lambda/\lambda}$ is one of the simplest respecting relations (4), and it is worth noting that the space dimension d appears only in these expressions. Like in the original system, changing λ amounts to dilate Λ and has no influence on p. The dynamics of Λ^t is particularly simple, and it is immediate to check that it is stable for any periodic motion of p^t (the reverse is, of course, not true). Our model also satisfies a RG relation similar to that of the original system [8], which guarantees

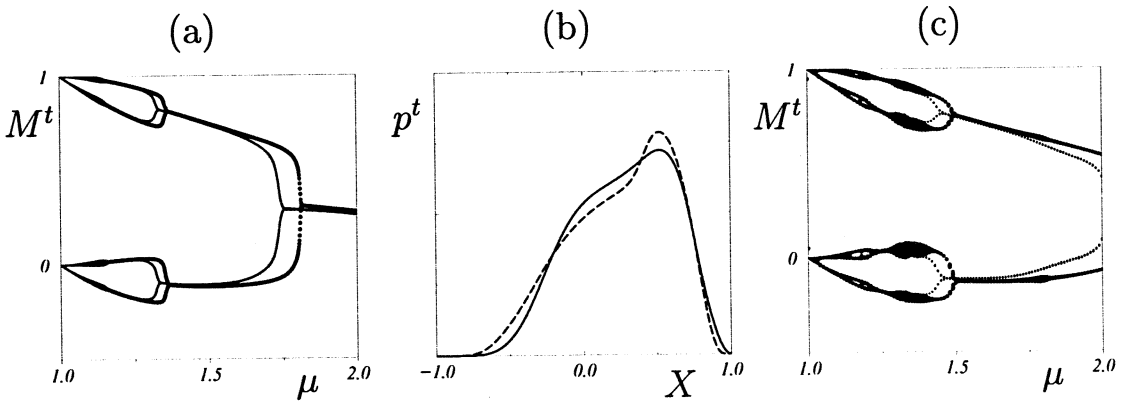

Figure 2: Comparison of the model with the non-trivial collective behaviour in democratically-coupled tent maps of Fig. 1. (a): bifurcation diagram of the instantaneous spatial average M^t in two dimension for the CML ($m = 1$, small circles) and for the model (large circles). (b): asymptotic single-site pdf $p(X)$ in the stationary regime of $\mathbf{\Delta}_g^m \circ \mathbf{S}_\mu$ at $\mu = 2$ and $m = 32$ (dashed line) compared with the fixed point regime obtained in the model (solid line). (c): Bifurcation diagrams for $d = 3$.

that it displays self-similarity and an infinite subharmonic cascade of global bifurcations.

We studied the dynamics of the model by direct numerical simulations. All initial pdfs tried lead to the same asymptotic behavior. Fig. 2 displays the bifurcation diagram of the average M^t in the model and the original, $m = 1$ CML in dimension $d = 2$ and 3. For $d = 2$, the whole bifurcation diagram is reproduced although the bifurcation points are slightly shifted to the right. The bifurcations seem to be discontinuous, although the hysteresis loops are very small (of the order of 10^{-2}). We are currently investigating whether the subcritical character of the bifurcations is an effect of the finiteness of the numerical simulations of pdf dynamics. The shapes of the pdfs obtained in the model compare fairly well to those measured in CMLs; they display the same asymmetry and inflexion points. For $d = 3$, the model accounts for periodic behavior and also for the dimension dependence of the transition points. However, a window of quasi-periodic behavior of p^t is observed, which does not seem to be observed in the continuous-limit (it is not observed for discrete CMLs with $m = 2, 3, 4$).

In higher space dimensions, the model often presents chaotic macroscopic behavior. We are unable, at this stage, to compare with the NTCB exhibited by the original CMLs in their continuous limit because this requires very large scale calculations, possibly out of reach of today's most powerful computers.

The model has also been tested with other local maps than the tent map. Similar results are obtained for piecewise linear maps with constant $|S'_\mu|$ (which justifies (5)). But this relation can also be used for more general maps, such as the logistic map, assuming that the field difference $\mathbf{X}_{\vec{r}} - \mathbf{X}_{\vec{r}+\vec{x}}$ depends only on $\vec{x}$ and is therefore independent of $\mathbf{X}_{\vec{r}}$. This also yields qualitatively good agreement, reproduces periodic behavior and their dependence on d, but the bifurcation points are strongly shifted to higher μ values. Better quantitative agreement can be expected from a more precise evaluation of coefficient $D(p^t)$.

Our work departs from standard mean-field approximations by the incorporation of fluctuations of the local mean-field and by taking into account the dynamics of short-range correlations, which is governed by a single coherence length in the space-continuous limit of CMLs. For coupled tent maps, our approximation leads to a parameter-free model in which the nonlinear PFO dynamics of the pdf p^t is coupled to a single scalar variable. In so far as the continuous-space limit is representative of the behavior of the original CMLs, the results obtained are qualitatively and even quantitatively good. For other maps, we expect equally-good results with a better treatment of the effect of the map on a pdf.

To our knowledge, this work constitutes the first macroscopic model for collective motion displayed by spatially-extended, chaotic, dynamical systems in the strong coupling limit. We hope it will trigger more rigorous, mathematical approaches, which have, so far, remained largely confined to the weak-coupling limit [11].

***

References

[1] H. Chaté, *Int. J. Mod. Phys. B*, **12**, 299 (1998).

[2] J.A.C. Gallas et al., *Physica A*, **180**, 19 (1992); J. Hemmingsson, *Physica A*, **183**, 255 (1992).

[3] H. Chaté and P. Manneville, *Prog. Theor. Phys.*, **87**, 1 (1992); *Europhys. Lett.*, **17**, 291 (1992); H. Chaté and J. Losson, *Physica D*, **103**, 51 (1997).

[4] See, e.g.: N. Nakagawa and Y. Kuramoto, *Physica D*, **80**, 307 (1995); M.-L. Chabanol, V. Hakim, and W.J. Rappel, *Physica D*, **103**, 273 (1997); K. Kaneko, *Physica D*, **86**, 158 (1995).

[5] N. Mousseau, *Europhys. Lett.*, **33**, 509 (1996).

[6] R.S. MacKay and T.A. Sépulchre, *Physica D*, **82**, 243 (1995); T.A. Sépulchre and R.S. MacKay, *Nonlinearity*, **10**, 679 (1997); S. Aubry, *Physica D*, **103**, 201 (1997); V.I. Nekorkin and V.A. Makarov, *Phys. Rev. Lett.*, **74**, 4819 (1995).

[7] A. Lemaître, H. Chaté and P. Manneville, *Europhys. Lett.*, **39**, 377 (1997).

[8] A. Lemaître and H. Chaté, *Phys. Rev. Lett.*, **80**, 5528 (1998); preprint, 1998.

[9] H. Chaté, L.-H. Tang and G. Grinstein, *Phys. Rev. Lett.*, **74**, 912 (1995).

[10] A. Lemaître, H. Chaté, and P. Manneville, *Phys. Rev. Lett.*, **77**, 486 (1996).

[11] L. A. Bunimovich and Ya G. Sinai, *Nonlinearity*, **1** (1988) 491; G. Keller and M. Künzle, *Ergod. Theor. Dyn. Sys.*, **12** (1992) 297. J. Bricmont and A. Kupiainen, *Comm. Math. Phys.*, **178**, 703 (1996); *Physica D*, **103**, 18 (1997).

Conclusion

Cette thèse m'a d'abord permis d'explorer dans plusieurs directions les comportements des réseaux d'itérations couplées : en faisant varier le couplage, la non linéarité, et même en définissant un paramètre supplémentaire lié à la discrétisation du réseau. L'écriture du groupe de renormalisation permet alors de relier la limite $\mu \to \mu_\infty$ à la limite des systèmes couplés continûment, et montre qu'il y a une cascade sous-harmonique infinie de comportements collectifs non triviaux. J'ai poursuivi en écrivant une hiérarchie d'équations qui gouvernent la dynamique d'un macro-état du système, pour enfin en proposer un modèle minimal. Je reprends maintenant ces différents points.

L'étude des différents régimes observés quand le couplage varie a permis de mettre en évidence l'existence d'une compétition entre structures mésoscopiques dès que l'attracteur du comportement collectif pur possède plusieurs composantes ergodiques. Afin de simplifier la présentation, la notion d'états par bandes est introduite : c'est une restriction de la notion d'états purs qui peuvent exister indépendamment des bandes de l'itération locale. Tant que le couplage est assez faible, des états mélangés peuvent être observés asymptotiquement : des amas correspondant aux phases temporelles de l'attracteur macroscopique coexistent en espace et sont séparés par des fronts bloqués sur les sites du réseau. Dès que le couplage est assez fort (en intensité, g ou en étendue, m) ces structures sont toutes instables, et seuls sont atteints asymptotiquement les états par bandes où toutes les variables locales participent à la même composante ergodique de l'attracteur. Dans le cas des itérations unimodales, l'asymétrie des bandes garantit que la synchronisation par bandes soit atteinte en temps fini pour des conditions initiales microscopiques génériques, c'est à dire prises selon la mesure de Lebesgue sur l'espace des phases.

La définition de variables de spins associées aux bandes offre une caractérisation simple des phases macroscopiques, indépendamment du couplage, et permet d'évaluer la dynamique de croissance de domaines qui s'instaure. La

recherche d'une méthode de mesure du seuil g_e^1 au delà duquel tous les fronts se propagent nous a conduit à l'étude numérique précise de la compétition entre les deux phases (dans le cas d'une dynamique à deux bandes), partant de la condition initiale macroscopique qui leur assure asymptotiquement des poids égaux. Au dessus du seuil g_e^*, la taille des domaines croît algébriquement en temps, $L(t) \propto t^{\phi}$, tandis que la persistance décroît comme $t^{-\theta}$. Les deux exposants θ et ϕ dépendent continûment de g pour s'annuler au point g_e^1, bien qu'il faille noter qu'une universalité faible semble être vérifiée, le rapport θ/ϕ étant constant. C'est un phénomène nouveau qui va à l'encontre des comportements observés habituellement dans ce type de systèmes où, partant de conditions initiales non corrélées en espace, ϕ prend toujours la valeur de $1/2$ ce qui est corroboré par des arguments liés à la dynamique des fronts [2, 7, 22].

Ce ralentissement de la propagation des fronts dans le milieu diphasique que constitue le réseau explique le gel des structures à faible couplage. Nous pouvons remarquer que les amas sont de forme plutôt carrée à très faibles couplage, et que les fronts suivent aussi des diagonales près de g_e^1 (voir fig. 1.5). Il semble donc que ce phénomène soit assez directement lié à l'anisotropie du réseau : la croissance des domaines a tendance à produire des fronts qui sont plats par morceaux, ce qui empêche alors leur propagation puisque par symétrie les fronts plats sont stationnaires. Reste à comprendre comment se forment ces fronts plats, et ce qui se passe près des défauts que sont les angles entre les parties linéaires d'un front. Que se passe-t-il en dimension supérieure, où les défauts sont plus complexes ? ou sur une réseau hexagonal ? Une idée de modélisation de ce phénomène consisterait donc à reprendre les théories usuelles de dynamique de fronts, en ajoutant un terme lié à l'anisotropie du système (indépendant du couplage ?) qui oriente les fronts vers les axes principaux du réseau. Les théories usuelles respectent la symétrie sphérique, et travaillent sur le rayon de courbure des fronts. La compétition entre la propagation normale de front courbes et cet effet anisotrope pourrait peut être rendre compte des variations des exposants, et pourquoi pas de leur comportement au seuil.

Nous avons remarqué que la synchronisation par bandes n'est pas *stricto sensu* le comportement collectif non trivial. La nuance est illustrée quand la dynamique locale n'a qu'une bande tandis que le comportement collectif est de période 2. Peut-il y avoir dans ce cas des structures gelées à faible couplage entre les composantes ergodiques du comportement collectif, à une échelle mésoscopique ? L'existence de telles structures requiert que les deux états purs soient définis à des valeurs du couplage qui autorisent aussi le blocage de fronts

et il faut alors s'attendre à ce que ces états s'hybrident. Quel est alors le rôle joué par l'unique bande de l'application locale ? Les variables de spins peuvent toujours être définies en prenant le point fixe X^*_μ comme frontière, mais le système autorise les spins à changer de phase, et la nucléation d'une phase dans l'autre devient permise ; l'influence de cette bande peut-elle être alors modélisée par une température ? Il semble en tout cas intéressant à ce stade de mettre en œuvre les techniques de mesure de persistance par blocs, qui permettent de caractériser la croissance de domaines à température non nulle [4].

Le groupe de renormalisation établit, par exemple dans le cas des applications circonflexes couplées, la conjugaison entre l'opérateur itéré $(\mathbf{\Delta}_g^m \circ \mathbf{S}_\mu)^2$ et $\mathbf{\Delta}_g^{2m} \circ \mathbf{S}_{\mu^2}$. C'est un outil puissant, qui permet d'accéder à la limite $\mu \to \mu_\infty$ par la considération des systèmes $\mathbf{\Delta}_g^m \circ \mathbf{S}_\mu$ pour $\mu \in [\bar{\mu}_1, \bar{\mu}_0]$. Ceci prouve, en particulier, que le comportement du système discret $\mathbf{\Delta}_g \circ \mathbf{S}_\mu$ aux points critiques $\mu_c^n \in [\bar{\mu}^{n+1}, \bar{\mu}^n]$ est directement relié aux comportements critiques des systèmes $\mathbf{\Delta}_g^{2^n m} \circ \mathbf{S}_\mu$ en leurs points $\mu_c^0 \in [\bar{\mu}_1, \bar{\mu}_0]$ respectifs. Dans le cas des applications circonflexes, cette relation est exacte, mais une relation similaire quoique plus compliquée est vérifiée dans le cas général.

L'étude numérique du comportement critique des réseaux d'itérations logistiques couplées près du point critique μ_c^0 a montré que le système présente des exposants critiques non triviaux, en tout cas différents des exposants d'Ising attendus dans le cadre d'une représentation à la Langevin, c'est à dire incluant un désordre extrinsèque [23]. À quel exposants peut-on s'attendre aux points μ_c^n, et en particulier dans la limite $\mu \to \mu_\infty$? Par application de groupe de renormalisation, cette question rejoint celle du comportement critique des systèmes à couplage itéré et de leur limite continue. Or, la mesure des exposants de persistance a montré que ceux-ci dépendent du couplage et de la discrétisation, mais qu'ils retrouvent un comportement universel dans la limite continue : il est donc envisageable que les exposants critiques retrouve de même un comportement de type «Ising» dans cette limite.

Notons à ce sujet que l'observation d'exposants non triviaux associés à cette transition de phase a été interprétée comme une conséquence de la mise à jour synchrone : ceci n'est pas du tout incompatible avec un rôle de l'anisotropie. En effet, la mise à jour synchrone contribue à faire jouer à plein la géométrie du réseau tandis qu'une mise à jour asynchrone «casse» la dépendance géométrique entre les différents sites. Les effets de discrétisation sont analogues aux effets de taille finie dans l'espace de Fourier, ce qui peut expliquer l'obser-

vation de comportements hors de la classe d'universalité attendue. Puisque le groupe de renormalisation est exact dans le cas des applications circonflexes couplées, ce système est le candidat inévitable qui permette d'éprouver ces idées, par la mesure du point critique μ_c^0 du système $\mathbf{\Delta}_g^m \circ \mathbf{S}_\mu$ et des exposants correspondants, pour plusieurs valeurs de m.

Venons-en maintenant à la modélisation des comportements collectifs purs. La dynamique des macro-états est définie de façon autonome par la hiérarchie des opérateurs de Perron-Frobenius marginaux. Le modèle de champ moyen conditionnel définit une approximation pour la dynamique de la distribution p^t couplées à celle de la longueur de cohérence. Cette approximation est définie pour la limite de «température nulle» que constituent les systèmes couplés continûment. Il est remarquable que ce modèle rende compte aussi correctement des comportements observés. Reste à comprendre ce que le modèle prédit au niveau du point critique : il est numériquement difficile d'y accéder, et la convolution, qui fait intervenir des puissances complexes non entières semble jouer un rôle subtil qui permet d'envisager que cette transition soit non seulement continue, mais en plus avec des exposants critiques non triviaux. Une analyse en forme normale pourrait être envisagée afin de mieux comprendre ce qui s'y passe.

Bien sûr, le modèle tel qu'il est défini est susceptible de nombreuses améliorations, la seule contrainte étant de coupler les dynamiques des corrélations et de la distribution p^t en respectant leurs effets respectifs. Il est particulièrement intéressant d'observer que le modèle lui même obéit à un groupe de renormalisation : en itérant ce groupe, comme pour les réseaux d'itérations couplées, le couplage se complexifie en faisant intervenir de plus en plus de variables. Ceci laisse alors espérer que le modèle itéré puisse rendre un meilleur compte des comportements du réseau ; malheureusement, ça ne semble pas évident au vu de premières tentatives dans cette direction, mais il est certainement trop tôt pour conclure.

Remarquons pour finir que la limite continue des systèmes d'itérations couplées est intéressante à plusieurs titres : non seulement pour son aspect universel et son importance dans la structure du groupe de renormalisation, mais aussi parce qu'elle constituent la limite naturelle de «température nulle» des itérations chaotiques couplées et permet donc d'élaborer les modèles qui nous renseignent sur les mécanismes à l'origine des comportements collectifs non triviaux.

Bibliographie

[1] S. Aubry. Breathers in non-linear lattices : Existence, linear stability and quantization. *Physica D*, **103** :201, 1997.

[2] A. J. Bray. Theory of phase ordering kinetics. *Adv. Phys.*, **43** :357, 1994.

[3] L. A. Bunimovich and Ya G. Sinai. Spacetime chaos in coupled map lattices. *Nonlinearity*, **1** :491–516, 1988.

[4] S. Ceuille and C. Sire. Block persistence. cond-mat/9803014, 1998.

[5] H. Chaté and P. Manneville. Collective behaviors in spatially extended systems with local interactions and synchronous updating. *Prog. Theor. Phys.*, **87**(1) :1–60, 1992.

[6] P. Collet and J. P. Eckmann. *Iterated Maps On the Interval as Dynamical Systems*, volume **1** of *Progress in Physics*. Birkhäuser, Boston, 1980.

[7] B. Derrida, A. J. Bray, and C. Godrèche. Non-trivial exponents in zero temperature dynamics of the 1D Ising and Potts models. *J. Phys A.*, **27**(11), 1994.

[8] K. Kaneko (Editor), editor. *Theory and applications of coupled map lattices*. John Wiley & Sons, New York, 1993.

[9] M. Feigenbaum. Universal behavior in nonlinear systems. *Physica D*, **7** :16, 1983.

[10] K. Kaneko. Period-doubling of kink-antikink patterns, quasiperiodicity of antiferro-like structures and spatial intermittency in coupled logistic lattice – Toward a prelude of a field theory of chaos. *Prog. Theor. Phys.*, 72 :480–486, 1984.

[11] K. Kaneko. Lyapunov analysis and information flow in coupled map lattices. *Physica D*, 23 :436–447, 1986.

[12] K. Kaneko. Pattern dynamics in spatio-temporal chaos. *Physica D*, **34** :1–41, 1989.

[13] K. Kaneko. Spatiotemporal chaos in one- and two-dimensional coupled map lattices. *Physica D*, 37 :60–82, 1989.

[14] K. Kaneko. Towards a thermodynamics of spatiotemporal chaos. *Prog. Theo. Phys. Suppl*, 99 :263–287, 1989.

[15] K. Kaneko, editor. *Coupled map lattices : theory and experiments*, Singapore, 1993. World scientific.

[16] G. Keller and M. Künzle. Transfer operators for coupled map lattices. *Ergod. Theor. Dyn. Sys.*, **12** :297–318, 1992.

[17] J. Komornik. Asymptotic periodicity of the iterates of weakly contrictive Markov operators. *Tohoku Math. J.*, **38** :15–27, 1986.

[18] A. Lasota and M. C. Mackey. *Chaos, Fractals and Noise : Stochastic Aspects of Dynamics.* Springer Verlag, New York, 1994.

[19] Joel L. Lebowitz. Microscopic reversibility and macroscopic behavior : physical explanations and mathematical derivations. cond-mat/9605183, 1996.

[20] J. Losson and M. C. Mackey. Statistical cycling in coupled map lattices. *Phys. Rev. E*, **50** :843–856, 1994.

[21] J. Losson and M.C. Mackey. Statistical cyling in two diffusively coupled maps. *Physica D*, **72** :324–342, 1994.

[22] M. Marcos-Martin, D. Beysens, J. P. Bouchaud, C. Godrèche, and I. Yekutieli. *Physica A*, 214 :396, 1995.

[23] P. Marcq, H. Chaté, and P. Manneville. Universal critical behavior in two-dimensional coupled map lattices. *Phys. Rev. Lett.*, **77** :4003–4007, 1996.

[24] J. Miller and D. A. Huse. Macroscopic equilibrium from microscopic irreversibility in a chaotic coupled map lattice. *Phys. Rev. E*, **48**(4) :2528–2535, 1993.

[25] O. Penrose. *Foundation of Statistical Mechanics.* Pergamon, Elmsford, N.Y., 1970.

[26] I. Prigogine. *From Being to Becoming.* Freeman, San Francisco, 1980.

[27] N. Provatas and M. C. Mackey. Asymptotic periodicity and banded chaos. *Physica D*, **53** :295–318, 1991.

[28] D. Ruelle. *Thermodynamic Formalism* in Encyclopedia of Mathematics and its Applications. Addison-Wesley, New York, 1978.

[29] T. Yoshida, H. Mori, and H. Shigematsu. Analytic study of chaos of the tent map : Band structures, power spectra and critical behaviors. *J. Stat. Phys.*, **31** :279–308, 1982.

Systèmes chaotiques couplés : comportements collectifs et universalité

Les systèmes dynamiques chaotiques à un grand nombre de degrés de liberté couplés peuvent présenter une dynamique autonome unique de leur observables macroscopiques associée aux trajectoires chaotiques des configurations dans l'espace des phases : c'est le comportement collectif non-trivial. Ce mémoire aborde l'étude de ce phénomène dans le cadre d'un modèle de chaos spatio-temporel : les réseaux d'itération couplées. L'étude de la transition entre les régimes faiblement/fortement couplés montre que l'unicité de l'attracteur macroscopique est l'aboutissement d'un processus de croissance de domaines, générique au dessus d'un seuil de couplage. L'écriture d'un groupe de renormalisation pour les itérations unimodales couplées assure que toutes les propriétés d'universalité des itérations elles-mêmes s'étendent aux systèmes fortement couplés avec un exposant supplémentaire lié à la forme du couplage. Enfin, la modélisation du comportement collectif à partir des équations locales est étudiée, par la mise en œuvre d'un développement hiérarchique d'équations pour les moments du système, et par la définition d'un opérateur de Perron-Frobenius non-linéaire effectif pour la dynamique des distributions.

Mots-clés : Chaos, itérations couplées, comportement collectif, groupe de renormalisation, universalité, croissance de domaines, équations hiérarchiques.

Coupled chaotic systems: collective behavior and universality

Chaotic dynamical systems with a large number of coupled degrees of freedom may exhibit a unique autonomous evolution of their macroscopic observables, associated to the chaotic trajectories of configurations in the phase space: this is called non-trivial collective behavior. This thesis tackles this phenomenon in the framework of a model of spatio-temporal chaos: coupled map lattices. Studying the transition between weak and strong coupling regimes shows that the unicity of the macroscopic attractor is the result of a phase ordering process which is generic above some threshold of the coupling strength. The definition of a renormalization group for coupled unimodal maps guarantees that all the universal properties of the maps themselves extend to the case of strongly-coupled systems, with an additional scaling exponent related to the form of the coupling. Finally, models for the collective behavior are derived from local equations, using a hierarchical expansion of equations governing the moments of the system, or via the definition of an effective non-linear Perron-Frobenius operator for the dynamics of (local) probability distribution functions.

Keywords: Chaos, coupled maps, collective behavior, renormalization group, universality, phase ordering, hierarchical equations.